Phenomenological Studies Towards the Improvement of Methodologies for Thermoluminescence Glow Curve Analysis

Dissertation submitted for the degree of
Doctor of Philosophy (Science)
of Jadavpur University

By

Mohan Kundu
Department of Physics
Jadavpur University
Kolkata – 700032, India

December – 2024

Phenomenological Studies Towards the Improvement of Methodologies for Thermoluminescence Glow Curve Analysis

Dissertation submitted for the degree of
Doctor of Philosophy (Science)
of Jadavpur University

By

Mohan Kundu
Ph. D. Registration no: SOPHY1514022 of 2022

Under the supervision of

Dr. Sukhamoy Bhattacharyya
Assistant Professor, Department of Physics
Jadavpur University
Kolkata – 700032, India

যাদবপুর বিশ্ববিদ্যালয়
কলকাতা-৭০০ ০৩২, ভারত

*JADAVPUR UNIVERSITY
KOLKATA-700 032,INDIA

FACULTY OF SCIENCE : DEPARTMENT OF PHYSICS

CERTIFICATE FROM THE SUPERVISOR

This is to certify that the thesis titled **"Phenomenological Studies towards the Improvement of Methodologies for Thermoluminescence Glow Curve Analysis"** submitted by **Mr. Mohan Kundu** who got his name registered on **09.06.2022** for the award of Ph. D. (Science) Degree of Jadavpur University, is absolutely based upon his own work under my supervision and that neither this thesis nor any part of it has been submitted for either any degree / diploma or any other academic award anywhere before.

Sukhamoy Bhattacharyya

Dr. Sukhamoy Bhattacharyya
Assistant Professor
Department of Physics
Jadavpur University

Dr. Sukhamoy Bhattacharyya
Assistant Professor
Department of Physics
Jadavpur University
Kolkata – 700 032

CERTIFICATE OF SIMILARITY CHECK

This is to certify that the plagiarism checking for this thesis titled **"Phenomenological Studies towards the Improvement of Methodologies for Thermoluminescence Glow Curve Analysis"** authored by **Mr. Mohan Kundu** has been performed using professional plagiarism prevention software **iThenticate**. According to the report generated after plagiarism checking there is a 10% similarity in this thesis, which is in the category **'Level 0'** (minor similarities) as per the 'Promotion of Academic Integrity and Prevention of Plagiarism in Higher Education Institutions Regulations, 2018' of the University Grants Commission (UGC) of India. The common knowledge or coincidental terms up to 10 (ten) consecutive words (as prescribed in the above said UGC Regulation up to 14 (fourteen) terms for such common knowledge or coincidental terms can be excluded) and own works of the candidate published in various peer-reviewed journals (those are attached in the thesis) are excluded from the similarity checking. It is certified that the present thesis submitted by Mr. Mohan Kundu is plagiarism-free and has followed standard norms of academic integrity and scientific ethics.

Sukhamoy Bhattacharyya

Dr. Sukhamoy Bhattacharyya
Asistant Professor
Department of Physics
Jadavpur University

Dr. Sukhamoy Bhattacharyya
Assistant Professor
Department of Physics
Jadavpur University
Kolkata – 700 032

Dedicated to the divine universe who has dragged everything to make it happen finally…

Contents

Acknowledgements

First and foremost, I would like to convey my heartfelt gratitude to my supervisor, Dr. Sukhamoy Bhattacharyya, for his continuous encouragement, guidance, and mentorship during this research project. I will be eternally thankful to him for introducing me to the domain of theoretical studies in Thermoluminescence. His skill, persistence, and hard efforts have helped shape my thesis significantly. Because of his kind and welcoming nature, he has become more like my elder brother than a guide.

Any appreciation will fall short of acknowledging Dr. Partha Sarathi Majumdar of Acharya Prafulla Chandra College. He has always been very enthusiastic and encouraging about the progress of my research work. His optimistic support during the difficult phases of the journey is actually priceless. He has always been very there to help me through the algebra, computer codes, and other skills required to conduct research. The discussion sessions with him always bring fresh air. He remains to be a constant source of inspiration for me.

I will ever remain grateful to Dr. Arabinda Das and Dr. Saurish Chakraborty of Acharya Prafulla Chandra College for their support during many phases of this course. Academic discussions with them always enriched me a lot. All of their appreciation and good wishes have boosted my confidence to explore new domains of study. I also acknowledge the support I received from the Dept. of Physics of APC College.

I am thankful to Prof. Tapan Kumar Mukhopadhyay of Narula Institute of Technology for his continuous encouragement and also for providing other necessary support in many ways to carry out my research. On the same note, I would like to express my sincere gratitude to Dr. Jayanta Kumar Saha of Aliah University.

I am extremely indebted to Jadavpur University for granting me permission to register for Ph. D. degree. I would like to thank Prof. Partha Pratim Ray, Prof. Subenoy Chakraborty, Dr. Kaustuv Das, Prof. Saikat Kumar Seth, and other faculties and staff of Jadavpur University for their all out support for seamlessly conducting the research work.

I want to express my gratitude to the authority Sadhanpur Uludanga Tulsiram

High School, Amdanga, N 24 PGS for giving permission to enroll into the Ph.D programme at Jadavpur University. I am also thankful to all my colleagues for their constant encouragement.

The best gift during the journey is the close association with Dr. Sayantan Dutta. I am really fortunate to have him as a friend during the entire period. I must thank all my lab mates Tushar, Salil, Soumya, Sayan for their association.

I want to express my heartfelt gratitude to Dr. Dwijesh Majumder who built the confidence of self learning during my B.Sc. at RKMVC college. I must thank Prof. Pratap Raychaudhuri at TIFR, Mumbai and Prof Subhananda Chakrabarti at IIT, Mumbai for providing opportunities to work in their labs which had immensely illuminated me. A special thanks is reserved for my friend Dr. Mintu Mondal from IACS, Kolkata for his constant support starting from my college days till the completion of this journey.

No mission is ever successful without the support of family. I am grateful to my mother, Smt. Manju Kundu and my father, Mr. Mrinal Kanti Kundu for providing all the comforts in life and providing unconditional support behind all my academic, personal and professional decisions. I am thankful to my wife, Smt. Kankana Kundu who has been encouraging me to pass through the process. Finally I must mention my eight month old son Master Sourish Kundu. Maybe, the entire project has been waiting for his arrival in my life.

I extend my thanks to my childhood friends Sanjoy and Biswajit for always being with me in every situation. Finally I thank the almighty to finally make it happen.

Date: 27.12.2024

Mohan Kundu

MOHAN KUNDU
Department of Physics
Jadavpur University
Kolkata – 700032, India

Abstract

Study of thermoluminescence (TL) involves recording optical glow on heating a previously irradiated TL material. Glow curve analysis (GCA) is a widely used technique to extract important information related to irradiation stage, trap states, charge transfer mechanism etc. For this reason, the TL phenomenon finds applicability in different fields of research like dosimetry, defect studies and dating. However, in an experimental scenario, GCA is quite critical and sometimes may become even misleading due to the lack of ab-intio theoretical background. Hence multiple methods depending on the nature of glow curves are needed to validate the results. For obvious reasons, theoretical analysis of TL is subject to various approximations and grossly depend on various models and methods. Therefore improving the present methodologies on the backdrop of various approximations and developing new methodologies with comparative analysis are in the active interest of researchers. Moreover, analyzing the TL data from a statistical viewpoint and hence to find suitable statistical distribution functions applicable to 'distribution' of intensity over temperature can be a potential approach to develop new methodologies.

This dissertation is organized in six chapters. The outline of the chapters are given below.

Chapter 1

In the 'Introduction' chapter, a brief description of the TL process and its importance in various fields of research is given. An account of the development in this field through different approaches based on various models has been discussed. The basic features of different methodologies of TL glow curve analysis are also included in this chapter. The focus and motivation of the present study on the backdrop of previous developments are discussed.

Chapter 2

The integral of the form $J(T_i, T_f, a) = \int_{T_i}^{T_f} T^a e^{-\frac{E}{kT}} dT$ occurs frequently in the theoretical analysis of various thermally stimulated process. The value of the exponent a may lie within the range $-2 \leq a \leq 2$. However, in traditional TL studies, $a = 0$ is mostly considered. For $a = 0$ the integral is called as 'temperature integral' and for $a \neq 0$, it may be referred to as 'extended temperature integral'. These integrals cannot be evaluated analytically in a closed form and various approximated methods have been reported in literature. In this chapter, we describe a new analytical method to evaluate the temperature integral using converging infinite series. The present method is not subject to any approximation other than truncating the converging infinite series after a suitable number of terms. The evaluation can be computationally realized through a simple computer code. A brief review of some of the previous approaches is also included here. The results of the present method has been compared with other methods for numerical validation of the present approaches.

Chapter 3

In this chapter we have developed two versions of peak shape relations for GCA on the basis of two newly introduced symmetry parameters: (i) average symmetry factor ($< \mu'_g >$) and (ii) skewness (S_k) of TL data. The applicability of both the methods is verified by applying them to simulated and experimental TL peaks. The present methods yield consistent results for all cases except for the highly saturated peaks with heavy retrapping. The reason behind the limitation is also explained by investigating the dependence of S_k and μ'_g and on the ratio of retrapping to recombination probabilities. The results of present peak shape methods are compared with other methods for further establishing their applicability in glow curve analysis.

Chapter 4

Frequency factor related to a trap state slowly varies with temperature. However in TL studies, it is assumed as a temperature independent quantity for experimental intricacies as well as theoretical realization. Such assumption may lead to certain inaccuracy in estimating trapping parameters. In this chapter, an account on the impact of temperature dependence of frequency factor on glow curve analysis is given. The temperature dependence of frequency factor is not known beforehand and hence to simulate the same glow curve for different temperature exponents is quite challenging. An efficient methodology to simulate the same glow peak for temperature dependent frequency factor (TDFF) has been discussed. Impact of TDFF in GCA is investigated by adopting different versions of 'peak shape methods' and 'area methods'. In 'area method' we have emphasized on the newly developed 'Three Point Area' method.

Chapter 5

The challenge in GCA of a complex glow curve is to isolate and analyze its component peaks. Glow curve deconvolution (GCD) is a potential method for this purpose. In this chapter we focus to develop a new GCD function on the basis of statistical distribution of data. At first we adopted the Gaussian distribution as a starting ground to proceed further in this direction. The suitability of Gaussian distribution in GCD have been critically examined, however, for obvious reasons, the results are not quite satisfactory. In the next phase, considering the skewed nature of TL data, we propose a version of skew-normal distribution characterized by five parameters. We investigate the suitability of this new probability function and apply it to a large number of TL glow curves simulated in various models. As a pilot investigation, we have considered the TL curves which are equivalent to first and second order kinetics. The quality of fitting is judged through residue plots as well as through the correlation between the TL data and fitted data. The present analysis shows good possibility of applying the skew-normal distribution for GCD in TL studies.

Chapter 6

We finally conclude all the findings reported in the dissertation in previous chapters. A consolidated account of the present work on developing new methodologies along with the theoretical developments is presented. We also discuss the potential future scopes of these works which will pave the way for further development towards the different fields of research engaging thermoluminescence as well as other thermally stimulated processes.

List of Publications

Peer reviewed publications included in the thesis:

1. "Three-Point Area Method for Thermoluminescence Glow Curve Analysis and Its Application to the Glow Peak of K2SrP2O7: Pr."

   M. Kundu, S. Bhattacharyya, M. Karmakar, and P. S. Majumdar

   Radiation Protection Dosimetry, (Oxford University Press), 193 (2021): 247-258,

   https://doi.org/10.1093/raddos/ncab048

2. "Reappraisal of peak shape method based on average geometrical symmetry factor and its application to thermoluminescence glow curves."

   M. Kundu, S. Chakrabarty, S. Bhattacharyya, and P. S. Majumdar.

   Physica Status Solidi (b), (Wiley), 258 (2021): 2100277

   https://doi.org/10.1002/pssb.202100277

3. "Thermoluminescence glow curve analysis using temperature dependent frequency factor in OTOR model."

   M. Kundu, S. Chakrabarty, S. Bhattacharyya, and P. S. Majumdar.

   Radiation Measurements (Elsevier), 156 (2022): 106820,

   https://doi.org/10.1016/j.radmeas.2022.106820

4. "Estimation of activation energy using skewness of TL data as symmetry parameter in peak shape method."

   M. Kundu, S. Chakrabarty, S. Bhattacharyya, and P. S. Majumdar.

   Nuclear Instruments and Methods in Physics Research Section B: Beam Interactions with Materials and Atoms, (Elsevier), 542 (2023): 214-222,

   https://doi.org/10.1016/j.nimb.2023.07.006

Conference Proceedings:

1. "Skew-Normal distribution function for deconvolution of thermoluminescence glow curves."

   M. Kundu, S. Sarkar, A. Das, S. Bhattacharyya.

   Presented at ICAMNOP-2023, Delhi; manuscript accepted for publication in Springer Nature conference proceedings.

List of Conferences Attended

1. "Participated in National Conference on Atomic, Molecular and Nano Sciences (NCAMNS - 2019)" held at Aliah University, Kolkata, India, during April 3-4, 2019

2. Participated and delivered a talk in 3rd International Conference on Recent Trends In Renewable Energy and Sustainable Development held at Bhilai Institute Of Technology, RAIPUR, India, during April 29–30, 2022

3. Participated in International Conference on Atomic, Molecular, Material, Nano and Optical Physics with Applications (ICAMNOP - 2023) held at Delhi Technological University, Delhi, India, during December 20-22

Chapter 1

Introductory ideas on thermoluminescence

1.1 Introductory discussion on Thermoluminescence

Luminescence refers to the phenomenon where luminous emission from a substance occurs after being excited by some form of external energy. Based on the form of absorption energy, the luminescence phenonemnon is categorized in different names which is tabulated below

Table 1.1.1: Different luminescence phenomena.

Type of luminescence	**Form of excitation energy**
Photoluminescence	Optical signal (generally UV)
Cathodoluminescence	Accelerated electrons
Radioluminescence	High energy radiation like X-ray, γ- ray, α- ray, accelerated protons *etc.*
Electroluminescence	Electric field
Triboluminescence	Mechanical force
Chemiluminescence	Chemical reaction
Bioluminescence	Biological process

The underlying process of luminescence can be described through a simple energy band diagram as shown in Fig. 1.1.1. By absorbing some excitation energy the system goes to a excited state. At time τ after excitation the system may emit luminous signal. Here τ is known as the life time of excited state. Depending on the order of τ the luminescence phenomenon is grouped into two categories; namely:

(i) Fluorescence ($\tau \sim 10^{-8}$s)

(ii) Phosphorescence ($\tau \geq 1$ s or more)

In fluorescence, the system returns immediately to ground state, therefore luminescence is observed instantly after excitation. In phosphorescence, from the excited state the system goes at first to a meta stable state. Hence the system does not change until an activation energy 'E' is supplied to the system to make a transition from metastable state to excited state followed by a transition to the ground state (or low lying state) and a luminous signal is obtained. The energy 'E', to escape from the meta stable state may be supplied via thermal or optical stimulation. This type of luminescence are categorized as stimulated luminescence.

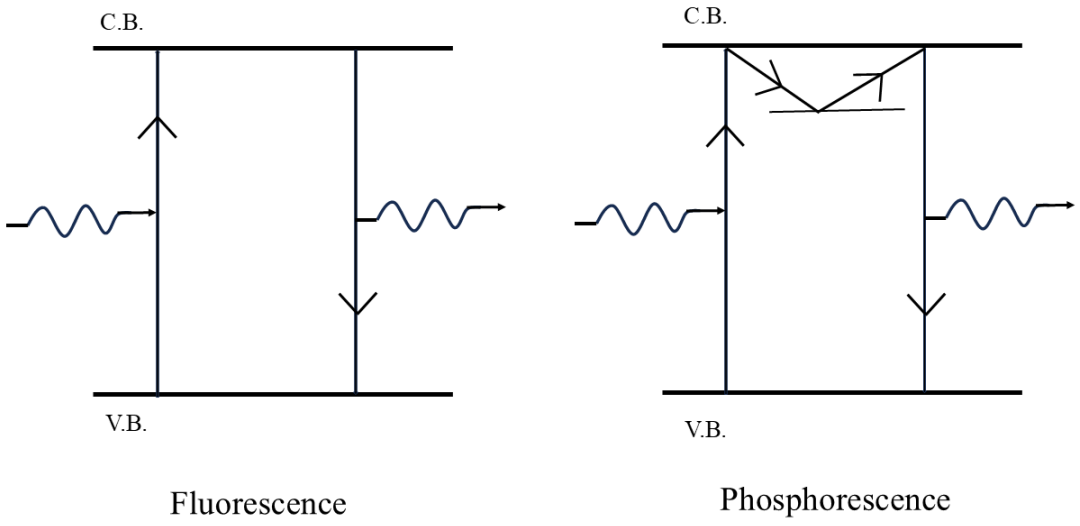

Figure 1.1.1: Schematic diagram describing the process of fluorescence and phosphorescence

1.1.1 Stimulated luminescence

It is understandable that 'Stimulated Luminescence' (SL) is a two stage process and based on the presence of localized energy levels within the forbidden energy band. Depending on different forms of stimulation energy, SL are known in different names (Bräunlich, 1979; Chen and Kirsh, 1981a; Chen and McKeever, 1997; Chen and Pagonis, 2011; Horowitz, 1984; Yukihara and McKeever, 2011). When the stimulation is thermal, the phenomenon is called 'Thermoluminescence' (TL). If optical signal *i.e.* visible light is used for stimulation, one is dealing with optically stimulated luminescence (OSL) and if infrared photons are used, we call it 'infrared stimulated luminescence' (IRSL). OSL and IRSL, can further be categorized as:

(i) Linearly Modulated OSL (LM-OSL): When stimulation rate is linear

(ii) Linearly Modulated IRSL (LM-IRSL): When stimulation rate is linear

(iii) Continuous Wave OSL (CW-OSL): constant light intensity is used for stimulation

(iv) Continuous Wave IRSL (CW-IRSL): constant light intensity is used for stimulation

(v) Pulsed OSL (POSL): Stimulation is done in pulsed mode

(vi) Pulsed IRSL (PIRSL): Stimulation is done in pulsed mode

1.1.2 Thermally stimulated processes

There are group of phenomenon in which certain property related to a substance is varied as a function of temperature when the sample is heated in a specific heating scheme. They are called thermally stimulated process in a combined manner. Some of them are:

(i) Thermally stimulated conductivity (TSC)

(ii) Thermally stimulated electron emission (TSEE)

(iii) Ionic thermoconductivity (ITC)

(iv) Thermal annealing

(v) Derivative thermogravity (DTG)

(vi) Differential thermal analysis (DTA)

(vii) Differential scanning calorimetry (DSC)

Thermoluminescence also falls under these category of phenomenon where luminous intensity is measured with temperature of heating.

1.1.3 The 'Thermoluminescence' phenomenon

Thermoluminescence (TL) or more specifically Thermally stimulated luminescence (TSL) is a phosphorescence which can be categorized as a stimulated luminescence as well as a thermally stimulated process. The focus of the present study is in the domain of thermoluminescence. The phenomenon is described here in detail.

TL was first observed in diamond by Sir Robert Boyle in the year 1663. In 1676 Elsholtz observed a similar effect in fluorspar. In 1705, Oldenberg described the phenomenon thermoluminescence in the mineral, fluorite. However, experimental and radiation induced TL in its present shape was perhaps first reported by Wiedemann and Schmidt in fluorite and $CaF_2 : Mn$ in the year 1895. The real boost in the field of thermoluminescence came after the pioneering work of Farrington Daniels and his group (Daniels et al., 1953) around 1950s at the University of Wisconsin (USA). They first suggested the use of TL as a technique in radiation dosimetry using Lithium fluoride (LiF) as a TL material. Later, LiF was used to measure the radiation dose after a test blast of an atomic bomb in USA. Soon the idea of incorporating TL in dosimetric study became popular and the field flourished as a new branch thermoluminescent dosimetry (TLD). Based on the work of Cameron et al.

(1961) in the material LiF: Mg,Ti the Harshaw Chemical Company in 1963 got a patent of TLD–100. In the last few decades there has been tremendous research in this field. Nowadays it has important application in different fields of radiation dosimetry including personnel dosimetry, environmental dosimetry, clinical dosimetry, retrospective dosimetry etc. TLD is a highly used method in monitoring the doses absorbed by radiation workers within a fixed time period. It is also used in radiation therapy.

Other than dosimetry, thermoluminescence (TL) finds application in diverse scientific disciplines which is described below (Murthy, 2013),

- Natural and artificial insulators and semiconductors along with several novel materials like crystalline nanophosphores have ample applications in various dispaly devices, signing devices, and several dosimetry based applications due to their manifestation of luminescent properties (Atlıhan, 2020; Dewangan et al., 2018; Khiem et al., 2020; Pardha Saradhi et al., 2014; Xu et al., 2014). Presence of appropriate metastable traps of suitable concentration within the band gap of the phosphors is crucial for their luminescent properties which facilitates their applications to optoelectronic devices. TL has been very useful in studying these features (Chen and Kirsh, 1981b; Chen and Mckeever, 1997; Pagonis et al., 2006) including characterizing the trap states. In fact TL based method provides very high sensitivity of detecting the presence of defect centers. It was estimated that the technique is capable of detecting as few as 10^9 defect levels in the material (Murthy, 2013). Apart from these, TL as a tool is very often used in determining surface impurities, in detecting precursor oxides in high-Tc superconductors (Murthy, 2013), detection of phases etc.

- TL has efficient application in archaeological and geological science. It has successfully applied in dating ancient pottery which is even 30,000 years old (Wagner et al., 1982).

- TL has very important application in space science. It is used to determine the thermal and irradiation history of meteorites, and celestial samples (*e.g.* martian and lunar sampels) (Hasan et al., 1986; Walker et al., 1972).

- In recent times TL is being used in biological and biochemical science. It has been successfully used in the study of different proteins including nucleic acids, different bacteria, algae and plant leaves (Murthy, 2013).

- TL is a useful technique in forensic sciences as the method is nondestructive. Generally evidentiary materials like soil, glass, safe insulation trails *etc* are analyzed using TL and compared with the similar material of same origin (Murthy, 2013).

- TL has been sometimes used in industry for quality control purpose. It is used in ceramic and glass industry, semiconductor products (Murthy, 2013).

1.1.4 Description of Thermoluminescence phenomenon

Like other stimulated luminescence, TL is yielded via a two stage process which is mostly observed in insulating or large band gap semiconducting materials. The phenomenon can be understood through the charge transition mechanism based on the band theory of solid. The complete process for observing TL can be described in two different stages namely: (i) irradiation stage and (ii) heating stage. In Fig. 1.1.2 this is shown schematically.

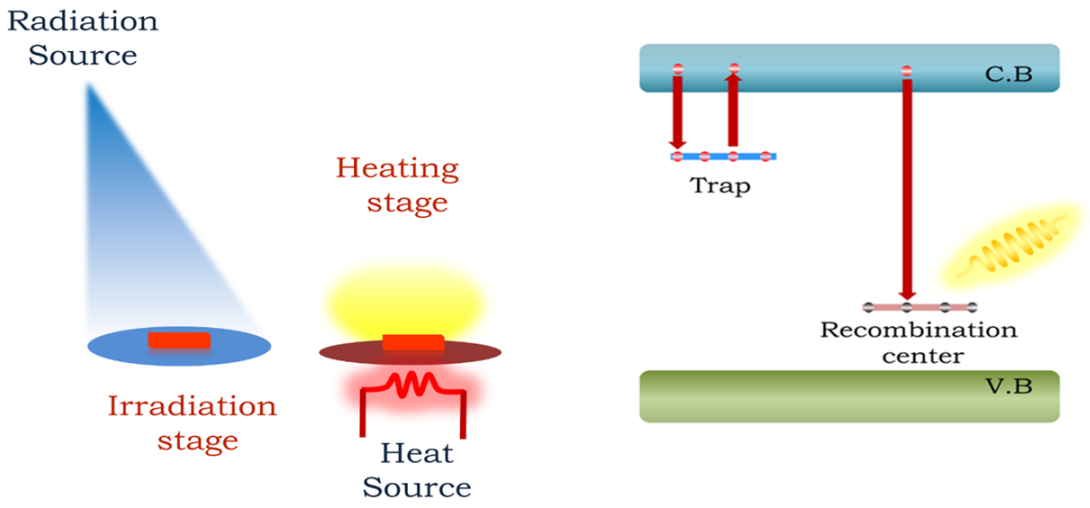

Figure 1.1.2: Schematic diagram describing the two stage TL process.

- **Irradiation stage:** the material is exposed to high energy radiation like x–ray, UV –ray, β–ray, γ–ray *etc.* Through irradiation the system is perturbed and electrons transit via conduction band to localized meta stable states within the forbidden gap region. In this way the system is set into a metastable state.

- **Heating stage:** During heating stage, the sample is heated in systematic scheme and the material starts to glow. As temperature of the sample is increased, the stored energy of irradiation stage is released as luminous signal.

A relaxation may be allowed between the two stages. Recording the glow intensity as function of temperature of heating, the **'TL glow curve'** is obtained. A typical experimentally obtained glow curve usually contains distinct peaks, which are subject to different trap levels.

There are some inherent subtle facts associated with the TL process. It has been mentioned that high energy radiations are used for irradiating the sample. But typical band gap of a TL material is of the order of $\sim$ 1 eV while an x–ray photon carries energy between $\sim$ 100 eV to 100 keV. It is important to understand why such high energy photon is required in irradiation stage. The irradiation process is not just a direct electron – photon interaction, rather a random interaction between crystal lattice and ionizing radiation occurs. The photon energy is spent to ionize the atoms at the lattice points and electronic excited states are created in crystalline TL materials. The generated excited states are trapped by localized defects for larger time period.

On the other hand, during heating stage, if we assume a typical glow peak is appearing at 450 K then the associated thermal energy of an electron is $\sim$ 48 meV while a typical trap depth is $\sim$ 1 eV. The phenomenon can be understood statistically. According to Maxwell-Boltzmann distribution the fraction of electron having thermal energy E over a base level is

$$\frac{N_T}{N_0} = e^{-\frac{E}{kT}} \tag{1.1.1}$$

where N_T is number of electron having energy E at temperature T and N_0 is the initial number of electrons. For $E = 1$ eV at $T = 450$ K, we find $\frac{N_T}{N_0} \sim 10^{-12}$. Therefore only 10^{-12} portion of total trapped electrons will have the sufficient energy (*i.e.* 1 eV) to overcome the energy gap to liberate in the conduction band. Evidently this fraction is very negligible to yield a significant TL intensity. But the probability that an electron escaping from the traps in a second is given by Arrhenius equation as,

$$p(t) = se^{-\frac{E}{kT}} = s\left(\frac{N_T}{N_0}\right) \tag{1.1.2}$$

where, s is named as frequency factor. If the trap is mimicked by a potential box then s is described as the product of the reflection coefficient at box wall and the frequency with which trapped electrons attempt to get free from the trap (Gurney and Mott, 1940). Thus its value will be slightly less than the lattice vibration frequency *i.e* Debye frequency ($\sim 10^{13}$). If typical value of s is considered to be 10^{12} sec^{-1} and $\frac{N}{N_0} \sim 10^{-12}$, then $p(t)$=1 in one second. This means, all the trapped electrons will be freed to conduction band within 1

sec at 450 K. Moreover the thermal equilibrium is re-established very quickly as soon as the charge carriers escape from the traps. This fact in TL study is incorporated by considering quasi equilibrium approximation.

1.1.5 Heating Scheme

A previously irradiated TL sample is heated in a systematic manner termed as heating scheme. It is very important to chose proper heating scheme with suitable heating rate since its impact is reflected in the nature of the glow curve. The popular heating schemes that are usually adopted in TL study are as follows:

- **Linear Heating scheme:** The sample is heated in such a way that the temperature is expressed as a function of time t as,

$$T(t) = T_0 + \beta t \tag{1.1.3}$$

T_0 is the initial temperature and T is temperature at time t. β is the constant equal to the heating rate ($= \frac{dT}{dt}$). So in linear heating scheme temperature is increased at a constant rate with time.

- **Hyperbolic heating scheme:** This scheme can be described through the functional form which is given by,

$$\frac{1}{T(t)} = \frac{1}{T_0} - \beta' \, t \tag{1.1.4}$$

Where β' is a constant. It is to mention that unlike linear heating scheme the heating rate does not remain constant because

$$\frac{dT}{dt} = \beta' T(t)^2 \tag{1.1.5}$$

- **Exponential heating scheme:** The exponential heating (Osada, 1960; Dijk and Julius, 1993; Kitis *et al.*, 2006) is expressed in Eq. 1.1.6 as

$$T(t) = T_e - (T_e - T_0)e^{-\alpha \, t} \tag{1.1.6}$$

Here T_g is the end temperature. α is a constant known as the decay parameter. The

heating rate is not constant and can be calculated as

$$\frac{dT}{dt} = \alpha(T_e - T)e^{-\alpha\ t} \tag{1.1.7}$$

1.1.6 Attempt to *ab-initio* quantum mechanical description of thermoluminescence

The primary motivation of the theoretical research in TL is based on describing the underlying process from theoretical formulation to yield the glow peak that will match the experimental data. Attempt has been made to develop the *ab-initio* quantum mechanical theory of TL process. Böhm and Scharmann (1985, 1987) made an attempt to explain the TL process from *ab-initio* quantum mechanical formalism. The Hamiltonian associated with the purturbation of the system was written as,

$$H' = V(x, X) - U(x, A) \tag{1.1.8}$$

where x is the coordinates of electrons, X represents the coordinates of the basis at lattice points and A is the coordinates of the lattice points at equilibrium. $V(x, X)$ is the potential energy subject to electron – electron interaction while $U(x, A)$ is addressing the potential energy associated to electron – lattice interaction. The time independent Schrödinger equation was solved assuming the basis related to the equilibrium positions while electrons are moving. The transition probability between two states were calculated using first order perturbation formalism under strong coupling condition and finally the expression for TL intensity was given by.

$$I(T) = I_0 \exp\left(-\frac{C}{\coth\left(\frac{\hbar\omega_i}{2kT}\right)}\right) \exp\left[-\frac{W_0}{q}\int_{T_0}^{T} \exp\left(-\frac{C}{\coth\left(\frac{\hbar\omega_i}{2kT'}\right)}\right) dT'\right]$$

Here I_0 is a constant, W_0 is pre-exponential factor related to transition probability of electron which may thought to be equivalent to frequency factor. q is the heating rate. However, the theoretical expression of glow peak intensity did not match with the actual experimentally obtained one. Thereafter the estimated value of trap depth is also in mismatch with the expected value. Therefore this attempt was not a very successful as compared to other formalisms that were adopted in theoretical TL study.

Due to the lack of *ab-initio* theory, the TL phenomenon has been usually studied

theoretically using phenomenological models. Depending on the system of study, suitable models are adopted to describe the TL process properly. The yielded glow peak is compared with the experimental one. Finally the glow peaks are analyzed in different methods to estimate different system properties and parameters.

1.2 Phenomenological models in TL studies

Significant research has been done to understand basic TL process by proposing various phenomenological models. The models are developed under the purview of band theory of solids. An account of previously developed models those are frequently used are presented below

The Kinetic Order (KO) formalism

Analysing a TL peak in the light of Kinetic Order (KO) model is a common practice. The term 'kinetic order' has its origin in chemical reaction kinetics and in this context relates to the dynamic concentrations of charge carriers. TL glow curves are analysed in the KO formalism which, though empirical, is very popular till date. The classification and description of different KO models are as follows.

1.2.1 First Order Kinetics (FOK)

Quantum mechanical transitions between localized and delocalized energy states in matter may be epitomized *via* various phenomenological models using band theory of solids. After the first prototype model proposed by Jabłoński (1935) explaining long life time and temperature dependent phosphorescence, the first significant theoretical insight of the TL process was given by Randall and Willkins (Randall and Wilkins, 1945a,b). They followed a semi-classical approach where TL intensity was expressed in terms of trapping parameters and the energy distribution of the trapped electrons was assumed to follow the Maxwell-Boltzmann statistics (Randall and Wilkins, 1945a,b) and hence the probability (p), that an electron would escape from a trap of trap depth E at temperature T was given by (Curie, 1963; Randall and Wilkins, 1945a)

$$p = se^{-\frac{E}{kT}} \tag{1.2.1}$$

where k is the Boltzmann constant and s is pre-exponential factor (in $\sec^{-1}$ unit) known as 'frequency factor' which may vary slowly with temperature. It is to mention that the

formulation was developed with the notion that all the electrons which were detrapped to the conduction band would recombine almost immediately at luminescent centers without further being retrapped. The TL intensity in such a case is found to be related to the first power of n and the formalism is named as 'first order kinetics'. The TL intensity is obtained as

$$I = -\frac{dn}{dt} = sne^{-\frac{E}{kT}} \tag{1.2.2}$$

where n is the instantaneous concentration of trapped electrons. For linear heating scheme with constant heating rate β, the solution of Eq. 1.2.2 yields the expression for TL intensity for a first order peak given by,

$$I(T) = sn_0e^{-\frac{E}{kT}} \exp\left[-\frac{s}{\beta}\int_{T_0}^{T} e^{-\frac{E}{kT'}}dT'\right] \tag{1.2.3}$$

Here n_0 is the concentration of trapped electrons at T_0 *i.e.* the starting temperature of heating. From Eq. (1.2.3), the peak maximum temperature (T_m) is determined by setting $\frac{dI}{dT} = 0$. The corresponding maximum condition is expressed as

$$\frac{\beta E}{kT_m^2} = se^{-\frac{E}{kT_m}} \tag{1.2.4}$$

1.2.2 Second Order Kinetics (SOK)

Garlick and Gibson (1948) adopted the similar approach of Randall and Wilkins (1945a,b) but with the notion that statistically there should not be any preference between recombination or retrapping. Thus the probabilities of recombination and retrapping for an electron should be equal. The TL intensity is then found to be related to the square of n and the formulation is known as second order kinetics. The expression of TL intensity is

$$I = -\frac{dn}{dt} = \frac{s}{N}n^2e^{-\frac{E}{kT}} = n^2s'e^{-\frac{E}{kT}} \tag{1.2.5}$$

Here N (cm^{-3}) is concentration of electron traps. s' is the pre-exponential factor expressed in cm^3s^{-1}. In linear hetaing scheme, the solution to Eq. 1.2.5 yields the intensity for second order case as

$$I = n_0^2se^{-\frac{E}{kT}}\left[1 + \int_{T_0}^{T}\frac{n_0s'}{\beta}e^{-\frac{E}{kT'}}dT'\right]^{-2} \tag{1.2.6}$$

$$= \quad sn_0 e^{-\frac{E}{kT}} \left[1 + \int_{T_0}^{T} \frac{s}{\beta} e^{-\frac{E}{kT'}} dT'\right]^{-2} \tag{1.2.7}$$

Here $s = s'n_0$. For second order preak the peak position can be determined from peak maximum condition (by setting $\frac{dI}{dT} = 0$ in Eq. 1.2.7) which is written as

$$\frac{\beta E}{kT_m^2} = se^{-\frac{E}{kT_m}} \left[1 + \frac{2kT_m}{E}\right] \tag{1.2.8}$$

1.2.3 General order Kinetics (GOK)

In practice, many TL peaks are observed experimentally which can be described neither by first order or second order equations (McKeever, 1988). Actually, from a broader perspective, the first and second order kinetics are two boundary conditions when the TL process is described by a 'One Trap One Recombination center' (OTOR) system. The intermediate TL peaks can be described from their geometrical characteristics (Halperin and Braner, 1960). Geometrical symmetry factor $\mu'_g = \frac{T_2 - T_m}{T_2 - T_1}$ (Chen, 1969a) is a very useful parameter in this purpose. It has been observed that for a first order peak $\mu'_g \simeq 0.42$ while for a second order peak $\mu'_g \simeq 0.52$. For the intermediate peaks, a range given by, $0.42 < \mu'_g < 0.52$, is satisfied.

The intermediate bridging between first and second order kinetics was mitigated by the adopting the general order kinetics formalism (May and Partridge, 1964). The formulation was further extended by Chen et al. (1981) to introduce the mixed order kinetics case which is discussed later. An empirical parameter, the order of kinetics (b) was introduced in GOK model to describe the nature of TL peak. For first and second order peaks the assigned value, of 'b' are 1 and 2 respectively. For GOK case 'b' lies between 1 and 2. The intensity in GOK case is obtained as (Chen and Kirsh, 1981a; May and Partridge, 1964; Rasheedy, 1993; Sunta, 2014).

$$I = -\frac{dn}{dt} = n^b \; s'' \; e^{-\frac{E}{kT}} \tag{1.2.9}$$

Here s'' is pre-exponential factor quantified in $cm^{3(b-1)}s^{-1}$. In linear heating scheme the expression for intensity in GOK formulation is given in Eq. 1.2.9 as

$$I = sn_0 \; e^{-\frac{E}{kT}} \left[1 + (b-1)\frac{s}{\beta} \int_{T_0}^{T} e^{-\frac{E}{kT'}} dT'\right]^{-\frac{b}{b-1}} \tag{1.2.10}$$

Here $s = s''n_0^{(b-1)}$ in sec^{-1}. Eq. 1.2.10 reduces to the FOK Eq. 1.2.3 in the limit b $\rightarrow$ 1. It

is to mention that for $b = 2$, Eq. 1.2.10 gives the second order (*i.e.* Eq. 1.2.7). The peak maximum condition is obtained from GOK equation as

$$\frac{sbkT_m^2}{\beta E} e^{-\frac{E}{kT_m}} = 1 + \frac{(b-1)s}{\beta} \int_{T_0}^{T_m} e^{-\frac{E}{kT'}} dT' \tag{1.2.11}$$

It may be expressed approximately in a simplified form as

$$\frac{\beta E}{kT_m^2} \simeq s e^{-\frac{E}{kT_m}} \left[1 + (b-1)\frac{2kT_m}{E}\right] \tag{1.2.12}$$

Though GOK model is formulated empirically in an approximated way, it is so far the most successful model which has been widely used in TL literature.

Modified versions of TL intensity in GOK model:

Kitis et al. (1998) gave a modified version of first, second and general order kinetics equations under linear heating scheme. The special feature of the expression is that the TL intensity is expressed as I (I_m, E, T_m, b, T) rather than I (n_0, E, s, b, T). The TL intensity is given by, taking $u_m = \dfrac{E}{kT_m}$,

$$\begin{aligned} I(T) &= I_m \exp\left[1 - \frac{2}{u_m} + u_m\left(1 - \frac{T_m}{T}\right) - \left(\frac{T}{T_m}\right)^2 \left(1 - \frac{2kT}{E}\right) \exp\left[u_m\left(1 - \frac{T_m}{T}\right)\right]\right] \quad \text{for b} = 1 \\ &= b^{\frac{b}{b-1}} \left[1 + (b-1)\left[\frac{2}{u_m} + \left(\frac{T}{T_m}\right)^2 \left(1 - \frac{2kT}{E}\right) \exp\left(u_m\left(1 - \frac{T_m}{T}\right)\right)\right]\right]^{-\frac{b}{b-1}} \exp\left[u_m\left(1 - \frac{T_m}{T}\right)\right] \\ &\qquad \text{for b} \neq 1 \end{aligned} \tag{1.2.13}$$

Another form of transformed equations for first and non first order cases were developed by Gartia et al. (1988), as

$$I = I_m \exp\left[(u_m - u) + F(u, u_m)\right] \quad \text{for b} = 1 \tag{1.2.14}$$

$$\text{and} \qquad I = I_m \exp(u_m - u)\left[1 - \frac{b-1}{b} F(u, u_m)\right]^{-\frac{b}{b-1}} \quad \text{for b} \neq 1 \tag{1.2.15}$$

$$\text{where} \qquad F(u, u_m) = u_m^2 \exp(u_m)\left[\frac{E_2(u_m)}{u_m} - \frac{E_2(u)}{u}\right] \tag{1.2.16}$$

$E_2(u)$ is the 2nd order exponential integral with argument u (Abramowitz and Stegun, 1972). Where $u = \dfrac{E}{kT_m}$

Though the kinetic order formalism has been very successful, yet its limitations are also reported in literature (Delgado et al., 1994; Levy, 1985; Wagner et al., 1982). Therefore

attempts were made in developing further suitable models that could describe different TL systems. Here we present some other band theory based models.

1.2.4 One trap one recombination center (OTOR) model

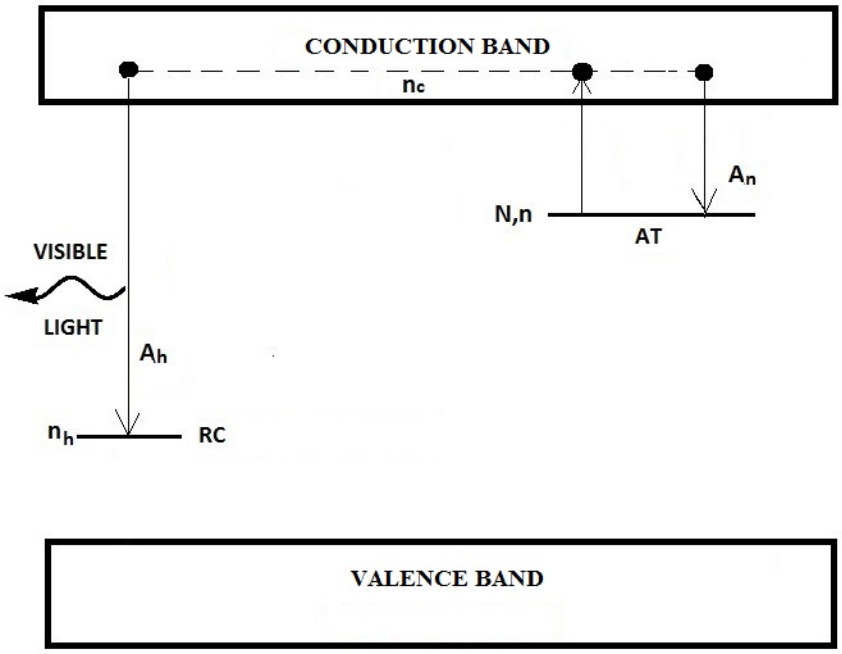

Figure 1.2.1: Schematic diagram describing TL process in one trap one recombination center (OTOR) model.

The one trap one recombination center (OTOR) model is a simplified yet efficient model to describe a TL process to yield glow peak. It has been schematically described in Fig. 1.2.1. The charge trafficking in OTOR model is mathematically presented as (Halperin and Braner, 1960; Sunta, 2014).

$$\frac{dn_c}{dt} = nse^{-\frac{E}{kT}} - A_n(N-n)n_c - A_h n_c n_h \tag{1.2.17}$$

$$\frac{dn}{dt} = -nse^{-\frac{E}{kT}} + A_n(N-n)n_c \tag{1.2.18}$$

$$I = -\frac{dn_h}{dt} = A_h n_c n_h \tag{1.2.19}$$

The parameters are listed below:

- n_c = the concentration of electrons at conduction band,
- n = concentration of trapped electrons,

- n_h = concentration of holes at recombination centre,
- N = concentration of available trap in the forbidden energy gap.
- s = frequency factor related to trap,
- A_n = probability of retrapping,
- A_h = probability of recombination and
- T = absolute temperature at time t.

The charge neutrality condition is expressed mathematically as

$$n_h = n + n_c \tag{1.2.20}$$

The quasi equilibrium condition

It is almost customary in TL analysis to assume the system under 'Quasi Equilibrium' (QE) condition during heating. Under QE approximation, it is assumed that during heating, the rates of detrapping is nearly equal to the sum of rates of recombination and retrapping. Though it is true that the liberated charge carriers will have some finite life time at the conduction band as a result of which some accumulation of charge carriers at conduction band may occur. But the process of thermal stimulation is not comparably fast and even if there is some charge accumulation at conduction band, it will be negligible in comparison to the trapped electron concentration. So it may safely be assumed that during heating the system remains almost in equilibrium that was attained before starting the heating process. Mathematically the QE condition can be expressed as,

$$\left|\frac{dn_c}{dt}\right| << \left|\frac{dn}{dt}\right| \qquad \text{and} \quad n_c << n \tag{1.2.21}$$

The TL intensity in OTOR model is obtained by solving Eqs. (1.2.17 – 1.2.19) by considering quasi equilibrium condition and expressed as

$$I(t) \simeq -\frac{dn}{dt} = \frac{n^2 s e^{-\frac{E}{kT}}}{n(1-R) + NR} \tag{1.2.22}$$

where $R = \dfrac{A_n}{A_h}$. From Eq. (1.2.22), the TL intensity in OTOR model is obtained in linear heating scheme as

$$I(T) \simeq -\frac{dn}{dT} = -\frac{1}{\beta}\frac{dn}{dt} = \frac{n^2 s e^{-\frac{E}{kT}}}{\beta\left[n(1-R)+NR\right]} \tag{1.2.23}$$

Eq. (1.2.23) reduces to first order (Eq. 1.2.2) and second order (Eq. 1.2.5) kinetic equations for $R = 0$ and 1 respectively. To produce the simulated TL data, Eq. (1.2.23) can be solved numerically or can be expressed analytically using lambert W function or wright ω function.

Analytical solution of OTOR equations

(Kitis and Vlachos, 2013) gave an analytical expression for TL intensity according to the OTOR model using the Lambert-W function which is written as

$$I = \frac{sNR\exp\left(-\frac{E}{kT}\right)}{(1-R)^2\left[W[e^{z_1}]+W[e^{z_1}]^2\right]} \quad \text{for} \quad R<1 \tag{1.2.24}$$

$$= \frac{sNR\exp\left(-\frac{E}{kT}\right)}{(1-R)^2\left[W[-1,-e^{-z_2}]^2+W[-1,-e^{z_2}]\right]} \quad \text{for} \quad R>1 \tag{1.2.25}$$

$$\text{where} \quad z_1 = \frac{1}{c} - \ln c + \frac{s}{(1-R)\beta}\int_{T_0}^{T}\exp\left(-\frac{E}{kT'}\right)dT'$$

$$z_2 = \frac{1}{|c|} - \ln(|c|) + \frac{s}{(1-R)\beta}\int_{T_0}^{T}\exp\left(-\frac{E}{kT'}\right)dT'$$

$$\text{and} \quad c = \frac{n_0(1-R)}{NR}$$

TL intensity in OTOR model may also be expressed in terms of Wright ω (denoted by $\omega(z)$) function when $R < 1$ (Singh and Gartia, 2013). However Wright ω function is related to the Lambert-W function as $\omega(z) = W_{k(z)}[e^z]$, where $k(z) = \dfrac{Im(z)-\pi}{2\pi}$. Thus for $R < 1$ we can easily obtain the expression of TL intensity that can be expressed as

$$I(T) = \frac{sNR\exp\left(-\frac{E}{kT}\right)}{\beta(1-R)^2\omega(z_1(T))(1+\omega(z_1(T)))} \tag{1.2.26}$$

The peak maximum condition is given by of the maximum of the TL peak in the OTOR/GOT model for $R < 1$ is

$$\frac{E}{kT_m^2} = \frac{s}{(1-R)\beta}\left[\frac{1+2W[e^{z_1(T_m)}]}{(1+W[e^{z_1(T_m)}])^2}\right]\exp\left(-\frac{E}{kT_m}\right) \tag{1.2.27}$$

It is interesting to note that this equation also work exactly for the case $R > 1$

Transformed OTOR equation

Sadek et al. (2015a) have transformed the expression for intensity in OTOR equation from the form $I(n_0, E, s, R, T)$ into the form $I(I_m, E, T_m, R, T)$ by using the condition for the maximum and given by,

$$I = I_m \exp\left(\frac{E(T-T_m)}{kTT_m}\right)\left[\frac{W[e^{z_{1m}}]+W[e^{z_{1m}}]^2}{W[e^{z_1}]+W[e^{z_1}]^2}\right] \quad \text{for} \quad R<1 \quad (1.2.28)$$

$$= I_m \exp\left(\frac{E(T-T_m)}{kTT_m}\right)\left[\frac{W[-1,-e^{-z_{2m}}]+W[-1,-e^{-z_{2m}}]^2}{W[-1,-e^{-z_2}]+W[-1,-e^{z_2}]^2}\right] \quad \text{for} \quad R>1 \quad (1.2.29)$$

It is to mention that the above expression has been successfully incorporated to develop a software package 'tgcd' in the open access software platform **R** by Peng et al. (2016).

1.2.5 Interactive Multitrap System (IMTS) Model

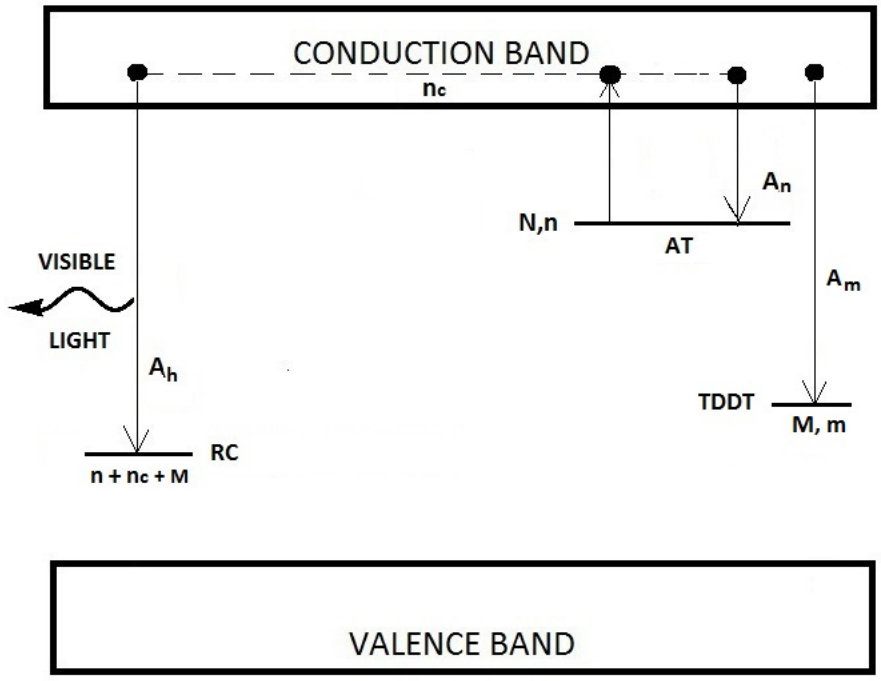

Figure 1.2.2: Schematic diagram describing TL process in interactive multi trap system (IMTS) model.

OTOR model has been further extended to develop Interactive Multitrap System (IMTS) Model. Here two types of trap states are considered,

- thermally active traps which is capable to release trapped elctrons on thermal stimulation
- thermally disconnected deep traps (TDDT) takes part in trapping or retrapping electrons but trapped electrons cannot be detrapped on thermal stimulation from TDDT.

A schematic digram describing basic IMTS model is presented in Fig. 1.2.2. The corresponding charge trafficking equations are given by Sadek et al. (2015b).

$$\frac{dn}{dt} = -nse^{-E/kT} + A_n n_c(N-n) \tag{1.2.30}$$

$$\frac{dm}{dt} = A_m n_c(M-m) \tag{1.2.31}$$

$$\frac{dn_c}{dt} = nse^{-E/kT} - A_n n_c(N-n) - A_m n_c(M-M) - A_h n_c(n+n_c+m) \tag{1.2.32}$$

$$I = -\frac{dn_h}{dt} = A_h n_c(n+n_c+m) \tag{1.2.33}$$

Here the parameters are described below:

- M (cm^{-3}) is the total concentration of TDDTs all of which are filled by electrons
- m (cm^{-3}) is the concentration of filled TDDTs
- A_m $(cm^3 s^{-1})$ is the probability of capturing electrons by TDDTs.

The charge neutrality condition is written as

$$n_h = n + n_c + m \tag{1.2.34}$$

Applying QE conditions *i.e.* $|\frac{dn_c}{dt}| << |\frac{dn}{dt}|, |\frac{dm}{dt}|, |\frac{dn_h}{dt}|$, the three differential equations may be solved to express the TL intensity as (Sunta, 2014)

$$I = -\frac{dn}{dt} - \frac{dm}{dt} = \frac{A_h(n+m)nse^{-\frac{E}{kT}}}{A_h(n+m) + A_n(N-n) + A_m(M-m)} \tag{1.2.35}$$

At lower trap occupancies ($n << N$ and $m << M$), the above equation reduces to the FOK form. Also first-order TL peaks are obtained both under slow retrapping and fast retrapping conditions (Sunta et al., 2001, 2004).

1.2.6 Non-interactive Multitrap System (NMTS) model

When, during the irradiation stage, TDDTs becomes saturated, these traps cannot capture electrons any more and thus they cannot take part in the retrapping process. Thus thermally

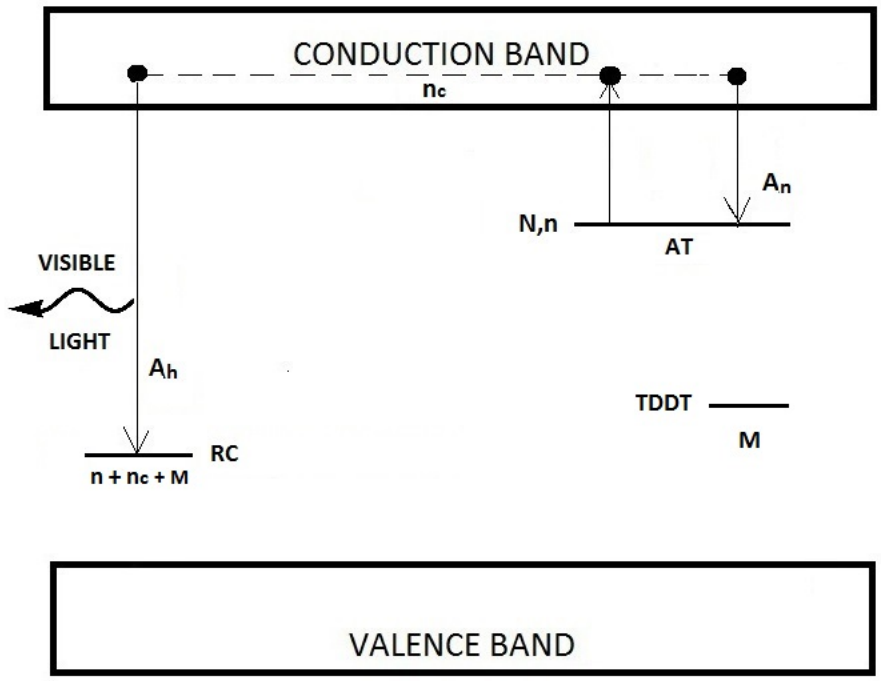

Figure 1.2.3: Schematic diagram describing TL process in non-interactive multi trap system (IMTS) model.

disconnected deep traps (TDDT) becomes non-interactive. The corrsponding model is known as Non-interactive Multitrap System (NMTS) model (Fig. 1.2.3). The differential equations describing the charge transitions in NMTS model are given by Sunta (2014)

$$\frac{dn}{dt} = -n\ s\ e^{-E/kT} + A_n n_c(N-n) \tag{1.2.36}$$

$$\frac{dn_c}{dt} = n\ s\ e^{-E/kT} - A_n n_c(N-n) - A_h n_c(n+n_c+M) \tag{1.2.37}$$

$$I(t) = -\frac{dn_h}{dt} = A_h n_c(n+n_c+M) \tag{1.2.38}$$

Considering the charge neutrality condition given as $n_h = n + n_c + M$, The general solution is given by Sunta (2014)

$$I = \frac{A_h(n+M)nse^{-\frac{E}{kT}}}{A_h(n+M) + A_n(N-n)} \tag{1.2.39}$$

The glow peaks of NMTS model attain the FOK form when trap occupancies $\left(\frac{n_0}{N}\right)$ are low. In addition to that, FOK is also attained at all trap occupancies if TDDTs are in greater abundance than active traps (Sunta, 2014).

Sadek et al. (2015b) presented an alternative analytical expression of the TL intensity in the NMTS model considering QE approximation which is given by

$$I(t) = \frac{NR\phi_{eff}}{(1-R\phi_{eff})^2}\frac{s\exp(-\frac{E}{kT})}{W[e^{z_1}]+W[e^{z_1}]^2} \quad \text{for } R<1 \tag{1.2.40}$$

$$= \frac{NR\phi_{eff}}{(1-R\phi_{eff})^2}\frac{s\exp(-\frac{E}{kT})}{W[-1,-e^{-z_2}]+W[-1,-e^{-z_2}]^2} \quad \text{for } R>1 \tag{1.2.41}$$

Here $\phi_{eff} = \frac{n}{m}$ and n is the concentration of trapped electrons in active traps and m is the concentration of holes in the luminescent centers.

1.2.7 Mixed Order Kinetics (MOK) Model

In case of low irradiation dose and fast retrapping, the condition can be written as $A_n(N-n) >> A_h(n+M)$ and $n << N$ (Chen et al., 1981; Kitis et al., 2019). In that situation NMTS equation for intensity reduces to

$$I = \frac{A_h}{A_n N} s\exp\left(-\frac{E}{kT}\right) n\,(n+M) \tag{1.2.42}$$

For the special case of $A_n = A_h$ (equivalent to b=2) NMTS equation for TL intensity reduces to

$$I = \frac{1}{N+M} s\exp\left(-\frac{E}{kT}\right) n\,(n+M) \tag{1.2.43}$$

Both the Eqs. (1.2.42) and (1.2.43) can be expressed in a compact form as

$$I = gs\exp\left(-\frac{E}{kT}\right) n\,(n+M) \tag{1.2.44}$$

Where $g = \frac{A_h}{A_n N}$ or $\frac{1}{N+M}$. Eq. (1.2.44) is the differential equation for the MOK model which is the sum of the two terms proportionate to n and n^2 related to first and second order kinetics respectively Chen et al. (1981).

In order to obtain analytical expression of intensity for MOK model, we use $I = -\frac{dm}{dt} \simeq -\frac{dn}{dt}$ and the final expression of TL intensity is given by (Kitis et al., 2019)

$$I(t) = gM^2\frac{\alpha F(t) s\exp\left(-\frac{E}{kT}\right)}{[F(t)-\alpha]^2} \tag{1.2.45}$$

Here the parameters are:

- $\alpha = \dfrac{n_0}{n_0 + M}$
- n_0 is the initial concentration of trapped electron at t=0
- $g = \frac{1}{N_1 + N_d}$
- N_1 = concentration total active traps and
- N_d = concentration total TDDT and
- $F(t) = \exp(gM \int_0^t exp(-\frac{E}{kT})dt)$

The above Eq. (1.2.45) have been applied successfully to simulated luminescence signals, as well as to address wide variety of experimental data (Gomez-Ros and Kitis, 2002; Kitis and Gomez-Ros, 2000; Yossian and Horowitz, 1997).

The peak maximum condition in MOK model is written as

$$\frac{\beta E}{kT_m^2} = \left[N_d g \frac{F_m - \alpha}{F_m + \alpha} \right] s e^{-\frac{E}{kT_m}} \tag{1.2.46}$$

Here F_m is the value of $F(t)$ at $T = T_m$.

Transformed analytical solution

Considering the peak maxima condition (Eq. 1.2.46), the MOK equation (Eq. 1.2.45) is transformed in terms of (T_m, I_m) and can be written as (Kitis and Gomez-Ros, 2000)

$$I(T) = I_m \exp\left(\frac{E(T - T_m)}{kTT_m}\right) \frac{[F(T_m) - \alpha]^2}{F(T_m)} \frac{F(T)}{[F(T) - \alpha]^2} \tag{1.2.47}$$

$$\text{Here } F(T) = \exp\left[\frac{1}{f_{MOK}} \left(\frac{T}{T_m}\right)^2 \exp\left(\frac{E(T - T_m)}{kTT_m}\right) \left(1 - \frac{2kT}{E}\right)\right] \tag{1.2.48}$$

$$\text{and } f_{MOK} = \frac{2.6 - 0.9203\alpha + 0.324\alpha^{3.338}}{2.6 - 2.9203\alpha + 0.324\alpha^{3.338}} \tag{1.2.49}$$

1.2.8 Simple localized transition model

Different versions of localized transition models have been proposed over the years (Bull, 1989; Mandowski, 2004; Pagonis, 2005; Pagonis et al., 2017; Templer, 1986). Simple localized transition model (SLT) (Kitis and Pagonis, 2018) is the simplest among all these. The preconceived notion of these model is that the transition probability between excited state of trap and recombination center is constant. In SLT model, During heating stage the trapped electrons raise to excited state of trap and subsequently recombine at recombination center

or it may recapture by ground state of trap (Jain et al., 2012; Kitis et al., 2019). The luminescent signal is yielded through the transition between localized energy levels only.

1.2.9 Tunneling localized transition model

In explaining the experimental observation like anomalous fading of luminescent signal reveals time dependent electronic transition probability between trap state and recombination center (Visocekas, 1985, 1988; Visocekas et al., 1994). The corresponding TL process described through Tunneling localized transition (TLT) model where quantum mechanical tunneling between ground state of trap and luminescent center is considered (Jain et al., 2012; Kitis and Pagonis, 2013; Kitis et al., 2019).

1.3 Methods of analysis.

The theoretical mechanism behind the TL process discussed above is related only to electrons trapped at a single trap level. However, in real phosphors, many different trap levels are usually present, each one due to a particular lattice defect or complex of defects. Each trap level gives rise to an associated glow peak maximum, which may or may not be resolved during readout. Hence a complex glow curve comprising of several peaks is obtained during TL read out. It is common that the values of trap depths for the same material obtained by different methods are found to be somewhat different from one another. Discrepancies in the results are observed when the same material from different origin, is used for the measurement of trapping parameters. Thus TL glow curve analysis itself is quite a complex job and involves lot of intricacies and uncertainties. One single method for glow curve analysis is not applicable for all material as because each material exhibits glow curve of different nature. Based on the shape and nature of complex glow curves a suitable method for glow curve analysis is adopted. Number of methods have been developed for glow curve analysis to determine trapping parameters. For developing different methods it is very important to have analytical expressions of TL intensity. Because these equations are used to compare directly with the experimental data, whether they consist of a single component or of multiple components. The advantage of using analytical equations is that it retains all the properties inherent to the system of differential equations related to the concerned model. For this reason, almost all the methods are developed on the basis of the TL expression obtained by FOK or GOK model. However, with the huge advantage in computational techniques, several attempts have been made where glow curve simulations are done in other models also. Software packages for computer based glow curve analysis are being developed where

different expressions are used to fit TL curves (Peng et al., 2016, 2021).

In glow curve analysis (GCA) different methodologies are used to estimate trapping parameters like activation energy (E), frequency factor (s). Various methods those have been developed over the years for glow curve analysis which may broadly be listed as (Chen, 1974; Chen and Kirsh, 1981a; Shalgaonkar and Narlikar, 1972; Sunta, 2014):

(i) Empirical method (Urbach, 1930)

(ii) Initial rise method (Garlick and Gibson, 1948; Halperin et al., 1960; Ilich, 1979; Nahum and Halperin, 1963)

(iii) Variable heating rate method (Bohun, 1954)

(iv) Peak shape methods (Chen, 1969a,b)

(v) Area method (Kirsh, 1992; Rasheedy, 1993)

(vi) Numerical curve fitting method (Shenker and Chen, 1971)

(vii) Computerized glow curve deconvolution (Peng et al., 2021)

In the following section, a brief account of various methods for determination of E, s and b from a TL glow curve is presented.

1.3.1 Empirical Methods

At the very early stage of TL studies, researchers tried to estimate the activation energy in an empirical way. The attempt was made to determine a relationship between the trap depth (E) related to the location (T_m) of a peak. Assuming the frequency factor to be same for all the peaks related to a TL sample, Urbach (1930) proposed the first empirical formula for the determination activation energy in case of the glow peak obtained from KCl crystal. The empirical relation is given by

$$E = \frac{T_m}{500} \tag{1.3.1}$$

This can also be written in an alternate form as $23kT_m$. Here k is the Boltzmann constant measured in eV/K. E is measured in eV and T_m in Kelvin. Similar relations have also been proposed to describe TL peak of different materials. For TL peak of NaCl, Halperin and Braner (1960) proposed $E = 38kT_m$, Miller and Bube (1970) gave $E = 39kT_m$ for glow peak of LiF *etc.* In case of the relation proposed by Urbach (1930), Chen (1969b) showed that

depending on the value of s, the error in estimating the pre-multiplicative factor to kT_m, may go by a factor of 2. Later on, from the proposition of Randall and Wilkins (1945a), a relation $E = kT_m \ln(s)$ was obtained which was similar to Eq. 1.3.1 for some particular value of s.

1.3.2 Initial rise (IR) method

The method was originally proposed by Garlick and Gibson (1948) where they considered the initial rising portion of glow intensity at the rising side of a glow peak such that $I \leq 0.15 I_m$ (Hagebeuk and Kivits, 1976). Around the initial temperature of heating, the glow intensity exhibits a linear relationship with $\frac{E}{kT_m}$ which is written by

$$I(T) \propto \exp\left(-\frac{E}{kT}\right). \tag{1.3.2}$$

Therefore a plot between $\ln(I)$ *vs* $\frac{1}{T}$ will yield a straight line while its gradient is $-\frac{E}{k}$. By measuring the slope of the straight line, E can be estimated directly

Later, during analyzing the TL signal in different alkaline halides Halperin and Braner (1960) suggested a modification to this method. They proposed a plot of $\ln \frac{I}{n^b}$ vs. $\frac{1}{T}$ to obtain the slope of the straight line if b is known beforehand. In this case also, the slope will be given by $\left(-\frac{E}{k}\right)$ from which E can be estimated easily.

Ilich method

Another version of the IR method was proposed by Ilich (1979). In this method, a particular point (I_i, T_i) is considered which lies within the initial rise range of glow intensity. E is measured by drawin a tangent to that point.

1.3.3 Various Heating Rates (VHR) method

The nature of glow peak very much depends on the rate of heating. Peak location for a glow curve changes as heating rate (β) changes. Exploiting this feature Bohun (1954) proposed a methodology to determine E in case of a first order glow peak. If a TL sample exhibits glow peaks with peak maximum at T_{m1} and T_{m2} corresponding to linear heating rates β_1

and β_2 respectively, then E may be expressed as

$$E = k\frac{T_{m1}T_{m2}}{T_{m1}-T_{m2}}\ln\left[\frac{\beta_1}{\beta_2}\left(\frac{T_{m2}}{T_{m1}}\right)^2\right] \tag{1.3.3}$$

Hoogenstraaten (1958) proposed a method where glow peak is generated for different linear heating rates. Thereafter a straight line can be obtained by plotting $\ln\frac{T_m^2}{\beta}$ vs. $\frac{1}{T_m}$. the slope of the straight line is $\left(\frac{E}{k}\right)$ and intercept $\ln\left(\frac{E}{sk}\right)$.

Using GOK equation (Eq. 1.2.10) Chen and Winer (1970) suggested a plot of $\ln\left[I_m^{(b-1)}\left(\frac{T_m^2}{\beta}\right)^b\right]$ against $\frac{1}{T_m}$. The slope of the straight line is $\left(\frac{E}{k}\right)$ from which E can be estimated easily.

By considering the approximated relation, $I_m \propto \exp\left(-\frac{E}{kT_m}\right)$ suggested by Chen and Winer (1970), a relation to estimate the activation energy was given by Pagonis et al. (2006) as

$$E = k\frac{T_{m1}T_{m2}}{T_{m1}-T_{m2}}ln\frac{I_{m1}}{I_{m2}} \tag{1.3.4}$$

1.3.4 Peak Shape method

Peak shape method is one of the popular methods where various shape and symmetry parameters of a well isolated single glow peak are used to determine the activation energy. In this dissertation we have performed in depth investigation on different versions of peak shape method. Detailed description of this method along with an account of earlier works have been given in later chapters.

1.3.5 Area method

In an experimental scenario a complex glow curve is obtained on heating a TL material. This experimental glow curve generally consists of several component glow peaks. Each of the peaks is related to different trap level lying in the forbidden energy gap between conduction and valence band in a TL material. These trap levels are characterized by their respective set of trapping parameters which govern the nature of their glow curves. Hence different features of glow peaks are correlated with different trapping parameters. Area of the glow peak is one of such features containing information regarding the activation energy of the trap associated to the peak.

Theoretically the phenomenon of thermoluminescence can be understood by describing a trap as a potential box. Considering the trapped electrons following Maxwell-Boltzmann distribution, the escape probability (p) of an electron out of a trap at temperature T is given by

$$p \propto e^{-\frac{E}{kT}}$$
$$\text{Hence, } p = se^{-\frac{E}{kT}}$$

The pre exponential factor 's' is known as frequency factor which is an important trapping parameter. If n is the concentration of trapped electrons at temperature T, then due to thermal stimulation on linear heating, the rate of detrapping of trapped electrons is given by;

$$\frac{dn}{dT} = -\frac{ns}{\beta}e^{-\frac{E}{kT}}$$
$$\text{Hence } \quad n = -\int \frac{s}{\beta}e^{-\frac{E}{kT}}dT \tag{1.3.5}$$

Here β is linear heating rate. The intensity of glow obtained on heating a TL material is proportionate to the rate of reaching the trapped electrons to the luminescent center after being liberated from trap. Hence,

$$I \quad \propto \quad \frac{dn}{dT}$$
$$i.e. \quad n \quad \propto \quad \int_{T}^{T_e} I(T)dT \tag{1.3.6}$$

From Eq. (1.3.6) it is evident that the number of trapped electrons at temperature T can be estimated by calculating the partial area under the glow curve in between the range T to T_e (Fig. 4.4.4). Here T_e being the end temperature of heating. From Eqs. (1.3.5) and (1.3.6) it is well understood that area under the glow curve can be exploited to estimate the trapping parameters since they are related to each other.

Different methodologies have been reported in literature which explore the area under the glow peak to estimate trapping parameters . The methods are broadly named as area method. The area under the glow curve reflects the instantaneous concentration of trapped electrons and is estimated through the area integral (Chen and Mckeever, 1997)

given by

$$n(T) = \frac{1}{\beta}\int_{T_0}^{T_e} I(T)dT \tag{1.3.7}$$

where β is the heating rate, T_0 is the starting temperature and T_e is the end-point temperature where TL intensity falls to zero. By partitioning the integral in different suitable temperature intervals, a straight line may be obtained by plotting $\ln\left[\frac{I}{n(T)}\right]$ against $\frac{1}{T}$ for first order kinetics. The activation energy (E) and an estimation of frequency factor (s) may be obtained from the slope and the intercept respectively (Halperin and Braner, 1960). For general order kinetics similar linear relation is obtained between $\ln\left(\frac{I}{n^b}\right)$ and $\frac{1}{T}$ when the best value of order of kinetics (b) is chosen (Muntoni et al., 1968). Moharil (1981), proposed an alternative method using GOK model to evaluate trapping parameters considering temperature dependent frequency factor where prior knowledge of the order of kinetics is not needed. Using the idea of Moharil's method (Moharil, 1981), Rasheedy (1996) reported a method for estimating trapping parameters for a complex TL glow curve consists of several peaks. Kirsh (1992) considered the linear correlation between $\frac{\Delta \ln I}{\Delta \ln\left(\frac{n}{N}\right)}$ and $\frac{\Delta\left(\frac{1}{T}\right)}{\Delta \ln\left(\frac{n}{N}\right)}$ to obtain E and b simultaneously, n and n_0 being the instantaneous and initial concentration of trapped electrons respectively. Recently a new method namely the 'Three point area (TPA)' method has been proposed. The method is reported to be capable of determining E and b simultaneously from a single (or well isolated) TL peak. In the following chapter the kirsh method and three point area method have been discussed in detail.

1.3.6 Numerical Curve Fitting method

In this method an experimentally obtained TL glow peak is fitted with suitable choice of theoretical expression of TL peak. The goodness of fit is quantified very often by Figure of Merit (FOM) (Balian and Eddy, 1977). Fitting is considered to be acceptable if the value of FOM $< 2.3\%$ (Gartia and Singh, 2011). Different fitting algorithms like least square fit (Mohan and Chen, 1970; Shenker and Chen, 1971) is adopted to fit a glow curve.

1.3.7 Computerized Glow Curve Deconvolution (CGCD)

Nowadays lot of effort has been devoted to analyze an experimentally obtained complex glow peak by using efficient algorithm. A complex glow peak generally comprises of a number of component peaks which may always not be well identifiable. Through CGCD, a complex glow peak is replicated by decomposing it into individual peaks through iterative process using a computer based software programme (Bos et al., 1993, 1994; Yossian and Horowitz, 1995). The availability of powerful computers and the emergence of advanced hardware techniques have led to a significant development in several software programs for GCA (Peng et al., 2021). Several programs that run on commercial software packages have been developed. An important step in establishing deconvolution as a reliable research tool was the GLOCANIN project by Bos *et al.*(Bos et al., 1993, 1994) which is an intercomparison of glow curve analysis programs. One of the widely used deconvolution software currently available is the 'GCA' program developed by CIEMAT (Delgado and Ros, 2001). A computer program, 'GlowFit' for CGCD based on first-order kinetics has been developed by Puchalska and Bilski (2006). A software 'PeakFit' has been developed (Singh et al., 2011) by a group of researcher at Manipur University, India in 2011. An open source R package 'tgcd' has been developed by Peng et al. (2016). In this package different shape parameters and resolution parameters are calculated according to the peak shape method by considering the geometrical properties of a glow peak (Halperin and Braner, 1960).

1.4 Scope of the present study

A thorough review of TL literature reveals that the phenomenological theories of thermoluminescence are sometimes subject to few approximated approaches. It is possible to improve the present theories in analytical methods on the backdrop of various approximated approaches. In TL study GCA is a widely used technique. As mentioned earlier, in an experimental scenario GCA is quite critical and even misleading sometimes. Hence multiple methods depending on the nature of glow curves are needed to verify the consistency of results. Number of methods have been developed over the years and critical analysis of existing methodologies for their improvement is important. At the same time, to explore the possibilities of new methods of TL analysis as well as gross study of recently proposed methods are always essential. Since GCA is primarily based on data analysis, it can be a highly potential and novel way to look forward towards the development methodologies by exploring the science of data from the aspect of statistical distribution. We aim to propose new methodologies using statistical approach which may provide a fresh view of the field.

In the theoretical study of thermally stimulated processes including TL, the prerequisite of mathematical procedure is the evaluation of the integral of the form $J = \int_{T_i}^{T_f} T^a e^{-\frac{E}{kT}} dT$, when the frequency factor is assumed to be temperature independent. However if temperature dependence of frequency factor is considered then the integral becomes $J = \int_0^{T_f} T^a e^{-\frac{E}{kT}} dT$. where a lies between -2 and 2. It is remarkable that the innocent integral cannot be evaluated analytically in a closed form and hence, a few approximated methods were adopted by researchers for the evaluation of the integral. In the present study we have developed a new analytical method to evaluate the temperature integral using converging infinite series and described in this chapter. The present method is not subject to any approximation, only the converging infinite series is to be truncated after considering suitable number of terms depending on the requirement of the accuracy. Moreover the evaluation can be computationally realized in a simple manner through a simple computer code.

Two versions of new peak shape relations for GCA on the basis of two newly introduced symmetry parameters namely average symmetry factor ($< \mu' g >$) and skewness (S_k). The applicability and limitations of both the methods are verified by applying them to various types of simulated and experimental TL peaks. The reason behind the limitation is also explained by investigating the dependence of S_k and μ'_g and on the ratio of retrapping to recombination probabilities. The present peak shape methods are compared with other methods for further establishing their applicability.

Frequency factor related to a trap state slowly varies with temperature. However in TL study it is usually assumed as a temperature independent quantity. MOreover, most of the methodologies developed for glow curve analysis have assumed that frequency factor to be the temperature independent. Such assumption may introduce some limitations in estimating trapping parameters. In this work, impact of temperature dependence of frequency factor on glow curve analysis is studied. The mathematical prerequisite of the study has been developed analytically and hence a successful methodology to simulate the same glow peak for different types of temperature dependence of frequency factor has been discussed. TL equations in OTOR model considering temperature dependent frequency factor (TDFF) has been solved and analytical expression to estimate the peak maxima condition is developed using Lambert-W function and Wright ω function. TDFF in GCA is investigated by adopting different versions of 'peak shape' methods and 'area' methods. In area method, a recently developed method known as 'Three Point Are' method has been adopted along with the existing method due to kirsh. The applicability of this method has been extensively studied by using it into various simulated and experimental glow peaks

along with systematic error analysis before applying it on the GCA of TL peaks considering TDFF.

The challenge in GCA of an experimentally obtained complex glow curve is to isolate and analyze its component peaks. Glow curve deconvolution (GCD) is a potential method for this purpose. In this study we attempt to develop a new GCD function on the basis of statistical distribution of data. At first we adopted Gaussian distribution as a starting ground to proceed further in this direction. the suitability of Gaussian distribution in GCD have been critically examined, however the results are not found to be satisfactory. Looking into the skewed nature of TL glow curve, we have tried a version of skew-normal distribution characterized by five parameters. For initial guess as the inputs of the iterative process some of the parameters are taken from a Gaussian fit of TL data which is done prior to the application of proposed skew-normal distribution function. We investigate the suitability of this new probability function and apply it to large number of TL glow curves simulated in OTOR and GOK model. As a pilot investigation we have considered the TL curves which are equivalent to first and second order kinetics. The quality of fitting is judged through residue plots as well as through the correlation between the TL data and fitted data.

Chapter 2

Evaluation of the temperature integral

2.1 Introduction to temperature integral

In theoretical study of different types of non isothermal kinetic reactions and different thermally stimulated processes like thermoluminescence, thermally stimulated conductivity, thermally stimulated electron emission, thermally stimulated depolarization, thermogravimetry, differential thermal analysis *etc,* the necessary mathematical procedure always involves the integral.

$$J(a, T_i, T_f) = \int_{T_i}^{T_f} T^a \exp\left(-\frac{E}{kT}\right) dT. \tag{2.1.1}$$

The origin of the above integral is embedded in the underlying mechanism during thermal stimulation.

In thermoluminescence, the electrons, those were trapped due to previous irradiation, become liberated on thermal stimulation in heating stage. The detrapping process is evidently random in nature and of course a quantum mechanical phenomenon. However, phenomenologically, the escape probability that a trapped electron will be freed in one second is obtained from Arrhenius law and given by.

$$p = s \exp\left(-\frac{E}{kT}\right) \tag{2.1.2}$$

the symbols have their usual meaning as mentioned earlier in this dissertation. This particular nature of probability is the origin of the integral in Eq. (2.1.1). It is to mention that this nature of escape probability is also observed to govern different thermal characteristics like diffusion coefficients, reciprocals of correlation times in dielectric, magnetic and viscoelastic relaxation, electronic and ionic mobilities, rates of internal rotation around chemical bonds *etc.* In Eq. (2.1.2), 's' is the frequency factor. Gibbs (1972) further studied and mentioned it's weak dependence on temperature. Later on, this temperature dependence is also observed experimentally and mathematically as well. It is grossly expressed as

$$s = s_0 T^a \tag{2.1.3}$$

The value of a is usually integer or half integer and reported to lie within the range of $-2 \leq a \leq 2$.

In TL study, due to theoretical as well as experimental intricacies, frequency factor is usually treated to be temperature independent (*i.e.* $a = 0$). Under this purview, the

integral in Eq. (2.1.1) takes the form

$$J(T_i, T_f) = \int_{T_i}^{T_f} \exp\left(-\frac{E}{kT}\right) dT. \tag{2.1.4}$$

Therefore to carry out any theoretical study involving thermally stimulated processes, it is a prerequisite to have a methodology for the evaluation of the integrals in Eq. (2.1.1) and (2.1.4).

In TL analysis, to carry out the theoretical study using temperature independent frequency factor, the integral in Eq. (2.1.4) arises and we call it as 'temperature integral'. In case of temperature dependent frequency factor the mathematical procedure involves the integral of Eq. (2.1.1), which is named as 'extended temperature integral'. Thus to to carry out the present study, it is inevitable to adopt a proper methodology for the evaluation of the temperature integral or the extended temperature integral. However the innocent looking integrals can not evaluated analytically in a closed form. Various attempts have been made earlier to have an approximated and lucid expression for the retrieval of the value of the integral. Here we present a brief account of the previous works and then elaborate on the present methodology of evaluation of these integrals.

2.2 Brief account of earlier works

Before we proceed, let us look towards the extended temperature integral. It can be easily evaluated in a closed analytical form for $a = -2$ and given by,

$$J(-2, T_i, T_f) = \frac{k}{E} \exp\left(-\frac{E}{kT}\right) \tag{2.2.1}$$

The usual case in TL study is due to $a = 0$ and for which the extended temperature integral reduces to the temperature integral *i.e.*

$$J(T_i, T_f) = \int_{T_i}^{T_f} \exp\left(-\frac{E}{kT} dT\right) \tag{2.2.2}$$

$J(T_i, T_f)$ can be written as

$$J(T_i, T_f) \quad = \quad J(0, T_f) - J(0, T_i) \tag{2.2.3}$$

Since $J(T_i, T_f)$ is a very strongly increasing function of T and T_i, T_f are not very close to each other, $J(0, T_i)$ can be neglected fairly in comparison to $J(0, T_f)$ and $J(T_i, T_f)$ can be

approximated as

$$J(T_i, T_f) = \int_{T_i}^{T_f} e^{-\frac{E}{kT}} dT \simeq J(0, T_i) = \int_{0}^{T_f} e^{-\frac{E}{kT}} dT \tag{2.2.4}$$

Grossweiner (1953) and Haake (1957) attempted the integral through repeated integration by parts and the expression can be approximated in a compact form as (Chen, 1969c)

$$\begin{aligned} J(T_i, T_f) &= \int_{T_i}^{T_f} e^{-\frac{E}{kT}} dT \simeq \int_{0}^{T_f} e^{-\frac{E}{kT}} dT \\ &= T_f e^{-\frac{E}{kT_f}} \sum_{r=1}^{\infty} \left(\frac{kT_f}{E}\right)^r (-1)^{r-1} r! \end{aligned} \tag{2.2.5}$$

The series in the above expression is actually a divergent series (Chen, 1969c), However it can return a good approximation for the integral. Chen (1969c) has also given an account of possible error in evaluating the integral. For example, for $\frac{E}{kT} \simeq 10$, the possible relative error would be about 2×10^{-3} if 10 terms in the series is considered. The error becomes smaller rapidly as value of $\frac{E}{kT}$ increases. For $\frac{E}{kT} \simeq 20$, the possible relative error becomes about 10^{-7} on considering 20 terms in the series.

Biegen and Czanderna (1972) gave a further approximated expression in terms of exponential integral function which is expressed as

$$J(T_i, T_f) = T_f \exp\left(-\frac{E}{kT_f}\right) + \frac{E}{k} E_i\left(-\frac{E}{kT_f}\right) \tag{2.2.6}$$

where $-E_i(-x) = \int_x^{\infty} \frac{e^{-z}}{z} dz$ is the well known exponential integral function (Abramowitz and Stegun, 1972). They have also mentioned about an idea of error occurred during evaluating the integral. For $\frac{E}{kT} \simeq 10$, the possible relative error is about 3.6×10^{-5} while for $\frac{E}{kT} \simeq 15$ it is around 4.5×10^{-7}.

Chen (1970) extended this procedure to the extended temperature integral (Eq. 2.1.1) which is valid when a is an integer and $a \geq -2$ and can be expressed as

$$J(a, E, T_i, T_f) = \frac{kT^{a+2}}{E}\left[1 - \frac{1}{\Gamma(a+2)} \sum_{n=2} (-1)^{n-1} \Gamma(a+n+1)\right] \exp\left(-\frac{E}{kT}\right) \tag{2.2.7}$$

Here $\Gamma(y)$ is the gamma function of y. Petty et al. (1977) made further improvement of equation (2.2.7) for $a < -2$ (Chen and Kirsh, 1981b; Petty et al., 1977) which is given by

$$J(a, E, T_i, T_f) = \left(\frac{k}{E}\right)^{(|a|-1)} (a-2)! \left[\sum_{n=0}^{|a|-2} \frac{(-\frac{E}{kT})^n}{n!}\right] \exp\left(-\frac{E}{kT}\right) \tag{2.2.8}$$

Keating (1961) gave an approximated formula for the extended temperature integral by an asymptotic series which involved $\sim 3\%$ error in estimating the integral and the expression is given by

$$J(a, E, T_i, T_f) \simeq \frac{kT^{a+2}}{E}\left[1 - (a+2)\frac{kT}{E}\right] \exp\left(-\frac{E}{kT}\right) \tag{2.2.9}$$

Gorbachev (Chen and Kirsh, 1981b; Gorbachev, 1976) presented another approximated solution to the temperature integral which can be written as

$$J(a, E, T_i, T_f) \simeq \left[\frac{kT^2}{(E+2)kT}\right] \exp\left(-\frac{E}{kT}\right) \tag{2.2.10}$$

Gorbachev (1976) further extended this procedure to yield an expression to the extended temperature integral which is given as

$$J(a, E, T_i, T_f) \simeq \left[\frac{kT^{a+2}}{E + (a+2)kT}\right] \exp\left(-\frac{E}{kT}\right) \tag{2.2.11}$$

Though the expression in Eq. (2.2.11) is easier to use but yields limited accuracy (Chen and Kirsh, 1981b). Balian and Eddy (1977) proposed an improved approximation for the temperature integral given by

$$J(T_i, T_f) = \left[\frac{kT^2}{E\sqrt{1 + \frac{4kT}{E}}}\right] \exp\left(-\frac{E}{kT}\right) \tag{2.2.12}$$

In a later work Balarin (1985) presented an account where the extended temperature integral was examined as a part of solution of a differential equation while the solution of the differential equation was discussed through different approximation like semiconvergent polynomial approximation, rational approximation, semi empirical approximation *etc.*

Christodoulides (1985) proposed another useful approximation using second exponential integrals to evaluate $J(T_i, T_f)$ as

$$J(T_i,T_f) = \int_{T_i}^{T_f} e^{-\frac{E}{kT}} dT \simeq \int_{0}^{T_f} e^{-\frac{E}{kT}} dT = -\frac{E}{k}\int_{u_f}^{\infty} \frac{e^{-u}}{u^2} du = \frac{E}{k}\frac{E_2(u_f)}{u_f} \tag{2.2.13}$$

where $\frac{E}{kT} = u$, $\frac{E}{kT_f} = u_f$ and the second exponential integral can be written as $E_2(u_f) = u_f \int_{u_f}^{\infty} \frac{e^{-u}}{u^2} du$.

Gartia et al. (1992) extended the approach of christodoulides to evaluate the extended temperature integral which is given by

$$\begin{aligned} J(a,T_i,T_f) &= \int_{T_i}^{T_f} T^a e^{-\frac{E}{kT}} dT \simeq \int_{0}^{T_f} T^a e^{-\frac{E}{kT}} dT \\ &= \left(\frac{E}{k}\right)^{a+1} \int_{u_f}^{\infty} u^{-(a+2)} e^{-u} du \\ &= \left(\frac{E}{k}\right)^{a+1} \frac{E_{a+2}(u_f)}{(u_f)^{a+1}} \end{aligned} \tag{2.2.14}$$

where $\frac{E}{kT} = u$ and $\frac{E}{kT_f} = u_f$ and the exponential integral, $E_{a+2}(u_f) = u_f^{a+1} \int_{u_f}^{\infty} \frac{e^{-u}}{u^{(a+2)}} du$
In an another attempt Gartia et al. (1992) presented a different way for the evaluation of extended temperature integral using complementary incomplete gamma function written as $\Gamma(a,x) = \int_{x}^{infy} e^{-t} t^{a-1} dt$. The expressions are given by,

- For integer value of a while $a \geq -1$:

$$J(a,T_i,T_f) = \left(\frac{E}{k}\right)^{a+1} \Gamma(-a-1,u) \tag{2.2.15}$$

- When a is a positive or negative half integer *i.e.* $a = m + \frac{1}{2}$, where m is a positive or negative integer:

$$J(a,T_i,T_f) = \left(\frac{E}{k}\right)^{m+\frac{3}{2}} \Gamma(-m-\frac{3}{2},u) \tag{2.2.16}$$

In a subsequent work Quanyin and Su (1995) considered the temperature integral and written it in terms of a function $P(u)$ as

$$J(T_i,T_f) = \int_{0}^{T_f} e^{-\frac{E}{kT}} dT = \int_{u_f}^{\infty} \frac{e^{-u}}{u^2} du = \frac{E}{k} P(u) \tag{2.2.17}$$

Therefore evaluation of the above integral involves finding an expression for $P(u)$. They mentioned that $P(u)$ is after all an infinite series which is needed to be approximated through appropriate truncation. In the same work Quanyin and Su (1995) provided two expressions for $P(u)$ was prposed as

$$\text{(i)} \quad P(u) = \frac{e^{-u}\left(\frac{1}{u^2}\right)\left(1-\frac{2}{u}\right)}{\left(1-\frac{5.2}{u^2}\right)} \tag{2.2.18}$$

$$\text{(ii)} \quad P(u) = \frac{e^{-u}\left(\frac{1}{u^2}\right)\left(1-\frac{2}{u}\right)}{\left(1-\frac{4.6}{u^2}\right)} \tag{2.2.19}$$

An estimation regarding the accuracy of the method was also reported. Using the expression for $P(u)$ in Eq. (2.2.18) better accuracy was achieved, with a deviation of less than 1% for $u \geq 7$ while the error is below 0.1% while $u \geq 10$. On the other hand the expression for $P(u)$ in Eq. (2.2.19) gave a wider scope of application, with errors less than 1% and 0.1% for $u \geq 4$ and $u \geq 35$ respectively.

It is thus understood that, for theoretical studies in thermoluminescence, one has to adopt one of the approximated ways for evaluating the temperature integral to proceed further. Such approximations will include some inherent deviation in the overall study. The motivation of the present attempt is to evaluate the integral in a more analytical way. The mathematical procedure includes converging series which can be evaluated using a simple computer programme. In the next section we describe the methodology at first for the 'temperature integral' and then for the 'extended temperature integral' is described.

2.3 Evaluation of Temperature integral: $\int_{T_i}^{T_f} e^{-\frac{E}{kT}} dT$

The temperature integral can be written in two parts as

$$J(T_i, T_f) = \int_{T_i}^{T_f} e^{-\frac{E}{kT}}\, dT = J_f - J_i \tag{2.3.1}$$

$$\text{where} \quad J_f = \int_0^{T_f} e^{-\frac{E}{kT}} dT \qquad \text{and} \qquad J_i = \int_0^{T_i} e^{-\frac{E}{kT}}\, dT \tag{2.3.2}$$

Let us consider $\frac{E}{kT} = u$. Hence $T = \frac{E}{ku}$, $dT = -\frac{E}{ku^2}du$. The limits in the integral J_f changes as:

$T = 0$	$u = \infty$
$T = T_f$	$u = \dfrac{E}{kT_f} = u_f$

Therefore, using the parameter u, the integral J_f can be written as

$$J_f = -\int_{\infty}^{u_f} e^{-u}\frac{E}{ku^2}du = \frac{E}{k}\int_{u_f}^{\infty} e^{-u}\frac{1}{u^2}du$$

Integrating by parts we get

$$\begin{aligned} J_f &= \frac{E}{k}\left[e^{-u}\int_{u_f}^{\infty}\frac{1}{u^2}du - \int_{u_f}^{\infty}\frac{d}{du}\left(e^{-u}\right)\int\frac{1}{u^2}du\right] \\ &= \frac{E}{k}\left[\left[e^{-u}\frac{1}{u}\right]_{\infty}^{u_f} + \int_{u_f}^{\infty}\frac{d}{du}\left(e^{-u}\right)\frac{1}{u}du\right] \\ &= \frac{E}{k}\left[\frac{e^{-u_f}}{u_f} - \int_{u_f}^{\infty} e^{-u}\frac{1}{u}du\right] \\ &= \frac{E}{k}\left[\frac{e^{-u_f}}{u_f} - J_1\right] \qquad (2.3.3) \\ \text{where } J_1 &= \int_{u_f}^{\infty}\frac{e^{-u}}{u}du \qquad (2.3.4) \end{aligned}$$

By incorporating another parameter substitution $u - u_f = y$, we have $u = y + u_f$ and $du = dy$. The limit in the integral (Eq. 2.3.4) changes as: when $u = u_f,\ y = 0$ and when $u = \infty,\ y = \infty$. Therefore the integral J_1 can be written as

$$\begin{aligned} J_1 &= \int_0^{\infty}\frac{e^{-y-u_f}}{y+u_f}dy = J_{11} + J_{12} \\ \text{where } J_{11} &= e^{-u_f}\int_0^{u_f}\frac{e^{-y}}{y+u_f}dy \qquad \text{and} \qquad J_{12} = \int_{u_f}^{\infty}\frac{e^{-y-u_f}}{y+u_f}dy \end{aligned}$$

- Using the series expansion of exponential function we write,

$$e^{-y} = \sum_{n_1=0}^{\infty}(-1)^{n_1}\frac{y^{n_1}}{n_1!} \qquad (2.3.5)$$

- Using binomial expansion we get,

$$\frac{1}{y+u_f} = \sum_{k_1=0}^{\infty}(-1)^{k_1}y^{k_1}u_f^{-k_1-1} \qquad (2.3.6)$$

Incorporating the expressions in Eqs. (2.3.5) and (2.3.6), integral J_{11} is now written as

$$\begin{aligned} J_{11} &= e^{-u_f}\int_0^{u_f}\sum_{n_1=0}^{\infty}(-1)^{n_1}\frac{y^{n_1}}{n_1!}\sum_{k_1=0}^{\infty}(-1)^{k_1}y^{k_1}u_f^{-k_1-1}\,dy \\ &= e^{-u_f}\sum_{n_1=0}^{\infty}\sum_{k_1=0}^{\infty}(-1)^{n_1+k_1}\frac{1}{n_1!}\frac{1}{u_f^{k_1+1}}\int_0^{u_f}y^{n_1+k_1}\,dy \\ &= e^{-u_f}\sum_{n_1=0}^{\infty}\sum_{k_1=0}^{\infty}(-1)^{n_1+k_1}\frac{1}{n_1!}\frac{1}{u_f^{k_1+1}}\left[\frac{y^{n_1+k_1+1}}{n_1+k_1+1}\right]_0^{u_f} \\ &= e^{-u_f}\sum_{n_1=0}^{\infty}\sum_{k_1=0}^{\infty}(-1)^{n_1+k_1}\frac{u_f^{n_1}}{n_1!(n_1+k_1+1)} \end{aligned} \tag{2.3.7}$$

We retrieve the variable $u = y + u_f$ in the integral J_{12} . Hence, $du = dy$ and the limit changes as:

$y = u_f$	$u = 2u_f$
$y = \infty$	$u = \infty$

Thus the J_{12} integral takes a remarkable form as

$$J_{12} = \int_{2u_f}^{\infty}\frac{e^{-u}}{u}du \tag{2.3.8}$$

Eqs. (2.3.4) and (2.3.8) show that the integrals J_1 and J_{12} are similar but the lower limit in J_{12} is twice that of J_1. Hence, J_{12} in Eq. (2.3.8) can be expanded in a series similar to that given in Eq. (2.3.7) where u_f is replaced by $2u_f$ plus another integral of the form $\int_{4u_f}^{\infty}\frac{e^{-u}}{u}du$ Fig. (2.3.1).

In this way, a converging infinite series is obtained to express J_f (in Eq. 2.3.3) as

$$\begin{aligned} J_f = \frac{E}{k}\frac{e^{-u_f}}{u_f} \quad - \quad \frac{E}{k}\Bigg[& e^{-u_f}\sum_{n_1=0}^{\infty}\sum_{k_1=0}^{\infty}(-1)^{n_1+k_1}\frac{u_f^{n_1}}{n_1!(n_1+k_1+1)} \\ & + e^{-2u_f}\sum_{n_2=0}^{\infty}\sum_{k_2=0}^{\infty}(-1)^{n_2+k_2}\frac{(2u_f)^{n_2}}{n_2!(n_2+k_2+1)} \\ & + e^{-4u_f}\sum_{n_3=0}^{\infty}\sum_{k_3=0}^{\infty}(-1)^{n_3+k_3}\frac{(4u_f)^{n_3}}{n_3!(n_3+k_3+1)} + \text{higher terms}\Bigg] \end{aligned}$$

$$\text{or} \quad J_f = \frac{E}{k}\frac{e^{-u_f}}{u_f} \quad - \quad \frac{E}{k}\sum_{p=0}^{\infty}\sum_{k_1=0}^{\infty}\sum_{n_1=0}^{\infty}(-1)^{n_1+k_1}e^{(-2^p u_f)}\frac{(2^p u)^{n_1}}{n_1!(n_1+k_1+1)} \tag{2.3.9}$$

It is to mention that the integral J_i in Eq. (2.3.2) is nothing but the same integral as J_f, the only difference is that the upper limit is changed to T_i in place of T_f. Hence the integral J_i is also evaluated in a similar manner and the value is obtained from Eq. (2.3.9) or (2.3.9) where u_f will be replaced by $u_i = \dfrac{E}{kT_i}$ and the final expression for $J(T_i, T_f)$ in Eq. (2.3.1) is obtained.

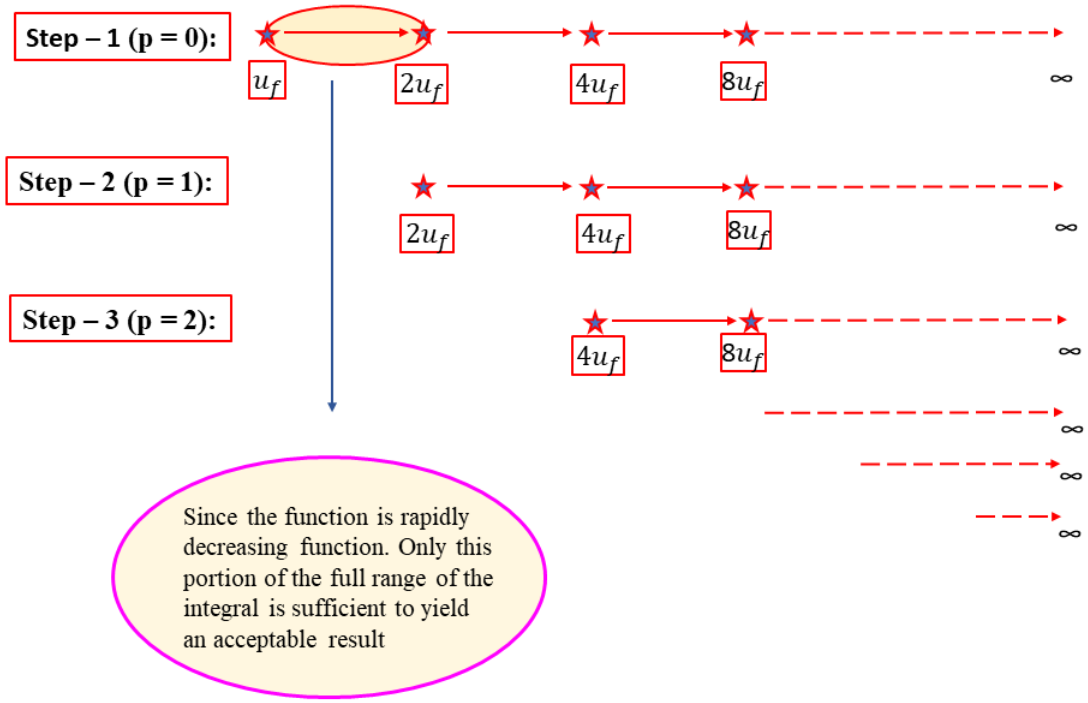

Figure 2.3.1: Schematic diagram describing the procedure to evaluate temperature integral.

2.4 Evaluation of extended temperature integral $\int_{T_i}^{T_f} T^a e^{-\frac{E}{kT}} dT$

In a similar procedure we extend the present methodology further. We describe an expression for the evaluation of the extended temperature integral $\int_{T_i}^{T_f} T^a e^{-\frac{E}{kT}} dT$ in an analytical

approach which does not assume any approximation but involves the truncation of a converging infinite series after a desired level of accuracy is achieved. The method is discussed below. We start as before by writing the integral in two parts,

$$J(a,E,T_i,T_f) = \int_{T_i}^{T_f} T^a e^{-\frac{E}{kT}} dT = J_f(a,E,T_f) - J_i(a,E,T_i) \tag{2.4.1}$$

$$\text{where} \quad J_f = \int_0^{T_f} T^a e^{-\frac{E}{kT}} dT \qquad \text{and} \qquad J_i = \int_0^{T_i} T^a e^{-\frac{E}{kT}} dT$$

We introduce a parameter substitution here. Using the parameter $u = \dfrac{E}{kT}$ as before, the integral J_f can be written as

$$J_f(a,E,T_f) = \left(\frac{E}{k}\right)^{a+1} \int_{u_f}^{\infty} \frac{e^{-u}}{u^{a+2}} du = \left(\frac{E}{k}\right)^{a+1} J_1 \tag{2.4.2}$$

$$\text{where} \quad J_1 = \int_{u_f}^{\infty} \frac{e^{-u}}{u^{a+2}} du \tag{2.4.3}$$

Adopting another transformation by substituting $u - u_f = u_1$, the integral J_1 is written as

$$J_1 = \int_0^{\infty} \frac{e^{-u_f-u_1}}{(u_f+u_1)^{a+2}} du_1 = J_{11} + J_{12} \tag{2.4.4}$$

$$\text{where} \quad J_{11} = e^{-u_f} \int_0^{\frac{u_f}{2}} \frac{e^{-u_1}}{(u_f+u_1)^{a+2}} du_1 \tag{2.4.5}$$

$$\text{and} \quad J_{12} = \int_{\frac{u_f}{2}}^{\infty} \frac{e^{-u_f-u_1}}{(u_f+u_1)^{a+2}} du_1 \tag{2.4.6}$$

From Eq. (2.4.4) we see that J_1 has been decomposed into a finite integral J_{11} and an infinite integral J_{12}.

It can be clearly seen from Eq. (2.4.5) that the integrand in the integral J_{11} is multiplication of two functions namely $(u_f+u_1)^{-(a+2)}$ and an exponential function e^{-u_1}. The function $(u_f+u_1)^{-(a+2)}$ could be expanded in a series using binomial expansion. However it can not be done using usual method, as because, the exponent *i.e.* $[-(a+2)]$ can take any values such as positive and negative integer or fraction.

- If $[-(a+2)]$ is positive then the situation is simple and bionomial expansion can be done using usual formula (Eq. 2.3.6).

- If the exponent $[-(a+2)]$ is fraction or negative integer then it cannot be expressed in terms of usual formula, as factorial of fraction or negative integer is undefined.

To resolve the situation and accommodate all the cases (*i.e.* positive integer, negative integer or fractional value of a) we expand the function $(u_f + u_1)^{-(a+2)}$ in series using bionomial expansion in terms of Pochhammer symbol (Graham et al., 1994) which is schematically expressed as

$$(\alpha)_m = \alpha(\alpha-1)(\alpha-2)...(\alpha-m+1) \tag{2.4.7}$$

Hence the function $(u_f + u_1)^{-(a+2)}$ is expanded in a series using binomial expansion and written as

$$\frac{1}{(u_f+u_1)^{a+2}} = (u_f+u_1)^{-(a+2)} = \sum_{k_1=0}^{\infty} \frac{(-a-2)_{k_1}}{k_1!} u_f^{-(a+2)-k_1} u_1^{k_1} \tag{2.4.8}$$

It is important to mention that for fractional or negative integer values of the exponent $-(a+2)$ in the above Eq. (2.4.8) the condition $u_1 < u_f$ must satisfy for bionomial expansion. For this reason, the upper limit of J_{11} in Eq. (2.4.5) is set to $\frac{u_f}{2}$ in order to facilitate the convergence of the binomial series (2.4.8). Further expressing the exponential function in series as $e^{-u_1} = \sum_{n_1=0}^{\infty} (-1)^{n_1} \frac{(u_1)^{n_1}}{n_1!}$ the integral J_{11} in Eq. (2.4.5) is recast as

$$\begin{aligned} J_{11} &= e^{-u_f} \int_0^{\frac{u_f}{2}} \sum_{n_1=0}^{\infty} (-1)^{n_1} \frac{u_1^{n_1}}{n_1!} \sum_{k_1=0}^{\infty} \frac{(-a-2)_{k_1}}{k_1!} u_f^{-(a+2)-k_1} u_1^{k_1} \, du_1 \\ &= e^{-u_f} \sum_{n_1=0}^{\infty} \sum_{k_1=0}^{\infty} (-1)^{n_1} \frac{(-a-2)_{k_1}}{n_1! k_1!} \frac{2^{-a-2-k_1}}{(n_1+k_1+1)} \left(\frac{u_f}{2}\right)^{n_1-a-1} \end{aligned} \tag{2.4.9}$$

The evaluation of the integral J_{12} (in Eq. 2.4.6) is carried out in a different manner. It is seen that on retrieval of the variable $u = u_f + u_1$, we get $du = du_1$ and the limit in the integral changes as,

$u_1 = \frac{u_f}{2}$	$u = \frac{3u_f}{2}$
$u_1 = \infty$	$u = \infty$

The integral J_{12} (Eq. 2.4.6) then takes a form similar to J_1 as given in Eq. (2.4.3)

except the lower limit and is expressed as

$$J_{12} = \int_{\frac{3u_f}{2}}^{\infty} \frac{e^{-u}}{u^{a+2}} du \tag{2.4.10}$$

The lower limit of the J_1 integral (Eq. 2.4.3) is u_f whereas for the J_{12} integral (Eq. 2.4.10) it becomes $\frac{3u_f}{2}$. Hence, J_{12} in Eq. (2.4.10) can be expanded in a similar manner as described for Eq. (2.4.9) in addition to another integral of the form $\int_{\frac{5u_f}{2}}^{\infty} \frac{e^{-u}}{u^{a+2}} du$ (Fig. 2.4.1). Finally, the integral J_f (2.4.3) is expressed in a converging infinite series as

$$\begin{aligned} J_f = \left(\frac{E}{k}\right)^{a+1} \Bigg[& e^{-u_f} \sum_{n_1=0}^{\infty} \sum_{k_1=0}^{\infty} (-1)^{n_1} \frac{(-a-2)_{k_1}}{n_1! k_1!} \frac{(2)^{-a-2-k_1}}{(n_1+k_1+1)} \left(\frac{u_f}{2}\right)^{n_1-a-1} \\ & + e^{-\frac{3u_f}{2}} \sum_{n_2=0}^{\infty} \sum_{k_2=0}^{\infty} (-1)^{n_2} \frac{(-a-2)_{k_2}}{n_2! k_2!} \frac{(\frac{3}{2})^{-a-2-k_2}}{(n_2+k_2+1)} \left(\frac{2u_f}{2}\right)^{n_2-a-1} \\ & + e^{-\frac{5u_f}{2}} \sum_{n_3=0}^{\infty} \sum_{k_3=0}^{\infty} (-1)^{n_3} \frac{(-a-2)_{k_3}}{n_3! k_3!} \frac{(\frac{5}{2})^{-a-2-k_3}}{(n_3+k_3+1)} \left(\frac{4u_f}{2}\right)^{n_3-a-1} \\ & + \text{higher order terms} \Bigg] \end{aligned}$$

A concise form of the J_f integral of equation (2.3.9) can be written as

$$J_f(a, E, T_f) = \left(\frac{E}{k}\right)^{a+1} \sum_{p=0}^{\infty} \sum_{n=0}^{\infty} \sum_{k=0}^{\infty} e^{-(2^p+1)\frac{u_f}{2}} (-1)^n \frac{(-a-2)_k}{n!k!} \frac{(1+\frac{1}{2^p})^{-a-2-k}}{(n+k+1)} \left(2^p \frac{u_f}{2}\right)^{n-a-1} \tag{2.4.11}$$

2.5 Results and Discussion

The temperature integral

To check the accuracy of the present method we compare the present values of the integral with those obtained from Eqs. (2.2.5) and (2.2.13). The results are displayed in Table 2.5.1 which show excellent agreement.

For evaluation of the integral in Eq. (2.3.9), considering only the $p = 0$ term in the series is enough to have an acceptable value for TL studies. The contribution of the next term with $p = 1$ is 10^{-12} order smaller than the previous sum and hence can be safely ignored. The present method seems to be working over a wide range of values of E and T_f whereas in other methods (Chen, 1969c; Christodoulides, 1985), several limitations were mentioned

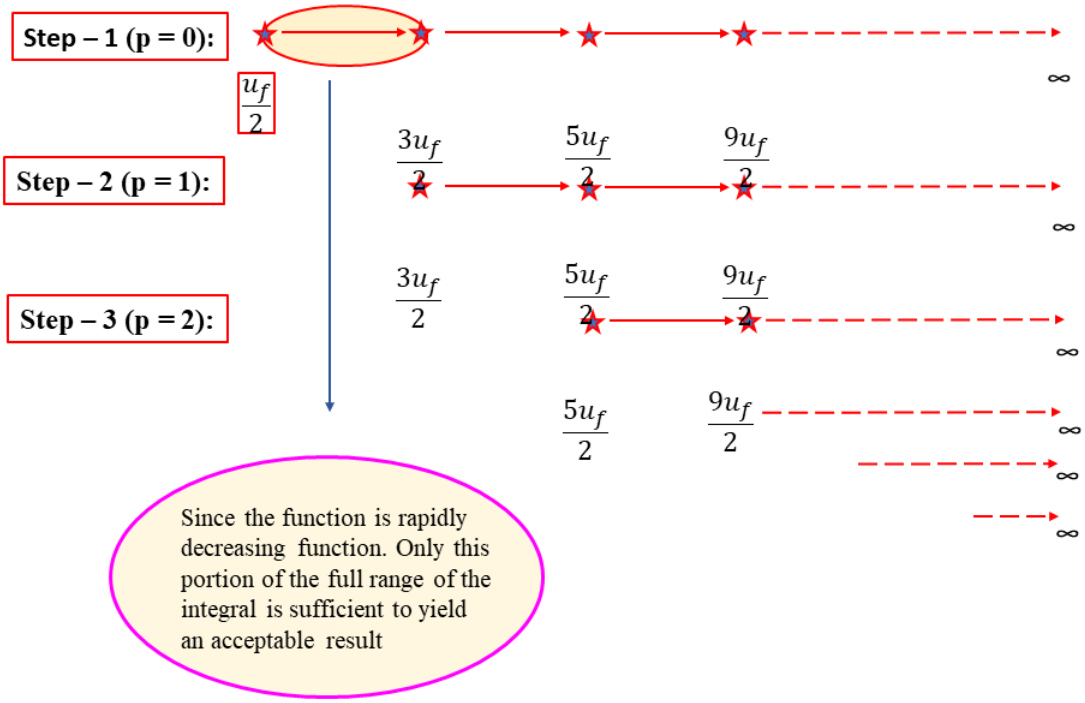

Figure 2.4.1: Schematic diagram describing the procedure to evaluate extended temperature integral.

regarding the accuracy depending on the value of $u_f = \frac{E}{kT_f}$. The series in Eq. (2.3.9) involving only $p = 0$ is found to be working successfully for $u_f < 173$ which covers almost the entire range in practical applications. For higher values of u_f, more terms in the sum over p are to be included. To achieve a desired accuracy, the number of terms required in the sums over k_1 and n_1 in Eq. (2.3.9) may be increased depending on the value of u_f. However, the integral in Eq. (2.3.9) converges almost instantly in a computer with modest hardware for any value of u_f. To ensure numerical accuracy, we have done the calculations in quadruple precision.

The extended temperature integral

We have estimated the extended temperature integral for different sets of parameters and the results are compared with those obtained from some of the other methods available in literature (Chen, 1970; Gorbachev, 1976; Keating, 1961; Petty et al., 1977). The calculations

Table 2.5.1: Values of the temperature integral evaluated from present analytical method (Eq. 2.3.9), Chen's approximation (Eq. 2.2.5) and Christodoulide's method (Eq. 2.2.13).

E (eV)	T_0 (K)	T (K)	Present method	Chen (1969c)	Christodoulides (1985)
1.0	250	400	3.24673×10^{-12}	3.24673×10^{-12}	3.24673×10^{-12}
1.0	250	500	1.65474×10^{-9}	1.65474×10^{-9}	1.65474×10^{-9}
1.0	250	600	1.12392×10^{-7}	1.12392×10^{-7}	1.12392×10^{-7}
1.5	250	400	1.10758×10^{-18}	1.10758×10^{-18}	1.10758×10^{-18}
1.5	250	500	1.03190×10^{-14}	1.03190×10^{-14}	1.03190×10^{-14}
1.5	250	600	4.87009×10^{-12}	4.87008×10^{-12}	4.87009×10^{-12}

are carried out in quadruple precision. The results are displayed in Table 2.5.2 which shows excellent agreement. In Table 2.5.2, we have given the values of the integral for both integer and fractional values of a within the range $-2 \leqslant a \leqslant 2$. However, we have verified that the integral works satisfactorily for other values of a beyond this range. The present results for $a = 0$ are also in excellent agreement with those reported in Table. 2.5.1.

Table 2.5.2: Comparison of the values of the extended temperature integral evaluated in different methods. Results are presented for $E = 1$ eV. Here the notation: $x(y) = x \times 10^y$.

			Value of the integral			
T_i (K)	T_f (K)	a	Present method	Chen (1970)	Keating (1961)	Gorbachev (1976)
0	200	–2.0	5.45108 (–30)	5.45107 (–30)	5.45107 (–30)	5.45107 (–30)
		–1.5	7.64421 (–29)	7.64420 (–29)	7.64255 (–29)	7.64312 (–29)
		0.0	2.10891 (–25)	2.10891 (–25)	2.10527 (–25)	2.10778 (–25)
			2.10891(–25) *			
		1.5	5.82157 (–22)	5.8216 (–22)	5.79517 (–22)	5.81634 (–22)
		2.0	8.16749 (–21)	8.16755 (–21)	8.12045 (–21)	8.15923 (–21)
0	600	–2.0	3.43354 (–13)	3.43354 (–13)	3.43354 (–13)	3.43354 (–13)
		–1.5	8.20801 (–12)	8.20808 (–12)	8.193 (–12)	8.19848 (–12)
		0.0	1.12480 (–7)	1.12504 (–7)	1.10826 (–7)	1.12023 (–7)
			1.12480(–7) *			
		1.5	1.54796 (–3)	1.54995(–3)	1.4879 (–3)	1.53828(–3)
		2.0	3.71277 (–2)	3.72039(–2)	3.52957(–2)	3.68728(–2)

*Present method for $a = 0$ (Eq.2.3.9)

In practical scenario, $J(a, E, T_i, T_f)$ is insensitive to T_i if T_f and T_i are not too close to each other since the integral is a very strongly increasing function of T. Thus

$J_i(a, E, T_i)$ can be ignored comfortably and the final expression for $J(a, E, T_i, T_f)$ equals $J_f(a, E, T_f)$ of Eq. (2.4.11). However, the $J_i(a, E, T_i)$ integral can similarly be evaluated as $J_f(a, E, T_f)$, by replacing T_f with T_i. It has been investigated that only the $p = 0$ term in the series in Eq. (2.4.11) is sufficient to have a value of the extended temperature integral appropriate for TL studies. In that case the integral takes the approximated form as

$$J_f = \int_0^{T_f} T^a e^{-\frac{E}{kT}} dT \simeq \left(\frac{E}{k}\right)^{a+1} e^{-u_f} \sum_{n_1=0}^{\infty} \sum_{k_1=0}^{\infty} (-1)^{n_1} \frac{(-a-2)_{k_1}}{n_1! k_1!} \frac{(2)^{-a-2-k_1}}{(n_1+k_1+1)} \left(\frac{u_f}{2}\right)^{n_1-a-1} \tag{2.5.1}$$

Chapter 3

Development of new peak shape relations and their applications

3.1 Introduction to peak shape method

It is quite remarkable that important information about the trapping parameters and change trafficking mechanism are reflected through the shape of TL glow curve. Since the early days of TL research, the shape of a TL peak has been exploited by researchers to extract the trapping parameters. In present days the peak shape method is one of the most widely used methods for TL glow curve analysis. The method can be applied to estimate activation energy from a well isolated single TL peak. Peak shape method has been developed on the basis of geometrical shape of a glow curve and it icludes different shape and symmetry parameters of glow curves.

3.1.1 The peak shape parameters

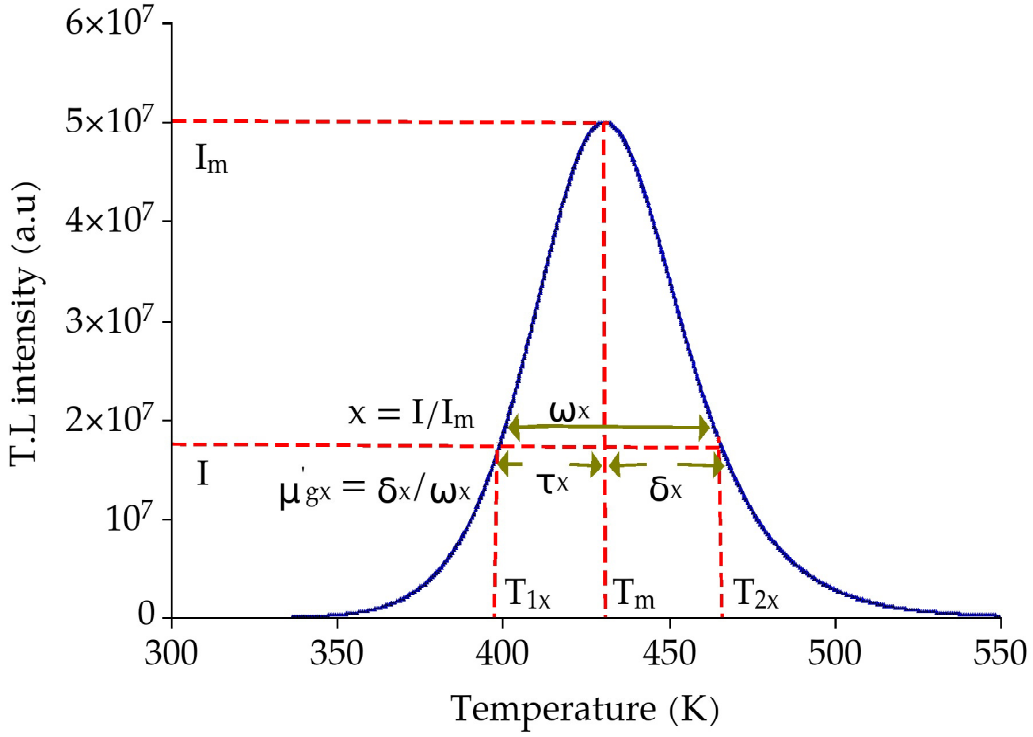

Figure 3.1.1: A sample TL peak showing the peak shape parameters (τ_x, δ_x, ω_x) at arbitrary fractional intensity $x = \frac{I}{I_m}$. For $x = \frac{1}{2}$, τ_x, δ_x, ω_x are denoted by τ, δ, ω respectively.

In peak shape method, shape of a glow curve is taken into account through different shape parameters. In constituting various peak shape relations, the peak temperature or full width at half maximum *etc.* have been used frequently as shape parameters to estimate activation energy (E). However shape parameters at other fractional intensity points are

also in use. A brief account of different peak shape parameters is discussed in following paragraph.

The fractional intensity points on the glow peak can be considered for which $x = \frac{I}{I_m}$. Here I is the intensity at those points of choice and I_m is the maximum intensity of the glow peak. A schematic diagram is given in Fig. 3.1.1 from which the following peak shape parameters can be defined using the temperature at fractional intensity points x.

i) $\tau_x = T_m - T_{1x}$

ii) $\delta_x = T_{2x} - T_m$

iii) $\omega_x = T_{2x} - T_{1x}$

Here T_m is the temperature at maximum intensity, T_{1x} and T_{2x} are the temperatures at which the fractional intensity is x $\left(= \frac{I}{I_m}\right)$ on rising side and falling side of the peak respectively. In different peak shape relations τ_x, δ_x and ω_x have been used to quantify the activation energy.

3.1.2 The symmetry parameters

In peak shape method the systematic variation of shape of glow peak is accounted by considering different symmetry parameters. Different researchers have explored various symmetry parameter to propose their peak shape relations. A brief description of different symmetry parameters are discussed here,

(i) **Geometrical symmetry factor:** The symmetry parameter, geometrical symmetry factor at fractional intensity point x is defined as, $\mu'_{gx} = \frac{\delta_x}{\omega_x} = \frac{T_{2x} - T_m}{T_{2x} - T_{1x}}$. For $x = \frac{1}{2}$, μ'_{gx} is written as μ'_g when $x = \frac{1}{2}$ (Chen, 1969a).

(ii) **Integral symmetry factor:** The integral symmetry factor (μ_i) related to a glow peak is defined as (Kitis et al., 2008)

$$\mu_i = \frac{\int_{T_m}^{T_e} I(T)dT}{\int_{T_0}^{T_e} I(T)dT} \tag{3.1.1}$$

Here the parameters are

- T_0 is the starting temperature of heating

- T_m is the peak temperature
- T_e is the end temperature of heating.

It is to mention that the value of μ_i somehow differs from μ'_g.

(iii) **Order of kinetics:** The empirical parameter, order of kinetics (b) is assigned to a glow peak when it is studied in GOK model, to address its systematic variation of skewed nature. $b = 1$ suggest a left skewed glow peak while $b = 2$ refers to right skewed glow peak. b has been explored as a shape parameter to propose peak shape relation Gartia et al. (1988).

In this work we have tried successfully with two new symmetry parameters: (iv) Average geometrical symmetry factor ($< \mu'_g >$) and (iv) skewness of data (S_k)

3.2 A brief review on Peak Shape method

Peak shape method in TL analysis has been developed as a result of continuous research carried out by different researchers over the years. The first version of peak shape formula was proposed by Grossweiner (1953) to calculate E from a first order TL peak. After incorporating the modification proposed by Dussel and Bube (1967) the formula is expressed as

$$E = 1.41 \left(\frac{kT_m T_1}{\tau} \right) \tag{3.2.1}$$

Here k is the Boltzmann constant, T_m is the peak temperature, T_1 is the half intensity temperature on rising side of the curve and $\tau = T_m - T_1$ is a peak shape parameter at half intensity points (*i.e.* $x = \frac{1}{2}$) (Fig. 3.1.1). Later, Lushchik (1956) gave the peak shape formulae for both first and second order peaks using another peak shape parameter $\delta = T_2 - T_m$ where T_2 is the half intensity temperature on the falling side of the curve (Fig. 3.1.1). The peak shape relations of Lushchik (1956) were modified by Chen (1969b) and can be expressed as

$$\begin{aligned} E &= 0.976 \left(\frac{kT_m^2}{\delta} \right) && \text{for first order} \\ &= 1.71 \left(\frac{kT_m^2}{\delta} \right) && \text{for second order} \end{aligned} \tag{3.2.2}$$

Halperin and Braner (1960) proposed another variant of peak shape relation for first order curves which can be written, after considering the numerical correction suggested by Chen

(1969b), as

$$E = 1.52\left(\frac{kT_m^2}{\tau}\right) - 1.58\,(2kT_m) \tag{3.2.3}$$

In formulating Eq. (3.2.3), the geometrical symmetry factor (μ_g') at half intensity points *i.e.* was used (Fig. 3.1.1). After revisiting all the earlier peak shape formulae (Halperin and Braner, 1960; Lushchik, 1956), Chen (1969a,b) proposed the peak shape relations using τ, δ and ω which can be summarized as

$$E_\alpha = C_\alpha \frac{kT_m^2}{\alpha} - D_\alpha(2kT_m) \tag{3.2.4}$$

Here α stands for the peak shape parameters τ, δ or ω. The peak shape coefficients (C_α, D_α) were estimated numerically and expressed in terms of μ_g' as.

$$C_\tau = 1.51 + 3.0(\mu_g' - 0.42), \qquad D_\tau = 1.58 + 4.2(\mu_g - 0.42) \tag{3.2.5}$$

$$C_\delta = 0.976 + 7.3(\mu_g' - 0.42), \qquad D_\delta = 0 \tag{3.2.6}$$

$$C_\omega = 2.52 + 10.2(\mu_g' - 0.42), \qquad D_\omega = 1 \tag{3.2.7}$$

Instead of the order of kinetics 'b' the above expressions Eq.(3.2.5–3.2.7) involve μ_g' which can be directly estimated from a glow curve. These peak shape relations are result of large number of simulations and linear interpolation-extrapolation technique. The applicability of the above method was examined for a broad range of activation energies starting from 0.1 eV to 1.6 eV (Chen, 1969b) and for values of frequency factor from 10^5 s^{-1} to 10^{13} s^{-1}. Chen (1969b) presented a curve of μ_g' $(0.36 \leq \mu_g' \leq 0.55)$ for values of b $(0.7 \leq b \leq 2.5)$ that may be used to estimate b of an experimental glow curve.

In later decades, several attempts were made to develop different variants of peak shape formula. Christodoulides (1985) proposed an alternative set of peak shape relations of the form

$$E(T_i, T_j) = \frac{T_i T_j}{C(T_i - T_j)} - \frac{T_j}{D} \qquad \text{for first order peaks} \tag{3.2.8}$$

Here the peak shape parameters $(\tau_x, \delta_x, \omega_x)$ were taken at different at fractional intensities $x = 0.25, 0.5, 0.75$. Here T_i, T_j are any two of T_{1x}, T_m and T_{2x} (Fig. 3.1.1) and the coefficients C, D were evaluated numerically (Christodoulides, 1985). In a subsequent work,

Christodoulides (1986a) reported another set of peak shape relations using general order kinetics theory in hyperbolic heating scheme. Mazumdar et al. (1988) further developed the expressions analogous to those of Christodoulides (1985) to extract E from non-first order TL peaks at fractional intensities $x = 0.5, 0.667, 0.8$. Gartia et al. (1988) reported another version of peak shape relations similar to those of Chen (1969a) where the peak shape coefficients were expressed as a quadratic function of b at various fractional intensities. Using the methodology suggested by Gartia et al. (1988), an empirical technique to estimate b in a modified peak shape method was suggested by Singh et al. (2013). Kitis and Pagonis (2007) reforged the peak shape method for general order kinetics where the peak shape coefficients were expressed analytically as a function of b multiplied by some pseudo-constants. In their work, Kitis and Pagonis (2007) made a comprehensive effort to improve the peak shape coefficients and to provide physical insights of them. Due to the accuracy it yields in estimating activation energy, the work of Kitis and Pagonis (2007) has drawn considerable attention among researchers (Karmakar et al., 2017; Singh et al., 2012; Talebi et al., 2019). In a subsequent work Kitis et al. (2008) also attempted an alternative approach to derive a set of peak shape formulas in terms of integral symmetry factor in mixed order kinetics (MOK) model.

3.3 Present development in peak shape method

In this dissertation we have performed an in depth study of existing peak shape methods those have been discussed above. After having proper insight, we thoroughly investigated the methodologies to derive the corresponding peak shape relations. The methodologies have been investigated from different possible perspectives. Finally we develop two new peak shape methods during the present study. The present developments can be classified into two broad categories:

i) Reapprisal of peak shape relations using average symmetry factor.

ii) Development of new peak shape method skewness of data.

3.4 Reapprisal of peak shape relations using average symmetry factor

Despite ample amount of research in developing the peak shape method, the most used formulae in literature is due to Chen (1969a) which is given in Eq. (3.2.5–3.2.7. The nature of symmetry of a TL curve is qualitatively estimated through the order of kinetics

related to a particular single peak. Chen (1969a) made a correspondence between b and directly measurable quantity μ'_g and peak shape coefficients were formulated in terms of μ'_g through numerical interpolation extrapolation technique. During the course of the work Chen assumed that b has only one-to-one dependence with μ'_g. However a little dependence of μ'_g on E and s was also mentioned but it was ignored in the development of the peak shape formula. This study focusses on this issue and examines the impact of the above mentioned dependence on peak shape relations.

It is to mention that the impact of s is reflected through T_m in a TL curve. Hence we considered $u_m = \dfrac{E}{kT_m}$ as a parameter to examine the dependence of μ'_g on E and s. To examine the dependence of μ'_g on u_m (Bhattacharyya and Majumdar, 2018; Gartia et al., 1988) along with b, we have simulated a large number of TL curves in a systematic way. For a fixed value of b, the TL peaks are simulated by taking values of E and s in such a way that u_m lies within the limit $10 \leqslant u_m \leqslant 100$. For a fixed value of b, μ'_{gx} is calculated from simulated TL curves at half intensity points (*i.e.* $x = \dfrac{1}{2}$) corresponding to each u_m value. This process is repeated by varying b in step 0.1 within the range $0.7 \leqslant b \leqslant 2.5$. The variation of μ'_g (*i.e.* μ'_{gx} at $x = 0.5$) with respect to u_m for $1 \leqslant b \leqslant 2$ is presented in Fig. 3.4.1 which shows a clear dependence of μ'_g on b and u_m.

The present procedure enables us to establish an empirical dependence of μ'_g on b and u_m by multi-parameter fitting. For $x = 0.5$, this relation may be written as

$$\mu'_g = -1.52 + 1.85b^{0.127} + \frac{1}{u_m}\left(0.094 + 0.919b - 0.227b^2\right) \tag{3.4.1}$$

Similar relations can be formulated for other fractional intensities.

3.4.1 Modification of Peak Shape coefficients

The dependence of μ'_g on both u_m and b may be realized through the average symmetry factor. We express the geometrical symmetry factor at any arbitrary fractional intensity (x) as

$$\mu'_{gx} = \frac{T_{2x} - T_m}{T_{2x} - T_{1x}} = \frac{(u_m - u_{2x})u_{1x}}{(u_{1x} - u_{2x})u_m} \tag{3.4.2}$$

u_{1x}, u_{2x} are similar to u_m calculated at the temperatures T_{1x}, T_{2x} (Fig. 3.1.1). To establish a one-to-one correspondence between b and μ'_{gx}, we proceed as follows. For a fixed value of b, μ'_{gx} is calculated for TL curves corresponding to various u_m within a range $u_{m_i} < u_m < u_{m_f}$.

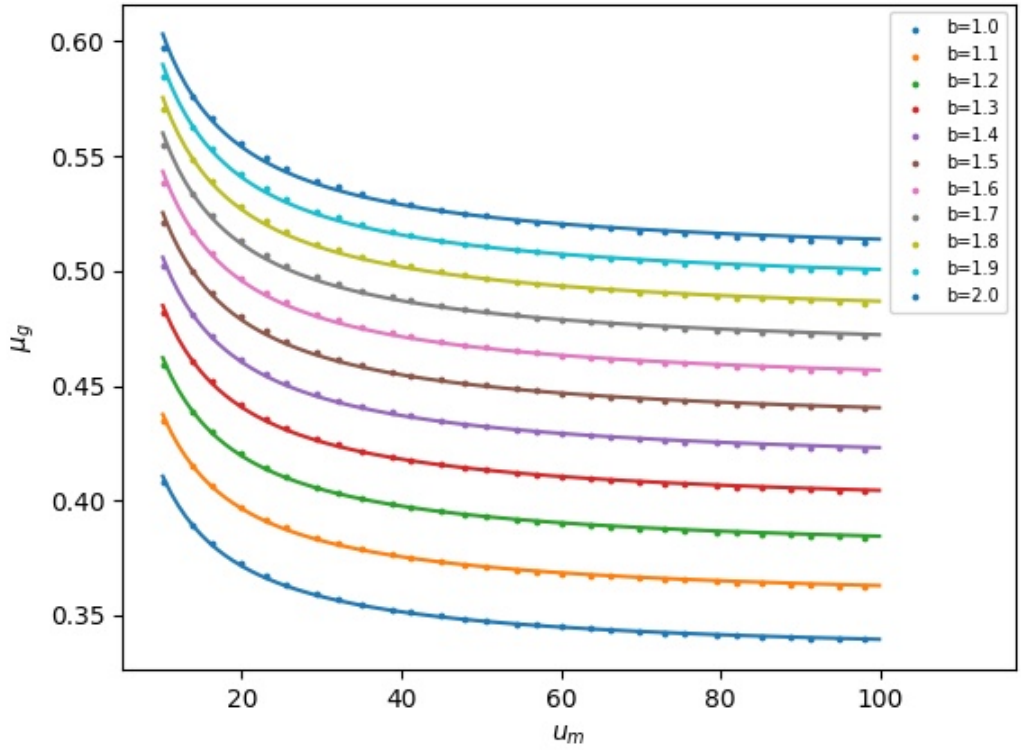

Figure 3.4.1: Variation of geometrical symmetry factor (μ'_{gx}) with $u_m = \dfrac{E}{kT_m}$ for different b at $x = 0.5$..

Then average μ'_{gx} *i.e.* $\langle \mu'_{gx} \rangle$ is defined as

$$\langle \mu'_{gx} \rangle = \frac{1}{u_{m_f} - u_{m_i}} \int_{u_{m_i}}^{u_{m_f}} \mu'_{gx} du_m \tag{3.4.3}$$

The integration may be evaluated numerically using any suitable algorithm, and in the present case, we have adopted the 16-point Gauss-Legendre quadrature method (Burden et al., 2001). This value of $\langle \mu'_{gx} \rangle$ corresponds to the input value of b that is used to generate TL peak.

In the next phase the peak shape coefficients are developed with respect to $\langle \mu'_{gx} \rangle$ for various values of fractional intensities. Retaining the forms of the original peak shape relations of Chen (1969a), we recast the new peak-shape relations as

$$E_{\alpha_x} = C_{\alpha_x} \frac{kT_m^2}{\alpha_x} - D_{\alpha_x}(2kT_m) \tag{3.4.4}$$

where x is the fractional intensity and α_x stands for $\tau_x, \delta_x, \omega_x$ (Fig. 3.1.1). Varying u_m over a wide range, a linear relation between u_m and $\frac{u_p u_q}{u_m|u_p - u_q|}$ can be fitted which yields the peak shape coefficients $C_{\alpha_x}, D_{\alpha_x}$. Here u_p and u_q are any two of u_m, u_{1x} and u_{2x}. The selection of peak shape parameter α_x from τ_x, δ_x and ω_x in Eq. (3.4.4) depends on the choice of u_p and u_q. C_{α_x} and D_{α_x} are fitted in a linear relation with $\langle \mu'_{gx} \rangle$ as

$$C_{\alpha_x} = C_{1\alpha_x} \langle \mu'_{gx} \rangle + C_{2\alpha_x} \tag{3.4.5}$$

$$D_{\alpha_x} = D_{1\alpha_x} \langle \mu'_{gx} \rangle + D_{2\alpha_x} \tag{3.4.6}$$

We summarize the entire procedure below to estimate peak shape coefficients for fractional intensity x.

(i) Initialize b.

(ii) Initialize u_m.

(iii) Estimate μ'_{gx}, u_{1x} and u_{2x} from the generated TL peak.

(iv) Increase u_m. Go to step (iii) and form new set of μ'_{gx}, u_{1x} and u_{2x}; repeat the process up to the highest value of u_m.

(v) Calculate $\langle \mu'_{gx} \rangle$.

(vi) Plot $\frac{u_p u_q}{u_m|u_p - u_q|}$ against u_m and fit the plot by a linear relation to find C_{α_x} and D_{α_x}.

(vii) Increase b. Go to step (ii) and form new set of $\langle \mu'_{gx} \rangle$, C_{α_x} and D_{α_x}; repeat the process up to the highest value of b.

(viii) Obtain a linear fit of C_{α_x} and D_{α_x} with respect to $\langle \mu'_{gx} \rangle$ to find out ($C_{1\alpha_x}$, $C_{2\alpha_x}$) and ($D_{1\alpha_x}$, $D_{2\alpha_x}$) for the particular value of x.

Peak shape coefficients at different fractional intensities

The peak shape coefficients (C_{α_x}, D_{α_x}) are needed to evaluate E according to Eq. (3.4.4). From Eqs. (3.4.5, 3.4.6) the dependence of (C_{α_x}, D_{α_x}) on $\langle \mu'_{gx} \rangle$ are expressed through the fitting constants $C_{1_{\alpha_x}}$, $C_{2_{\alpha_x}}$, $D_{1_{\alpha_x}}$, $D_{2_{\alpha_x}}$ which are obtained in linear regression method. In Table 3.4.1 we have listed the values of $C_{1_{\alpha_x}}$, $C_{2_{\alpha_x}}$, $D_{1_{\alpha_x}}$, $D_{2_{\alpha_x}}$ corresponding to different values of fractional intensities (x). We have given the fitting constants to estimate peak shape coefficients in Table. 3.4.1 for fractional intensities at $x = 0.11,\ 0.25,\ 0.5,\ 0.667$ and 0.8. These coefficients can be used directly for estimation of activation energy from the geometrical symmetry factor of a single TL peak. Here α stands τ, δ and ω. Final peak

shape coefficients (C_{α_x}, D_{α_x}) have been applied to evaluate E from TL curve generated in GOK model and OTOR model.

Table 3.4.1: Fitting constants in Eqs. (3.4.5, 3.4.6) to evaluate peak shape coefficients in Eq. (3.4.4) calculated at various fractional intensities.

$x = \frac{I}{I_m}$	α	$C_{1\alpha x}$	$C_{2\alpha x}$	$D_{1\alpha x}$	$D_{2\alpha x}$
0.8	τ	3.6701	−0.9010	8.0509	−2.8304
	δ	6.3094	−2.2376	6.9813	−2.8956
	ω	9.9768	−3.1377	6.9644	−2.5935
0.667	τ	3.3405	−0.3900	5.8890	−1.6311
	δ	6.9339	−2.2181	4.7095	−1.8662
	ω	10.2689	−2.6063	4.5399	−1.3810
0.5	τ	2.9865	0.2260	4.3810	−0.7228
	δ	7.7658	−2.2194	3.0187	−1.1556
	ω	10.7414	−1.9904	2.6723	−0.4477
0.25	τ	2.4611	1.3484	2.8957	0.3388
	δ	9.4782	−2.2821	1.0579	−0.4413
	ω	11.9081	−0.9264	0.3977	0.6851
0.11	τ	2.0872	2.4286	2.1323	1.0754
	δ	11.3057	−2.3975	−0.3198	−0.0337
	ω	13.3205	0.0464	−1.2923	1.5175

3.4.2 Results and discussions

We have applied the present peak shape coefficients on TL graphs simulated in GOK and OTOR models and compared with other established versions of peak shape methods. Some experimental curves are also considered.

Application to GOK model TL peaks

For the sake of initial standardization of the present method, we have applied the peak shape formula (Eq. 3.4.4) to extract activation energy from TL peaks generated in GOK model. TL glow curves from GOK model are generated by using Eqs. (1.2.3, 1.2.10) in linear heating scheme with temperature independent frequency factor. The heating rate (β) is taken as 1 K.sec^{-1}. The output values $E_{\tau x}$, $E_{\delta x}$ and $E_{\omega x}$ are listed in Table 3.4.2 where first order, second order and general order kinetics are considered. Table 3.4.2 reveals

Table 3.4.2: Activation energies $E_{\tau x}$, $E_{\delta x}$, $E_{\omega x}$ (eV) derived by using the present peak shape method from TL peaks simulated in GOK model for different order of kinetics (b). Here $E_{in} = 1$ eV, $s_{in} = 10^{12}$ sec^{-1} and $\beta = 1$ K.sec^{-1}.

$x = \frac{I}{I_m}$	b	T_m (K)	τ_x	δ_x	ω_x	μ'_{gx}	$E_{\tau x}$	$E_{\delta x}$	$E_{\omega x}$
0.8	1	384.57	9.09	7.54	16.63	0.4533	1.01	1.03	1.02
	1.5	384.22	10.32	9.79	20.11	0.4869	1.02	1.05	1.03
	2	383.88	11.26	11.71	22.97	0.5098	1.01	1.02	1.01
0.667	1	384.57	12.70	9.87	22.56	0.4373	1.01	1.04	1.02
	1.5	384.22	14.17	13.21	27.38	0.4824	1.02	1.06	1.04
	2	383.88	15.29	16.13	31.42	0.5134	1.01	1.02	1.01
0.5	1	384.57	17.36	12.48	29.84	0.4183	1.01	1.04	1.02
	1.5	384.22	19.03	17.38	36.41	0.4773	1.01	1.07	1.04
	2	383.88	20.29	21.82	42.10	0.5181	1.01	1.02	1.02
0.25	1	384.57	26.56	16.7	43.26	0.3860	1.01	1.05	1.03
	1.5	384.22	28.38	25.09	53.48	0.4692	1.01	1.09	1.05
	2	383.88	29.75	33.24	62.99	0.5278	1.01	1.03	1.02
0.11	1	384.57	35.96	20.11	56.07	0.3587	1.00	1.06	1.03
	1.5	384.22	37.77	32.64	70.41	0.4635	1.01	1.12	1.06
	2	383.88	39.12	45.62	84.74	0.5383	1.01	1.04	1.03

that the extracted values of activation energy are quite consistent with the input value $E_{in} = 1$ eV. From theoretical perspective, the present method should work for any value of x, whereas it is observed that admissible values of activation energies are not obtained for $x < 0.11$. It is also evident that the $E_{\tau x}$ values are in greater agreement with E_{in} as compared to $E_{\delta x}$ and $E_{\omega x}$. $E_{\delta x}$ shows highest deviation from E_{in}.

Application to OTOR model TL peaks

We have studied the OTOR glow curves for a fairly large number of TL peaks corresponding to a wide range of parameters. For curve generation, the input values of activation energy are taken in the range $0.8 \leqslant E_{in} \leqslant 1.5$ eV and the frequency factor lies in the range $10^8 \leqslant s_{in} \leqslant 10^{12}$ sec^{-1}. The filling ratio $f = \dfrac{n_0}{N}$ is taken from 0.01 to 1 to cover almost the entire range of trap saturation corresponding to different irradiation stages. Retrapping to recombination ratio (R) is considered from 10^{-2} to 10^2 to cover low to high retrapping situations during heating stage. The extracted values of $E_{\tau x}$, $E_{\delta x}$ and $E_{\omega x}$ are displayed in Table 3.4.3 for some selected set of input parameters. From Table 3.4.3 it is observed that $E_{\tau x}$ values are more consistent with E_{in} whereas $E_{\delta x}$ values show maximum deviation, as is observed in case of GOK glow curves. The results are consistent for $0 \leqslant R \leqslant 1$. However, for $R > 1$, *i.e.* in case of heavy retrapping, $E_{\tau x}$, $E_{\delta x}$ and $E_{\omega x}$ yield acceptable values when f is quite small which corresponds to low dose rates. In case of saturated or almost saturated

cases ($f \leqslant 1$) with heavy retrapping ($R > 1$), the output values of activation energy are quite away from the input value. Table 3.4.3 shows that even for $f = 0.5$, $E_{\tau x}$, $E_{\delta x}$ and $E_{\omega x}$ show deviation from E_{in} and are underestimated by as much as 9%.

Table 3.4.3: Activation energies $E_{\tau x}$, $E_{\delta x}$, $E_{\omega x}$ (eV) derived by using the present peak shape method from TL peaks simulated in OTOR model. Here $E_{in} = 1$ eV, $s_{in} = 10^{12}$ sec^{-1} and $\beta = 1$ K.sec^{-1}.

x	f	R	T_m (K)	τ_x	δ_x	ω_x	μ'_{gx}	$E_{\tau x}$	$E_{\delta x}$	$E_{\omega x}$
0.8	0.01	0	384.57	9.09	7.54	16.63	0.4536	1.02	1.05	1.03
		0.5	436.68	14.39	15.04	29.43	0.5109	1.02	1.07	1.02
		1	447.37	15.11	15.80	30.91	0.5112	1.01	1.08	1.02
		10	487.17	17.81	18.70	36.51	0.5122	1.02	1.08	1.02
	0.5	0	384.57	9.09	7.54	16.63	0.4536	1.02	1.04	1.02
		0.5	388.30	10.78	10.79	21.57	0.5002	1.05	1.07	1.06
		1	392.29	11.74	12.22	23.96	0.5100	1.01	1.02	1.01
		10	416.38	14.92	16.25	31.17	0.5214	0.92	0.91	0.91
	1	0	384.57	9.09	7.54	16.63	0.4536	1.02	1.04	1.05
		0.5	383.31	10.13	9.85	19.98	0.4929	1.06	1.09	1.09
		1	383.87	11.26	11.72	22.97	0.5099	1.01	1.02	1.03
		10	400.08	20.04	20.02	40.06	0.4997	0.56	0.59	0.60
0.667	0.01	0	384.57	12.7	9.88	22.58	0.4374	1.01	1.04	1.02
		0.5	436.68	19.54	20.74	40.28	0.5149	1.01	1.05	1.02
		1	447.37	20.5	21.8	42.31	0.5154	1.01	1.05	1.02
		10	487.17	24.15	25.83	49.98	0.5168	1.01	1.06	1.02
	0.5	0	384.57	12.7	9.88	22.58	0.4374	1.01	1.04	1.02
		0.5	388.30	14.75	14.81	29.55	0.5010	1.04	1.07	1.06
		1	392.29	15.95	16.85	32.8	0.5138	1.01	1.02	1.01
		10	416.38	20.02	22.43	42.46	0.5284	0.92	0.92	0.92
	1	0	384.57	12.7	9.88	22.58	0.4374	1.01	1.04	1.06
		0.5	383.31	13.93	13.45	27.38	0.4913	1.05	1.09	1.11
		1	383.87	15.3	16.15	31.44	0.5136	1.01	1.02	1.05
		10	400.08	26.95	27.12	54.07	0.5016	0.57	0.61	0.63
0.5	0.01	0	384.57	17.35	12.49	29.84	0.4185	1.01	1.04	1.03
		0.5	436.68	25.89	28.06	53.95	0.5201	1.01	1.05	1.02
		1	447.37	27.15	29.51	56.66	0.5208	1.01	1.05	1.02
		10	487.17	31.94	34.99	66.93	0.5228	1.01	1.06	1.03
	0.5	0	384.57	17.35	12.49	29.84	0.4185	1.01	1.04	1.02
		0.5	388.30	19.72	19.93	39.65	0.5027	1.04	1.07	1.06
		1	392.29	21.14	22.77	43.92	0.5185	1.01	1.02	1.02
		10	416.38	26.17	30.28	56.45	0.5364	0.93	0.93	0.93
	1	0	384.57	17.35	12.49	29.84	0.4185	1.01	1.04	1.07
		0.5	383.31	18.71	18.02	36.73	0.4907	1.05	1.10	1.12
		1	383.87	20.28	21.82	42.10	0.5182	1.01	1.02	1.06

Table (3.4.3) continued..

x	f	R	T_m (K)	τ_x	δ_x	ω_x	μ'_{gx}	$E_{\tau x}$	$E_{\delta x}$	$E_{\omega x}$
		10	400.08	34.94	35.83	70.77	0.5063	0.58	0.63	0.66
0.25	0.01	0	384.57	26.56	16.7	43.26	0.3861	1.01	1.05	1.03
		0.5	436.68	37.88	42.86	80.75	0.5308	1.01	1.04	1.03
		1	447.37	39.69	45.1	84.79	0.5319	1.01	1.05	1.03
		10	487.17	46.6	53.57	100.17	0.5348	1.01	1.05	1.04
	0.5	0	384.57	26.56	16.7	43.26	0.3861	1.01	1.05	1.03
		0.5	388.30	29.26	30.34	59.61	0.5090	1.03	1.08	1.06
		1	392.29	30.99	34.71	65.7	0.5284	1.01	1.03	1.02
		10	416.38	37.46	45.77	83.23	0.5499	0.94	0.95	0.94
	1	0	384.57	26.56	16.7	43.26	0.3861	1.01	1.05	1.03
		0.5	383.31	27.97	27.3	55.28	0.4939	1.04	1.11	1.08
		1	383.87	29.74	33.25	62.99	0.5278	1.01	1.03	1.02
		10	400.08	48.04	52.26	100.3	0.5210	0.63	0.69	0.66
0.11	0.01	0	384.57	35.95	20.11	56.07	0.3588	1.00	1.06	1.03
		0.5	436.68	49.71	58.99	108.7	0.5427	1.01	1.03	1.04
		1	447.37	52.04	62.09	114.13	0.5440	1.01	1.03	1.04
		10	487.17	60.98	73.9	134.88	0.5479	1.01	1.04	1.05
	0.5	0	384.57	35.95	20.11	56.07	0.3588	1.00	1.06	1.03
		0.5	388.30	38.83	41.86	80.68	0.5188	1.03	1.09	1.06
		1	392.29	40.74	47.66	88.39	0.5391	1.01	1.04	1.03
		10	416.38	48.35	62.06	110.4	0.5621	0.95	0.97	0.96
	1	0	384.57	35.95	20.11	56.07	0.3588	1.00	1.06	1.10
		0.5	383.31	37.31	37.67	74.98	0.5024	1.04	1.12	1.15
		1	383.87	39.12	45.62	84.74	0.5384	1.01	1.04	1.10
		10	400.08	58.93	68.84	127.78	0.5388	0.68	0.75	0.80

We have shown the variation of average activation energy $\left[E = \frac{1}{3}\left(E_\tau + E_\delta + E_\omega\right)\right]$ plotted against R for different filling ratios at fractional intensities $x = 0.8$, 0.67, 0.5 and 0.11 in Fig. 3.4.2. Similar pattern is observed for other x values also. It is evident that for very low values of f (say, $f = 0.01$), the output energy is slightly overestimated near $R = 0$. The error decreases with increase of R and even in heavy retrapping domain ($R > 1$), the activation energy is quite consistent with E_{in}. For higher filling ratio, the error is less near $R = 0$ and 1, but within this range, the extracted activation energy is overestimated. The method starts to fail for heavy retrapping cases ($R > 1$) and the departure becomes more prominent with the gradual filling of trap states. This behaviour is uniform for all values of fractional intensities and input parameters for glow curve generation.

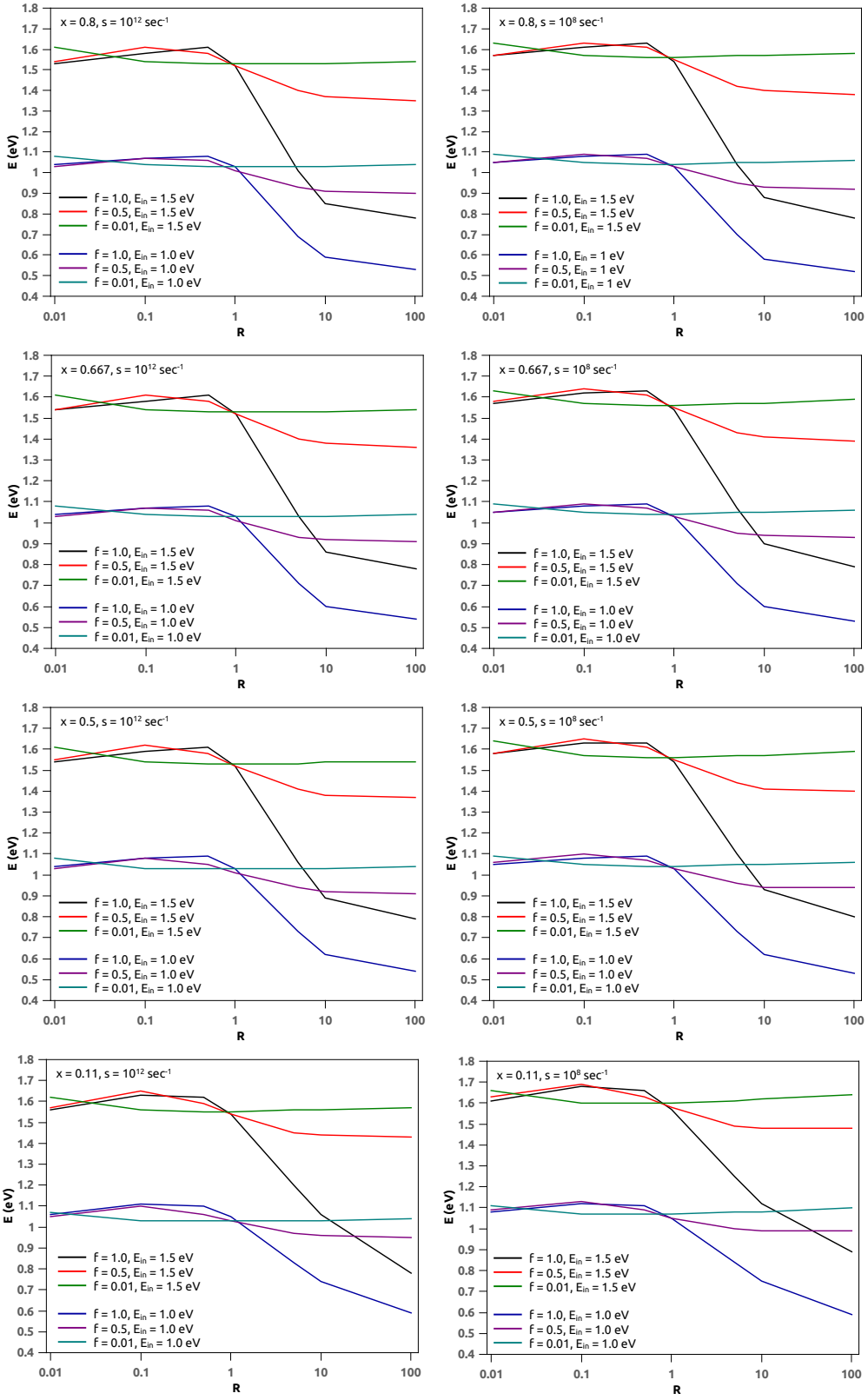

Figure 3.4.2: Average activation energy (E) plotted against R for fractional intensities $x = 0.8, 0.67, 0.5, 0.11$. Here $E_{in} = 1$ eV and 1.5 eV, $s_{in} = 10^{12}$ and 10^{8} sec^{-1}, $\beta = 1$ K.sec^{-1}.

Table 3.4.4: Comparison of present results at $x = 0.5$ with other peak shape methods (Chen, 1969a; Kitis and Pagonis, 2007). Here $E_{in} = 1$ eV, $s_{in} = 10^{12}$ sec^{-1}, $\beta = 1$ K.sec^{-1} and, for OTOR model, $f = 0.5$.

Model	Input parameters	T_m (K)	μ_g	Activation energy (eV)		
				E_τ	E_δ	E_ω
GOK	$b = 1.0$	384.57	0.4183	1.01	1.04	1.02
				1.00[a]	0.98[a]	1.00[a]
				0.99[b]	1.00[b]	0.99[b]
	$b = 1.5$	384.22	0.4773	1.01	1.07	1.04
				1.00[a]	1.02[a]	1.02[a]
				0.99[b]	1.00[b]	0.99[b]
	$b = 2.0$	383.88	0.5181	1.01	1.02	1.01
				1.00[a]	0.98[a]	1.00[a]
				0.99[b]	1.01[b]	0.99[b]
OTOR	$R = 0.0$	384.57	0.4185	1.01	1.04	1.02
				1.00[a]	0.98[a]	1.00[a]
				0.99[b]	1.00[b]	0.99[b]
	$R = 0.5$	388.30	0.5027	1.04	1.07	1.05
				1.03[a]	1.03[a]	1.04[a]
				1.01[b]	0.98[b]	0.99[b]
	$R = 1.0$	392.29	0.5186	1.01	1.02	1.01
				1.00[a]	0.99[a]	1.00[a]
				0.99[b]	1.01[b]	0.99[b]

[a] Chen (1969a)
[b] Kitis and Pagonis (2007)

Comparison of the present method with other peak shape methods

In Table 3.4.4, we have given a comparison of the present activation energies for some selected input parametrs with those derived by using the methods due to Chen (1969a) and Kitis and Pagonis (2007). We note that both the existing methods (Chen, 1969a; Kitis and Pagonis, 2007) are applicable only for $x = 0.5$. The present results for $x = 0.5$ are given in Table 3.4.4 for a ready comparison though this method can yield activation energies at various fractional intensity points. It is evident from Table 3.4.4 that the output values activation energies are quite consistent and in reasonable agreement with other methods. Moreover, the activation energies derived from a particular TL curve at different fractional intensities should be consistent and the present method provides a scope to verify this.

Application to experimental TL peaks

We have applied the present peak shape relations (Eq. 3.4.4) to extract the activation energy from some experimental TL peaks reported in literature. This method works for an

isolated component peak deconvoluted from a composite experimental peak. Kucuk et al. (2015) reported the TL curves along with the component peaks of γ-irradiated phosphor $ZnB_2O_4 : 0.02La$ recorded at a heating rate of 5 K.sec^{-1}. The recorded TL data show a multipeak system of this phosphor and we have considered the first two component peaks with maxima at 456K and 472K. We have picked the datapoints from the deconvoluted $I - T$ curves (Kucuk et al., 2015) for which we have used the browser-based software tool WebPlotDigitizer. It is to note that datapoints picked up in this manner are not equispaced whereas it is preferred to have equispaced data in order to carry out some systematic numerical analysis. Moreover, accurate $I - T$ data are essential to estimate the peak shape parameters τ, δ and ω for a given fractional intensity (x). We have, therefore, adopted the method of interpolation to generate the intermediate data at equal temperature intervals by using the divided difference algorithm (Burden et al., 2001) which is a standard process for non-equispaced data (Gill and Miller, 1972). The $I - T$ data thus obtained are now exploited to extract the activation energy as per the present version of peak shape formulas. In Table 3.4.5, we have given the present results ($E_{\tau x}, E_{\delta x}$ and $E_{\omega x}$) of activation energies corresponding to the experimental curves. The reported experimental values (E_{expt}) are also given here for a ready comparison of the present results. Moreover, in Table 3.4.5, we have also given the activation energies (E_τ, E_δ and E_ω) estimated according to the formulas of Chen (1969a) and Kitis and Pagonis (2007) which are valid for $x = 0.5$ only. It is evident from Table 3.4.5 that the $E_{\tau x}, E_{\delta x}$ and $E_{\omega x}$ values of $ZnB_2O_4 : 0.02La$ are quite consistent among themselves and are also in agreement with those otained by other methods (Chen, 1969a; Kitis and Pagonis, 2007). The average values of present activation energy of $ZnB_2O_4 : 0.02La$ are 1.45 eV and 1.59 eV for peak 1 and 2 respectively which are marginally overestimated as compared to E_{expt} values (Kucuk et al., 2015). The relative standard deviation is measured using the formula: $\sigma = \frac{1}{E_{avg}} \sqrt{\frac{1}{n} \sum_n (E_{\alpha x} - E_{avg})^2} \times 100\%$. Here, from the values listed in Table 3.4.5, $E_{\alpha x}$ are the activation energies ($\alpha = \tau, \delta, \omega$) for all values of x, n is the number of $E_{\alpha x}$ values (15 for each peak) and E_{avg} is the average of these $E_{\alpha x}$ values. For $ZnB_2O_4 : 0.02La$, the $E_{\tau x}, E_{\delta x}$ and $E_{\omega x}$ values yield $\sigma = 2.80\%$ and 2.75% for peak 1 and 2 respectively.

In a similar manner, we have also determined the activation energies from the component peaks 1 and 2 of the experimental TL curve of X-ray irradiated Sillimanite (Al_2SiO_5) mineral reported by Kalita and Wary (2017). The sample was annealed at 773K and heated at a rate of 2 K.sec^{-1}. The reported peak maxima were at 359.6K and 387.3K (Kalita and Wary, 2017). The present results as given in Table 3.4.5 yield $E_{avg} = 0.85$ eV for peak 1 with $\sigma = 8.14\%$. It is evident that for peak 1, $E_{\tau x}, E_{\delta x}$ and $E_{\omega x}$ values of Al_2SiO_5

Table 3.4.5: Activation energies derived by using the present peak shape method from experimental TL peaks.

Material	Peak	E_{expt} (eV)	$x = \frac{I}{I_m}$	Activation energy (eV)		
				$E_{\tau x}$	$E_{\delta x}$	$E_{\omega x}$
$ZnB_2O_4 : 0.02La$	1	1.36 ± 0.07^{k}	0.8	1.49	1.53	1.51
(phosphor)			0.667	1.42	1.49	1.46
(Kucuk et al., 2015)			0.5	1.43	1.46	1.44
				1.43^{a}	1.40^{a}	1.43^{a}
				1.39^{b}	1.31^{b}	1.35^{b}
			0.25	1.39	1.44	1.41
			0.11	1.39	1.46	1.42
	2	1.48 ± 0.07^{k}	0.8	1.63	1.67	1.65
			0.667	1.58	1.63	1.59
			0.5	1.57	1.62	1.60
				1.56^{a}	1.54^{a}	1.57^{a}
				1.51^{b}	1.40^{b}	1.46^{b}
			0.25	1.52	1.58	1.54
			0.11	1.52	1.59	1.55
Sillimanite (Al_2SiO_5)	1	0.88^{kw}	0.8	0.75	0.76	0.76
(mineral)			0.667	0.79	0.82	0.80
(Kalita and Wary, 2017)			0.5	0.86	0.91	0.88
				0.85^{a}	0.86^{a}	0.86^{a}
				0.85^{b}	0.89^{b}	0.87^{b}
			0.25	0.87	0.95	0.90
			0.11	0.87	0.98	0.92
	2	1.08^{kw}	0.8	1.14	1.18	1.16
			0.667	1.12	1.17	1.15
			0.5	1.11	1.17	1.14
				1.10^{a}	1.11^{a}	1.11^{a}
				1.08^{b}	1.05^{b}	1.06^{b}
			0.25	1.09	1.18	1.13
			0.11	1.07	1.19	1.13

[a] Chen (1969a)
[b] Kitis and Pagonis (2007)
[k] Kucuk et al. (2015)
[kw] Kalita and Wary (2017)

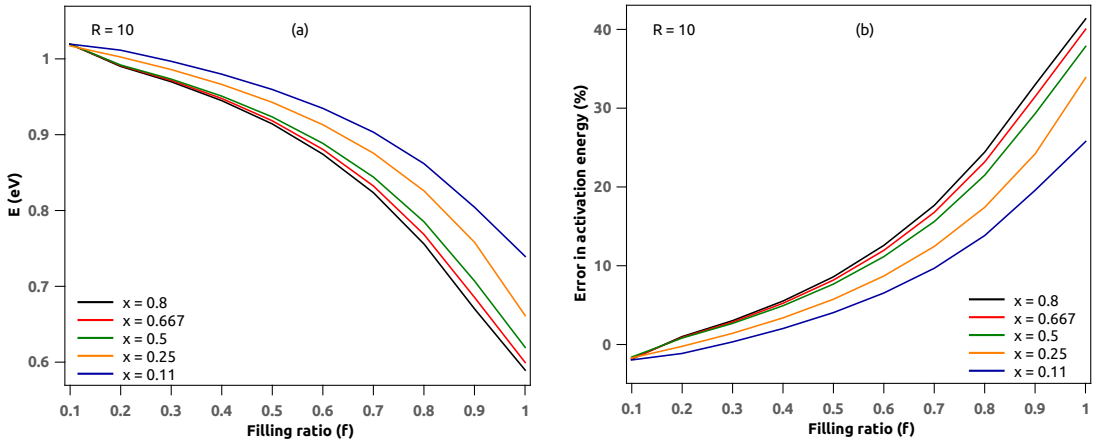

Figure 3.4.3: Estimated Values of (a) activation energy (E) and (b) the error inherent in it as derived from TL peaks simulated in OTOR model for different x plotted against f for heavy retrapping ($R = 10$). Here $E_{in} = 1$ eV and $s_{in} = 10^{12}$ sec^{-1}, $\beta = 1$ K.sec^{-1}.

are consistent except for $x = 0.8$ and 0.667 and also in agreement with the values derived from other methods (Chen, 1969a; Kitis and Pagonis, 2007). Given that $E_{expt} = 0.88$ eV for peak 1, the results corresponding to $x = 0.8$ are quite underestimated. Compared to peak 1, the results of peak 2 of (Al_2SiO_5) show more consistency and yield $E_{avg} = 1.14$ eV with $\sigma = 2.93\%$. The probable reason behind such inflated value of σ corresponding to peak 1 of Al_2SiO_5 might be inherent in the quality of the $I - T$ data picked up from the experimental plot. However, for all the cases, the $E_{\tau x}$ results are always consistent and in better agreement with experimental values.

3.4.3 Limitation of peak shape method

It has been evident, both from literature and present study, that the peak shape method fails for heavy retrapping cases when the initial trap saturation is quite high. To have a deeper insight on the limitation of these peak shape relations for heavy retrapping cases with higher filling ratio, we have plotted the average activation energy measured at different values of x along with the corresponding error for $R = 10$ in Fig. 3.4.3. We observe a gradual decrease in the output value of E as f increases and the departure is minimum for the parameters corresponding to the lower portion of the curve.

To investigate the primary reason of the failure of present peak shape method for saturated curves with heavy retrapping, we have performed a detailed study on the symmetry factor (μ'_{gx}) of TL peaks generated with various R and f. The dependence of μ'_{gx} on R and f are shown in Fig. 3.4.4 for $x = 0.8$ and 0.11. Similar patterns are observed for other values of x also. It is found that for $0 \leqslant R \leqslant 1$, μ'_{gx} increases gradually. Beyond

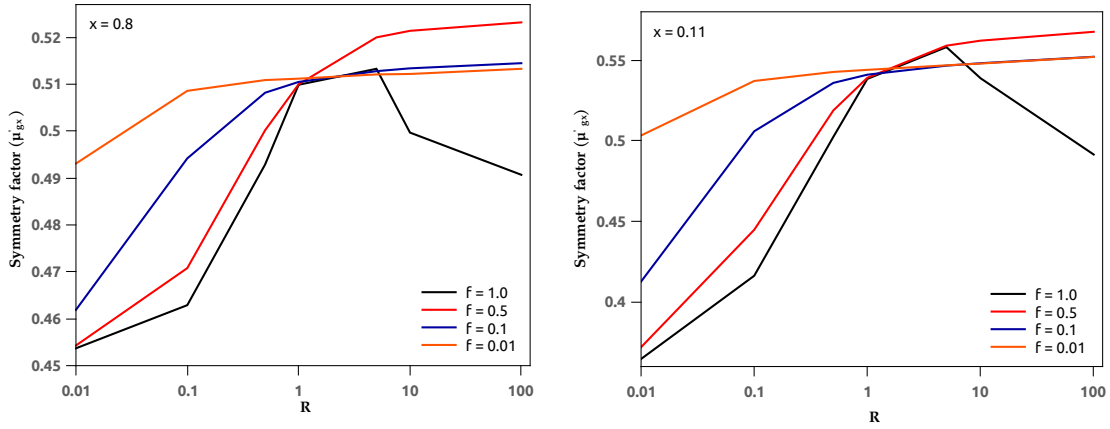

Figure 3.4.4: Variation of symmetry factor (μ'_{gx}) plotted against R for TL peaks simulated in OTOR model for various filling ratios with fractional intensities $x = 0.8$ and 0.11. Here $E_{in} = 1$ eV, $s_{in} = 10^{12}$ sec^{-1}, $\beta = 1$ K.sec^{-1}.

$R > 1$ it increases very slowly in an almost well-behaved way for low values of f. For higher values of f (say, $f = 0.5$) the growth rate of μ'_{gx} with respect to R is quite high as is seen from Fig. 3.4.4, and above $R = 1$, μ'_{gx} increases and the extracted values of activation energy starts deviating. Even the $E_{\tau x}$ values, which are otherwise consistent for $0 \leqslant R \leqslant 1$, show a considerable departure from E_{in} for $R > 1$. The behaviour of μ'_{gx} for $f = 1$ is quite remarkable. The rate of increase of μ'_{gx} is maximum in this case and above $R = 1$ it shows an anomalous behaviour showing initial growth and then an abrupt fall which finally reflects through the spurious values of activation energies.

It is to note that in OTOR model, b does not occur explicitly, whereas R does not appear in GOK model. However, a functional relation between these two can be written as (Sunta, 2014)

$$b(T) = 1 + \frac{\ln\left[1 + R\left(\frac{N}{n(T)} - 1\right)\right]}{\ln \frac{N}{n(T)}} \tag{3.4.7}$$

Eq. (3.4.7) shows that b has no temperature dependence only for $R = 0$ and 1 which yield $b = 1$ and 2 respectively. For all other values of R, b has a dependence on T due to the temperature dependence of $n(T)$ and hence an entire TL curve should not be described using a fixed value of b. Instead, the temperature average of $b(T)$ (*i.e.* b_{av}) is supposed to provide a more reliable correspondence to R. This average is defined as

$$b_{av} = \frac{1}{T_f - T_i} \int_{T_i}^{T_f} b(T) dT \tag{3.4.8}$$

Table 3.4.6: Average value of order of kinetics (b_{av}) for OTOR peaks. The input parameters are: $E_{in} = 1.0$ eV, $s = 1.0 \times 10^{12}$ sec^{-1}, $N = 1.0 \times 10^{10}$ m^{-3} and $\beta = 1$ K.sec^{-1}.

R	f	b_{av}
0.5	0.01	1.9
	0.1	1.8
	0.5	1.7
	1	1.7
1	0.01	2.0
	0.1	2.0
	0.5	2.0
	1	2.0
10	0.01	2.4
	0.1	2.6
	0.5	3.3
	1	5.2
100	0.01	2.8
	0.1	3.3
	0.5	5.1
	1	28.6

To estimate $b(T)$, we need to integrate Eq. (1.2.23) so that the required values of $n(T)$ are obtained. The integration in Eq. (3.4.8) is done here using composite Simpson's rule (Burden et al., 2001). The detail discussion regarding the issue is included later in Section (4.4.8). We have estimated b_{av} for a large number of TL peaks generated with different values of R and initial filling ratio $f = \dfrac{n_0}{N}$. In Table 3.4.6 we have given a representative set of these values. Table 3.4.6 reveals that for $R \leqslant 1$, the b_{av} values lie below 2.5 irrespective of the values of f. Even for $R = 10$, we find $b_{av} < 2.5$ for low filling ratio ($f = 0.01$). For all such cases, the activation energies derived from peak shape relations are quite acceptable, as is evident from Table 3.4.3. This is because the present peak shape coefficients are determined for b lying between 0.7 and 2.5. When trap saturation (*i.e.* f) increases for $R > 1$, the b_{av} values exceed 2.5 and the peak shape results fail. For $R >> 1$, the peak shape results fail entirely, irrespective of the value of f. The same argument also holds for the failure (Sunta et al., 1999) of conventional peak shape relations for saturated or highly saturated TL peaks with heavy retrapping.

3.5 New peak shape method using skewness of TL data.

In peak shape method, the shape of a TL curve is incorporated in the calculations through the geometrical symmetry factor μ'_g. In experimental scenario, μ'_g can be estimated easily from a TL peak as it involves only three points on a glow curve *viz.* (T_{1x}, I_{1x}), (T_m, I_m),

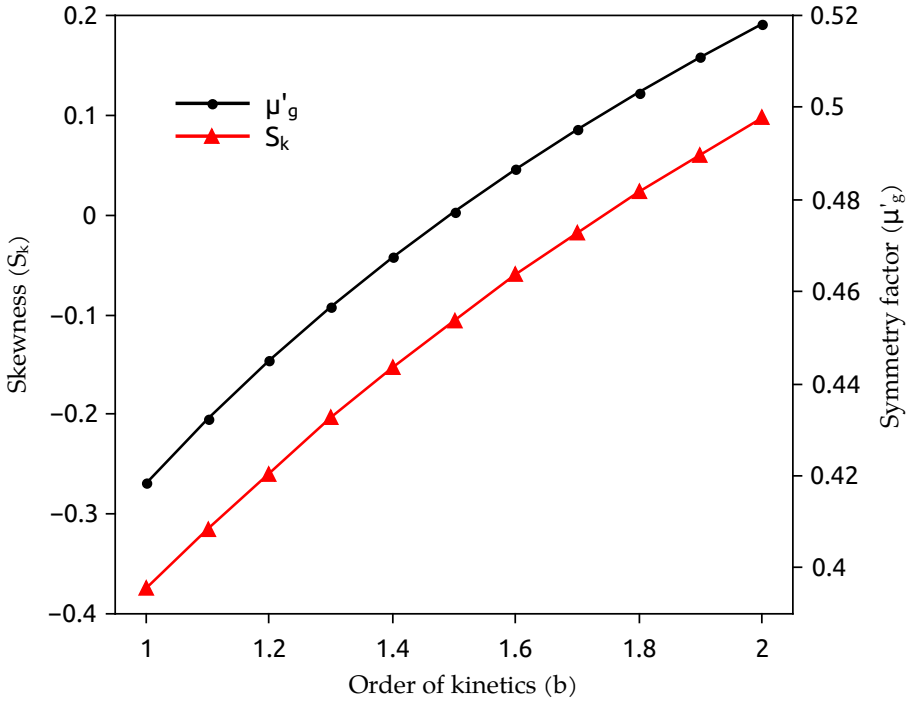

Figure 3.5.1: Variation of skewness (S_k) and geometric symmetry factor (μ'_g) with order of kinetics (b).

(T_{2x}, I_{2x}) (see Fig. 3.1.1). For obvious reasons, μ'_g varies at different fractional intensities (Fig. 3.1.1) and all the choices of x may not yield results with same accuracy. The primary motivation of the work is to develop a peak shape method using a symmetry parameter which is unique to a set of TL data and can involve the whole data set instead of choosing few particular points. The nature of symmetry of TL curve has direct dependence on the retrapping-recombination mechanism in a material at the heating stage of TL process. This retrapping-recombination mechanism is reflected through b in GOK model and through R ($= \frac{A_n}{A_h}$) in OTOR model. Here A_n and A_h are the probabilities of retrapping and recombination respectively. The dependence of the shape of a glow curve on b (or R) can be reflected through the skewness which is unique for a particular dataset. In fact, the variations of skewness and μ'_g as a function b exhibit almost similar nature as is shown in Fig. 3.5.1. Hence, as a measure of asymmetry of a glow curve, skewness can be a useful parameter to represent the shape of a TL peak. The calculation of skewness involves the entire TL dataset and thus avoids the limitation of choosing particular points or portion of the curve.

In the present study we have carried out a thorough investigation on the shape and nature of asymmetry of glow curves by studying their skewness (S_k). Within the perview

of GOK framework glow curves are simulated by varying E, s and b and the variation of S_k with respect to these parameters are studied in detail. We note that variation of S_k with the combined effect of E and s is studied through the parameter $u_m = \frac{E}{kT_m}$. In OTOR model, S_k is estimated from glow curves simulated for different values of R and trap filling ratio (f). The heavy retrapping cases ($R > 1$) are also considered exhaustively. A new set of peak shape relations similar to Eq. (3.2.4) are developed for τ_x, δ_x and ω_x where the peak shape coefficients are formulated in terms of skewness of the TL data. The present peak shape relations are applied to extract E from TL peaks simulated in GOK and OTOR models. Finally, the present method is successfully employed to estimate E from well known experimental TL glow curves of (i) 110^{o}C peak of quartz (Lovedy, 2017; Petrov and Bailiff, 1995) and (ii) peaks of MgO (Thomas and Houston, 1964).

3.5.1 Skewness as peak shape parameter for TL study

Skewness is a statistical parameter that represents the extent of asymmetry in a set of recorded data. When the frequency distribution of the data set is symmetric, skewness is zero. A longer tail toward left in distribution represents negative skewness while the opposite condition yields positive skewness. Skewness of a set of TL data estimated from Pearson's first measure (Dodge, 2008) can be given by

$$
\begin{aligned}
S_k = \frac{\text{mean} - \text{mode}}{\text{standard deviation}} &= \frac{\overline{T} - T_m}{\sigma} \\
\text{where,} \quad \text{mean} = \overline{T} &= \frac{\sum_j T_j I_j}{\sum_j I_j} \\
\text{mode} = T_m &= \text{Peak temperature} \\
\text{standard deviation} = \sigma &= \sqrt{\frac{\sum_j \left(T_j - \overline{T}\right)^2 I_j}{\sum_j I_j}}
\end{aligned}
\tag{3.5.1}
$$

In the usual language of statistics, the intensity I_j can be considered as the equivalent frequency of occurrence of the variable T_j *i.e.* temperature in this case.

Skewness is measured by considering the departure of data from the central tendency, *i.e.*, from the mean temperature in the present case. However the mean temperature which is a weighted average, has a dependence on the intensity values (Eq. 3.5.1). Though the temperature is increased systematically to simulate a TL curve, the mean temperature

depends on the data distribution in 'I – T' plot and not on the initial and the final temperatures only. The 'I – T' data distribution depends on system properties. For example if we generate the 'I – T' data with input parameters E = 1 eV, s = 10^{12} sec^{-1}, β = 1 K/s between the temperatures T_i = 300 K and T_f = 500 K, then the mean temperature is 379 K for first order TL peaks and 386 K for second order peak respectively. Clearly the mean values differ as the charge dynamics in the system changes and they are in general not equal to the arithmetic mean which is 400 K in the example given above, irrespective of order of kinetics.

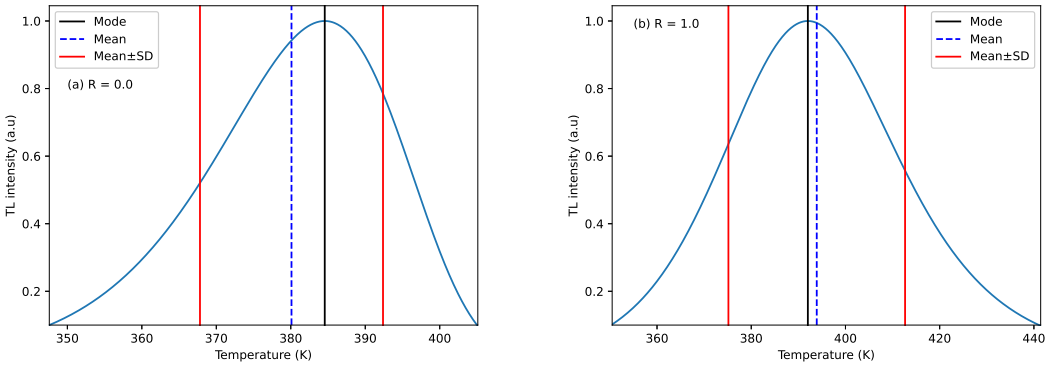

Figure 3.5.2: Schematic diagram to calculate S_k of a TL peak generated in OTOR model (a) for $R = 0$ (b) for $R = 1$. The input parameters are: $E = 1$ eV, s= 10^{12} sec^{-1}, $f = 0.5$.

In Fig. 3.5.2, a schematic diagram related to the calculation of skewness from a TL data set is given. A TL peak with negative skewness is shown in Fig. 3.5.2(a) where the peak is simulated in OTOR model with $R = 0$ (equivalent to first order kinetics). The blue vertical dotted line indicates the position of mean whereas the vertical solid black line indicates the mode (*i.e.* T_m) of TL data. The two vertical red lines indicate the range of temperature representing standard deviation. It is seen from Fig. 3.5.2(a) that the mean is on the left to the mode which corresponds to negative skewness. In Fig. 3.5.2(b), another TL peak simulated in OTOR model with $R = 1$ (equivalent to second order kinetics) is shown. It is evident from Fig. 3.5.2(b) that the mean is on the right to the mode which is the signature of positive skewness. Since skewness is associated to a particular data set, therefore S_k of a TL dataset depends on the initial and final data points and also on stepsize (ΔT). To have an accurate estimation of skewness of a glow curve, it is imperative to include as many datapoints as possible. In an experimental scenario it is sometimes difficult to get clean data at low intensity regions due to presence of various noise signals. Keeping this in mind, we have calculated S_k considering all the data points for which $I(T) \geq \frac{I_m}{10}$. The stepsize for simulation of TL peaks is ΔT = 0.1K. We note that $\overline{T}$ does not significantly

depend on the size of ΔT.

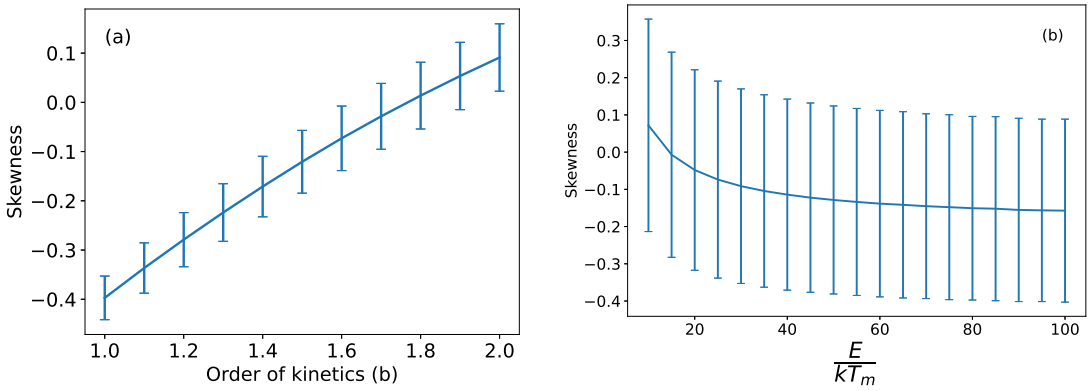

Figure 3.5.3: Variation of S_k of TL peak with: (a) b and (b) $u_m = \dfrac{E}{kT_m}$.

The shape of a TL curve depends on the retrapping and recombination kinetics represented through the empirical parameter b (or R). However, small dependence on E and s is also observed (Chen, 1969a; Kundu et al., 2021). Since in case of a TL curve, S_k relates to the shape and symmetry, it is expected to have some dependence on b as well as on E and s. To have a close insight in this context we have carried out an exhaustive study with a large number of TL peaks. Glow curves are simulated in systematic manner using Eq. (1.2.13) by varying b in step 0.1 within the range $1.0 \leq b \leq 2.0$. For each b, E is varied from 0.2 to 2.0 eV in step 0.1, whereas for each set of b and E, s is chosen in such a way that u_m varies from 10 to 100 in step 5. We estimate S_k of the synthetic glow peaks using Eq. (3.5.1) and the results are presented in Fig. 3.5.3. From Fig. 3.5.3(a) it is seen that S_k varies with b in a systematic manner. As b increases S_k also increases gradually from –ve to +ve values. For a fixed value of b, the possible variation in S_k due to change in u_m is also studied and the results are depicted in Fig. 3.5.3(a) through vertical error bars. Dependence of S_k on u_m is presented in Fig. 3.5.3(b) from which it appears that S_k decreases by a small amount from positive to negative value as u_m increases. However, for $u_m > 50$ the change in S_k is almost negligible. For a fixed u_m, significant variation in S_k is observed due to variation in b and presented through vertical error bars in Fig. 3.5.3(b).

3.5.2 Determination of Peak Shape coefficients using skewness

The above study reveals that S_k of a TL peak for a particular b cannot be defined specifically because of the simultaneous dependence of S_k on u_m. However, the shape of a TL curve has direct dependence on b and hence, to use S_k as a symmetry parameter for glow curve analysis in peak shape method, it is required to establish a one-to-one correspondence between b and

S_k. For this purpose, we propose to use the average value of skewness *i.e.* $\langle S_k \rangle$ to determine peak shape coefficients where the averaging is done over a range of u_m ($u_{m_i} \leq u_m \leq u_{m_f}$) for a fixed value of b. Therefore,

$$\langle S_k \rangle = \frac{1}{u_{m_f} - u_{m_i}} \int_{u_{m_i}}^{u_{m_f}} S_k \, du_m \tag{3.5.2}$$

Retaining the forms of the original peak shape relations (Eq. 3.2.4) as suggested by Chen (1969a), the new peak-shape relations are given by

$$E_{\alpha_x} = C_{\alpha_x} \frac{kT_m^2}{\alpha_x} - D_{\alpha_x}(2kT_m) \tag{3.5.3}$$

where C_{α_x} and D_{α_x} are peak shape coefficients estimated at the fractional intensity x and α_x stands for $\tau_x, \delta_x, \omega_x$ (Fig. 3.1.1). We express C_{α_x} and D_{α_x} in a linear relation with S_k as

$$C_{\alpha_x} = C_{1\alpha_x} S_k + C_{2\alpha_x} \tag{3.5.4}$$

$$D_{\alpha_x} = D_{1\alpha_x} S_k + D_{2\alpha_x} \tag{3.5.5}$$

Now we proceed to determine $C_{1\alpha_x}$, $C_{2\alpha_x}$, $D_{1\alpha_x}$, $D_{2\alpha_x}$ in Eq. (3.5.4) and (3.5.5) using $\langle S_k \rangle$. For a particular value of b, we generate TL peaks by varying u_m. For calculation of S_k, we consider all the datapoints for which $I(T) \geq \frac{I_m}{10}$ where the stepsize is $\Delta T = 0.1$ K. From each of these curves S_k, u_m and $\frac{u_p u_q}{u_m |u_p - u_q|}$ are estimated. Here u_p and u_q are any two of u_{1x}, u_m and u_{2x} where u_{1x}, u_{2x} are similar to u_m calculated at the temperatures T_{1x}, T_{2x} respectively (Fig. 3.1.1). For the three peak shape parameters $\tau_x, \delta_x, \omega_x$, we mention that

i) If $u_p = u_{1x}$ and $u_q = u_m$, in Eq. (3.5.3) $\alpha_x = \tau_x$ is to be considered.

ii) $u_p = u_m$ and $u_q = u_{2x}$ are to be considered to obtain the peak shape relation using δ_x.

iii) Peak shape coefficients for ω_x are obtained when $u_p = u_{1x}$ and $u_q = u_{2x}$.

For a particular value of b, Eq. (3.5.2) is used to calculate $\langle S_k \rangle$ from the set of S_k values obtained from each curve corresponding to different values of u_m. From $\left(u_m, \frac{u_p u_q}{u_m |u_p - u_q|} \right)$ data of all the curves generated for a particular b, a linear relation between u_m and $\frac{u_p u_q}{u_m |u_p - u_q|}$ can be fitted to obtain $C_{\alpha_x}, D_{\alpha_x}$ in Eq. (3.5.3) for that particular b. In this way we obtain C_{α_x}, D_{α_x}, $\langle S_k \rangle$ corresponding to a particular b. Now, by varying b in suitable stepsize and following the procedure discussed above, we obtain the sets of $[C_{\alpha_x}, D_{\alpha_x}, \langle S_k \rangle]$

corresponding to different values of b. The coefficients $C_{1\alpha_x}, C_{2\alpha_x}, D_{1\alpha_x}, D_{2\alpha_x}$ (Eqs. 3.5.4 and 3.5.5) are obtained from a linear fit of C_{α_x} and D_{α_x} with $\langle S_k \rangle$.

Summary of the methodology to estimate peak shape coefficients at arbitrary fractional intensity:

(i) Initialize b.

(ii) Initialize u_m.

(iii) Generate TL data by varying temperature systematically in step $\Delta T = 0.1$ K from $T_{0.1}^-$ to $T_{0.1}^+$. Where $T_{0.1}^-$ and $T_{0.1}^+$ are the temperatures at intensity $I = 0.1I_m$ on rising and falling side respectively.

(iv) Estimate S_k, u_{1x} and u_{2x} from the generated TL peak.

(v) Increase u_m. Go to step (iii) and calculate new set of S_k, u_x^- and u_x^+; repeat the process up to the highest value of u_m.

(vi) Calculate $\langle S_k \rangle$.

(vii) Plot $\dfrac{u_p u_q}{u_m |u_p - u_q|}$ against u_m and fit the plot by a linear relation and hence calculate C_{α_x} and D_{α_x}. Thus a set of $\langle S_k \rangle$, C_{α_x} and D_{α_x} is obtained for the initialized b.

(viii) Increase b. Go to step (ii) and form new set of $\langle S_k \rangle$, C_{α_x} and D_{α_x}; repeat the process up to the highest value of b.

(ix) Obtain a linear fit of C_{α_x} and D_{α_x} with respect to $\langle S_k \rangle$ to find out ($C_{1\alpha_x}$, $C_{2\alpha_x}$) and ($D_{1\alpha_x}$, $D_{2\alpha_x}$) for the particular value of x.

(x) Change the fractional intensity x as needed, repeat the entire procedure from (i).

Peak shape coefficients at different fractional intensities

The present peak shape formulae provide an opportunity to estimate E at different fractional intensities of the same TL curve using τ_x, δ_x, ω_x and by estimating skewness of the TL data. Thus the peak shape coefficients are to be determined for various x. For generating TL curves, we considered b within the range $0.7 \leqslant b \leqslant 2.5$ in step $\Delta b = 0.1$. For each value of b, we have taken E (eV) in step 0.1 within the range $0.2 \leqslant E \leqslant 2.0$ and varied s (in $\sec^{-1}$) in a wide range so that u_m lies within the limits $10 \leqslant u_m \leqslant 100$. In the present work we have increased u_m systematically in step of 5 for simulating glow curves. For a fixed value of b, S_k is calculated for simulated TL data corresponding to each u_m value.

In Table 3.5.1 we have listed the values of $C_{1\alpha_x}$, $C_{2\alpha_x}$, $D_{1\alpha_x}$, $D_{2\alpha_x}$ (Eqs. 3.5.4, 3.5.5) to determine C_{α_x}, D_{α_x} (Eq. 3.5.3) corresponding to different fractional intensities

Table 3.5.1: Linear constants in Eqs. (3.5.4, 3.5.5) for the determination of peak shape coefficients in Eq. (3.5.3) estimated at different values of x.

x	α	$C_{1\alpha_x}$	$C_{2\alpha_x}$	$D_{1\alpha_x}$	$D_{2\alpha_x}$
1/4	τ	0.7627	2.5570	0.8984	1.7609
	δ	2.9453	2.3730	0.3309	0.0784
	ω	3.6983	4.9219	0.1250	0.8806
1/2	τ	0.6591	1.6971	0.9685	1.4354
	δ	1.7186	1.6064	0.6711	0.3318
	ω	2.3753	3.3012	0.5931	0.8689
2/3	τ	0.5652	1.2603	0.9985	1.2783
	δ	1.1760	1.2075	0.8022	0.4608
	ω	1.7402	2.4669	0.7719	0.8620

using the shape parameters τ_x, δ_x and ω_x. We note that by adopting the present methodology it is possible to determine peak shape coefficients for any reasonable value of x. In Table 3.5.1, the coefficients at $x = \frac{1}{4}, \frac{1}{2}, \frac{2}{3}$ are listed that can be used directly on simulated as well as experimental glow curves to extract E using skewness of the TL data.

It is important to note that the role of average skewness in the present work is only to estimate the coefficients C_{α_x} and D_{α_x}. For practical purposes the skewness of a TL dataset can be used directly in Eqs. 3.5.4 and 3.5.5. The required coefficients are given above in Table 3.5.1.

3.5.3 Results and discussions on applicability of present peak shape method to different TL peaks

To check the applicability of the present method we have applied the peak shape coefficients (C_{α_x}, D_{α_x}) to evaluate E from TL curves generated in GOK and OTOR models and finally applied them on some experimental TL peaks.

Application to TL peaks simulated in GOK model

TL glow curves in GOK model are generated by using Eqs. (1.2.3, 1.2.10) in linear heating scheme. The heating rate (β) is 1 K.sec^{-1} and the input values of activation energy (E_{in})

Table 3.5.2: Values of $E_{\tau x}$, $E_{\delta x}$, $E_{\omega x}$ (eV) estimated using the present peak shape method from TL curves simulated in GOK model. Here $E_{in} = 1$ eV, $s_{in} = 10^{12}$ sec^{-1} and $\beta = 1$ K.sec^{-1}.

b	T_m (K)	S_k	x	τ	δ	ω	$E_{\tau x}$	$E_{\delta x}$	$E_{\omega x}$
1	384.57	–0.3745	1/4	26.56	16.70	43.26	1.00	1.04	1.02
			1/2	17.36	12.48	29.84	1.01	1.03	1.02
			2/3	12.70	9.87	22.56	1.01	1.02	1.02
1.5	384.22	–0.1062	1/4	28.38	25.09	53.48	1.00	1.07	1.04
			1/2	19.03	17.38	36.41	1.01	1.05	1.03
			2/3	14.17	13.21	27.38	1.01	1.04	1.02
2	383.88	0.0973	1/4	29.75	33.24	62.99	1.00	1.02	1.01
			1/2	20.29	21.82	42.10	1.00	1.02	1.01
			2/3	15.29	16.13	31.42	1.01	1.01	1.01

and frequency factor (s_{in}) are 1 eV and 10^{12} sec^{-1} respectively. The coefficients given in Table 3.5.1 are used to estimate the output values $E_{\tau x}$, $E_{\delta x}$ and $E_{\omega x}$. The results are given in Table 3.5.2 where first order, second order and general order (b=1.5) kinetics are taken into account. It is evident from Table 3.5.2 that the extracted values of activation energy are quite consistent with the input value $E_{in} = 1$ eV. Table 3.5.2 also reveals that $E_{\tau x}$ values show comparatively better agreement with E_{in} whereas $E_{\delta x}$ shows maximum deviation.

Application to TL peaks simulated in OTOR model

In the next phase, we investigate the applicability of the present peak shape formulae in case of OTOR glow curves. For curve simulation, the input values of activation energy and frequency factor are taken in the range $0.5 \leqslant E_{in} \leqslant 1.5$ eV and $10^7 \leqslant s_{in} \leqslant 10^{13}$ sec^{-1} respectively. The filling ratio $f = \dfrac{n_0}{N}$ is taken from 0.1 to 1 to cover almost the entire range of trap saturation. The ratio of retrapping to recombination probabilities (R) is considered by varying it in step $\Delta R = 0.01$ when $0 \leq R \leq 1$ and in step $\Delta R = 1$ when $1 < R \leq 100$ corresponding to heavy retrapping situations during the heating stage.

In Table 3.5.3, $E_{\tau x}$, $E_{\delta x}$ and $E_{\omega x}$ extracted from TL peaks generated for some selected values of f and R with input values $E_{in} = 1$eV and $s_{in} = 10^{12}$ sec^{-1} are given.

Table 3.5.3: Activation energies $E_{\tau x}$, $E_{\delta x}$, $E_{\omega x}$ (eV) estimated using the present peak shape method from TL curves simulated in OTOR model. Here $E_{in} = 1$ eV, $s_{in} = 10^{12}$ $\sec^{-1}$ and $\beta = 1$ K.$\sec^{-1}$.

f	R	T_m (K)	S_k	x	τ	δ	ω	$E_{\tau x}$	$E_{\delta x}$	$E_{\omega x}$
0.1	0	384.57	–0.3633	1/4	26.56	16.70	43.26	1.01	1.06	1.03
				1/2	17.35	12.49	29.84	1.01	1.05	1.03
				2/3	12.70	9.88	22.58	1.01	1.04	1.02
	0.5	405.08	0.0900	1/4	32.60	36.03	68.63	1.01	1.04	1.03
				1/2	22.18	23.62	45.80	1.02	1.04	1.03
				2/3	16.70	17.48	34.18	1.02	1.04	1.03
	1	413.28	0.1052	1/4	34.19	38.51	72.70	1.01	1.03	1.02
				1/2	23.35	25.24	48.59	1.01	1.02	1.02
				2/3	17.62	18.67	36.29	1.01	1.02	1.01
	10	446.07	0.1250	1/4	39.87	46.04	85.91	1.00	1.02	1.01
				1/2	27.36	30.15	57.51	1.00	1.01	1.01
				2/3	20.70	22.27	42.97	1.00	1.01	1.00
0.5	0	384.57	–0.3633	1/4	26.56	16.70	43.26	1.01	1.06	1.03
				1/2	17.35	12.49	29.84	1.01	1.05	1.03
				2/3	12.70	9.88	22.58	1.01	1.04	1.02
	0.5	388.31	0.0395	1/4	29.27	30.33	59.60	1.03	1.08	1.06
				1/2	19.73	19.92	39.65	1.04	1.08	1.06
				2/3	14.76	14.80	29.56	1.05	1.08	1.06
	1	392.29	0.1006	1/4	30.99	34.71	65.70	1.00	1.02	1.02
				1/2	21.14	22.77	43.91	1.01	1.02	1.01
				2/3	15.95	16.85	32.80	1.01	1.02	1.01
	10	416.38	0.1676	1/4	37.46	45.77	83.23	0.94	0.93	0.93
				1/2	26.17	30.28	56.45	0.92	0.91	0.91
				2/3	20.02	22.43	42.45	0.91	0.90	0.90
1	0	384.57	–0.3633	1/4	26.56	16.7	43.26	1.01	1.06	1.03
				1/2	17.35	12.49	29.84	1.01	1.05	1.03
				2/3	12.70	9.88	22.58	1.01	1.04	1.02
	0.5	383.31	–0.0081	1/4	27.97	27.3	55.27	1.04	1.10	1.07
				1/2	18.71	18.03	36.74	1.06	1.11	1.09
				2/3	13.93	13.45	27.38	1.06	1.11	1.09
	1	383.88	0.0985	1/4	29.75	33.24	62.99	1.00	1.02	1.01
				1/2	20.29	21.81	42.10	1.00	1.02	1.01
				2/3	15.30	16.14	31.44	1.01	1.02	1.01
	10	400.09	0.0673	1/4	48.04	52.25	100.29	0.63	0.68	0.66
				1/2	34.94	35.82	70.76	0.59	0.64	0.62
				2/3	26.96	27.11	54.07	0.57	0.63	0.60

It is observed that $E_{\tau x}$ values are more in agreement with E_{in} whereas $E_{\delta x}$ values show maximum departure, similar to GOK curves. The results are consistent for the TL peaks when $0 \leqslant R \leqslant 1$. As trap saturation increases, the error in activation energy for $R = 0.5$ goes up to 6% and 11% when $E_{\tau x}$ and $E_{\delta x}$ are considered respectively. For $R > 1$, *i.e.* in case of heavy retrapping, $E_{\tau x}$, $E_{\delta x}$ and $E_{\omega x}$ yield acceptable values only when f is quite small which corresponds to low-dose irradiation. In case of saturated or nearly saturated TL peaks (*i.e.* $f \simeq 1$) with heavy retrapping ($R > 1$), the output values of activation energy are quite away from the input value. Table 3.5.3 shows that even for $f = 0.5$ and $R = 10$, $E_{\tau x}$, $E_{\delta x}$ and $E_{\omega x}$ show deviation from E_{in} and are underestimated by as much as 10%. The results show that for $f = 1$ and $R = 10$, the version of peak shape method using skewness as a symmetry parameter does not work at all. This observation is consistent with earlier reports of other versions of peak shape method (μ'_g as symmetry parameter) (Karmakar et al., 2017; Sadek et al., 2014; Sunta et al., 1999) on the limitation of peak shape methods in case of saturated TL peaks with heavy retrapping.

Table 3.5.4: Activation energies estimated by present peak shape method from OTOR glow peaks simulated with different input parameters.

Input parameters				T_m	S_k	$E_{out} = E_{\tau_x}$		
E	s	f	R			$x = \frac{1}{4}$	$x = \frac{1}{2}$	$x = \frac{2}{3}$
0.5	10^7	0.1	0.1	314.76	0.0458	0.52	0.53	0.54
			10	387.87	0.1935	0.51	0.51	0.51
		0.9	0.1	306.08	–0.1933	0.52	0.53	0.53
			10	327.10	0.2356	0.38	0.36	0.34
	10^{13}	0.1	0.1	186.08	–0.0018	0.52	0.52	0.53
			10	210.92	0.1197	0.50	0.50	0.50
		0.9	0.1	182.81	–0.2351	0.51	0.52	0.52
			10	191.20	0.1319	0.37	0.35	0.34
1.5	10^7	0.1	0.1	896.07	0.0399	1.57	1.59	1.61
			10	1092.93	0.1843	1.51	1.52	1.52
		0.9	0.1	872.41	–0.1985	1.56	1.58	1.59
			10	930.14	0.2235	1.13	1.06	1.03
	10^{13}	0.1	0.1	540.36	–0.0043	1.55	1.57	1.58
			10	610.07	0.1159	1.49	1.49	1.49
		0.9	0.1	531.13	–0.2361	1.54	1.56	1.57
			10	554.83	0.1271	1.10	1.03	1.01

For the sake of completeness we have given a representative set of present results corresponding to some other values of input parameters in Table 3.5.4. However, as output values of activation energy (E_{out}) we have presented $E_{\tau x}$ only. In Fig. 3.5.4 we have plotted

$E_{\tau x}$ measured at $x = \frac{1}{2}$ against R for different filling ratios (f). Fig. 3.5.4 represents the data corresponding to $E_{in} = 1$eV and $s_{in} = 10^{12}$ used as input parameters, though similar variation of $E_{\tau x}$ is observed for other values of E_{in} and s_{in} with different x. Moreover, in all the cases, $E_{\delta x}$ and $E_{\omega x}$ also exhibit similar pattern. It is seen from Fig. 3.5.4 that the present method yields quite consistent values of activation energy (E_{out}) near $R = 0$ and 1 whereas, within the range $0 < R < 1$, the estimated activation energy is marginally overestimated. In heavy retrapping region ($R > 1$), the activation energy is quite consistent with E_{in} for low values of f (*i.e.* $f \leq 0.4$). It is also evident from Fig. 3.5.4 that for heavy retrapping cases ($R > 1$) the deviation of output values (E_{out}) from E_{in} grows higher as trap filling increases.

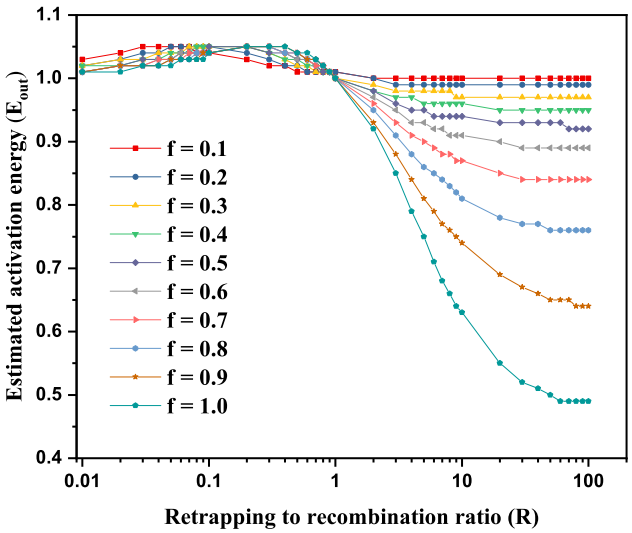

Figure 3.5.4: Estimated values of activation energy plotted against R measured at fractional intensity $x = 0.5$. Here $E_{in} = 1\ eV$, $s_{in} = 10^{12}$ sec^{-1} and $\beta = 1 K sec^{-1}$.

3.5.4 Comparative discussion on applicability of present method with other versions peak shape methods

To validate the applicability of skewness as symmetry parameter in peak shape method we have compared the present results with some other variants of peak shape methods (Chen, 1969a; Kitis and Pagonis, 2007). The activation energies derived from TL curves simulated in GOK and OTOR models using different methods are given in Table 3.5.5. It is evident that the present results are quite in agreement with those obtained by other established methods.

Table 3.5.5: Comparison of activation enrgies (eV) obtained using present peak shape method and other established peak shape methods (Chen, 1969a; Kitis and Pagonis, 2007). Here E_{in} =1 eV, $s_{in} = 10^{12}$ sec^{-1} are used.

Model	Input parameters		T_m (K)	$x = \frac{I}{I_m}$	Present method			Other methods		
					E_τ	E_δ	E_ω	E_τ	E_δ	E_ω
GOK	b = 1		384.57	1/4	1.00	1.04	1.02	1.01[a]	1.05[a]	1.03[a]
				1/2	1.01	1.03	1.02	1.01[a]	1.04[a]	1.02[a]
								1.00[b]	0.98[b]	1.00[b]
								0.99[c]	1.00[c]	0.99[c]
				2/3	1.01	1.02	1.02	1.01[a]	1.04[a]	1.02[a]
	b = 1.5		384.22	1/4	1.00	1.07	1.04	1.01[a]	1.09[a]	1.05[a]
				1/2	1.01	1.05	1.03	1.01[a]	1.07[a]	1.04[a]
								1.00[b]	1.02[b]	1.02[b]
								0.99[c]	1.00[c]	0.99[c]
				2/3	1.01	1.04	1.02	1.02[a]	1.06[a]	1.04[a]
	b = 2		383.88	1/4	1.00	1.02	1.01	1.01[a]	1.03[a]	1.02[a]
				1/2	1.00	1.02	1.01	1.01[a]	1.02[a]	1.02[a]
								1.00[b]	0.99[b]	1.00[b]
								0.99[c]	1.01[c]	0.99[c]
				2/3	1.01	1.01	1.01	1.01[a]	1.02[a]	1.01[a]
OTOR	f = 0.5	R = 0	384.57	1/4	1.01	1.06	1.03	1.01[a]	1.05[a]	1.03[a]
				1/2	1.01	1.05	1.03	1.01[a]	1.04[a]	1.02[a]
								1.00[b]	0.99[b]	1.00[b]
								0.99[c]	1.00[c]	0.99[c]
				2/3	1.01	1.04	1.02	1.01[a]	1.04[a]	1.02[a]
		R = 0.5	388.30	1/4	1.03	1.08	1.06	1.03[a]	1.08[a]	1.06[a]
				1/2	1.04	1.08	1.06	1.04[a]	1.07[a]	1.05[a]
								1.03[b]	1.03[b]	1.04[b]
								1.01[c]	0.99[c]	0.99[c]
				2/3	1.05	1.08	1.06	1.04[a]	1.07[a]	1.06[a]
		R = 1	392.29	1/4	1	1.02	1.02	1.01[a]	1.03[a]	1.02[a]
				1/2	1.01	1.02	1.01	1.01[a]	1.02[a]	1.01[a]
								1.00[b]	0.99[b]	1.00[b]
								0.99[c]	1.01[c]	0.99[c]
				2/3	1.01	1.02	1.01	1.01[a]	1.02[a]	1.01[a]

a: present peak shape method using μ'_g

b: Chen (1969a)

c: Kitis and Pagonis (2007)

It is to note that both the methods of Chen (1969a) and Kitis and Pagonis (2007) are applicable for $x = 0.5$ whereas the present method provides a scope to compare the present results for various values of x. Table 3.5.5 exhibits that present peak shape method using skewness as the symmetry parameter more often than not yields better results than the present method where the symmetry factor was used as symmetry parameter.

3.5.5 Application to experimental TL peaks

We have applied the present peakshape method in case of some widely studied TL peaks. We note that the present peakshape method is applicable for single or well isolated glow peaks and hence we have selected few such peaks reported in literature. In all the cases we have picked up the data from the experimental curves by using the browser-based software tool WebPlotDigitizer and the skewness (S_k) is calculated using Eq. (3.5.1). For the 110^{o}C peak of quartz, we have used the glow curves reported by Petrov and Bailiff (1995) as well as by Lovedy (2017) where the values of activation energy were reported as 0.99 and 0.973 eV respectively. The present method yields the activation energies as 1.03 eV for the dataset of Petrov and Bailiff (1995) and 1.05 eV for that of Lovedy (2017). We have also considered the TL peaks of MgO which are well separated and applied the present method on the 1st peak of the glow curve reported by Thomas and Houston (1964). The reported value (Thomas and Houston, 1964) of activation energy was 0.66 eV and the present calculation comes out to be 0.71 eV.

3.5.6 Limitation of peak shape method

To have a deeper insight on the limitation of peak shape relations for heavy retrapping cases, we have plotted in Fig. 3.5.5 the percentage error in activation energy $\delta E_{\tau_x}(\%)$ measured at $x = \frac{1}{2}$ with respect to f for different values of R. We observe that the error in E becomes significant for $R > 1$. To be precise, for $R > 1$, the activation energy is underestimated and the magnitude of error gradually increases as f increases. For lower filling ratios, (*i.e.* when $f \leq 0.4$) the present method works well even for $R > 1$ as $|\delta E_{\tau_x}|$ lie within 5%. The magnitude of error increases with increase in R also, however, Fig. 3.5.5 reveals that this error does not change much for $R > 50$.

Results of the study on S_k of TL peaks generated with various values of R are shown in Fig. 3.5.6 for f. For $0 \leqslant R \leqslant 1$, S_k increases gradually with R when f is fixed. When R is fixed within this range, S_k decreases as f increases. Values of S_k for all f are equal at $R = 1$. The pattern of variation of S_k changes remarkably beyond $R > 1$ where

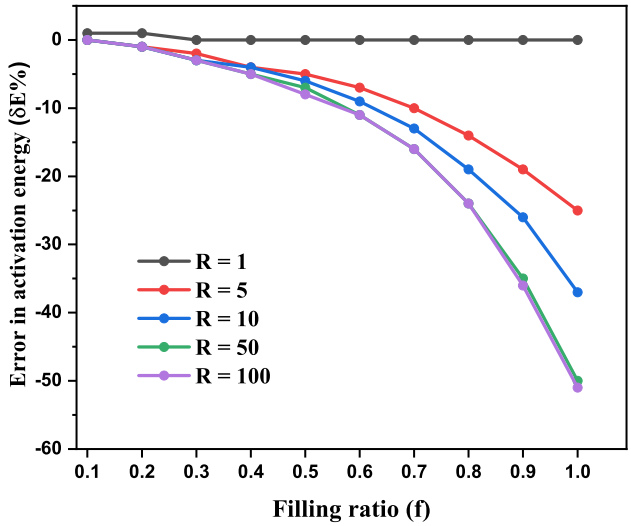

Figure 3.5.5: Inherent error (δE%) plotted against f for different values of R. Here $E_{in} = 1\ eV$, $s_{in} = 10^{12}$, $x = 0.5$ and $\beta = 1 K sec^{-1}$ is considered

crossing of the plots takes place. For low values of f, S_k slowly increases with R in an almost well-behaved manner. For high values of f, this pattern becomes quite anomalous for $R > 1$ and the present peak shape method fails in such cases.

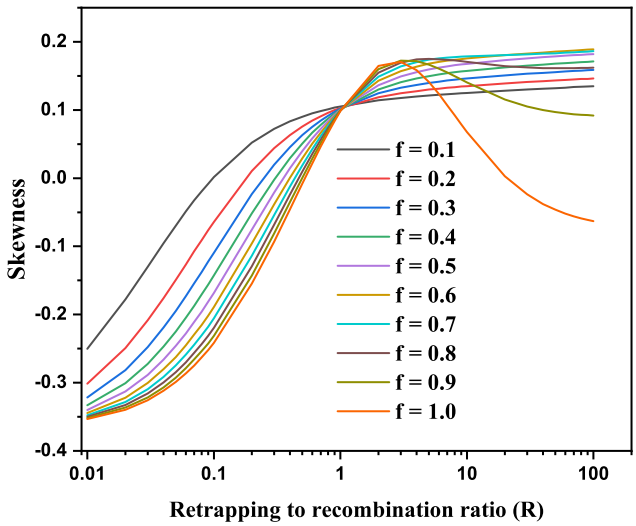

Figure 3.5.6: Variation of skewness (S_k) plotted against R for TL peaks simulated in OTOR model. Here $E_{in} = 1$ eV, $s_{in} = 10^{12}$ sec^{-1}, $\beta = 1$ K.sec^{-1}.

Chapter 4

Temperature dependence of frequency factor

4.1 Introduction to temperature dependent frequency factor

Insulating materials can possess localized energy levels within their forbidden energy gap which are created either naturally or artificially. When such a material is exposed to radiation *e.g.* γ-ray, X-ray *etc.*, electrons and holes are generated in conduction and valence band respectively. Subsequently the electrons from the conduction band are trapped in electron traps and the holes in hole traps (luminescence centres). Various stimulation methods are used to detrap those trapped electrons to produce the respective stimulated luminescence signals. Depending on the type of stimulation, the processes are named as thermally stimulated luminescence (TSL), optically stimulated luminescence (OSL) *etc.* For thermoluminescence the stimulating function is written as

$$p(t) = se^{-\frac{E}{kT(t)}} \tag{4.1.1}$$

where E is the activation energy or trap depth, k is the Boltzmann constant and s is the pre-exponential factor (in $\sec^{-1}$) known as frequency factor which varies slowly with temperature. The temperature dependence of 's' is in the focus of the present study. To impart a physical significance to s, the trap may be regarded as a potential box (Chen, 1969a) and s may be considered as the product of the reflection coefficient and the frequency with which the trapped electron strikes the wall of the box (Gurney and Mott, 1940). The pre-exponential factor was reported more explicitely from comprehensive theoretical background (Bosacchi et al., 1974; Bube, 1960; Simmons and Taylor, 1971) and can be expressed as

$$s(T) = N_c(T)v_t(T)\sigma_n(T) \tag{4.1.2}$$

Here N_c is the effective density of states in the conduction band and v_t is the thermal velocity of electrons which are approximated as

$$N_c = 2\left(\frac{km^*T}{2\pi\hbar^2}\right)^{3/2} \qquad \text{and} \qquad v_t = \sqrt{\frac{3kT}{m^*}} \tag{4.1.3}$$

m^* is the effective mass of electron. σ_n is the transition cross section for trapped electrons to transit into conduction band which is same as the retrapping cross section according to the principle of detailed balance (Salzmann, 1998). Though there is no explicit expression available in literature for σ_n, it has been reported to vary with temperature differently for different materials (Bemski, 1958; Lax, 1960; Lewandowski and McKeever, 1991). The

capture cross section may depend on temperature as $\sigma_n \sim T^{-l}$, where l is a positive number that has been observed to have values in the range $0 \leq l \leq 4$ (Lax, 1960). Thus using Eq. (4.1.3) the temperature dependence of frequency factor (Bhattacharya et al., 2000; Chen, 1969a; Fleming, 1990; Karmakar et al., 2010; Keating, 1961; Shambhunath Singh et al., 2000) can be expressed from equation (4.1.2) as

$$s(T) = s_0 T^a \tag{4.1.4}$$

where a is a number with values $-2 \leq a \leq 2$ and s_0 is the temperature independent part of the frequency factor.

A theoretical account explaining the impact of temperature dependent frequency factor (TDFF) on TL peaks and subsequently a method that estimates the activation energy and temperature exponent a from such peaks was reported by Keating (1961) using General Order Kinetic (GOK) model. In a later work, Fleming (1990) showed that it is not possible to determine the value of a from TL measurements alone. Thus determination of the index a from separate experiment not only enhances experimental intricacy, it also introduces additional experimental error. For this reason all the widely used methods (Chen and Kirsh, 1981b) assume the frequency factor to be temperature independent (*i.e.* $a = 0$) for TL analysis. However, the quantitative idea about the error originating from this approximation is important for having a deeper physical insight of the underlying processes and also for practical measurements.

Theoretical studies of TL processes considering TDFF is quite limited in literature and almost all of them are carried out using the GOK model. However, GOK model has its inherent limitations for which it is imperative to go beyond GOK model. Models based on the band theory *e.g.* One Trap One Recombination center (OTOR), Interactive Multi Trap System (IMTS) *etc.* may be adopted for this purpose. Lovedy Singh (2020) studied the TL process in OTOR model considering TDFF, where only T^2 dependence of s (*i.e.* $a = 2$ in Eq. 4.1.4) was considered and a significant mismatch was visible between the TL curves generated for $a = 2$ and $a = 0$. Thus an elaborate study of the TL process in OTOR model for the entire range of a should be carried out which may find importance not only for TL studies but also for other thermally stimulated processes like thermally stimulated conductivity (TSC) *etc.*

The primary difficulty in the theoretical analysis using TDFF is to reproduce the same curve for different values of a (which is not known beforehand in experimental scenario) by tuning other TL parameters, which has been also mentioned by Lovedy Singh

(2020). In this work, a comprehensive study using OTOR model for investigating the effect of TDFF on TL peaks is reported. Analytical expression for TL intensity is derived by solving relevant differential equations. An account of the procedure to simulate the same TL peak for different values of a ($-2 \leq a \leq 2$) is given. The applicability of the present method of peak simulation is tested in IMTS model also for a sample dataset using different values of a. However, the present work is in the purview of OTOR model and hence, for further analysis, only the OTOR model is considered.

During glow curve analysis in an experimental scenario it is a usual practice to avoid the temperature dependence of frequency factor of an experimentally obtained glow peak. All the methods of analysis also have been developed with the same notion. Therefore it is an important issue to assess the level of compromise made with the accuracy of the extracted parameters, particularly the activation energy, when derived from a glow curve where frequency factor was considered to be temperature independent. We have carried out a detail investigation in this chapter. Firstly we discuss the method of simulating the same glow curve considering TDFF in OTOR and IMTS model. Then we have extracted E from these glow curves using different methods of TL analysis which were primarily developed considering $a = 0$. Hence we have investigated the inherent error in the output due to the impact of TDFF.

4.2 TL equations in OTOR model using temperature dependent frequency factor

The basic charge trafficking equations in OTOR model (Sunta, 2014) can be recast considering TDFF as

$$\frac{dn_c}{dt} = ns_0T^a e^{-\frac{E}{kT}} - A_n(N-n)n_c - A_h n_c n_h \tag{4.2.1}$$

$$\frac{dn}{dt} = -ns_0T^a e^{-\frac{E}{kT}} + A_n(N-n)n_c \tag{4.2.2}$$

$$\text{and} \quad I(t) = -\frac{dn_h}{dt} = A_h n_c n_h \tag{4.2.3}$$

The parameters used in the equations (4.2.1–4.2.3) are: n_c = concentration of conduction band electrons, n = concentration of trapped electrons, N = total trap concentration, n_h = concentration of holes or recombination centre, k = Boltzmann constant, A_n = retrapping probability, A_h = recombination probability and T = absolute temperature at heating time t. The charge neutrality condition is given by: $n_h = n + n_c$. The quasi-equilibrium (QE)

approximations *i.e.* $\left|\frac{dn_c}{dt}\right| << \left|\frac{dn}{dt}\right|$ and $n_c << n$ can also be applied here as, during the TL process, the heating is generally done rather slowly Dussel and Bube (1967); Sunta (2014). Considering this, the TL intensity may be expressed as

$$I(t) \simeq -\frac{dn}{dt} = \frac{n^2 s_0 T^a e^{-\frac{E}{kT}}}{n(1-R)+NR} \tag{4.2.4}$$

where $R = \frac{A_n}{A_h}$. It may be noted that, in an earlier work, Halperin and Braner (1960) mentioned the dependence of σ_n on A_n and v_t as $\sigma_n = \frac{A_n}{v_t}$ where A_n was considered independent of tempereature. In the present study, A_n and A_h are incoporated in the process of peak generation through the parameter R. As R is the ratio of retrapping to recombination probabilities, it is approximated here as independent of temperature.

In linear heating scheme *i.e.* $T = T_0 + \beta t$ where T_0 is the initial temperature and β is the heating rate, equation (4.2.4) reduces to

$$I(T) \simeq -\frac{dn}{dT} = -\frac{1}{\beta}\frac{dn}{dt} = \frac{n^2 s_0 T^a e^{-\frac{E}{kT}}}{\beta\left[n(1-R)+NR\right]} \tag{4.2.5}$$

The initial condition $n = n_0$ at $T = T_0$ is employed to solve Eq. (4.2.5). Here n_0 is the initial concentration of trapped electrons. The initial trap filling ratio is defined as $f = \frac{n_0}{N}$. Eq. (4.2.5) can be solved numerically or in terms of Lambert-W function to yield TL intensity in OTOR model considering TDFF. The analytical solution of Eq. (4.2.5) can be expressed as (Kitis and Vlachos, 2013)

- For $R < 1$

$$\begin{aligned} I(T) &= \frac{s_0 T^a N R \exp\left(-\frac{E}{kT}\right)}{\beta\left(1-R\right)^2 W[e^{z_1(T)}]\left(1+W[e^{z_1(T)}]\right)} \\ \text{where } z_1(T) &= \frac{1}{c} - \ln c + \frac{s_0}{\beta(1-R)}\int_{T_0}^{T} T'^a \exp\left(-\frac{E}{kT'}\right) dT' \\ \text{and } c &= \frac{n_0}{N}\frac{(1-R)}{R} = f\frac{(1-R)}{R} \end{aligned} \tag{4.2.6}$$

- For $R > 1$

$$\begin{aligned} I(T) &= \frac{s_0 T^a N R \exp\left(-\frac{E}{kT}\right)}{\beta\left(1-R\right)^2 W[-1,-e^{-z_2(T)}]\left(1+W[-1,-e^{z_2(T)}]\right)} \\ \text{where } z_2(T) &= \frac{1}{|c|} + \ln(|c|) + \frac{s_0}{(1-R)\beta}\int_{T_0}^{T} T'^a \exp\left(-\frac{E}{kT'}\right) dT' \end{aligned} \tag{4.2.7}$$

In the present study we have considered the cases where R lies between 0 and 1.

For simulating same glow peak for different values of a, the value of s_0 for various a (Eq. 4.1.4) is to be evaluated which can be obtained from peak maximum condition. During the study the peak maximum condition with TDFF in OTOR model is developed analytically using Lambert-W function (Corless et al., 1997) as well as Wright ω function (Corless and Jeffrey, 2002). The peak position can be located from the maximum condition that can be obtained from Eq. (4.2.6) by setting $\frac{dI(T)}{dT} = 0$. However for mathematical convenience we set $\frac{d\ln I(T)}{dT} = 0$ and obtain

$$\frac{d\ln I(T)}{dT} = \frac{a}{T} + \frac{E}{kT^2} - \frac{d\ln[W[e^{z_1(T)}] + W[e^{z_1(T)}]^2]}{dW[e^{z_1(T)}]}\frac{dW[e^{z_1(T)}]}{dz_1(T)}\frac{dz_1(T)}{dT} \tag{4.2.8}$$

The derivative of $W[e^{z_1(T)}]$ is given by Corless et al. (1997)

$$\frac{dW[e^{z_1(T)}]}{dz_1(T)} = \frac{W[e^{z_1(T)}]}{1+W[e^{z_1(T)}]} \tag{4.2.9}$$

Setting $\frac{d\ln I(T)}{dT} = 0$ in Eq. (4.2.8) and using Eq. (4.2.9), the maximum condition can be expressed after simplification as

$$\frac{a}{T_m} + \frac{E}{kT_m^2} = \frac{s_0}{(1-R)\beta}\left[\frac{1+2W[e^{z_1(T_m)}]}{(1+W[e^{z_1(T_m)}])^2}\right] T_m^a \exp\left(-\frac{E}{kT_m}\right) \tag{4.2.10}$$

The TL intensity in OTOR model can also be expressed in terms of Wright ω (denoted by $\omega(z)$) function when $R < 1$ (Singh and Gartia, 2013). The Wright ω function is related to the Lambert-W function as $\omega(z) = W_{k(z)}[e^z]$, where $k(z) = \frac{Im(z)-\pi}{2\pi}$ and hence the TL intensity for TDFF in Eq. (4.2.6) can be recast as

$$I(T) = \frac{s_0 T^a N R \exp\left(-\frac{E}{kT}\right)}{\beta\,(1-R)^2\,\omega(z_1(T))(1+\omega(z_1(T)))} \tag{4.2.11}$$

The peak maximum condition takes the form

$$\frac{a}{T_m} + \frac{E}{kT_m^2} = \frac{s_0}{(1-R)\beta}\left[\frac{1+2\omega(z_1(T_m))}{(1+\omega(z_1(T_m)))^2}\right] T_m^a \exp\left(-\frac{E}{kT_m}\right) \tag{4.2.12}$$

where the derivative of $\omega(z_1(T))$ is given by (Corless and Jeffrey, 2002)

$$\frac{d\omega(z_1(T))}{dz_1(T)} = \frac{\omega(z_1(T))}{1+\omega(z_1(T))}. \tag{4.2.13}$$

4.3 Glow curve simulation

The prerequisite in investigating the effect of temperature dependence of frequency factor on TL peaks is to simulate the same peak for different values of a (Eq. 4.1.4) which poses a challenge before theoretical analysis. If a particular TL curve can not be reproduced for different values of a, it will not be possible to apply any method to extract trapping parameters from experimental peaks by glow curve analysis. In this study we have been able to simulate the same TL curve for different values of a lying in the range $-2 \leq a \leq 2$. For obvious reasons the determined values of s_0 and E corresponding to a peak will vary if a is varied. It is reported in literature that when TDFF is taken into account, a correction term akT_m is to be incorporated in E (Aramu et al., 1966; Chen, 1969a,b; Chen and Kirsh, 1981b; Ingraham and Marier, 1964). Since T_m is known for an experimental TL peak, s_0 can be determined for a particular value of a from the peak maximum condition (Eqs. 4.2.10 or 4.2.12) with $E = E_0 - akT_m$ where E_0 is the input value of E for $a = 0$. We have observed that the exclusion of the correction factor akT_m results in a mismatch in peak height and a deviation in peak position (T_m) occurs if s_0 is not estimated properly. We have simulated glow curves for various values of a and the matching among the glow curves are quite remarkable as depicted in Fig. 4.3.1.

Table 4.3.1: The input parameters used for different values of a to yield the same glow peak simulated in OTOR model when s depends on temperature. The peaks are given in Fig. 4.3.1(a)–(c). Here $E = E_0 - akT_m$. $E_0 = 1$ eV and $f = 0.5$ are considered for all the cases.

a	E (eV)	s_0 $(sec^{-1}K^{-a})$	$R = 0.0$		$R = 0.5$		$R = 1.0$	
			T_m (K)	$s_m(sec^{-1})$	T_m (K)	$s_m(sec^{-1})$	T_m (K)	$s_m(sec^{-1})$
–2	1.067	9.18×10^{17}	386.8	6.14×10^{12}	390.6	6.02×10^{12}	394.6	5.90×10^{12}
–1	1.033	8.71×10^{14}		2.25×10^{12}		2.23×10^{12}		2.21×10^{12}
0	1.0	8.30×10^{11}		8.30×10^{11}		8.30×10^{11}		8.30×10^{11}
1	0.967	7.90×10^{08}		3.05×10^{11}		3.08×10^{11}		3.12×10^{11}
2	0.933	7.49×10^{05}		1.12×10^{11}		1.14×10^{11}		1.17×10^{11}

In Fig. 4.3.1(a) TL glow peaks for $R = 0$ and $f = 0.5$ simulated in OTOR model are shown where s is temperature dependent. The $R = 0$ peak is equivalent to the first order case in GOK model. Fig. 4.3.1(a) exhibits that the same TL peak with $T_m = 386.8K$ is generated with various values of a. Similar glow curves for $R = 0.5$ (general order case in GOK model) and $R = 1$ (second order in GOK model) are given in Fig. 4.3.1(b) and (c) respectively. The input parameters used for simulating the peaks in Fig. 4.3.1(a)–(c) are

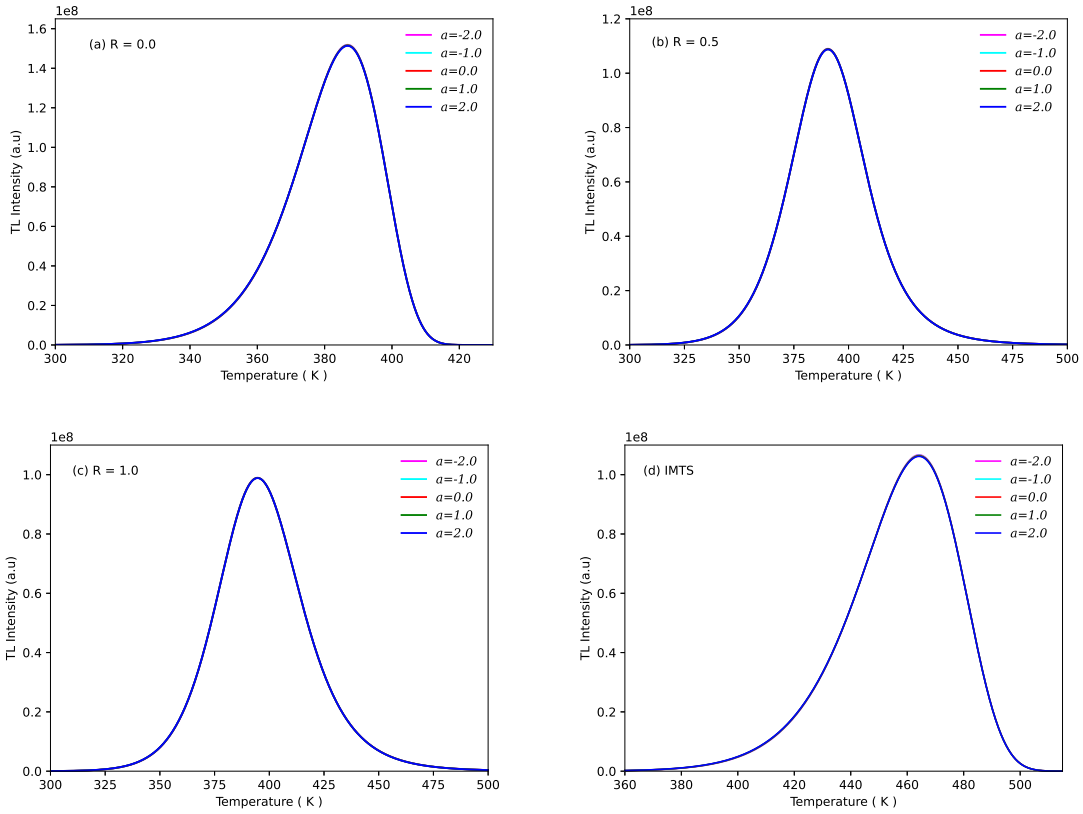

Figure 4.3.1: Simulation of TL glow peaks for TDFF. (a)–(c) Particular TL peak simulated in OTOR model with different values of a where $s = s_0 T^a$. Here a has been considered in the range $-2 \leq a \leq 2$. Corresponding input parameters are given in Table 4.3.1. (d) IMTS glow peak, equivalent to first order peak in GOK model, simulated for temperature dependent s by varying a. For peak generation, we have taken $E_0 = 1$ eV and $\beta = 1$ Ksec^{-1}.

given in Table 4.3.1. The peak maximum (T_m) is seen to shift as R changes and the values of T_m are also tabulated. In addition to that, we have also given the values of frequency factor at peak temperature $s_m = s(T_m) = s_0 T_m^a$ in Table 4.3.1 for convenience. We have studied numerous TL curves for different values of input parameters (E, s_0, f, R) covering a wide range of T_m and observed that the present methodology can reproduce the same TL curve for different values of a. We have extended the present method of peak simulation in IMTS model also and found it to be equally applicable which is evident from Fig. 4.3.1(d). The required differential equations governing the TL process for $a = 0$ in IMTS model are given in Eqs. (1.2.30 – 1.2.33) at introduction chapter. The necessary modification for $a \neq 0$ is done in a similar way as it is done in OTOR model in Eqs. (4.2.1 – 4.2.3).

We have also investigated the variation of frequency factor with respect to temperature for different values of a related to a particular peak and repeated the study for a

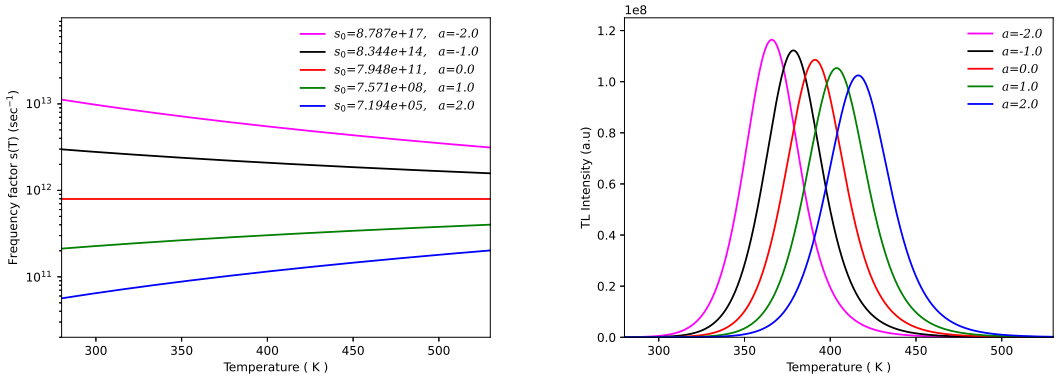

Figure 4.3.2: (a)Variation of frequency factors with temperature for different values of a. Here s_0 values are given in unit sec^{-1}/K^a. The vertical axis is presented in log scale. (b) The TL peaks corresponding to each $s(T)$ in figure (a) are shown. Here $E = 1$, $R = 0.5$ and $f = 0.5$ is used for curve simulation.

large number of TL curves. Here we present the analysis in Fig. 4.3.2(a) in respect of the TL curves using $\frac{E}{kT_m} = 30$. Corresponding values of s_0 (unit sec^{-1}/K^a) are also given in log scale in Fig. 4.3.2(a). It is observed that $s(T)$ decreases with temperature for $a < 0$ whereas the reverse behavior is seen for $a > 0$. The impact of TDFF on TL peaks are visible when we simulate TL peaks using these values of $s(T)$ corresponding to different a keeping E, f, R fixed and it is displayed in Fig. 4.3.2(b). As the values of a vary from -2 to 2, the peak maxima show a rightward shift with almost a monotonic decrease in peak height.

4.4 Investigating the impact of TDFF in glow curve analysis

Before analyzing glow peaks with TDFF we first looked into the variation in different characteristics of a particular glow peak which has been simulated in OTOR model for different values of a. We examined how the symmetry of a glow peak may vary for possible variations in values of a. In this regard we picked up the geometrical symmetry factor $\mu'_g = \frac{T_2 - T_m}{T_2 - T_1}$ as a symmetry parameter. Here T_1, T_2 are the temperatures at rising side and falling side respectively of the glow curve at half intensity points. In Fig. 4.4.1 we have shown the variation of μ'_g with respect to $\frac{E}{kT_m}$ for the glow curves generated with $R = 0.5$ and $f = 0.5$. It is seen that μ'_g does not exhibit much difference with respect to a when $\frac{E}{kT_m} > 30$.

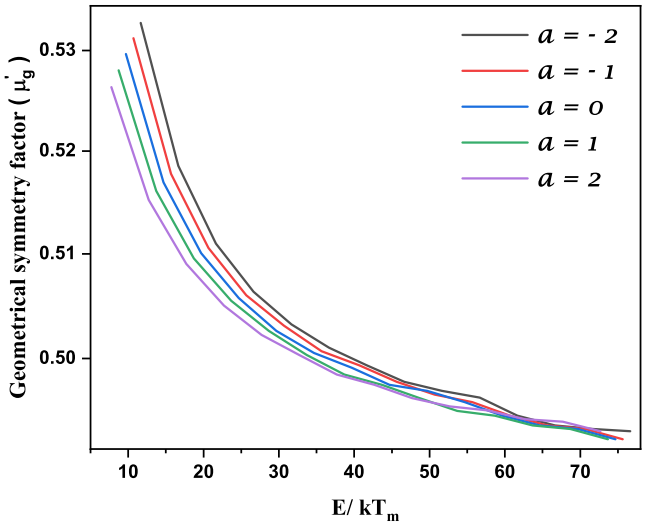

Figure 4.4.1: Comparative variation of geometrical symmetry factor of TL peaks with TDFF with respect to $\frac{E}{kT_m}$ for different values of a. Here $R = 0.5$ and $f = 0.5$ are taken.

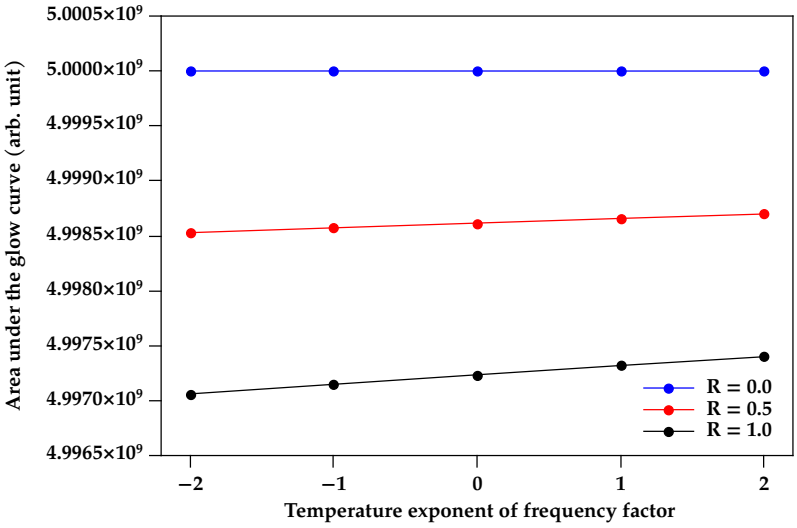

Figure 4.4.2: Comparison of area under the curve plotted against a. Here TL peaks in Figure 4.3.1(a)–(c) for different R have been used.

Next we have estimated the area under the curves and the variation in area under the curve for different a related to a particular peak is given in Fig. 4.3.1(a–c). The observation has been depicted in Fig. 4.4.2. From Fig. 4.4.2 it is seen that, in case of $R = 0$, area under the curves is almost insensitive to a and a gradually increasing trend

with respect to a is there as R goes from 0 to 1, though not much variation is seen. The above observations lead us to pick up methods based on area for analyzing glow curves with TDFF.

In the next phase, based on the above observations, we have adopted different methods of glow curve analysis to examine the effect of variation of symmetry factor and area under the curve on the outcome of TL analysis for different value of a. In particular we have chosen different versions of (i) peak shape method and (ii) area method for this purpose.

4.4.1 TL analysis with TDFF using different versions of peak shape method.

In this section, we describe the procedure to extract activation energy from the TL curves simulated in OTOR model with TDFF using the peak shape method. We have considered different values of input parameters to generate TL peaks in such a way that the value of $u_m = \frac{E}{kT_m}$ remains in the range of experimental interest. At first, the peak for $R = 0$ is simulated with $a = 0$ and $u_m = 30$ where $E = 1.0$ eV that corresponds to $T_m = 386.8$ K. The value of s_0 comes out to be $s_0 = 8.296 \times 10^{11} sec^{-1}$ from the maximum condition. Setting this glow peak as reference, we simulate the same peak (similar to $a = 0$) for other values of a ($-2 \leq a \leq 2$) keeping T_m unaltered. Adopting the present peak shape method in Eq. 3.4.4, we have estimated the activation energy (E_τ) using the peak shape parameter $\tau_x = \frac{T_m - T_{1x}}{T_{2x} - T_{1x}}$ where $x = \frac{I}{I_m}$ is the fractional intensity. T_{1x}, T_{2x} are the temperatures at rising side and falling side of the glow curve respectively at fractional intensity x. We have taken $x = \frac{1}{4}, \frac{1}{2}, \frac{2}{3}$ in this work. Moreover, for $x = \frac{1}{2}$, we have also used the peak shape method proposed by Chen (1969a) to estimate the activation energy. The results are listed in Table 4.4.1. E_{in} is the input values of activation energy used in peak simulation and E_{out} is the output activation energy derived by peak shape method. It is to note that in both the versions of peak shape method, the geometrical symmetry factor (μ'_g) plays a central role and the difference in μ'_g values for different a, as is shown in Fig. 4.4.1, is reflected through the output values of E. The results extracted by using two versions of peak shape method as given in Table 4.4.1 are quite in agreement. The same procedure is followed to investigate other peaks corresponding to $R = 0.5$ and 1.0 and the results are also displayed in Table 4.4.1.

In experimental scenario, T_m is directly measured from a TL peak where a is unknown and E is usually estimated from the recorded TL data considering $a = 0$. Hence there is a scope to investigate theoretically the effect of non-zero values of a on the extracted values of activation energy using peakshape method. We have carried out a systematic error

analysis in extracting activation energy from TL data. In Table 4.4.1 we have also given the error ($\delta E = \frac{E_{out} - E_{in}}{E_{in}} \times 100\%$) explicitly for each TL peak corresponding to different values of a. It can be seen from Table 4.4.1 that for $R = 0$ and 1, the inherent error in activation energy arising due to the temperature variation of frequency factor lie within 8% whereas for $R = 0.5$, the error may go beyond 11%. In Fig. 4.4.3 we have given the variation of error $\delta E(\%)$ as a function of $\frac{E}{kT_m}$. For this purpose we have generated a sufficiently large number of TL peaks where $u_m = \frac{E}{kT_m}$ is varied from 10 to 75. Each peak is reproduced for five values of a *i.e.* $\pm 2, \pm 1, 0$. The plot in Fig. 4.4.3 for $R = 0$, 0.5, 1 are presented in the same scale to facilitate a comparative study. In all the cases it is seen that the magnitude of error increases as $\frac{E}{kT_m}$ decreases and the amount of error becomes quite significant when $\frac{E}{kT_m}$ goes below 30. Moreover, for $R = 0$ and 1, δE is minimum with $a = 0$ when $\frac{E}{kT_m} > 20$ whereas, for $R = 0.5$, δE is minimum for $a = -1$.

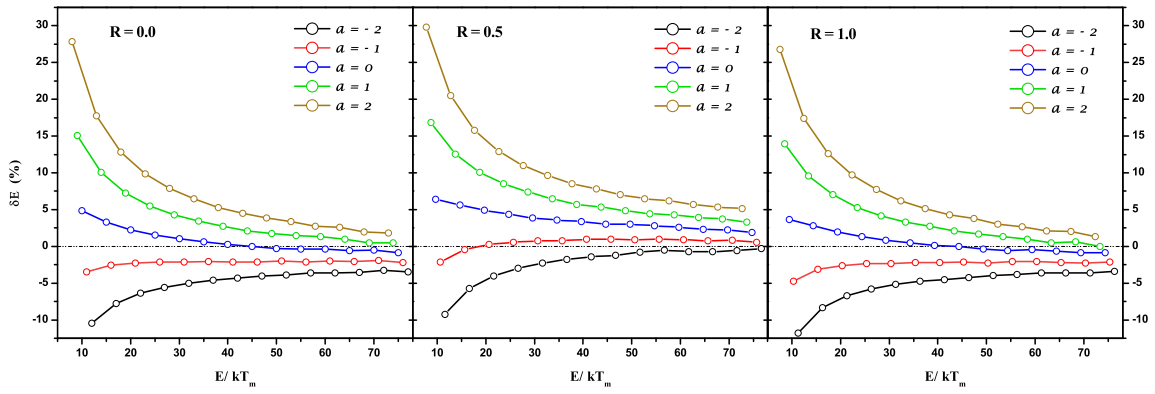

Figure 4.4.3: Variation in error $\delta E\%$ due to temperature dependence of frequency factor plotted against $\frac{E}{kT_m}$. Here $f = 0.5$ has been used for peak generation.

In order to verify the applicability of the present study in case of experimental TL peaks, we have considered the glow curve of $Sr_2P_2O_7 : Cu, Pr$ reported by Yazici et al. (2010) where the sample was exposed to β-radiation with dose $\sim$ 12 Gy and the heating rate was 1 $Ksec^{-1}$. The composite TL signal was deconvoluted into two component peaks. In this work we have considered only the peak-1 and carried out the analysis based on OTOR model for different values of a to estimate E using the peak shape method given in Eqs. (3.4.4, 3.4.5, 3.4.6) and the method given by Chen (1969a). In the original work of Yazici et al. (2010) the glow curve analysis was carried out in GOK model and the order

Table 4.4.1: Activation energies (E) and corresponding error ($\delta E\%$) for fractional intensities $x = \frac{1}{4}$, $\frac{1}{2}$ and $\frac{2}{3}$ estimated using the peak shape relations proposed in Eqs.(3.4.4, 3.4.5, 3.4.6). For $x = \frac{1}{2}$, Chen's Chen (1969a) peakshape results are also given that are marked by asterisks. Here $f = 0.5$ has been considered for all the peaks.

		Input parameters				Output values of activation energy (E_{out} *in eV*)					
T_m	$\frac{E}{kT_m}$	R	a	s_0	E_{in}	$x=\frac{1}{4}$		$x=\frac{1}{2}$		$x=\frac{2}{3}$	
(K)				$(sec^{-1}K^{-1})$	(eV)	E_τ	$\delta E(\%)$	E_τ	$\delta E(\%)$	E_τ	$\delta E(\%)$
386.8	32.00	0.0	–2	9.182×10^{17}	1.067	1.010	–5.34	1.013	–5.06	1.014	–4.97
								1.004*	–5.90		
	31.00		–1	8.714×10^{14}	1.033	1.008	–2.42	1.011	–2.13	1.013	–1.94
								1.002*	–3.00		
	30.00		0	8.296×10^{11}	1.000	1.006	0.60	1.010	1.00	1.012	1.20
								1.001*	0.10		
	29.00		1	7.898×10^{8}	0.967	1.005	3.93	1.008	4.24	1.010	4.45
								0.999*	3.31		
	28.00		2	7.495×10^{5}	0.933	1.003	7.50	1.007	7.93	1.008	8.04
								0.998*	6.97		
391.1	31.65	0.5	–2	8.787×10^{17}	1.067	1.037	–2.81	1.042	–2.34	1.045	–2.06
								1.033*	–3.19		
	30.66		–1	8.344×10^{14}	1.033	1.035	0.19	1.041	0.77	1.044	1.06
								1.031*	–0.19		
	29.67		0	7.948×10^{11}	1.000	1.033	3.30	1.039	3.90	1.042	4.20
								1.029*	2.90		
	28.68		1	7.571×10^{8}	0.967	1.032	6.72	1.038	7.34	1.041	7.65
								1.028*	6.31		
	27.69		2	7.194×10^{5}	0.933	1.03	10.40	1.036	11.04	1.039	11.36
								1.026*	9.97		
395.3	31.31	1.0	–2	8.642×10^{17}	1.067	1.010	–5.34	1.011	-5.25	1.011	–5.25
								1.001*	–6.19		
	30.33		–1	8.208×10^{14}	1.033	1.009	–2.32	1.009	–2.32	1.010	–2.23
								0.998*	–3.39		
	29.35		0	7.821×10^{11}	1.000	1.007	0.70	1.009	0.90	1.008	0.80
								0.998*	–0.20		
	28.37		1	7.451×10^{8}	0.967	1.005	3.93	1.007	4.14	1.007	4.14
								0.996*	3.00		
	27.39		2	7.083×10^{5}	0.933	1.004	7.61	1.005	7.72	1.005	7.72
								0.995*	6.65		

*Ref. Chen (1969a)

of kinetics was reported as $b = 1.1$ for peak-1 of $Sr_2P_2O_7 : Cu, Pr$. As the present study is done in terms of OTOR model where b does not arise explicitly, we have estimated the

value of R corresponding to $b = 1.1$ using the empirical relation.

$$b = 1 + \frac{\ln\left[1 + R(\frac{N}{n} - 1)\right]}{\ln \frac{N}{n}} \tag{4.4.1}$$

In the present study, the activation energy for peak-1, estimated by using peak shape method, is found to lie within the range from 0.948 to 0.936 eV when a is varied from -2 to 2. To compare, Yazici et al. (2010) estimated the value of E for the same peak to be 0.933 eV while temperature dependence of frequency factor was ignored.

4.4.2 TL analysis with TDFF using methods based on area under glow curve

In the next phase of present study *i.e.* to understand the impact of TDFF on glow curve analysis we have considered the area method proposed by Kirsh (1992) and the TPA method for analysis. Both the area methods have been described in following section. Since the TPA method is newly proposed, it is imperative to verify the validity of the method in as many ways as possible. For that we have performed a thorough investigation on the applicability of TPA method. At first the method have been applied to simulated TL peaks generated in GOK and OTOR model. Then we have applied TPA method to analyze the glow peak numerically generated using hyperbolic heating scheme. In every case, the results of TPA method have been compared with the result obtained by using other established area method (Kirsh, 1992). Finally we have applied this method to analyze experimental glow peaks reported in literature (Kumar et al., 2020; Yazici et al., 2010). In the experimental case we have also compared the present result with that obtained by using other established method and the result reported in literature. This way once the applicability of the TPA method is established then we proceed to to analyze glow peaks with TDFF.

4.4.3 Description of Kirsh method and Three Point Area method

The expressions for TL intensity for first order kinetics can be obtained from the differential Eq. (4.4.2) (Randall and Wilkins, 1945a,b)

$$I = -\frac{dn}{dt} = nse^{-\frac{E}{kT}} \tag{4.4.2}$$

For $b = 2$, the corresponding differential equation becomes (Garlick and Gibson, 1948)

$$I = -\frac{dn}{dt} = \frac{n^2}{N}se^{-\frac{E}{kT}} \tag{4.4.3}$$

The glow intensity (I) for general order kinetics (GOK) is obtained by solving the differential Eq. (4.4.4) (Chen and Kirsh, 1981b)

$$I = -\frac{dn}{dt} = \left(\frac{n}{N}\right)^b sNe^{-\frac{E}{kT}} \tag{4.4.4}$$

For $b = 1$, Eq. (4.4.4) becomes the first order equation of Randall and Wilkins (1945a,b) and for $b = 2$, the second order equation of Garlick and Gibson (1948) is obtained. For an arbitrary point (T_i, I_i) on the curve, we can write from Eq. (4.4.4)

$$\ln I_i = -\frac{E}{kT_i} + b \ln \frac{n_i}{N} + \ln sN \tag{4.4.5}$$

n_i is the concentration of trapped electrons at temperatures T_i.

4.4.4 Kirsh method

Let us consider a pair of data points namely $(T_1,\ I_1)$ and $(T_2,\ I_2)$ on the glow peak. Using Eq. (4.4.5) we can write at the points $(T_1,\ I_1)$ and $(T_2,\ I_2)$,

$$\ln I_1 = -\frac{E}{kT_1} + b \ln \frac{n_1}{N} + \ln sN \tag{4.4.6}$$

$$\ln I_2 = -\frac{E}{kT_2} + b \ln \frac{n_2}{N} + \ln sN \tag{4.4.7}$$

From Eqs. (4.4.6) and (4.4.7) we can write

$$\ln I_2 - \ln I_1 = -\frac{E}{k}\left(\frac{1}{T_2} - \frac{1}{T_1}\right) + b\left[\ln \frac{n_2}{N} - \ln \frac{n_1}{N}\right] \tag{4.4.8}$$

Eq. (4.4.8) can be written as

$$\frac{\Delta \ln I}{\Delta \ln\left(\frac{n}{N}\right)} = -\left(\frac{E}{k}\right)\left[\frac{\Delta\left(\frac{1}{T}\right)}{\Delta \ln\left(\frac{n}{N}\right)}\right] + b \tag{4.4.9}$$

If numbers of such pair of data points are considered it can be seen from Eq. (4.4.9) that a plot between $\dfrac{\Delta \ln I}{\Delta \ln\left(\frac{n}{N}\right)}$ and $\dfrac{\Delta\left(\frac{1}{T}\right)}{\Delta \ln\left(\frac{n}{N}\right)}$ will yield a straight line with slope $\left(-\dfrac{E}{k}\right)$ and intercept b.

4.4.5 Three point area method

For a pair of arbitrary points (T_i, I_i) and (T_j, I_j), using Eq. (4.4.5), we obtain

$$Y_{ij} \quad = \quad b - \frac{E}{k} X_{ij} \tag{4.4.10}$$

$$\text{where } Y_{ij} = \frac{\ln I_j - \ln I_i}{\ln \frac{n_j}{n_0} - \ln \frac{n_i}{n_0}}; \quad X_{ij} = \frac{\frac{1}{T_j} - \frac{1}{T_i}}{\ln \frac{n_j}{n_0} - \ln \frac{n_i}{n_0}} \tag{4.4.11}$$

Here we have used $\frac{n_i}{n_j} = \frac{n_i}{n_0}.\frac{n_0}{n_j}$. n_0 is the initial concentration of trapped electrons and is proportional to the area under the entire glow curve. $\frac{n_i}{n_0}$ and $\frac{n_j}{n_0}$ are estimated by measuring the area under the TL curve (Fig. 4.4.4) starting from temperature T_i and T_j respectively to the end-point temperature (T_e). Similarly, for another pair of points (T_j, I_j) and (T_l, I_l) (one point is common in both the pairs), we obtain

$$Y_{jl} = b - \frac{E}{k} X_{jl} \tag{4.4.12}$$

Solving Eqs. (4.4.10) and (4.4.12) we get the expressions of E and b as

$$E = -k \frac{Y_{ij} - Y_{jl}}{X_{ij} - X_{jl}}; \quad b = \frac{X_{jl} Y_{ij} - X_{ij} Y_{jl}}{X_{ij} - X_{jl}} \tag{4.4.13}$$

Thus the TPA method yields the activation energy and order of kinetics simultaneously. From the knowledge of E and b, the frequency factor (s) is determined from the 'maximum condition' (Chen and Kirsh, 1981b)

$$s = \beta \left[\frac{bkT_m^2}{E} \exp\left(-\frac{E}{kT_m} \right) - (b-1) J(T_0, T_m) \right]^{-1} \tag{4.4.14}$$

In this way, the TPA method needs two pairs of points on the curve and thus, a set of at least three distinct points (one point being common in each pair) are selected. The partial area (A_i) from each datapoint to the end-point (T_e) is estimated along with the total area (A_0) under the entire glow curve. The partial area A_i corresponds to the concentration of trapped electrons at temperature T_i whereas A_0 corresponds to the initial concentration of trapped electrons. A schematic diagram is presented in Figure 4.4.4. The temperatures and intensities at three points along with the ratios of partial areas to the total area are used to determine E and b using Eq. (4.4.13).

Estimation of area

Considering the initial concentration of trapped electrons n_0 to be proportional to the area under the whole TL peak and the instantaneous concentration of trapped electrons n to be proportional to the partial area under the glow peak from temperature T to T_e, we can write (Kirsh, 1992)

$$\frac{n}{n_0} = \frac{A(T, T_e)}{A_0(T_0, T_e)} \tag{4.4.15}$$

$A(T, T_e)$ is the area of the TL glow curve from T to T_e ($T_e >> T_m$) and is given by

$$A(T, T_e) = \int_T^{T_e} I(T')dT' \tag{4.4.16}$$

$A_0(T_0, T_e)$ is the area of the TL glow curve from T_0 to T_e *i.e.* the area of the whole curve (Fig. 4.4.4). The expression for TL intensity can be obtained by solving the differential

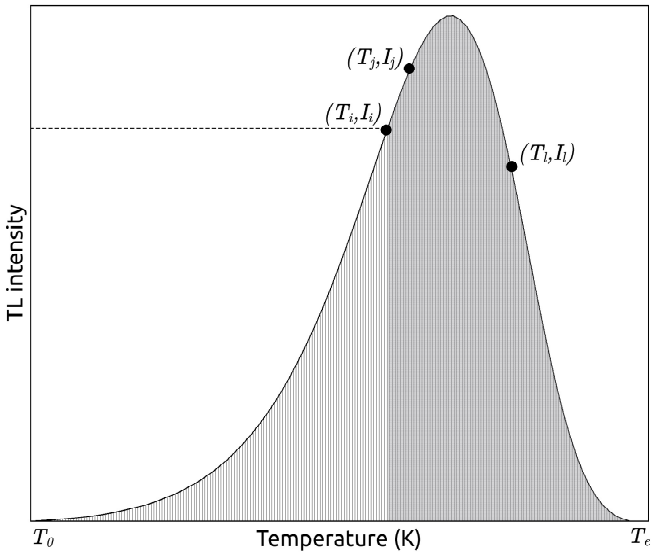

Figure 4.4.4: Schematic diagram of a TL peak with three arbitrary points (T_i, I_i), (T_J, I_j) and (T_L, I_l) placed on it. The striped area shows the area under the complete curve from T_0 to T_e. The shaded region shows the partial area from T_i to T_e.

Eqs. (4.4.2) - (4.4.4) and can be summarized as

$$I(T) = sn_0 e^{-\frac{E}{kT}} \exp\left[-\frac{s}{\beta}\int_{T_0}^{T} e^{-\frac{E}{kT'}}dT'\right] \quad \text{for b} = 1 \tag{4.4.17}$$

$$\text{and} \quad I(T) = sn_0 e^{-\frac{E}{kT}}\left[\frac{(b-1))s}{\beta}\int_{T_0}^{T} e^{-\frac{E}{kT'}}dT' + 1\right]^{-\frac{b}{b-1}} \quad \text{for b} \neq 1 \tag{4.4.18}$$

Writing $u = \dfrac{E}{kT}$ and $u_m = \dfrac{E}{kT_m}$ where (T_m, I_m) being the peak coordinates, Eqs. (4.4.17) and (4.4.18) can be recast as

$$\frac{I}{I_m} = \exp\left[(u_m - u) + F(u, u_m)\right] \quad \text{for b} = 1 \tag{4.4.19}$$

$$\text{and} \quad \frac{I}{I_m} = \exp(u_m - u)\left[1 - \frac{b-1}{b}F(u, u_m)\right]^{-\frac{b}{b-1}} \quad \text{for b} \neq 1 \tag{4.4.20}$$

$$\text{with} \quad F(u, u_m) = u_m^2 \exp(u_m)\left[\frac{E_2(u_m)}{u_m} - \frac{E_2(u)}{u}\right] \tag{4.4.21}$$

Here $E_2(u)$ is the 2nd order exponential integral with argument u (Abramowitz and Stegun, 1972).

Now, for non-first order ($b \neq 1$) kinetics (Eq. 4.4.20), the area under the portion of the peak from temperature T to T_e is given by

$$A(u, u_e) = \frac{E}{k} \int_u^{u_e} \exp(u_m - u') \left[1 - \frac{b-1}{b} F(u', u_m)\right]^{-\frac{b}{b-1}} u'^{-2} du' \tag{4.4.22}$$

where $u_e = \dfrac{E}{kT_e}$. The end-point temperature T_e is taken at which the intensity of the falling side of the curve becomes 1% of the maximum intensity (I_m). The integral occurring in Eq. (4.4.22) has been evaluated by splitting the total range of integration (T, T_e) into suitable number of subranges and applying composite Simpson's rule (Burden et al., 2001). This area is now used to estimate $\dfrac{n}{n_0}$ (Eq. 4.4.15) and then E and b are calculated from Eq. (4.4.13).

4.4.6 Application of TPA method to simulated glow peak

As mentioned earlier the Three-point area (TPA) method is newly proposed, hence its applicability is checked from all aspect before we proceed. The applicability and accuracy of the TPA method for extracting trapping parameters has been tested at first on simulated glow curve by extracting E and b and thereof comparing them with the input values. To note that in GOK model only input value of b can be directly compared with the corresponding value extracted from the TPA method. However, b does not appear exclusively in OTOR model, although a correlation exists between R and b. So, accuracy in this context may be checked indirectly in OTOR model. The activation energy from an OTOR glow peak can be extracted directly using TPA method.

4.4.7 Glow curves simulated in GOK model

At first we have employed the GOK model (Eqs. 4.4.20 and 4.4.21 to generate the TL curve using different set of input values of activation energy (E_{in}), order of kinetics (b_{in}) and frequency factor (s_{in}). In the set of input values, we have considered

- E within the range $0.5 \leq E \leq 1.5$ in eV
- b in the range $1.0 \leq b \leq 2.0$
- s in the range $10^8 \leq s \leq 10^{12}$ in sec^{-1}

Table 4.4.2: Kinetic parameters derived by TPA method from numerically simulated TL peaks generated in GOK model in linear heating scheme. The heating rate is $\beta = 1$ Ksec^{-1}.

Input values			Output values					
E_{in} (eV)	s_{in} (sec^{-1})	b_{in}	T_m (K)	E_T (eV)	b_T	s_T (sec^{-1})	E_k (eV)	b_k
0.5	1.0×10^{10}	1.0	229.93	0.4999	0.9995	9.95×10^{9}	0.5000	0.9995
		1.6	229.58	0.4999	1.5977	9.85×10^{9}	0.4999	1.5972
		2.0	229.35	0.4998	1.9957	9.73×10^{9}	0.4998	1.9950
	1.0×10^{12}	1.0	196.52	0.4999	0.9996	9.94×10^{11}	0.5000	0.9995
		1.6	196.29	0.4999	1.5977	9.85×10^{11}	0.4999	1.5973
		2.0	196.15	0.4998	1.9959	9.76×10^{11}	0.4998	1.9953
1	1.0×10^{10}	1.0	448.44	0.9999	0.9995	9.97×10^{9}	0.9999	0.9995
		1.6	447.79	0.9997	1.5977	9.82×10^{9}	0.9998	1.5972
		2.0	447.37	0.9995	1.9958	9.74×10^{9}	0.9997	1.9951
	1.0×10^{12}	1.0	384.57	0.9999	0.9996	9.97×10^{11}	0.9999	0.9995
		1.6	384.15	0.9997	1.5976	9.81×10^{11}	0.9998	1.5973
		2.0	383.87	0.9996	1.9957	9.74×10^{11}	0.9997	1.9954
1.5	1.0×10^{10}	1.0	663.02	1.4998	0.9995	9.96×10^{9}	1.4999	0.9995
		1.6	662.07	1.4995	1.5977	9.83×10^{9}	1.4997	1.5972
		2.0	661.47	1.4993	1.9957	9.73×10^{9}	1.4995	1.9951
	1.0×10^{12}	1.0	569.68	1.4998	0.9995	9.96×10^{11}	1.4999	0.9995
		1.6	569.06	1.4995	1.5978	9.82×10^{11}	1.4997	1.5973
		2.0	568.67	1.4994	1.9960	9.74×10^{11}	1.4995	1.9954

All the input parameters are increased systematically in a step-by-step manner and TPA method is applied to all the numerical glow curves. In Table 4.4.2 we have given a representative set of the results of TPA method corresponding to some selective input parameters (E_{in}, b_{in}, s_{in}). The agreement between input values (E_{in}, b_{in}) and output values (E_T and b_T) is evident from Table 4.4.2 which shows that the TPA method quite accurately performs simultaneous extraction of activation energy and order of kinetics. The frequency factor has been calculated using Eq. 4.4.14 and the results are given in Table 4.4.2. We observe that the output s-values are slightly lower than the input values and this is consistent throughout the dataset. This marginal difference in s values may be due to the approximations inherent in the derivation of Equation (4.4.14). For a comparison of the present results, we have evaluated E and b from the same curve using Kirsh method (Kirsh, 1992) also. The results derived from Kirsh method (Kirsh, 1992) are listed in Table 4.4.2 as E_k and b_k respectively. It is evident that the present results E_T, b_T are quite consistent with the values E_k, b_k.

4.4.8 Glow curves simulated in OTOR model

We have generated TL glow curves in OTOR model using Eqs. (1.2.17 – 1.2.19), for different values of R and filling ratio $\left(f = \frac{n_0}{N}\right)$. The linear heating scheme is adopted with heating rate $\beta = 1\ Ks^{-1}$. The TPA method is applied on these curves to extract the activation energy (E_T) and order of kinetics (b_T). The results are displayed in Table 4.4.3 where the values of input parameters required to generate the curves are also mentioned. Three arbitrary points on the glow curve are chosen and Eq. (4.4.13) is applied to determine E_T and b_T as output values. From 'm' number of points on the curve, we can calculate ${}^{m}C_3$ sets of values of E_T and b_T. We consider a large number of dataset ($m = 19$) and after averaging we obtain the final values of E_T and b_T. However, we note here that for all the simulated curves, the lower half of the falling side of the TL curve is excluded while taking the required three points for extraction of trapping parameters. For experimental curves, points are chosen from the rising side of the curve. The reason behind this is explained later in section 4.4.12. Table 4.4.3 shows that E_T is quite in agreement with the input value of activation energy (E_{in}).

In OTOR model b does not occur explicitly in the expression of TL intensity. Similarly in GOK model, R does not occur. However, a correlation between R and b exists which is given in Eq. (3.4.7) (Sunta, 2014). Eq. (3.4.7) reveals that for $R = 0$, $b = 1$ and for $R = 1$, $b = 2$ and b thus becomes independent on temperature for $R = 0$ and 1. For all other values of R, b has a dependence on T, as n varies with T. $n(T)$ is estimated from Eq. (1.3.6) which is further employed to evaluate $b(T)$ for a particular input value of R. therefore a unique value of b should not be assigned to a TL peak due to its temperature dependence, rather average value of b (b_{av}) can be an appropriate parameter which can be estimated using Eq. (3.4.8)

The integration has been carried out numerically using composite Simpson's rule Burden et al. (2001). We have studied the temperature variations of n as well as of b in detail and the variations are displayed in Fig. 4.4.5 for $R = 0.5$ corresponding to an unsaturated ($f = 0.5$) and a saturated ($f = 1$) TL peak. b_{av} is estimated (Eq. 3.4.8) for these curves and compared with b_T obtained from TPA method. Results displayed in Table 4.4.3 show reasonable agreement between the extracted value (b_T) and the average value (b_{av}). To have a further check on the reliability of the parameter b_{av} as an equivalent to R, we reproduce the value of R from b_{av} by rearranging Eq. (3.4.7) as

$$R = \frac{\left(\frac{N}{n}\right)^{b_{av}-1} - 1}{\frac{N}{n} - 1} \tag{4.4.23}$$

Table 4.4.3: Kinetic parameters derived by TPA method from numerically simulated TL peaks generated in OTOR model in linear heating scheme. The input parameters are: $E_{in} = 1.0\ eV$, $s = 1.0 \times 10^{12}\ sec^{-1}$, $N = 1.0 \times 10^{10}\ m^{-3}$ and $\beta = 1.0$ Ksec^{-1}. b_{av} is estimated using Equation (3.4.8).

Input parameters			Output from TPA method	
f	R_{in}	b_{av}	b_T	E_T (eV)
0.1	0.0	1.0056	1.0004	0.9999
	0.001	1.0328	1.0092	1.0000
	0.25	1.6419	1.7932	1.0001
	0.50	1.8030	1.8631	1.0001
	0.75	1.9208	1.9609	1.0001
	1.0	2.0070	2.0517	1.0000
0.5	0.0	1.0056	1.0004	0.9999
	0.001	1.0238	1.0022	1.0000
	0.25	1.5506	1.4182	1.0002
	0.50	1.7257	1.6632	1.0003
	0.75	1.8819	1.8710	1.0001
	1.0	2.0067	2.0118	1.0001
1.0	0.0	1.0057	1.0004	0.9999
	0.001	1.0213	1.0018	1.0000
	0.25	1.5179	1.2662	1.0002
	0.50	1.6881	1.5074	1.0006
	0.75	1.8588	1.7647	1.0003
	1.0	2.0067	2.0062	1.0002

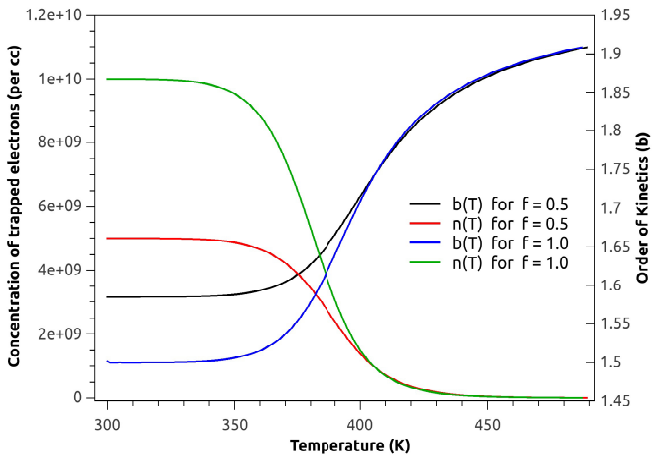

Figure 4.4.5: Variation of n and b with respect to T for $R = 0.5$. The input parameters are: $E_{in} = 1.0\ eV$, $s = 1.0 \times 10^{12}\ sec^{-1}$, $N = 1.0 \times 10^{10}\ m^{-3}$ and $\beta = 1.0 Ksec^{-1}$.

Table 4.4.4: Average value of R (*i.e.* R_{av}) estimated from b_{av} using Eqs. (4.4.23, 4.4.24) from simulated TL peaks generated in OTOR model in linear heating scheme. The input parameters are same as Table 4.4.3.

f	R_{in}	b_{av}	R_{av}
0.1	0.0	1.0056	0.0010
	0.001	1.0328	0.0061
	0.25	1.6419	0.2519
	0.50	1.8030	0.4898
	0.75	1.9208	0.7453
	1.0	2.0070	1.0287
0.5	0.0	1.0056	0.0027
	0.001	1.0238	0.0119
	0.25	1.5506	0.2653
	0.50	1.7257	0.4648
	0.75	1.8819	0.7030
	1.0	2.0067	1.0243
1	0.0	1.0057	0.0041
	0.001	1.0213	0.0153
	0.25	1.5179	0.2795
	0.50	1.6881	0.4568
	0.75	1.8588	0.6784
	1.0	2.0067	1.0232

We obtain a set of values of R at different temperatures as n varies with T. Numerical average of R (R_{av}) is then obtained as

$$R_{av} = \frac{1}{T_f - T_i} \int_{T_i}^{T_f} R(T) dT \tag{4.4.24}$$

We now employ the b_{av} values listed in Table 4.4.3 along with other parameters to reproduce R_{av} according to Eq. (4.4.24) and the results are listed in Table 4.4.4. It is evident that R_{av} values are in close agreement with the input values of R and hence b_{av} can be treated as a reliable parameter equivalent to R.

4.4.9 Systematic error analysis

Because of the inherent approximations, any phenomenological analysis involves systematic errors. In case of interpretation of experimental data using theoretical methods, experimental errors merge with theoretical errors. So the analysis of systematic errors in theoretical studies gives the lower limit of errors in that method. We have calculated the percentage errors δE and δb in the determination of E and b using TPA method from the simulated

glow curves for different values of E, s, b by using the relations $\delta E = \dfrac{E_T - E_{in}}{E_{in}} \times 100\%$ and $\delta b = \dfrac{b_T - b_{in}}{b_{in}} \times 100\%$. It is noted that in TPA method the calculated values of E_T and b_T are always less than the input values in GOK model. The fact that E_T is less than E_{in} is somewhat similar to the case of initial rise method (Chen and Mckeever, 1997) which underestimates activation energy. Fig. 4.4.6 shows the variation of δE with respect to b and $\log s$ for $E = 1$ eV. Though the percentage error ($\delta E\%$) for the simulated curve is very nominal, Fig. 4.4.6 displays that δE has dependence on both b and s. δE increases with the increase of b and decreases with increase of $\log s$. However, δE is more sensitive on variations of b than s. For all other values of E_{in}, our observation is that δE does not have much dependence on E_{in} (*i.e.* on trap depth). In Fig. 4.4.7(a), δb is presented as a function of $\log s_{in}$ for different values of E_{in} and Fig. 4.4.7(b) shows the variation of δb with respect to E_{in} for different values of s_{in}. A decrease in δb is observed as $\log s$ increases whereas δb is almost independent of E_{in}.

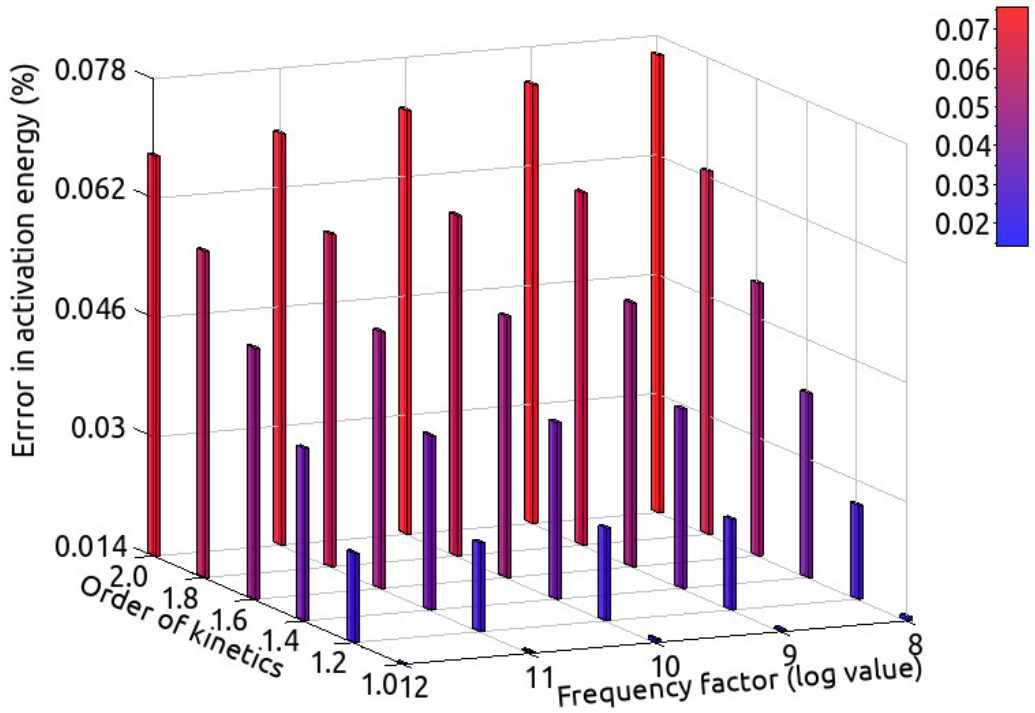

Figure 4.4.6: δE (%) plotted against different values of b_{in} and s_{in}. Here $E_{in} = 1$ eV.

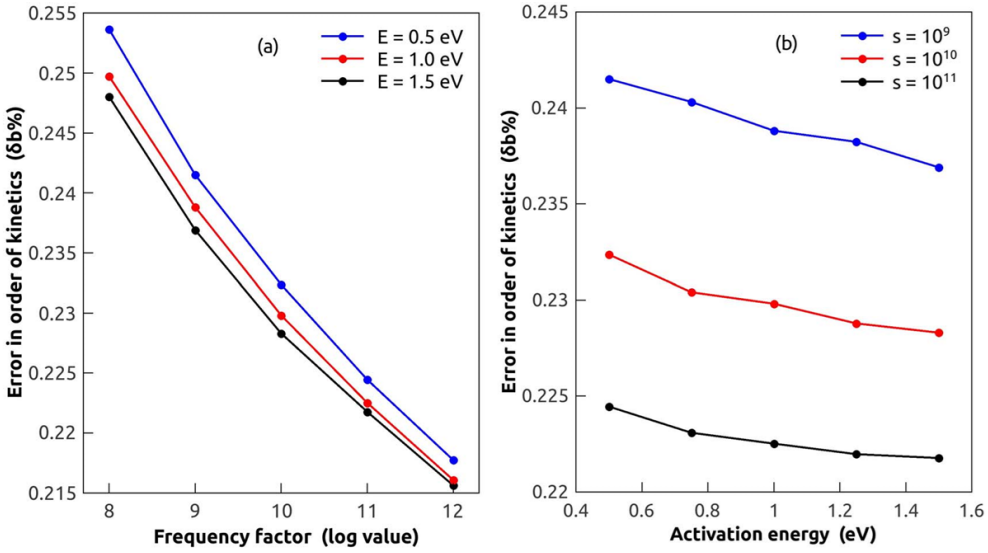

Figure 4.4.7: (a) Variation of δb (%) against $\log s_{in}$ for different values of E_{in}, (b) Variation of δb (%) against E_{in} for different values of s_{in}.

4.4.10 Application of TPA method to glow curves generated in hyperbolic heating scheme

We have also applied the TPA method on simulated glow curves generated in GOK model in hyperbolic heating scheme. The heating procedure in hyperbolic heating scheme is expressed as $\frac{1}{T} = \frac{1}{T_0} - \beta' t$, β' is a constant (Christodoulides, 1986b). Hence,

$$\frac{dn}{dt} = \frac{dn}{dT}\frac{dT}{dt} = \beta' T^2 \frac{dn}{dT} \tag{4.4.25}$$

Thus the heating rate $\frac{dT}{dt}$ varies with temperature in a quadratic manner. In hyperbolic heating scheme, we write

$$\frac{n}{n_0} = \frac{1}{\beta'} \int_{T_i}^{T_e} \frac{I(T')}{T'^2}\, dT' \tag{4.4.26}$$

Now proceeding as the same way as in the case of linear heating scheme, the expression of TL intensity under hyperbolic heating scheme can be expressed according to Eqs. (1.2.14) and (4.4.20) where $F(u, u_m)$ is given by Christodoulides (1986b) as;

$$F(u, u_m) = 1 - e^{u_m - u} \tag{4.4.27}$$

With this $F(u, u_m)$, the ratio $\frac{n}{n_0}$ is determined by following Eqs. (4.4.15) and (4.4.22). The rest of the procedure is similar to as discussed before. Knowing E and b, s can be determined from the expression Christodoulides (1986b)

$$s = \frac{\beta_m E}{kT_m^2}\left[\exp\left(-\frac{E}{kT_m}\right) + (b-1)\exp\left(-\frac{E}{kT_0}\right)\right]^{-1} \tag{4.4.28}$$

where $\beta_m = \beta' T_m^2$ is the heating rate at peak temperature T_m. However, in practice, it is found that the last term $(b-1)\exp\left(-\frac{E}{kT_0}\right)$ in Eq. (4.4.28) has almost negligible contribution and $s \simeq \frac{\beta_m E}{kT_m^2}\exp\left(\frac{E}{kT_m}\right)$ is a good approximation in hyperbolic heating.

Table 4.4.5: Kinetic parameters derived by TPA method from numerically simulated TL peaks generated in GOK model in hyperbolic heating scheme. The notation $x(y)$ means $x \times 10^y$.

Input values			Output values					
E_{in} (eV)	s_{in} (sec^{-1})	b_{in}	T_m (K)	E_T (eV)	b_T	s_T (sec^{-1})	E_k (eV)	b_k
0.5	1.0(10)	1.0	229.93	0.4934	1.0394	7.14(09)	0.4940	1.0321
		1.6	229.58	0.4915	1.7244	6.73(09)	0.4922	1.7123
		2.0	229.36	0.4910	2.2241	6.73(09)	0.4916	2.2097
	1.0(12)	1.0	196.52	0.4943	1.0332	7.13(11)	0.4947	1.0269
		1.6	196.29	0.4926	1.7037	6.67(11)	0.4932	1.6932
		2.0	196.15	0.4920	2.1850	6.57(11)	0.4926	2.1726
1.0	1.0(10)	1.0	448.44	0.9871	1.0384	7.14(09)	0.9882	1.0312
		1.6	447.79	0.9833	1.7208	6.70(09)	0.9848	1.7089
		2.0	447.37	0.9823	2.2173	6.70(09)	0.9836	2.2031
	1.0(12)	1.0	384.57	0.9888	1.0324	7.13(11)	0.9897	1.0263
		1.6	384.15	0.9854	1.7011	6.64(11)	0.9866	1.6909
		2.0	383.87	0.9843	2.1802	6.56(11)	0.9855	2.1680
1.5	1.0(10)	1.0	663.02	1.4809	1.0378	7.13(09)	1.4825	1.0307
		1.6	662.07	1.4753	1.7187	6.70(09)	1.4774	1.7071
		2.0	661.47	1.4737	2.2134	6.68(09)	1.4757	2.1995
	1.0(12)	1.0	569.68	1.4834	1.0320	7.13(11)	1.4847	1.0259
		1.6	569.06	1.4783	1.6996	6.63(11)	1.4802	1.6896
		2.0	568.67	1.4767	2.1775	6.55(11)	1.4785	2.1655

For glow curve generation in GOK model considering hyperbolic heating scheme, the input parameters for peak generation are kept same as in case of linear scheme. The heating rate at peak temperature (β_m) is taken as 1 $K^{-1}sec^{-1}$. The input parameters E_{in}, b_{in}, s_{in} to generate the glow peak and the output values E_T and b_T derived from TPA method are displayed in Table 4.4.5. As in case of linear heating scheme, E_T is slightly underestimated than E_{in} in hyperbolic scheme also. But unlike linear heating, order of

kinetics (b_T) evaluated by TPA method is higher than the corresponding input value (b_{in}) and the difference can go up to 11% for second order kinetics ($b = 2$). Our results of E_T and b_T are consistent with those estimated by Kirsh method (E_k, b_k) (Kirsh, 1992) which is evident from Table 4.4.5. We further use T_m, E_T and b_T to compute the frequency factor (s_T) from the 'maximum condition' (Eq. 4.4.28) and the values are given in Table 4.4.5. We observe that s_T is also underestimated, as is discussed in case of linear heating scheme.

4.4.11 Application to experimental TL peaks

Table 4.4.6: Trapping parameters of TL peaks of different phosphors taken from literature. The notation $x(y)$ means $x \times 10^y$.

Material	Peak	Present work: TPA method				Literature		
		T_m (K)	E_T (eV)	b_T	s_T	E_{gcd} (eV)	b_{gcd}	s
$Sr_2P_2O_7 : Cu, Pr$	1	368.52	0.9329	1.0887	4.55(11)	0.933	1.1	
Yazici et al. (2010)	2	446.21	1.2279	1.3904	5.25(12)	1.228	1.4	
$LiF : Sm^{3+}, Dy^{3+}$	1	373.16	0.8288	0.9947	5.39(10)	0.82	1	5.40(10)
Kumar et al. (2020)	2	408.21	1.0320	1.7857	1.88(12)	1.03	2	1.89(12)

In the next phase, we apply the TPA method to experimental TL curves reported in literature. At first, we have taken the glow peaks reported by Yazici et al. (2010) where they analyzed the TL signal of $Sr_2P_2O_7 : Cu, Pr$ exposed to β-radiation of dose $\sim$ 12 Gy. The glow curve was recorded at a heating rate of 1 $Ksec^{-1}$. The sample exhibited two distinct TL peaks with very small overlapping and the peak maxima were reported near 363 K and 453 K. From the glow curve (Yazici et al., 2010), we have picked up the $I-T$ datapoints using the browser-based software platform WebPlotDigitizer. It is worthwhile to mention that to run a numerical code in a systematic manner for calculating the area under the curve, the datapoints are preferred to be equispaced which is not possible for experimental data. To avoid this difficulty we have interpolated the intermediate data to generate the intensities for temperatures in equal interval by using the divided difference algorithm (Burden et al., 2001) which is a standard technique in case of irregularly spaced data (Gill and Miller, 1972; Salzer, 1964). The composite Simpson's rule (Burden et al., 2001) is now employed to estimate the area under the glow curve and TPA method is employed to extract the values of activation energy (E_T) and order of kinetics (b_T) for both the peaks. The results are shown in Table 4.4.6. Yazici et al. (2010) reported the values of activation energy and order of kinetics derived by glow curve deconvolution (GCD) technique which are quoted

in Table 4.4.6 and good agreement with the present values (E_T, b_T) is observed. The values of T_m, E_T, and b_T are used to estimate the frequency factors (s_T) and the values are given in Table 4.4.6.

In a similar manner, we have analyzed the TL curve of γ-irradiated LiF : Sm^{3+}, Dy^{3+} reported by Kumar et al. (2020) where the dose was 30 kGy and heating rate was 5 $Ksec^{-1}$. Five deconvoluted peaks were reported by Kumar et al. (2020) from which we have considered the fist two peaks. The results are quite in agreement and are displayed in Table 4.4.6. The present values of T_m, E_T, and b_T are used to estimate the frequency factors (s_T) which are in conformity with those reported by Kumar et al. (2020).

4.4.12 Dependence of the results on the location of data points

It remains an important issue to verify if the outcome of TPA method has a considerable dependence on the location of data points. Therefore we have verified the consistency of the results obtained from the TPA method choosing three points from different locations of the curve. For this purpose, we have divided the TL curve in four 'zones',

(i) **Zone-I:** lower half of the rising side (T_0 to $T^-_{\frac{1}{2}}$)

(ii) **Zone-II:** upper half of the rising side ($T^-_{\frac{1}{2}}$ to T_m)

(iii) **Zone-III:** upper half of the falling sidee (T_m to $T^+_{\frac{1}{2}}$)

(iv) **Zone-IV:** lower half of the falling side ($T^+_{\frac{1}{2}}$ to T_e)

Here $T^-_{\frac{1}{2}}$ and $T^+_{\frac{1}{2}}$ are half maxima temperatures in rising and falling sides respectively. We have examined the simulated and experimental TL curves and a representative data set showing how the final results are influenced by the location of the chosen points are given in Table 4.4.7. It is observed for all the cases that the results are quite consistent if the points are chosen from Zone-I and Zone-II. The activation energy is marginally lowered if the points are chosen from Zone-III. But, in Zone-IV, the results are quite inconsistent. These deviations are not much significant for first order simulated curves but becomes noticeable for second order, as is evident from Table 4.4.7. In case of experimental peaks, the deviations of the results are prominent for Zone-III and quite large for Zone-IV. In Table 4.4.7, the TL data of peak no. 1 of $Sr_2P_2O_7 : Cu, Pr$ (Yazici et al., 2010) taking points from different zones are reported showing such behavior. We have also considered the cases where the points are chosen from different zones and found that if the points from Zone-IV are excluded, then the results are quite satisfactory. On the basis of such findings, we have

excluded Zone-IV for simulated curves and considered only the rising part of experimental curves for TL analysis in TPA method.

Table 4.4.7: Activation energy and order of kinetics derived from three datapoints chosen from various locations of the TL curve. For simulated curves, E_{in} = 1.0 eV, $s_{in} = 1.0 \times 10^{12}\ sec^{-1}$, $\beta = 1.0\ K sec^{-1}$.

Peak	T_m (K)	$T_{\frac{1}{2}}^{-}$ (K)	$T_{\frac{1}{2}}^{+}$ (K)	Location of three points	Coordinates of the points (T_1, I_1)	(T_2, I_2)	(T_3, I_3)	E_T (eV)	b_T
Simulated peak with $b_{in} = 1.0$	384.6	367.2	397.1	Zone-I	(347.6, 0.1)	(355.3, 0.2)	(360.3, 0.3)	0.99	0.99
				Zone-II	(372.8, 0.7)	(375.5, 0.8)	(378.5, 0.9)	0.99	0.99
				Zone-III	(392.1, 0.8)	(393.9, 0.7)	(395.5, 0.6)	0.99	0.99
				Zone-IV	(397.1, 0.5)	(398.6, 0.4)	(400.3, 0.3)	0.99	0.99
				Mixed zone	(360.3, 0.3)	(375.5, 0.8)	(397.1, 0.5)	0.99	0.99
Simulated peak with $b_{in} = 2.0$	383.9	363.6	405.7	Zone-I	(351.4, 0.2)	(356.4, 0.3)	(360.3, 0.4)	0.99	1.99
				Zone-II	(366.6, 0.6)	(369.6, 0.7)	(372.6, 0.8)	0.99	1.99
				Zone-III	(391.8, 0.9)	(395.6, 0.8)	(398.9, 0.7)	0.99	1.99
				Zone-IV	(405.7, 0.5)	(409.6, 0.4)	(414.3, 0.3)	0.96	1.95
				Mixed zone	(360.3, 0.4)	(372.6, 0.8)	(395.6, 0.8)	0.99	1.99
Peak no. 1 of $Sr_2P_2O_7$:Cu,Pr*	362.5	351.3	382.1	Zone-I	(336, 0.1)	(342, 0.2)	(346, 0.3)	0.93	1.10
				Zone-II	(354, 0.6)	(358, 0.7)	(361, 0.9)	0.93	1.10
				Zone-III	(375, 0.8)	(378, 0.7)	(380, 0.6)	0.92	1.09
				Zone-IV	(383, 0.4)	(385, 0.3)	(388, 0.2)	0.79	1.03
				Mixed zone	(344, 0.3)	(358, 0.8)	(376, 0.8)	0.93	1.10

*: Yazici et al. (2010)

4.4.13 Study the Impact of TDFF in glow curve analysis using area method

In the last phase we attempt to understand the impact of TDFF on glow curve analysis when the analysis is performed using area methods in OTOR model. For this purpose we have taken the newly developed TPA method and an well established method (Kirsh, 1992). We have considered different values of input parameters to generate TL peaks in such a way that the value of $u_m = \dfrac{E}{kT_m}$ remains within the range of experimental interest. At first, the peak for $R = 0$ is simulated with $a = 0$ and $u_m = 30$. For $E = 1.0$ eV it yields $T_m = 386.8$ K. Hence the value of s_0 comes out to be $s_0 = 8.296 \times 10^{11} sec^{-1}$ from maximum condition given in Eq. (4.2.10). We have taken the same peak (similar to $a = 0$) with other possible values of a (*i.e.* $-2 \leq a \leq 2$).

We analyze the simulated TL peaks using TPA and Kirsh (1992) method. Considering the preference in choosing locations of data points in case of TPA method we have taken the three data points from rising side of glow curve. The results are shown in Table 4.4.8. E_{in} is the input values of activation energy used in peak simulation and E_{out} is the output activation energy derived by area methods. It is to note that in both the versions of area method, the area under the curve is important. The difference in area under the glow

Table 4.4.8: Activation energies (E) and corresponding error ($\delta E\%$) estimated using TPA and Kirsh (1992) method. Here $f = 0.5$ has been considered for all the peaks.

T_m (K)	$\frac{E}{kT_m}$	Input parameters				Output values of activation energy			
		R	a	s_0 $(sec^{-1}K^{-1})$	E_{in} (eV)	E_T (eV)	δE_T (%)	E_K (eV)	δE_K (%)
386.8	32.00	0	– 2	9.182×10^{17}	1.067	1.005	-5.81	1.005	-5.81
	31.00		– 1	8.714×10^{14}	1.033	1.002	-3.00	1.002	-3.00
	30.00		0	8.296×10^{11}	1.000	1.000	0.00	1.000	0.00
	29.00		1	7.898×10^{8}	0.967	0.997	3.10	0.997	3.10
	28.00		2	7.495×10^{5}	0.933	0.995	6.64	0.995	6.64
391.1	31.65	0.5	– 2	8.787×10^{17}	1.067	1.014	-4.97	1.014	-4.97
	30.66		– 1	8.344×10^{14}	1.033	1.011	-2.13	1.012	-2.03
	29.67		0	7.948×10^{11}	1.000	1.009	0.9	1.010	1.0
	28.68		1	7.571×10^{8}	0.967	1.007	4.13	1.007	4.13
	27.69		2	7.194×10^{5}	0.933	1.004	7.60	1.005	7.71
395.3	31.31	1.0	– 2	8.642×10^{17}	1.067	1.004	-5.90	1.004	-5.90
	30.33		– 1	8.208×10^{14}	1.033	1.002	-3.00	1.002	-3.00
	29.35		0	7.821×10^{11}	1.000	1.000	0.00	1.000	0.00
	28.37		1	7.451×10^{08}	0.967	0.998	3.21	0.998	3.21
	27.39		2	7.083×10^{05}	0.933	0.995	6.64	0.995	6.64

peak related to different a for different values of R, as is shown in Fig. 4.4.2, is reflected through the output values of E. The results extracted by using two versions of area method as given in Table 4.4.8 are quite in agreement.

It is to mention that in an experimental scenario, T_m is measured from a TL peak where a is unknown and hence E is usually estimated from the recorded TL data considering $a = 0$. Hence the impact of TDFF on accuracy of glow curve analysis using area method can be predicted at least theoretically. We have carried out a systematic error analysis in extracting activation energy from TL data. In Table 4.4.8 we have also given the error ($\delta E = \frac{E_{out} - E_{in}}{E_{in}} \times 100\%$) explicitly for each TL peak corresponding to different values of a. It can be seen from Table 4.4.8 that for $R = 0$ and 1, the inherent error in activation energy arising due to the temperature variation of frequency factor lie within 7 % whereas for $R = 0.5$, the error is within 8 %. On the other hand the range of error in peak shape method was beyond 11% for $R = 0.5$. In that sense the area method may be more preferable so that the error due to ignoring TDFF may be less.

Chapter 5

Skew-normal distribution for glow curve deconvolution

5.1 Introduction to glow curve deconvolution

Glow curve analysis (GCA) is the most used technique for the estimation of trapping parameters from an experimental thermoluminescence glow curve. However this involves a lot of intricacies and uncertainties, because an experimental glow curve in general is a complex one which is constituted by superposition of several prominent or satellite peaks. Various methodologies have been developed over the years for glow curve analysis, *e.g.* peak shape methods (Chen, 1969a,b), Initial rise method (Garlick and Gibson, 1948; Halperin et al., 1960; Nahum and Halperin, 1963), Variable heating rate method (Bohun, 1954), Curve Fitting (Mohan and Chen, 1970; Shenker and Chen, 1971) and Computerized Glow Curve Deconvolution (CGCD) (Horowitz and Moscovitch, 2012; Puchalska and Bilski, 2006; Singh et al., 2011) *etc.* Each technique has its own merits and demerits as well. Most of the methods are applied to single peak. So isolating the single peaks from the complex glow curve is a prerequisite in most of the cases. Depending on the nature of experimental glow curve, various experimental techniques like*e.g.* $T_M - T_{stop}$ (McKeever, 1980), isothermal thermal cleaning, dynamic heating method of thermal cleaning (Chithambo and Niyonzima, 2014; Pagonis and Shannon, 2000; Taylor and Lilley, 1978)) are adopted to deconvolute the component peaks from the complex glow curve. Different simulation based techniques *e.g.* non-linear least square fitting, division of glow curve by reference glow curve, glow curve subtraction *etc.*(Perks and Marshall, 1991), step-fitting simulation technique(Rasheedy, 2005)) for this pupose have been also reported. Glow curve deconvolution (GCD) is one of the most efficient methods which is frequently used in deconvoluting complex glow curves.

In recent past CGCD has emerged as one of the popular methods for analysis of complex glow curves. Several software programs which run on different commercial software packages (Peng et al., 2021) have been developed for CGCD to analyze complex TL data (Bos et al., 1993, 1994; Yossian and Horowitz, 1995). An important development towards establishing CGCD as a reliable research tool was the GLOCANIN project developed by Bos *et al.*(Bos et al., 1993, 1994) which is an intercomparison of glow curve analysis program. One of the widely used deconvolution softwares currently available is the 'GCA' program developed by CIEMAT (Delgado and Ros, 2001). A computer program, 'GlowFit' for CGCD based on first-order kinetics has been developed by Puchalska and Bilski (2006). A software 'PeakFit' has been developed (Singh et al., 2011) by a group of researcher at Manipur University in 2011. Within the framework of the open source R package 'tgcd' has been developed by Peng et al. (2016).

In CGCD the experimentally obtained complex TL glow curve is reconstituted

by iterative process using proper glow curve deconvoluting (GCD) function to build up the constituent single TL glow peaks. Therefore use of an appropriate GCD function is crucial for an efficient CGCD program. Many functions have been proposed and tried by researchers (Bos et al., 1993, 1994; Yossian and Horowitz, 1995) to describe the constituent peaks used in various CGCD programs. Some of GCD functions were developed on the basis of kinetic order formalism while others were formulated from the point of view of statistical distribution of TL data.

5.1.1 Deconvolution funtions using kinetic order equations

Kitis *et. al.* have proposed GCD functions for first, second and general order of kinetics (Kitis et al., 1998). The functions have been derived from the basic expression of intensity obtained from GOK model and expressed as.

$$I(T) = I_m \exp\left[1 + \frac{E}{kT}\left(\frac{T-T_m}{T_m}\right) - \frac{T^2}{T_m^2}\exp\left(\frac{E}{kT}\,\frac{T-T_m}{T_m}\right)\left(1-\frac{2kT}{E}\right) - \frac{2kT_m}{E}\right] \tag{5.1.1}$$

$$= I_m\,(b)^{\frac{b}{b-1}} \exp\left(\frac{E}{kT}\,\frac{T-T_m}{T_m}\right)\left[(b-1)\left(1-\frac{2kT}{E}\right)\frac{T^2}{T_m^2}\exp\left(\frac{E}{kT}\,\frac{T-T_m}{T_m}\right) + 1 + (b-1)\frac{2kT_m}{E}\right]^{-\frac{b}{b-1}} \tag{5.1.2}$$

Using this expression, activation energy may be obtained from TL data.

5.1.2 Deconvolution funtions using Weibull distribution function

A few probability distribution functions have been tried to describe single TL peak for the development of proper GCD function. Pagonis et al. (2001) have proposed a GCD function using 3 parameter Weibull probability function which can only be used to describe first order TL peaks. The GCD function is given by (Pagonis et al., 2001),

$$W(T) = 2.713 I_m \left(\frac{T-T_m}{\zeta} + 0.996\right)^{15} \exp\left[-\left(\frac{T-T_m}{\zeta} + 0.996\right)^{16}\right] \tag{5.1.3}$$

Here w is the width of the Weibull distribution and related to the full width half maxima (ω) of the Weibull function (5.1.3) and related as $b = 6.4368\omega$. The activation energy is estimated as,

$$E = \frac{2.417kT_m^2}{\omega} - kT_m \tag{5.1.4}$$

5.1.3 Deconvolution funtions using logistic asymmetric distribution function

In a later work, Pagonis and Kitis (2001) proposed another GCD function where logistic asymmetric statistical probability function was used which could describe second order TL curves only. The GCD function has been reported as (Pagonis and Kitis, 2001),

$$LA(T) = 5.2973 I_m \left(1 + \exp\left[-\left(\frac{T - T_m}{a_2} + 0.38542\right)\right]^{2.4702}\right) \exp\left[-\left(\frac{T - T_m}{a_2} + 0.38542\right)\right] \quad (5.1.5)$$

Here $a_2 = 0.3121\omega$, a_2 is the width of the LA function (5.1.5) and ω = full width at half maxima.

Moreover, in TL literature, (Chandrasekhar and Gartia, 2018; Perepelitsa et al., 2018) the application of Gaussian function to deconvolute complex TL data is also available. However, Chandrasekhar and Gartia (2018) have shown that Gaussian function is not suitable for this purpose. Conceptually it is also understandable as the Gaussian function is composed of two parameters (the mean (λ) and variance (σ^2)), whereas a single TL peak is characterized by at least three kinetic parameters (E, s, b) in GOK model or four parameters in band theory based OTOR model (E, s, f, R). It is further remarkable that the Gaussian (normal) distribution is symmetric in nature whereas the shape of a single TL peak is usually asymmetric. The nature of asymmetry in TL curve depends on the retrapping-recombination mechanism during the heating stage. This dependence can be systematically reflected through the skewness of a TL dataset and that skewness of TL data may be exploited to reflect the shape of a single TL curve. Hence a probability distribution function which includes skewness of the data to the normal distribution function may be a potential candidate for developing an appropriate GCD function. Apart from this, it is to mention that all the proposed GCD functions Eqs. (5.1.1, 5.1.3, 5.1.5) mentioned above were derived on the basis of GOK model. Hence development of a GCD function based on band theory based OTOR model can be a significant improvement towards this direction.

During this study we have made an attempt to explore the above mentioned possibilities. The primary motivation of this work is to develop a GCD function from a statistical view point on the basis of OTOR model. Since in OTOR model a TL intensity is characterized by four parameters (E, s, f, R), the probability distribution function is likely to be composed of at least four parameters. Keeping all this in mind we adopted a version of skew normal distribution function for this purpose. But investigating the skew normal distribution function needs prior insight of normal distribution function for describing experimental TL peaks. Hence we critically investigate the normal distribution function to describe some experimental TL peaks mentioned by Chandrasekhar and Gartia (2018), simulated using

GOK model and highlight the limitations. In the next step, we consider the OTOR model and apply the skew normal distribution to examine its suitability as GCD function. It is to note that the present work is carried out in OTOR model using $R = 0$ and 1 which corresponds to first and second order kinetics respectively.

5.2 Glow curve Simulation

Glow curves have been simulated in kinetic order model as well as in OTOR model. A set of "intensity (I) – temperature (T)" data set is obtained as output of simulation where charge neutrality and quasi equilibrium condition given in Eqs. (1.2.20) and (1.2.21) was considered. The TL data was simulated under linear heating scheme where the heating rate (β) was kept fixed. The initial concentration of trapped electrons (n_0) at initial temperature T_0 was used as initial condition. For simulation in kinetic order model we have used the first, second and general order kinetic equations for TL intensity which is given in introduction chapter in Eqs. (1.2.3), (1.2.7) and (1.2.10). The input parameters are activation energy (E), frequency factor (s) and order of kinetics (b).

For data simulation in OTOR model under linear heating scheme, given in Eqs. (1.2.17), (1.2.18) and (1.2.19) have been adopted. For input parameters, apart from E and s, initial trap filling ratio $\left(f = \frac{n_0}{N}\right)$ and retrapping to recombination ratio $\left(R = \frac{A_n}{A_h}\right)$ was considered. Here N is the total trap concentration and A_n, A_h are probability of retrapping and recombination respectively.

5.3 Critical investigation on suitability of Gaussian function for GCD

The Gaussian function is symmetric in nature and characterized by two parameters, mean and variance. On the other hand, an well isolated TL glow curve is generally asymmetric in nature. Moreover, to describe a single TL peak, at least three parameters are needed. So limitations of Gaussian function as a GCD function to describe a TL peak is inherent in its nature. However, Gaussian function may fairly be used to have a primary idea about the peak locations and number of constituent peaks in a complex glow curve. It is to mention that deconvolution of complex TL glow curve using Gaussian function have also been reported in literature (Chen et al., 2016; Kang et al., 2012; Mu et al., 2011; Xu et al., 2010). However, further investigation and conceptual clarity are required in this aspect.

5.3.1 Fitting with Gaussian functions

The TL curves simulated in kinetic order model and OTOR model are fitted using Gaussian distribution functions. The basic form of the function is given by

$$I_g(T) = I_0 + \frac{A}{\sigma_g}\sqrt{\frac{2}{\pi}}\ \exp\left[-2\left(\frac{T - T_{mg}}{\sigma_g}\right)^2\right] \tag{5.3.1}$$

where $I_g(T)$ is the TL intensity at temperature T, I_0 = offset, A = area. The peak maxima occurs at the mean position (T_{mg}) and σ_g is the width at inflection points (T_i^- in the rising side and T_i^+ in the falling side of the curve). Hence,

$$\frac{d^2 I_g}{dT^2} = 0 \qquad \text{at} \quad T = T_i^{\pm} = T_{mg} \pm \frac{\sigma_g}{2} \tag{5.3.2}$$

The Gaussian fitting is carried out using a computer code written in programming language R. We have also estimated mode *i.e.* T_{mg} and variance σ_g as the fitting parameter.

5.3.2 Estimation of mode (T_m) and variance (σ) from simulated TL data

From the simulated TL data T_m and σ are calculated through a suitable computer program. The simulated TL data were fed to the code as input. T_m were located using iterative process. To find out σ, differentiation of TL data were performed numerically using forward difference method (Abramowitz and Stegun, 1972). After performing double derivative of simulated $I - T$ data, the temperatures were extracted iteratively where $\frac{d^2 I}{dT^2} = 0$.

5.4 Preliminary analysis of the results obtained from Gaussian fittings

To investigate the suitability of Gaussian function in GCD, we have simulated a fairly large number of TL curves in GOK and OTOR model. TL curves were simulated with the input values of activation energy in the range $0.5 \leq E_{in} \leq 1.5$ eV, the frequency factor lies in the range $10^8 \leq s_{in} \leq 10^{12}$ sec^{-1}. In case of TL curves in GOK model, the order of kinetics is varied within the range $1 \leq b \leq 2$ in step 0.1. For OTOR TL curves the initial filling ratio (f) is taken from 0.1 to 1 in step 0.1 and the retrapping to recombination ratio R is considered from 0 to 1 in step 0.1 and then 1 to 10 in step 1. It is to mention that $R = 0$ is equivalent to first order peak (*i.e.* $b = 1$), For $0 < R < 1$ TL curves are similar to GOK curves that covers the range *i.e.* $1 < b < 2$ cases and for $R = 1$ the glow peak represents

the second order case *i.e.* $b = 2$. The heating rate in all the cases is 1.0 Ks^{-1}.

5.4.1 Gaussian fit of GOK curves

The TL data generated in GOK model are fitted using Eq. (5.3.1). Quality of fit for some representative cases are depicted in Fig. 5.4.1 (a) – (d). It is clear that quality of fit using Gaussian function is not at all satisfactory. In particular, glow peaks similar to first order peak yield very poor fitting results. In case of second order peaks, the quality of fit improves marginally because th esecond order peaks are nearly symmetric in nature, (*i.e.* $\mu'_g = 0.42$). However it may be concluded that a normal distribution function is not a suitable candidate to provide a proper GCD function.

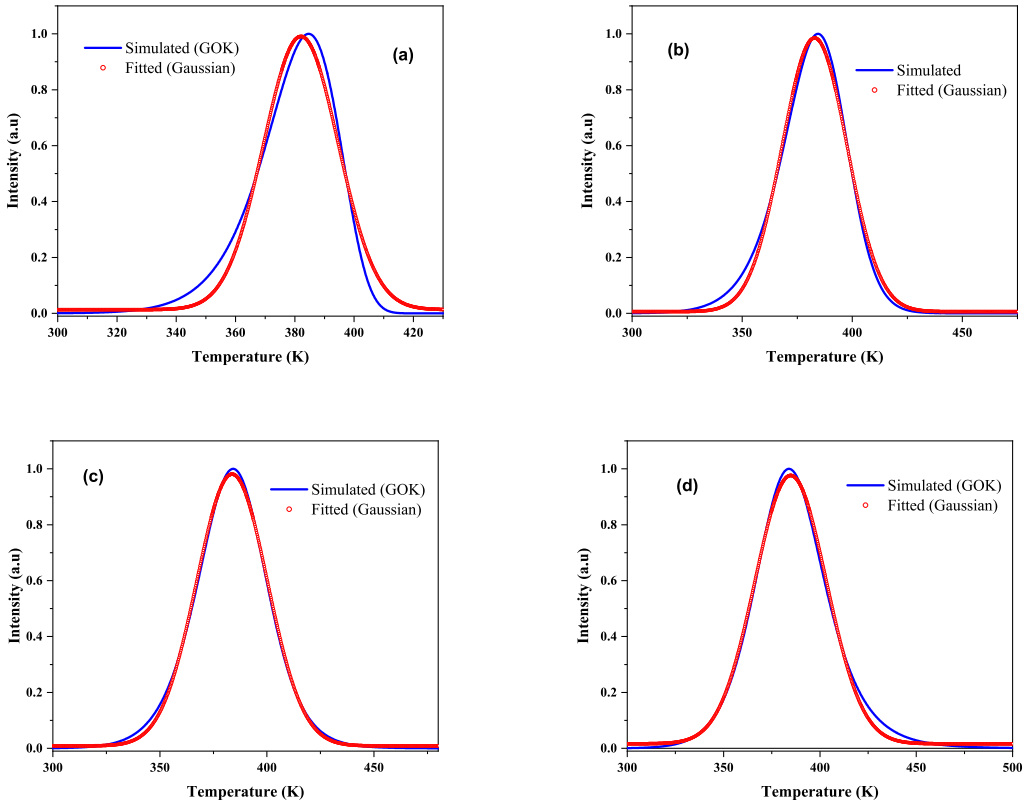

Figure 5.4.1: Fitting of GOK TL glow curve using Gaussian distribution function. For all the cases input values of trapping parameters are: $E = 1$ eV, $s = 10^{12}$ sec^{-1}, $\beta = 1$K/sec. The values of b for: (a) $b = 1.0$, (b) $b = 1.3$, (c) (a) $b = 1.6$, (d) $b = 2.0$.

The parameters (*i.e.* T_{mg} and σ_g) yielded after Gaussian fitting the GOK curves are presented in table 5.4.1 for the representative cases give in Fig. 5.4.1. The calculated value of the same parameters (*i.e.* T_m and σ) obtained from simulated curves along with

the input parameters for curve simulation are also presented in Table 5.4.1. It is seen from the Table 5.4.1, that the values of T_m and σ given in column-II which are obtained from fitting do not show satisfactory agreement with the values estimated from TL data which is shown in column-III. Nevertheless there may be one advantage that can be extracted from Gaussian fit. The values of T_m and σ obtained from the fit may serve as initial guess which can be used in further deconvolution process.

Table 5.4.1: Gaussian fit of TL curves simulated in kinetic order approximation. The input parameters for curve simulation, the parameters estimated from simulated curve and parameters obtained after fitting are listed. Here linear heating rate $\beta = 1.0\ K.s^{-1}$ is adopted.

Input parameters for simulation			parameters estimated from simulated curve		Gaussian fit parameters	
$E(eV)$	$s(sec^{-1})$	b	$T_{ms}(K)$	$\sigma_s(K)$	$T_{mg}(K)$	$\sigma_g(K)$
1	10^{12}	1	384.64	24.19	382.05	25.23
1	10^{12}	1.3	384.43	26.68	382.86	29.48
1	10^{12}	1.6	384.22	28.9	383.71	33.04
1	10^{12}	2	383.94	31.47	384.81	37.09

5.4.2 Gaussian fit of OTOR curves

Table 5.4.2: Gaussian fit of TL curves simulated in OTOR model. The input parameters for curve simulation, the parameters estimated from simulated curves and parameters obtained after fitting are depicted. Here linear heating rate $\beta = 1.0\ K.s^{-1}$ is adopted.

Input parameters for simulation				parameters estimated from simulated curve		Gaussian fit parameters	
$E(eV)$	$s(sec^{-1})$	f	R	$T_{ms}(K)$	$\sigma_s(K)$	$T_{mg}(K)$	$\sigma_g(K)$
1	10^{12}	0.5	0	384.56	23.86	381.95	25.57
1	10^{12}	0.5	0.5	388.1	29.41	388.52	35.51
1	10^{12}	0.5	1	392.02	32.38	393.22	39.05
1	10^{12}	0.5	10	415.97	43.65	418.55	49.33

In a similar manner we continue to examine the quality of fit using Gaussian distribution when the glow curves are simulated in OTOR model. Some representative cases have been shown in Fig. 5.4.2 (a) – (d). It is to mention that Fig. 5.4.2 (d) exhibits the heavy retrapping case ($R = 10$). Fig. 5.4.2 again shows the limitation of Gaussian function to be used in deconvoluting experimental complex glow curves. The results obtained from Gaussian fitting are listed in Table 5.4.2 along with the input parameters for the simulated curves. The values of peak position (T_m) and variance (σ) are also estimated and listed

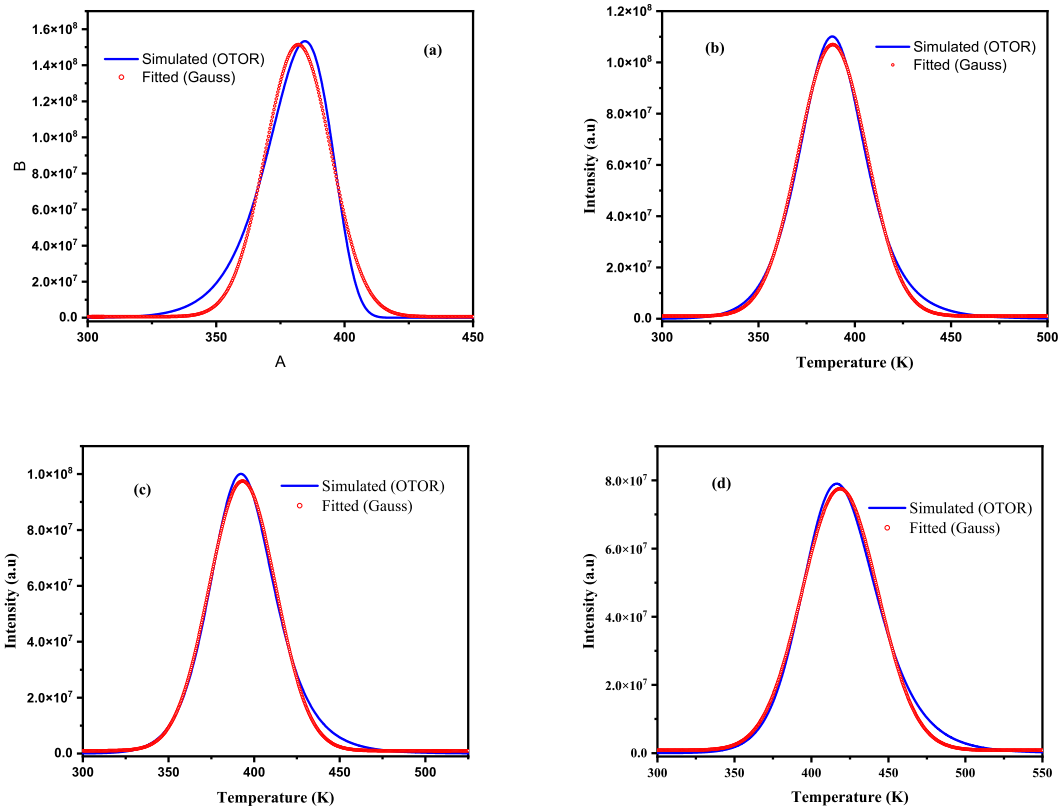

Figure 5.4.2: Fitting of OTOR glow curve using normal distribution function. For all the cases input values of trapping parameters are: $E = 1$ eV, $s = 10^{12}$ sec^{-1}, $f = 0.5$, $\beta = 1$K/sec. The values of R for: (a) $R = 0.0$, (b) $R = 0.5$, (c) $R = 1.0$, (d) $R = 10$.

in Table 5.4.2 for comparison. Table 5.4.2 shows significant mismatch between the output parameters which confirms the incapability of normal distribution to yield a GCD function.

5.5 Investigating the suitability of skew normal distribution function for GCD

From the above study it is evident from all aspects that the Gaussian distribution function is not quite a suitable choice for developing a proper GCD function. The skewed nature of TL curves can not be addressed properly by normal distribution function. Hence different methodologies applied to deconvoluted data are expected to misleading results in TL analysis. Hence we extend our study to explore the suitability of skew normal distribution function to develop proper GCD function based on OTOR model. It is to mention that under the purview of the present study using skew normal distribution we have adopted the

OTOR model only.

5.5.1 Methodology of fitting the OTOR glow curves using skew normal distribution function

The basic version of a skew normal distribution function is characterized by mainly three parameters, *viz.* the mean (λ), variance (σ^2) and skewness (S_k). However, depending on the nature of the system and quality of data, more number of parameters may be needed in order to improve the quality of fit. In the present procedure we started with three parameters (β_1, β_2, β_3) in the distribution functions and then increased it to four (β_1, β_2, β_3, β_4) but finally our study reveals that to fit TL data simulated in OTOR model, the skew normal distribution function characterized by five parameters is better suitable.

The computation is done in programming language 'R' which is widely used for statistical computation and data visualization. According to the present proposition the TL intensity in skew normal distribution is expressed as

$$I(T) = \frac{2}{\sqrt{\pi}} exp\left[\frac{1}{2}\left(\frac{T-\beta_1}{\beta_2}\right)^2\right] pnorm\left(\beta_3 T, \beta_3\beta_1, \beta_2\right)\beta_4 + \beta_5 \tag{5.5.1}$$

'pnorm' is the function in 'R' that returns the value of the cumulative density function (cdf) of the normal distribution of a random variable x, with population mean μ, and population standard deviation σ. Cumulative density function (cdf) of normal distribution of a random variable x:

$$\phi\left(\lambda\frac{x-\mu}{\sigma}\right) = \int_{-\infty}^{\frac{\lambda(x-\mu)}{\sigma}} \frac{1}{2\pi} e^{-\frac{z^2}{2}} dz \tag{5.5.2}$$

The characteristic parameters in the probability function are related to the glow data which is to be fitted (Fig. 5.5.1). The relations are as follows:

i) β_1 = Peak temperature (T_m).

ii) β_2 = peak width at inflection points.

iii) β_3 = skewness of TL data.

iv) β_4 = Peak height (*i.e.* (I_{max} - I_{min})).

v) $\beta_5 = I_{max}$.

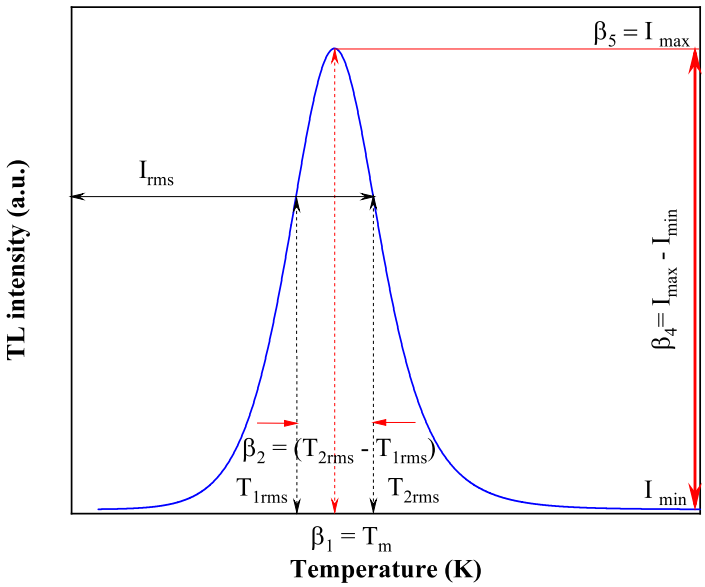

Figure 5.5.1: Schematic diagram showing relations between the characteristic parameters of proposed skew normal distribution and the various features of TL glow curve

The simulated TL data in OTOR model is fed to the 'R' code and a set of initial (guess) values for β_1, β_2 and β_3 are given as input. Based on these initial values, iteration is performed to yield the best values of the fitting parameters. For obvious reasons, if the initial guess values are close to the actual values, the process of iteration converges rapidly. To do away with this difficulty we first fit the input TL data by using a normal distribution function to have better initial guess of β_1 and β_2. The initial guess of β_3 is given intuitively by seeing the skewed nature of input TL data. The code does not require initial values of β_4 and β_5 as they are calculated within the process and final iterated values of all the fitting parameters are obtained as output.

5.5.2 Results obtained on the investigating the of skew normal distribution function for GCD

We now proceed to verify the applicability of the skew normal distribution function as GCD function. In this work we have only considered $R = 0$ and 1 cases that correspond to first and second order TL curves.

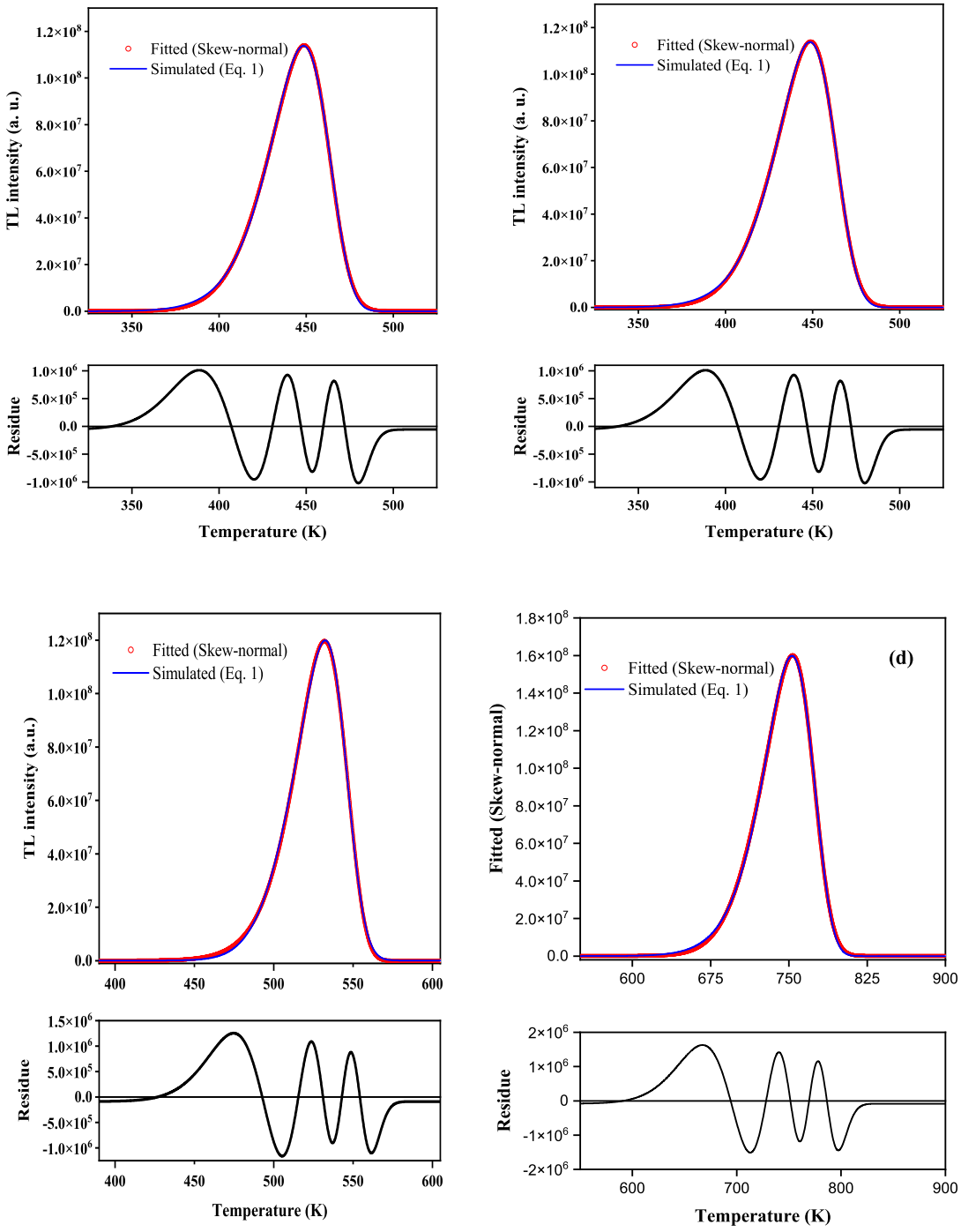

Figure 5.5.2: Fitting of TL glow curve using skew normal distribution function. Glow curves are simulated in OTOR model where R = 0 and f = 0.5 were taken. The left glow curve is simulated with $E = 1$ eV and $s = 10^{10}\ s^{-1}$ whereas the right glow curve is for $E = 1.5$ eV and $s = 10^{13}\ s^{-1}$

.

5.5.3 Fitting of OTOR glow curves

For generating OTOR TL curves for $R = 0$ and 1, we have taken E (eV) within $0.1 \leq E \leq 2.0$ in step 0.1. For every E the values of s (s^{-1}) are $10^7, 10^8, 10^9, 10^{10}, 10^{11}, 10^{12}, 10^{13}$ while f varied within $0.1 \leq f \leq 1.0$ in step 0.1. The OTOR curves are fitted with the proposed skew normal distribution function (Eq. 5.5.1) and the results are given in Fig.(5.5.2) for $R = 0$. The residues *i.e.* the difference between simulated data and fitted data are also plotted here. That results show quite satisfactory fitting. In Table 5.5.1 we have given the output values of the characteristic parameters of the skew normal distribution for some randomly chosen set of input TL parameters corresponding to $R = 0$. The correlation between the TL data and fitted data are also given in Table 5.5.1 and the results are quite satisfactory.

Table 5.5.1: The input values used for TL curve simulation (Eq. 4.2.6) along with the fitted parameters of skew normal distribution function (Eq. (5.5.1)). Here $R = 0$ and linear heating rate $\beta = 1.0\ K.s^{-1}$ is adopted.

Input parameters			**Parameters obtained after fitting**					
E (eV)	s (s^{-1})	f	β_1 (K)	β_2 (K)	β_3	β_4	β_5	Correlation
0.1	10^{07}	0.1	69.51	5.84	-2.43	1.71×10^8	1.86×10^4	0.99995
0.2	10^{10}	0.5	98.36	6.25	-2.64	7.96×10^8	2.27×10^5	0.99991
0.3	10^{13}	1.0	114.52	5.87	-2.76	1.69×10^9	5.17×10^5	0.99989
0.4	10^{07}	0.5	258.81	20.54	-2.48	2.43×10^8	4.58×10^4	0.99994
0.5	10^{10}	1.0	237.39	14.64	-2.66	6.79×10^8	2.54×10^5	0.99991
0.6	10^{13}	0.1	224.24	11.28	-2.77	8.81×10^7	3.28×10^4	0.99988
0.7	10^{07}	1.0	440.54	34.20	-2.50	2.91×10^8	7.96×10^4	0.99993
0.8	10^{10}	0.1	373.19	22.68	-2.67	4.39×10^7	1.44×10^4	0.99991
0.9	10^{13}	0.5	332.28	16.53	-2.77	3.00×10^8	1.60×10^5	0.99988
1.0	10^{07}	0.1	618.55	47.37	-2.51	2.10×10^8	5.09×10^4	0.99993
1.1	10^{10}	0.5	507.13	30.52	-2.67	1.63×10^8	4.75×10^4	0.99991
1.2	10^{13}	1.0	439.26	21.69	-2.78	4.58×10^8	1.97×10^5	0.99988
1.3	10^{07}	0.5	794.09	60.22	-2.52	8.28×10^7	1.74×10^4	0.99993
1.4	10^{10}	1.0	639.76	38.22	-2.68	2.60×10^8	7.81×10^4	0.99991
1.5	10^{13}	0.1	545.46	26.78	-2.78	3.71×10^7	1.77×10^4	0.99988
1.6	10^{07}	1.0	967.78	72.81	-2.52	1.37×10^8	2.84×10^4	0.99993
1.7	10^{10}	0.1	771.38	45.80	-2.68	2.17×10^7	6.91×10^3	0.99991
1.8	10^{13}	0.5	651.06	31.81	-2.78	1.56×10^8	7.03×10^4	0.99988
1.9	10^{07}	0.1	1139.99	85.22	-2.53	1.17×10^7	2.41×10^3	0.99993
2.0	10^{13}	0.5	721.16	35.14	-2.78	1.41×10^8	7.26×10^4	0.99988

In a similar manner, OTOR model TL curves are simulated for $R = 1$ and fitted with the skew normal function. In Fig.(5.5.3) a few representative cases are depicted to show the quality of fitting along with the residue plot.

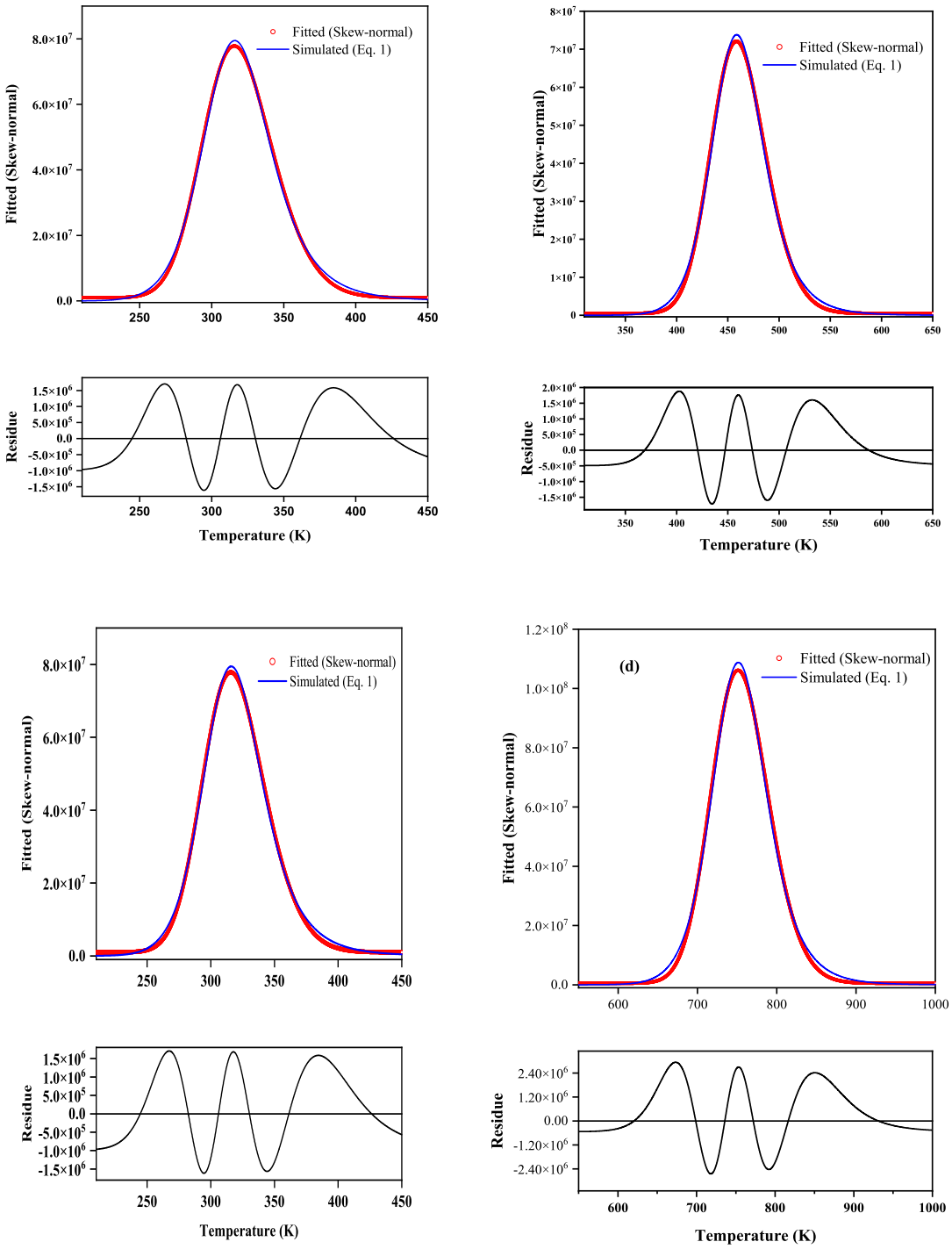

Figure 5.5.3: Fitting of TL glow curve using skew normal distribution function. Glow curves are simulated in OTOR model where $R = 1$ and $f = 0.5$ were taken. The left glow curve is simulated with $E = 1$ eV and $s = 10^{10}\ s^{-1}$ whereas the right glow curve is for $E = 1.5$ eV and $s = 10^{13}\ s^{-1}$

The input values for simulation of some TL curves and the fitting parameters obtained from skew normal distribution are shown in the Table 5.5.2 for $R = 1$. The values of correlation given in Table 5.5.2 confirms the suitability of the proposed probability distribution to derive a GCD function for OTOR glow curve equivalent to second order kinetics.

Table 5.5.2: The input values used for TL curve simulation (Eq. 4.2.6) along with the fitted parameters of skew normal distribution function (equation (5.5.1)). Here $R = 1$ and linear heating rate $\beta = 1.0\ K.s^{-1}$ is adopted.

Input parameters			**Parameters obtained after fitting**					
E (eV)	s (s^{-1})	f	β_1 (K)	β_2 (K)	β_3	β_4	β_5	Correlation
0.1	10^{07}	0.1	69.60	9.58	1.68	9.85×10^{7}	6.56×10^{5}	0.99914
0.2	10^{10}	0.5	93.03	8.04	1.41	5.94×10^{8}	2.24×10^{6}	0.99914
0.3	10^{13}	1.0	107.60	6.94	1.28	1.38×10^{9}	3.25×10^{6}	0.99912
0.4	10^{07}	0.5	240.26	27.72	1.57	1.70×10^{8}	1.09×10^{6}	0.99919
0.5	10^{10}	1.0	219.60	17.71	1.38	5.38×10^{8}	2.36×10^{6}	0.99914
0.6	10^{13}	0.1	225.67	15.29	1.30	6.25×10^{7}	2.18×10^{5}	0.99912
0.7	10^{07}	1.0	397.50	42.72	1.52	2.20×10^{8}	1.64×10^{6}	0.99919
0.8	10^{10}	0.1	375.25	32.62	1.41	2.92×10^{7}	1.36×10^{5}	0.99914
0.9	10^{13}	0.5	319.10	20.13	1.26	2.37×10^{8}	1.06×10^{6}	0.99912
1.0	10^{07}	0.1	620.67	74.03	1.58	1.27×10^{7}	9.87×10^{4}	0.99915
1.1	10^{10}	0.5	481.40	38.85	1.38	1.23×10^{8}	4.09×10^{5}	0.99913
1.2	10^{13}	1.0	413.81	25.44	1.26	3.76×10^{8}	1.22×10^{6}	0.99911
1.3	10^{07}	0.5	740.30	80.54	1.53	5.89×10^{7}	3.16×10^{5}	0.99916
1.4	10^{10}	1.0	593.46	46.20	1.36	2.07×10^{8}	6.49×10^{5}	0.99913
1.5	10^{13}	0.1	549.10	35.91	1.28	2.65×10^{7}	1.18×10^{5}	0.99912
1.6	10^{07}	1.0	876.17	91.32	1.51	1.04×10^{8}	4.81×10^{5}	0.99915
1.7	10^{10}	0.1	775.70	65.42	1.40	1.46×10^{7}	6.23×10^{4}	0.99914
1.8	10^{13}	0.5	625.76	38.76	1.26	1.23×10^{8}	4.40×10^{5}	0.99911
1.9	10^{07}	0.1	1144.00	132.50	1.57	7.14×10^{6}	4.40×10^{4}	0.99917
2.0	10^{13}	0.5	693.32	42.68	1.25	1.12×10^{8}	4.64×10^{5}	0.99911

5.5.4 Relation between fitting parameters and trapping parameters

For further progress in the direction of study, we have carried out some preliminary investigation about estimating the trapping parameters (mainly the activation energy) after deconvolution using skew normal distribution function as GCD function. In this case, it is instructive to explain the relationship between the fitting parameters of the proposed GCD function and trapping parameters of the glow curves.

An useful GCD technique is expected to have the scope to retrieve the value of activation energy. It needs a relationship among trapping parameters and fitting parameters of the GCD function. Therefore we considered a large number of simulated TL curves with

wide range of input parameters: $0.1 \leq E \leq 2.0$ in step 0.1 eV, $10^7 \leq s \leq 10^{13}$ in order of 10 sec^{-1}, $0.1 \leq f \leq 1$ in step 0.1 and $R = 0$, 1. In fitting parameters, we consider β_1, β_2 and β_3 as these are physically and mathematically significant. In Fig. 5.5.4 we show a graphical presentation to study relation between β_1, β_2, β_3 and the activation energy for different values of frequency factors. It is seen that a systematic linear relation between activation energy and β_1, β_2 is prominent whereas it does not depend much on β_3 (*i.e.* skewness). A similar study has been performed for $R = 1$ cases and the results are graphically shown in Fig. 5.5.5. The findings are similar to $R = 0$ cases. It is to mention that in previous reports (Kitis et al., 1998; Pagonis and Kitis, 2001; Pagonis et al., 2001) it can be observed that the formula to estimate E depends on peak height, width and asymmetry which is also obvious from the present study. However, to formulate a direct mathematical expression of E in terms of the fitting parameters (β_1, β_2, β_3) more studies are needed. It seems quite possible to derive a new formula based on OTOR model which can be used to estimate trapping parameters. Thus it can be said this study establishes the proposed skewnormal function as a fairly potential candidate to be used as a GCD function.

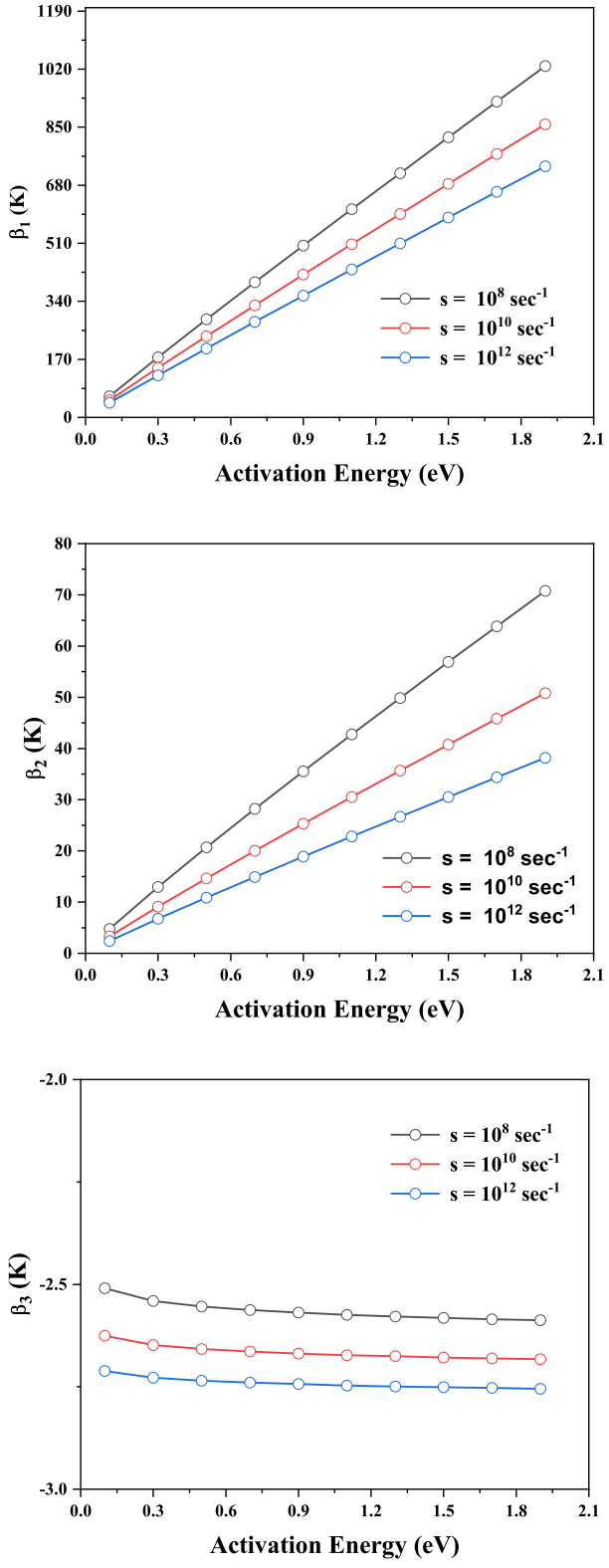

Figure 5.5.4: Plot between fitting parameters of skew normal distribution and the trapping parameters related to glow curves. Here $f = 0.5$ and $R = 0$ are considered as input parameters of curve simulation for all the cases.

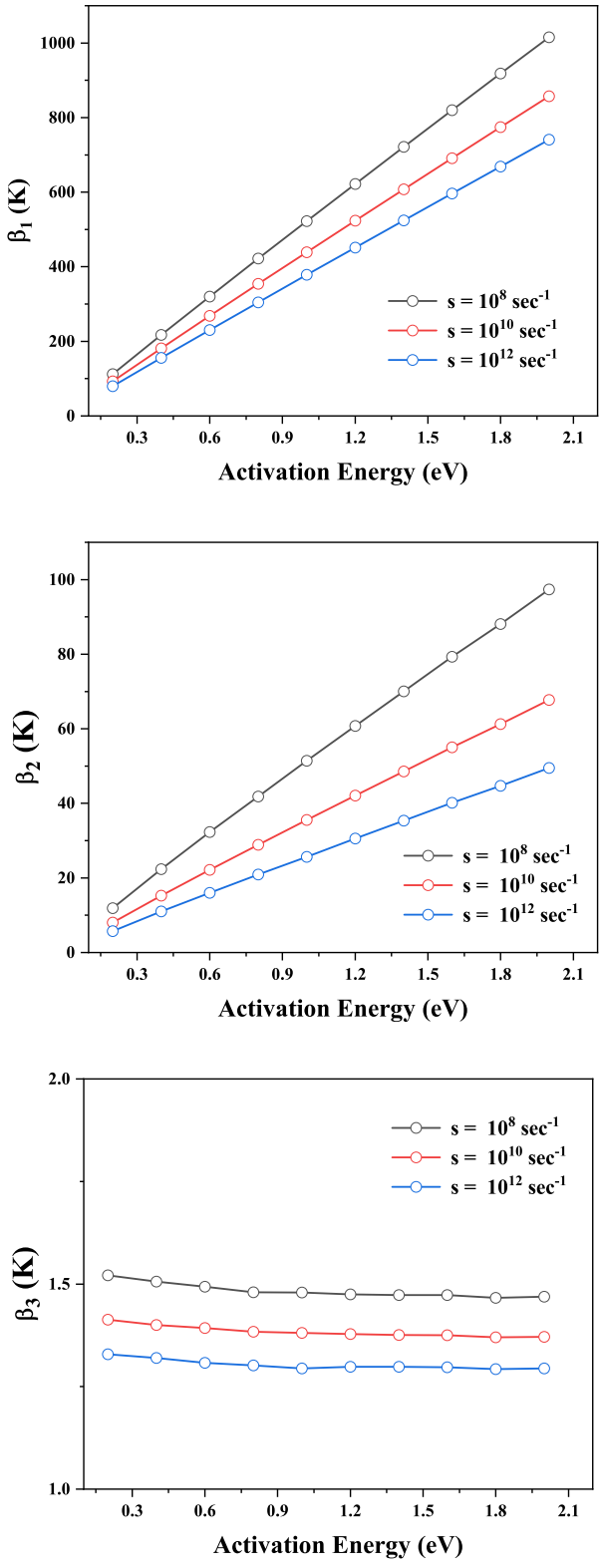

Figure 5.5.5: Plot between fitting parameters of skew normal distribution and the trapping parameters related to glow curves. Here $f = 0.5$ and $R = 0$ are considered as input parameters of curve simulation for all the cases.

Chapter 6

Concluding remarks and future outlook

In this dissertation detailed study has been performed regrading different aspect of thermoluminescence. The primary motivation behind this endeavor is to explore the possibilities to improve the present methodologies of thermoluminescence glow curve analysis and propose new methodologies for the same purpose. The whole work can be classified into three phases. At first we have focused on analytical development of mathematical procedures involved in TL study. In this regard, the TL process has been investigated engaging the temperature dependent frequency factor using band theory based models. In the next phase, we have worked towards the development of critical analysis of new methodologies for the improvement in glow curve analysis. Finally a new approach based on statistical distribution has been proposed aiming the development of computer based glow curve analysis.

During the present study a new analytical procedure to evaluate temperature integral *i.e.* $\int_{T_i}^{T_f} e^{-\frac{E}{kT}} dT$ using converging infinite series is developed. It is to mention that the integral is not exactly analytically solvable in a closed form and it appears everywhere in the mathematical procedure involved in TL and also in many other thermally stimulated processes. So far, researchers adopted different approximated expressions for the evaluation of the integral. In this work a completely analytical way for the evaluation of the integral has been discussed. In a similar way an analytical evaluation of the 'extended temperature integral' of the form $\int_{T_i}^{T_f} T^a e^{-\frac{E}{kT}} dT$ is also developed. The novelty of the present method is that it is not subject to any approximation. Since the solution is obtained in a convergent infinite series form, its value can be obtained by truncating the series after considering suitable number of terms to achieve the desired level of accuracy. Also the described method can be easily realized computationally in a simple manner. Nowadays computer based TL analysis is being popular and therefore, the present method has the potential to be exploited towards the development of a library function in both commercial and open source software packages for TL analysis.

In this study two versions of peak shape relations have been developed. Set of peak shape formulae using different fractional intensity points have been developed for the estimation of activation energy from well isolated glow curves. The peak shape coefficients are determined using the average symmetry factor $< \mu'_g >$ of TL curve. A numerical relationship to express $< \mu'_g >$ in terms of b and $\frac{E}{kT_m}$ has been formulated. On the other hand another set of peak shape relations are developed where activation energy related to a well isolated peak can be estimated by using skewness of the TL data as a symmetry parameter. The applicability of both the methods have been critically examined. At first they are applied to simulated peaks generated using GOK model. The results have been

consistent. When applied to TL peaks simulated in OTOR model, the present methods found to work successfully except for saturated peaks which are subject to heavy retrapping. However this limitation is consistent with the general nature of peak shape methods as reported in literature. The reason of failure has been investigated and found that both the parameters *i.e.* $< \mu'_g >$ and S_k exhibit an anomalous pattern of variation with retrapping to recombination ratio for heavy retrapping cases. This limitation indicates the scope of future study and hence the need of the development of new methodologies for the cases where heavy retrapping prevails. The application of present peak shape methods in case of experimental peaks produces encouraging results. The activation energies derived from the τ parameter appears to be more accurate and the lower portion of the curve seems to produce better results.

Applicability of the recently developed 'Three-Point Area' (TPA) method, as a tool to analyze well isolated TL glow curves for simultaneous determination of activation energy and order of kinetics, has been critically discussed. The method has been succssfully applied to OTOR and GOK model glow curves in linear heating scheme. Systematic error analysis has been carried out. The application of this method on experimental peaks also show reasonable agreement. During this process, a relation between the ratio of retrapping to recombination probabilities and the temperature average of order of kinetics is established. It is observed that any set of three points excluding those on the lower half portion of the falling side of the curve can yield reasonably good output of activation energy and order of kinetics, given the entire area and the relevant partial areas under the curve are estimated properly. However, the results are more accurate if the datapoints are chosen from the rising side of the curve. The present results are quite consistent and encouraging enough to employ the TPA method further on TL curves based on other models like NMTS, IMTS *etc.* However, future works are to be carried out in this direction with emphasis on comparative analysis of experimental data by various state-of-the-art methods. The cases of heavy retrapping along with those beyond quasi-equilibrium approximations in different models are also under the future purview.

Temperature dependence of frequency factor (TDFF) has been taken into consideration as a major part of the study. At first the required development in theoretical background including the mathematical procedure has been carried out. The TL equations have been solved in OTOR model considering TDFF. Analytical expressions for peak maxima condition using Lambert-W function and Wright ω function in OTOR model are also developed. For simulation it has been possible to generate a particular TL peak for different values of temperature exponent 'a' lying within the range $-2 \leqslant a \leqslant 2$ by tuning other

relevant parameters. We have also been able to simulate a sample IMTS peak for different values of 'a' to check the validity of the present methodology. The activation energies are derived from the TL curves using two different versions of 'peak shape' method and two versions of 'area' method. The error incurred in activation energy due to the approximation of temperature independent frequency factor is estimated quantitatively. It has been found the error in activation energy becomes significant if the value of $\frac{E}{kT_m}$ goes below 20. The overall outcome of the present study is quite encouraging and expected to be useful in future research in the backdrop of recent advancements in experimental as well as computational techniques. The role of TDFF on TL curves simulated in different heating schemes like hyperbolic heating, exponential heating *etc.* are also to be explained in future.

Finally TL data has been analyzed statistically to describe the data distribution by adopting a suitable statistical distribution function. At first a critical examination has been carried out to investigate the suitability of Gaussian distribution as a GCD function for TL glow curve analysis and the results obtained are not at all satisfactory. Looking into the skewed nature of TL glow curve, a version of skew normal distribution characterized by five parameters is proposed. The suitability of this new probability function is investigated by applying it to large number of TL glow curves simulated in OTOR model. As a pilot investigation the TL curves which are equivalent to first and second order kinetics are considered. The quality of fitting is judged through residue plots as well as through the correlation between the TL data and fitted data. The outcome is quite encouraging which will definitely pave the way to formulate an efficient GCD function that may lead to the development of a CGCD technique based on OTOR model.

Bibliography

[1] Abramowitz, M. and Stegun, I. A. (1972). *Handbook of Mathematical Functions*. Dover, New York.

[2] Aramu, F., Brovetto, P., and Rucci, A. (1966). Activation energy in the nacl thermoluminescence. *Physics Letters*, 23(5):308–309.

[3] Atlıhan, M. A. (2020). Thermoluminescence properties of two natural colorful fluorite samples of anatolian origin for dosimetric applications. *Nuclear Instruments and Methods in Physics Research Section B: Beam Interactions with Materials and Atoms*, 467:33 – 39.

[4] Balarin, M. (1985). Accuracy of various approximations to the exponential integral in glow curve theory. *Journal of Computational Physics*, 57(1):26–42.

[5] Balian, H. and Eddy, N. W. (1977). Figure-of-merit (FOM), an improved criterion over the normalized chi-squared test for assessing goodness-of-fit of gamma-ray spectral peaks. *Nuclear Instruments and Methods*, 145(2):389–395.

[6] Bemski, G. (1958). Recombination properties of gold in silicon. *Physical Review*, 111(6):1515.

[7] Bhattacharya, M., Singh, W. S., and Mazumdar, P. (2000). Determination of the temperature exponent for the case of the temperature-dependent frequency factor in thermoluminescence. *Canadian Journal of Physics*, 78(4):253–260.

[8] Bhattacharyya, S. and Majumdar, P. S. (2018). An overview on peak shape method for thermoluminescence glow curve analysis: Application on tremolite and actinolite glow peaks. In *Emerging Synthesis Techniques for Luminescent Materials*, pages 26–52. IGI Global.

[9] Biegen, J. R. and Czanderna, A. W. (1972). Analysis of thermal processes: The exponential integral. *Journal of thermal analysis*, 4(1):39–45.

[10] Böhm, M, E. O. and Scharmann, A, A. P. A. (1985,). Quantum mechanical treatment of the escape probability from traps in thermally stimulated processes,. *Appl. Phys. A*, 37,(165.).

[11] Böhm, M. and Scharmann, A. (1987). The pre-exponential factor of the escape probability in thermally stimulated processes. *Appl. Phys. A*, 43(29).

[12] Bohun, A. (1954). Thermoemission und photoemission von natriumchlorid. *Cechoslovackij fiziceskij zurnal*, 4(1):91–93.

[13] Bos, A., Piters, T., Gómez-Ros, J., and Delgado, A. (1993). An Intercomparison of Glow Curve Analysis Computer Programs: I. Synthetic Glow Curves. *Radiation Protection Dosimetry*, 47(1-4):473–477.

[14] Bos, A., Piters, T., Gómez-Ros, J., and Delgado, A. (1994). An Intercomparison of Glow Curve Analysis Computer Programs: II. Measured Glow Curves. *Radiation Protection Dosimetry*.

[15] Bosacchi, A., Franchi, S., and Bosacchi, B. (1974). Thermoluminescence and continuous distributions of traps. *Physical Review B*, 10(12):5235–5238.

[16] Bräunlich, P. (1979). *Basic principles inThermally stimulated relaxation in solids*. Springer-Verlag, Berlin.

[17] Bube, R. H. (1960). *Photoconductivity of solids*, page 50. Wiley, New York.

[18] Bull, R. K. (1989). Kinetics of the localised transition model for thermoluminescence. *Journal of Physics D: Applied Physics*, 22(9):1375–1379.

[19] Burden, R. L., Faires, J. D., and Reynolds, A. C. (2001). *Numerical Analysis: 9th Ed.* Brooks/Cole Cengage Learning, Boston, USA.

[20] Cameron, J. R., Daniels, F., Johnson, N., and Kenney, G. (1961). Radiation dosimeter utilizing the thermoluminescence of Lithium Fluoride. *Science*, 134(3475):333–334.

[21] Chandrasekhar, N. and Gartia, R. K. (2018). Gaussian approximation of thermoluminescence (TL) peaks: A common misconception for analysis of TL of persistent luminescent materials. *Journal of Alloys and Compounds*, 745:773–778.

[22] Chen, R. (1969a). Glow curves with general order kinetics. *Journal of The Electrochemical Society*, 116:1254–1257.

[23] Chen, R. (1969b). On the calculation of activation energies and frequency factors from glow curves. *Journal of Applied Physics*, 40:570–585.

[24] Chen, R. (1969c). On the computation of the integral appearing in glow curve theory. *Journal of Computational Physics*, 4:415–418.

[25] Chen, R. (1970). On the computation of the generalized integral in glow curve theory. *Journal of Computational Physics*, 6(2):314–316.

[26] Chen, R. (1974). On the methods for determining trap depth from glow curves. *Journal of Materials Science*, 9(2):345–347.

[27] Chen, R. and Kirsh, Y. (1981a). *Analysis of thermally stimulated processes*, page 163. Pergamon Press, Oxford.

[28] Chen, R. and Kirsh, Y. (1981b). *Analysis of thermally stimulated processes*. Pergamon Press, Oxford.

[29] Chen, R., Kristianpoller, N., Davidson, Z., and Visocekas, R. (1981). Mixed first and second order kinetics in thermally stimulated processes. *Journal of Luminescence*, 23(3-4):293–303.

[30] Chen, R. and McKeever (1997). *Theory of thermoluminescence and related phenomena*. World Scientific.

[31] Chen, R. and Mckeever, S. W. S. (1997). *Theory of Thermoluminescence and Related Phenomena*. World Scientific Publishing Company, Singapore.

[32] Chen, R. and Pagonis, V. (2011). *Thermally and optically stimulated luminescence: a simulation approach*.

[33] Chen, R. and Winer, S. A. A. (1970). Effects of various heating rates on glow curves. *Journal of Applied Physics*, 41(13):5227–5232.

[34] Chen, W., Wang, Y., Zeng, W., Li, G., and Guo, H. (2016). Enhancement of yellow persistent luminescence in Eu^{2+}-doped $\beta - Ba_3P_4O_{13}$ phosphor by Ga^{3+} codoping. *RSC Advances*, 6(54):48411–48414.

[35] Chithambo, M. and Niyonzima, P. (2014). On isothermal heating as a method of separating closely collocated thermoluminescence peaks for kinetic analysis. *Journal of Luminescence*, 155:70–78.

[36] Christodoulides, C. (1985). Determination of activation energies by using the widths of peaks of thermoluminescence and thermally stimulated depolarisation currents. *Journal of Physics D: Applied Physics*, 18:1501–1510.

[37] Christodoulides, C. (1986a). Parameter determination for general-order thermoluminescence peaks measured with hyperbolic heating. *physica status solidi (a)*, 94:251–258.

[38] Christodoulides, C. (1986b). Use of peak widths for the determination of the trap parameters of thermoluminescence glow curves recorded with hyperbolic heating. *Journal of Physics D: Applied Physics*, 19(8):1555–1562.

[39] Corless, R. M. and Jeffrey, D. J. (2002). The wright ω function. In *Artificial intelligence, automated reasoning, and symbolic computation*, pages 76–89. Springer.

[40] Corless, R. M., Jeffrey, D. J., and Knuth, D. E. (1997). A sequence of series for the lambert w function. In *Proceedings of the 1997 international symposium on Symbolic and algebraic computation*, pages 197–204.

[41] Curie, D. (1963). *Luminescence in crystals*, pages 142–145. Methuen.

[42] Daniels, F., Boyd, C. A., and Saunders, D. F. (1953). Thermoluminescence as a research tool. *Science*, 117(3040):343–349.

[43] Delgado, A., Muñiz, J., and Ros, J. (1994). On the peculiarities of peak 4 in LiF TLD-100. *Radiation Measurements*, 23(4):693–701.

[44] Delgado, A. and Ros, J. M. G. (2001). Computerised glow curve analysis: A tool for routine thermoluminescence dosimetry. *Radiation Protection Dosimetry*, 96(1):127–132.

[45] Dewangan, P., Bisen, D., Brahme, N., Tamrakar, R. K., Upadhyay, K., Sharma, S., and Sahu, I. P. (2018). Studies on thermoluminescence properties of alkaline earth silicate phosphors. *Journal of Alloys and Compounds*, 735:1383–1388.

[46] Dodge, Y. (2008). *The Concise Encyclopedia of Statistics*. Springer, New York.

[47] Dussel, G. A. and Bube, R. H. (1967). Theory of thermally stimulated conductivity in a previously photoexcited crystal. *Physical Review*, 155(3):764–779.

[48] Fleming, R. (1990). Activation energies and temperature-dependent frequency factors in thermally stimulated luminescence. *Journal of Physics D: Applied Physics*, 23(7):950.

[49] Garlick, G. F. J. and Gibson, A. F. (1948). The electron trap mechanism of luminescence in sulphide and silicate phosphors. *Proceedings of the Physical Society*, 60(6):574–590.

[50] Gartia, R. and Singh, L. L. (2011). Evaluation of trapping parameter of quartz by deconvolution of the glow curves. *Radiation Measurements*, 46(8):664–668.

[51] Gartia, R., Singh, S. D., Subodh, T., Singh, T., and Mazumdar, P. (1992). Determination of the activation energy of a thermally stimulated luminescence peak for the case of a temperature-dependent frequency factor. *Journal of Physics D: Applied Physics*, 25(3):530.

[52] Gartia, R. K., Singh, S. J., and Mazumdar, P. S. (1988). Symmetry factor and order of kinetics in thermally stimulated luminescence. *Physica Status Solidi (a)*, 106:291–296.

[53] Gibbs, J. H. (1972). Sufficient conditions for the arrhenius rate law. *The Journal of Chemical Physics*, 57(10):4473–4478.

[54] Gill, P. E. and Miller, G. (1972). An algorithm for the integration of unequally spaced data. *The Computer Journal*, 15:80–83.

[55] Gomez-Ros, J. M. and Kitis, G. (2002). Computerised glow curve deconvolution using general and mixed order kinetics. *Radiation Protection Dosimetry*, 101(1):47–52.

[56] Gorbachev, V. (1976). Algorism for the solution of the exponential integral in non-isothermal kinetics at linear heating. *Journal of Thermal Analysis and Calorimetry*, 10(3):447–449.

[57] Graham, R. L., Knuth, D. E., Patashnik, O., and Liu, S. (1994). *Concrete mathematics: a foundation for computer science*. 2nd edition, Addison-Wesley Publishing Company, Reading, USA.

[58] Grossweiner, L. I. (1953). A note on the analysis of first-order glow curves. *Journal of Applied Physics*, 24:1306–1307.

[59] Gurney, R. and Mott, N. (1940). *Electronic processes in ionic crystals*, page 136. University press, oxford.

[60] Haake, C. H. (1957). Critical comment on a method for determining electron trap depths. *Journal of the Optical Society of America*, 47(7):649.

[61] Hagebeuk, H. and Kivits, P. (1976). Determination of trapping parameters from the conventional model for thermally stimulated luminescence and conductivity. *Physica B+C*, 83(3):289–294.

[62] Halperin, A., Braner, A., Ben-Zvi, A., and Kristianpoller, N. (1960). Thermal activation energies in NaCl and KCl crystals. *Physical Review*, 117(2):416–422.

[63] Halperin, A. and Braner, A. A. (1960). Evaluation of thermal activation energies from glow curves. *Phys. Rev.*, 117:408–415.

[64] Hasan, F. A., Keck, B. D., Hartmetz, C., and Sears, D. W. (1986). Anomalous fading of thermoluminescence in meteorites. *Journal of Luminescence*, 34(6):327–335.

[65] Hoogenstraaten, W. (1958). Electron traps in zinc sulphide phosphors. *Philips Research Report*, 13:515–693.

[66] Horowitz, Y. S. (1984). *Thermoluminescence and thermoluminescent dosimetry*, volume 1. CRC Press Boca Raton.

[67] Horowitz, Y. S. and Moscovitch, M. (2012). Highlights and pitfalls of 20 years of application of computerised glow curve analysis to thermoluminescence research and dosimetry. *Radiation Protection Dosimetry*, 153:1–22.

[68] Ilich, B. M. (1979). Method of determination of trap depth. *Sov. Phys. Solid State*, 21:1880–1882.

[69] Ingraham, T. R. and Marier, P. (1964). Activation energy calculation from a linearly-increasing-temperature experiment. *The Canadian Journal of Chemical Engineering*, 42(4):161–163.

[70] Jabłoński, A. (1935). Über den mechanismus der photolumineszenz von farbstoffphosphoren. *Zeitschrift für Physik*, 94(1-2):38–46.

[71] Jain, M., Guralnik, B., and Andersen, M. T. (2012). Stimulated luminescence emission from localized recombination in randomly distributed defects. *Journal of Physics: Condensed Matter*, 24(38):385402.

[72] Kalita, J. M. and Wary, G. (2017). Temperature assisted radiative and non-radiative recombination mechanisms in sillimanite (Al_2SiO_5) mineral. *Spectrochimica Acta Part A: Molecular and Biomolecular Spectroscopy*, 175:61–66.

[73] Kang, F., Hu, Y., Wu, H., Mu, Z., Ju, G., Fu, C., and Li, N. (2012). Luminescence and red long afterglow investigation of $Eu^{3+}Sm^{3+}$ Co-doped $CaWO_4$ phosphor. *Journal of Luminescence*, 132(4):887–894.

[74] Karmakar, M., Bhattacharyya, S., Sarkar, A., Mazumdar, P. S., and Singh, S. D. (2017). Analysis of thermoluminescence glow curves using derivatives of different orders. *Radiation Protection Dosimetry*, 175:493–502.

[75] Karmakar, M., Sarkar, B., Azharuddin, S., Mazumdar, P., Singh, S. D., Singh, W. S., and Bhattacharya, M. (2010). On the temperature dependent frequency factor in thermoluminescence. *Indian Journal of Physics*, 84(5):529–537.

[76] Keating, P. N. (1961). Thermally stimulated emission and conductivity peaks in the case of temperature dependent trapping cross sections. *Proceedings of the Physical Society*, 78:1408–1415.

[77] Khiem, D. D., Matsuura, H., and Akiyoshi, M. (2020). Measurement of dose distribution from a crookes tube using thermoluminescent dosimeter. *Radiation Measurements*, 134:106312.

[78] Kirsh, Y. (1992). Kinetic analysis of thermoluminescence. *physica status solidi (a)*, 129:15–48.

[79] Kitis, G., Chen, R., and Pagonis, V. (2008). Thermoluminescence glow-peak shape methods based on mixed order kinetics. *physica status solidi (a)*, 205:1181–1189.

[80] Kitis, G. and Gomez-Ros, J. (2000). Thermoluminescence glow-curve deconvolution functions for mixed order of kinetics and continuous trap distribution. *Nuclear Instruments and Methods in Physics Research Section A: Accelerators, Spectrometers, Detectors and Associated Equipment*, 440(1):224–231.

[81] Kitis, G., Gomez-Ros, J., and Tuyn, J. W. (1998). Thermoluminescence glow-curve deconvolution functions for first, second and general orders of kinetics. *Journal of Physics D: Applied Physics*, 31(19):2636–2641.

[82] Kitis, G. and Pagonis, V. (2007). Peak shape methods for general order thermoluminescence glow-peaks: A reappraisal. *Nuclear Instruments and Methods in Physics Research Section B: Beam Interactions with Materials and Atoms*, 262:313–322.

[83] Kitis, G. and Pagonis, V. (2013). Analytical solutions for stimulated luminescence emission from tunneling recombination in random distributions of defects. *Journal of Luminescence*, 137:109–115.

[84] Kitis, G. and Pagonis, V. (2018). Localized transition models in luminescence: A reappraisal. *Nuclear Instruments and Methods in Physics Research Section B: Beam Interactions with Materials and Atoms*, 432:13–19.

[85] Kitis, G., Polymeris, G. S., and Pagonis, V. (2019). Stimulated luminescence emission: From phenomenological models to master analytical equations. *Applied Radiation and Isotopes*, 153:108797.

[86] Kitis, G. and Vlachos, N. (2013). General semi-analytical expressions for TL, OSL and other luminescence stimulation modes derived from the OTOR model using the Lambert W-function. *Radiation Measurements*, 48:47–54.

[87] Kucuk, N., Gozel, A. H., Yüksel, M., Dogan, T., and Topaksu, M. (2015). Thermoluminescence kinetic parameters of different amount La-doped ZnB_2O_4. *Applied Radiation and Isotopes*, 104:186–191.

[88] Kumar, A., Kumar, A., Dogra, R., Manhas, M., Sharma, S., and Kumar, R. (2020). Effect of gamma irradiation on thermoluminescence studies of LiF:Sm3+,Dy3+ nanophosphor. *Emerging Materials Research*, 9(1):122–131.

[89] Kundu, M., Chakrabarty, S., Bhattacharyya, S., and Majumdar, P. S. (2021). Reappraisal of peak shape method based on average geometrical symmetry factor and its application to thermoluminescence glow curves. *physica status solidi (b)*, 258(11):2100277.

[90] Lax, M. (1960). Cascade capture of electrons in solids. *Physical Review*, 119(5):1502.

[91] Levy, P. W. (1985). Thermoluminescence kinetics in materials exposed to the low doses applicable to dating and dosimetry. *Nuclear Tracks and Radiation Measurements (1982)*, 10(4-6):547–556.

[92] Lewandowski, A. and McKeever, S. (1991). Generalized description of thermally stimulated processes without the quasiequilibrium approximation. *Physical Review B*, 43(10):8163.

[93] Lovedy, L. (2017). Glow curve analysis of the 110^oC glow peak of quartz in the simplified got equation. *International Journal of Luminescence and applications*.

[94] Lovedy Singh, L. (2020). Formulation of OTOR differential equation for thermoluminescence using temperature dependent frequency factor. *Nuclear Instruments and Methods in Physics Research Section B: Beam Interactions with Materials and Atoms*, 474:63 – 67.

[95] Lushchik, C. B. (1956). The investigation of trapping centers in crystals by the method of thermal bleaching. *Sov. Phys. JETP*, 3:390–399.

[96] Mandowski, A. (2004). Semi-localized transitions model for thermoluminescence. *Journal of Physics D: Applied Physics*, 38(1):17–21.

[97] May, C. and Partridge, J. (1964). Thermoluminescent kinetics of alpha-irradiated alkali halides. *The Journal of Chemical Physics*, 40(5):1401–1409.

[98] Mazumdar, P. S., Singh, S. J., and Gartia, R. K. (1988). The determination of activation energy from the shape of a thermoluminescence peak. *Journal of Physics D: Applied Physics*, 21:815–819.

[99] McKeever (1988). *Thermoluminescence of solids*, volume 3. Cambridge University Press.

[100] McKeever, S. W. S. (1980). On the analysis of complex thermoluminescence. glow-curves: Resolution into individual peaks. *Physica Status Solidi (a)*, 62(1):331–340.

[101] Miller, L. D. and Bube, R. H. (1970). Luminescence, trapping, and f centers in Lithium Fluoride crystals. *Journal of Applied Physics*, 41(9):3687–3697.

[102] Mohan, N. S. and Chen, R. (1970). Numerical curve fitting for calculating glow parameters. *Journal of Physics D: Applied Physics*, 3(2):243–247.

[103] Moharil, S. (1981). A new method for obtaining trapping parameters from glow curves. *physica status solidi (a)*, 66(2):767–772.

[104] Mu, Z., Hu, Y., Wang, Y., Wu, H., Fu, C., and Kang, F. (2011). The structure and luminescence properties of long afterglow phosphor $Y_{3-x}Mn_xAl_{5-x}Si_xO_{12}$. *Journal of Luminescence*, 131(4):676–681.

[105] Muntoni, C., Ricci, A., and Sergi, A. (1968). On the analysis of thermoluminescence glow curves. *Ric. Sci.*, 9:762.

[106] Murthy, K. (2013). Thermoluminescence and its applications: A review. *Defect and Diffusion Forum*, 347:35–73.

[107] Nahum, J. and Halperin, A. (1963). Thermoluminescence and the relation between thermal and optical activation energies in diamond. *Journal of Physics and Chemistry of Solids*, 24(7):823–834.

[108] Pagonis, V. (2005). Evaluation of activation energies in the semi-localized transition model of thermoluminescence. *Journal of Physics D: Applied Physics*, 38(13):2179–2186.

[109] Pagonis, V., Chen, R., Kulp, C., and Kitis, G. (2017). An overview of recent developments in luminescence models with a focus on localized transitions. *Radiation Measurements*, 106:3–12.

[110] Pagonis, V. and Kitis, G. (2001). Fit of second order thermoluminescence glow peaks using the logistic distribution function. *Radiation Protection Dosimetry*, 95(3):225–229.

[111] Pagonis, V., Kitis, G., and Furetta, C. (2006). *Numerical and Practical Exercises in Thermoluminescence*. Springer New York.

[112] Pagonis, V., Mian, S., and Kitis, G. (2001). Fit of first order thermoluminescence glow peaks using the weibull distribution function. *Radiation Protection Dosimetry*, 93(1):11–17.

[113] Pagonis, V. and Shannon, C. (2000). An improved experimental procedure of separating a composite thermoluminescence glow curve into its components. *Radiation Measurements*, 32(5–6):805–812.

[114] Pardha Saradhi, M., Lakshminarasimhan, N., Boudin, S., Vijay Kumar Gupta, K., Varadaraju, U., and Raveau, B. (2014). Enhanced luminescence of $Sr_2SiO_4 : Dy^{3+}$ by sensitization (Ce^{3+}/Eu^{2+}) and fabrication of white light-emitting-diodes. *Materials Letters*, 117:302–304.

[115] Peng, J., Dong, Z., and Han, F. (2016). tgcd: An R package for analyzing thermoluminescence glow curves. *SoftwareX*, 5:112 – 120.

[116] Peng, J., Kitis, G., Sadek, A. M., Asal, E. C. K., and Li, Z. (2021). Thermoluminescence glow-curve deconvolution using analytical expressions: A unified presentation. *Applied Radiation and Isotopes*, 168:109440.

[117] Perepelitsa, A., Smirnov, M., Ovchinnikov, O., Latyshev, A., and Kotko, A. (2018). Thermostimulated luminescence of colloidal Ag_2S quantum dots. *Journal of Luminescence*, 198:357–363.

[118] Perks, C. and Marshall, M. (1991). Techniques for thermoluminescence glow curve analysis. *Radiation Protection Dosimetry*, 38(4):261–269.

[119] Petrov, S. and Bailiff, I. (1995). The '110^{o}C' TL peak in synthetic quartz. *Radiation Measurements*, 24(4):519–523.

[120] Petty, H. R., Arakawa, E. T., and Baird, J. K. (1977). Methods to determine the temperature dependence of the pre-exponential factor of the arrhenius equation from thermogravimetric data. *Journal of Thermal Analysis*, 11(3):417–422.

[121] Puchalska, M. and Bilski, P. (2006). GlowFit—a new tool for thermoluminescence glow-curve deconvolution. *Radiation Measurements*, 41(6):659–664.

[122] Quanyin, R. and Su, Y. (1995). New approximations of the temperature integral for nonisothermal kinetics. *Journal of Thermal Analysis*, 44(5):1147–1154.

[123] Randall, J. and Wilkins, M. (1945a). Phosphorescence and electron traps-I. the study of trap distributions. *Proceedings of the Royal Society of London. Series A. Mathematical and Physical Sciences*, 184(999):365–389.

[124] Randall, J. and Wilkins, M. (1945b). Phosphorescence and electron traps-II. the interpretation of long-period phosphorescence. *Proceedings of the Royal Society of London. Series A. Mathematical and Physical Sciences*, 184(999):390–407.

[125] Rasheedy, M. (2005). A new evaluation technique for analyzing the thermoluminescence glow curve and calculating the trap parameters. *Thermochimica Acta*, 429(2):143–147.

[126] Rasheedy, M. S. (1993). On the general-order kinetics of the thermoluminescence glow peak. *Journal of Physics: Condensed Matter*, 5(5):633.

[127] Rasheedy, M. S. (1996). A new method for obtaining the trap parameters of complex thermoluminescence glow peaks. *Journal of Physics D: Applied Physics*, 29(5):1340–1344.

[128] Sadek, A., Eissa, H., Basha, A., Carinou, E., Askounis, P., and Kitis, G. (2015a). The deconvolution of thermoluminescence glow-curves using general expressions derived from the one trap-one recombination (OTOR) level model. *Applied Radiation and Isotopes*, 95:214–221.

[129] Sadek, A., Eissa, H., Basha, A., and Kitis, G. (2014). Resolving the limitation of the peak fitting and peak shape methods in the determination of the activation energy of thermoluminescence glow peaks. *Journal of Luminescence*, 146:418–423.

[130] Sadek, A. M., Eissa, H. M., Basha, A. M., and Kitis, G. (2015b). Properties of the thermoluminescence glow peaks simulated by the interactive multiple-trap system (IMTS) model. *physica status solidi (b)*, 252(4):721–729.

[131] Salzer, H. E. (1964). Divided differences for functions of two variables for irregularly spaced arguments. *Numerische Mathematik*, 6:68–77.

[132] Salzmann, D. (1998). *Atomic physics in hot plasmas*. Oxford University Press.

[133] Shalgaonkar, C. and Narlikar, A. (1972). Review: a review of the recent methods for determining trap depth from glow curves. *Journal of Materials Science*, 7(12):1465–1471.

[134] Shambhunath Singh, W., Bhattacharya, M., Dorendrajit Singh, S., and Mazumdar, P. (2000). Activation energies and temperature dependent frequency factors in thermoluminescence recorded with hyperbolic heating scheme. *physica status solidi (a)*, 179(1):265–273.

[135] Shenker, D. and Chen, R. (1971). Numerical curve fitting of general order kinetics glow peaks. *Journal of Physics D: Applied Physics*, 4(2):287–291.

[136] Simmons, J. and Taylor, G. (1971). Nonequilibrium steady-state statistics and associated effects for insulators and semiconductors containing an arbitrary distribution of traps. *Physical Review B*, 4(2):502–511.

[137] Singh, L. L. and Gartia, R. (2013). Theoretical derivation of a simplified form of the OTOR/GOT differential equation. *Radiation measurements*, 59:160–164.

[138] Singh, S. J., Karmakar, M., Bhattacharya, M., Singh, S. D., Singh, W. S., and Azharuddin, S. (2012). On the reappraisal of the peak shape method for general order thermoluminescence. *Indian Journal of Physics*, 86(2):113–116.

[139] Singh, S. J., Karmakar, M., and Singh, S. D. (2013). On the determination of the order of kinetics in thermoluminescence by peak-shape method. *Radiation Effects and Defects in Solids*, 168:352–357.

[140] Singh, T. B., Rey, L., and Gartia, R. (2011). Applications of peakfit software in thermoluminescence studies. *NISCAIR-CSIR, India*.

[141] Sunta, C., Feria, A. W., Piters, T., and Watanabe, S. (1999). Limitation of peak fitting and peak shape methods for determination of activation energy of thermoluminescence glow peaks. *Radiation Measurements*, 30:197–201.

[142] Sunta, C. M. (2014). *Unraveling thermoluminescence; Springer Series in Materials Science*, volume 202. Springer India, New Delhi.

[143] Sunta, C. M., Ayta, W. E. F., Chubaci, J. F. D., and Watanabe, S. (2001). A critical look at the kinetic models of thermoluminescence: I. first-order kinetics. *Journal of Physics D: Applied Physics*, 34(17):2690–2698.

[144] Sunta, C. M., Ayta, W. E. F., Chubaci, J. F. D., and Watanabe, S. (2004). A critical look at the kinetic models of thermoluminescence—II. non-first order kinetics. *Journal of Physics D: Applied Physics*, 38(1):95–102.

[145] Talebi, M., Zahedifar, M., and Sadeghi, E. (2019). UVC dosimetry properties of Mn and Ce doped KCl thermoluminescent phosphor produced by co-precipitation method. *Nuclear Instruments and Methods in Physics Research Section B: Beam Interactions with Materials and Atoms*, 458:97–104.

[146] Taylor, G. C. and Lilley, E. (1978). The analysis of thermoluminescent glow peaks in LiF (TLD-100). *Journal of Physics D: Applied Physics*, 11(4):567–581.

[147] Templer, R. (1986). The localised transition model of anomalous fading. *Radiation Protection Dosimetry*, 17(1-4):493–497.

[148] Thomas, B. and Houston, E. (1964). Correlation of optical absorption and thermoluminescence curves for single crystals of magnesium oxide. *British Journal of Applied Physics*, 15(8):953.

[149] Urbach, F. (1930). Zur Lumineszenz der Alkalihalogenide. II. Mitteilung. *Wiener Berichte*, 139:363–372.

[150] Visocekas, R. (1985). Tunnelling radiative recombination in labradorite: Its association with anomalous fading of thermoluminescence. *Nuclear Tracks and Radiation Measurements (1982)*, 10(4-6):521–529.

[151] Visocekas, R. (1988). Comparison between tunnelling afterglows following alpha or beta irradiations. *International Journal of Radiation Applications and Instrumentation. Part D. Nuclear Tracks and Radiation Measurements*, 14(1-2):163–168.

[152] Visocekas, R., Spooner, N., Zink, A., and Blanc, P. (1994). Tunnel afterglow, fading and infrared emission in thermoluminescence of feldspars. *Radiation Measurements*, 23(2-3):377–385.

[153] Wagner, G., Aitken, M. J., and Mejdahl, V. (1982). *Thermoluminescence dating*. European Science Foundation.

[154] Walker, R. M., Zimmerman, D. W., and Zimmerman, J. (1972). Thermoluminescence of lunar samples: Measurement of temperature gradients in core material. *The Moon*, 4(3–4):308–314.

[155] Xu, X., Wang, Y., Gong, Y., Zeng, W., and Li, Y. (2010). Effect of oxygen vacancies on the red phosphorescence of $Sr_2SnO_4 : Sm^{3+}$ phosphor. *Optics Express*, 18(16):16989.

[156] Xu, X., Zhang, X., Wang, T., Qiu, J., and Yu, X. (2014). Color variation of photo-stimulated luminescence in strontium ortho-silicate with the assistance of trap centers. *Materials Letters*, 127:40–43.

[157] Yazici, A. N., Seyyidoğlu, S., Toktamiş, H., and Yilmaz, A. (2010). Thermoluminescent properties of $Sr_2P_2O_7$ doped with copper and some rare earth elements. *Journal of Luminescence*, 130:1744–1749.

[158] Yossian, D. and Horowitz, Y. (1995). Computerized glow curve deconvolution applied to the analysis of the kinetics of peak 5 in LiF: Mg, Ti (TLD-100). *Journal of Physics D: Applied Physics*, (7):1495.

[159] Yossian, D. and Horowitz, Y. (1997). Mixed-order and general-order kinetics applied to synthetic glow peaks and to peak 5 in LiF:Mg, Ti (TLD-100). *Radiation Measurements*, 27(3):465–471.

[160] Yukihara, E. G. and McKeever, S. W. S. (2011). *Optically stimulated luminescence: fundamentals and applications*. John Wiley & Sons.

Published Papers and Participation in Conferences

Radiation Protection Dosimetry (2021), Vol. 193, No. 3–4, pp. 247–258 doi:10.1093/rpd/ncab048
Advance Access publication 4 May 2021

THREE-POINT AREA METHOD FOR THERMOLUMINESCENCE GLOW CURVE ANALYSIS AND ITS APPLICATION TO THE GLOW PEAK OF $K_2SrP_2O_7$: Pr

M. Kundu[1,2], S. Bhattacharyya[1,*], M. Karmakar[3] and P. S. Majumdar[1]
[1]Department of Physics, Acharya Prafulla Chandra College, New Barrackpore, Kolkata 700131, India
[2]Sadhanpur Uludanga Tulsiram High School (H.S), Amdanga, 24 Parganas (N) 743221, India
[3]Department of Physics, Raghunathpur College, Purulia 723133, India

*Corresponding author: sukhamoy.b@gmail.com

Received 10 December 2020; revised 17 February 2021; editorial decision 10 March 2021; accepted 10 March 2021

A method has been proposed to evaluate the kinetic parameters, viz. activation energy (E) and order of kinetics (b) from a single or isolated thermoluminescence (TL) glow peak. Along with the area under the entire curve, this method uses a set of three arbitrary data points and calculates the partial area under the curve from each point to the endpoint. In this way, the entire information associated with the curve is used and the method is named as 'Three-Point Area' (TPA) method. We have applied it successfully on a number of theoretically simulated TL curves generated in One Trap One Recombination centre (OTOR) model and General-Order Kinetics (GOK) model under quasi-equilibrium approximations with linear heating scheme. The activation energies are found in good agreement with input values for both the models. For OTOR model, temperature average of order of kinetics is estimated to compare with the present result. Systematic analysis is carried out for estimation of errors inherent in the method in the purview of GOK model. A closer look on the results reveals that any set of three points, preferably chosen from the rising side of the curve, can yield activation energy and order of kinetics. The validity of the method to extract E and b from experimental glow curves is exemplified by considering experimental TL data reported in literature. Finally, a complete study starting from the synthesis of a new phosphor $K_2SrP_2O_7$: Pr and analysis of the recorded TL data to estimate E and b employing the TPA method has been reported.

INTRODUCTION

Natural and artificial insulators and semiconductors along with several novel materials like crystalline nanophosphores have ample applications in various display devices, signing devices and several dosimetry-based applications due to their manifestation of luminescent properties[1–5]. Presence of appropriate metastable traps of suitable concentration within the band gap of the phosphors is crucial for their luminescent properties, which facilitates their applications to optoelectronic devices. Knowledge of the trap levels in solids is a crucial field of interest in defect studies in solid state physics[6]. Thermally stimulated luminescence or thermoluminescence (TL) has been a very useful technique for studying these features[7–9]. TL also serves as an important tool in the field of dosimetry[10] and even in archaeological[11] and geophysical research[12].

Charge carriers that are created due to exposure of a phosphor to the field of high-frequency ionizing radiation, e.g. X-ray, gamma ray can be trapped into metastable energy levels, i.e. traps. On thermal stimulation, these electrons get detrapped and excited to conduction band followed by recombination with trapped holes at recombination centers producing TL signals if the recombination process is radiative in nature[7]. TL intensity plotted as a function of temperature is known as a glow curve. The shape and symmetry of the glow curve along with the peak position are governed by the intrinsic physical properties of the traps[13–15]. So glow curve analysis based on different analytical and numerical methods gives information about the trap levels and also about charge carrier trafficking that includes the retrapping–recombination mechanism in the solid.

Based on the band theory of solids, several models, e.g. One Trap One Recomination centre (OTOR), Non-interactive Multi-Trap System (NMTS), Interactive Multi-Trap System (IMTS) have been developed[16, 17] to simulate a TL curve, and the OTOR model is the simplest of them. First-order and second-order kinetic models can be approximated from the provisions of OTOR model. The General-Order Kinetics (GOK) model is one of the very widely used ones in literature[7, 18]. Since TL involves trapping of electrons and holes in defect and recombination centers, theoretically, it is modeled in terms of some trapping parameters. In this work, we have adopted GOK and OTOR model to simulate

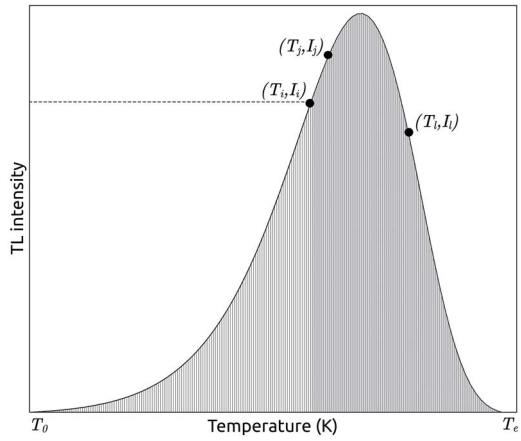

Figure 1: Schematic diagram of a TL peak with three arbitrary points $(T_i, I_i), (T_J, I_j)$ and (T_L, I_l) placed on it. The striped area shows the area under the complete curve from T_0 to T_e. The shaded region shows the partial area from T_i to T_e.

the TL curves. In GOK model, the TL process is explained in terms of three parameters: activation energy (E), order of kinetics (b) and frequency factor (s). In OTOR model, b does not appear explicitly, but the ratio (R) of retrapping and recombination probabilities plays an equivalent role. However, b is well analyzed in literature and can be considered as a parameter providing an intermediate platform between microscopic and macroscopic pictures. The order of kinetics can be correlated with the quantity R[17], which has been attempted in the present work.

The trapping parameters governing the nature of a glow curve are determined by various methods developed over the years[8]. In the present work, we discuss a method for simultaneous determination of E and b from a single (or well isolated) TL peak. The calculations involve two pairs of points on the curve, and thus, a set of at least three distinct points (one point being common in each pair) are selected. The partial area (A_i) from each data point to the endpoint (T_e) is estimated along with the total area (A_0) under the entire glow curve. The partial area A_i corresponds to the concentration of trapped electrons at temperature T_i, whereas A_0 corresponds to the initial concentration of trapped electrons. A schematic diagram is presented in Figure 1. The temperatures and intensities at three points along with the ratios of partial areas to the total area are used to determine E and b. Since this method uses three points on the glow curve, we call it 'Three-Point Area' (TPA) method; nevertheless, the entire information of the curve is inherent in it through the total area. In principle, TPA method can be employed to evaluate E and b simultaneously by using any arbitrary set of three points on the glow curve. However, some limitations are found on the accuracy of extracted TL parameters depending on the location of data points, which are discussed later.

As a testing ground of the applicability of TPA method in experimental cases, we attempt to synthesize a new phosphor and analyze its TL data. Rare earth-activated pyrophosphates have emerged as promising materials for their various interesting properties and application to different luminescent-based industries[19]. In this work, the phosphor praseodymium-doped potassium strontium pyrophosphate [$K_2SrP_2O_7 : Pr(0.1mole\%)$] is synthesized in combustion method[20] and exposed to gamma irradiation. The irradiated sample is linearly heated and the recorded TL signal is analyzed in TPA method to calculate trap level energy (E) and nature of electronic trafficking between different energy levels given by the order of kinetics (b).

The article is organized as follows: the relevant theoretical background of OTOR and GOK models along with the TPA method is discussed in Section 2. The results for simulated glow curves in linear heating scheme are discussed in Section 3.1. Application of this method to the experimental TL curves of $Sr_2P_2O_7 : Cu, Pr$[21] and gamma-irradiated $LiF : Sm^{3+}, Dy^{3+}$[22] are given in Section 3.2. Synthesis and TL analysis of the new phosphor $K_2SrP_2O_7 : Pr$ in TPA method is discussed in Section 3.4. A final conclusion is included in Section 4.

METHODOLOGY

The basic set of differential equations for OTOR model can be written as

$$\frac{dn_c}{dt} = nse^{-\frac{E}{kT}} - n_c(N-n)A_n - A_h n_c n_h \quad (1)$$

$$\frac{dn}{dt} = -nse^{-\frac{E}{kT}} + n_c(N-n)A_n \quad (2)$$

The charge neutrality condition in OTOR model is

$$n_c = n + n_h \quad (3)$$

where n and N are concentration of trapped electrons and concentration of traps, respectively; n_h is the hole concentration; n_c is the concentration of electrons in the conduction band and k is the Boltzmann constant. A_n and A_h are retrapping and recombination probabilities, respectively. Using quasi-equilibrium (QE) approximations

$$\frac{dn_c}{dn_t} << \frac{dn}{dt} \quad (4)$$

and $n_c << n$ (5)

the TL intensity is given by

$$I = -\frac{dn_h}{dt} = A_h n_c n_h \tag{6}$$

From Equations (1 – 6), we obtain

$$I \simeq -\frac{dn}{dt} = \frac{n^2 s e^{-\frac{E}{kT}}}{n(1-R)+NR} \tag{7}$$

where $R = \frac{A_n}{A_h}$. Now for $R << 1$ leading to $NR << 1$, Equation (7) reduces to the first-order kinetics equations of Randall and Wilkins[23, 24]

$$I = -\frac{dn}{dt} = nse^{-\frac{E}{kT}} \tag{8}$$

and for $R = 1$, Equation (7) yields the second-order kinetics equation of Garlick and Gibson[25]

$$I = -\frac{dn}{dt} = \frac{n^2}{N} s e^{-\frac{E}{kT}} \tag{9}$$

The intensity (I) of a TL peak at temperature T in GOK model[7] is given by

$$I = -\frac{dn}{dt} = \left(\frac{n}{N}\right)^b sNe^{-\frac{E}{kT}} \tag{10}$$

For $b = 1$, Equation (10) becomes the first-order equation of Randall and Willkins[23, 24], and for $b = 2$, the second-order equation of Garlick and Gibson[25] is obtained.

In OTOR model, b does not occur explicitly in the expression of TL intensity. Similarly, in GOK model, R does not occur. However, we can correlate R and b by equating the expressions for intensity originating from GOK (Equation 10) and OTOR (Equation 6) models. Hence, we can write

$$I = \frac{n^2 s e^{-\frac{E}{kT}}}{n(1-R)+NR} = \left(\frac{n}{N}\right)^b sNe^{-\frac{E}{kT}} \tag{11}$$

which yields

$$b = 1 + \frac{\ln\left[1 + R\left(\frac{N}{n} - 1\right)\right]}{\ln \frac{N}{n}} \tag{12}$$

Equation (12) reveals that for $R = 0$, $b = 1$ and for $R = 1$, $b = 2$, and b thus becomes independent on temperature for $R = 0$ and 1. For all other values of R, b has a dependence on T as n varies with T. Simulating the TL curve in OTOR model, $n(T)$ is estimated by integrating Equation (7), which is further employed to evaluate $b(T)$ for a particular input value of R. Average value of b (b_{av}) is then obtained as

$$b_{av} = \frac{1}{T_f - T_i}\int_{T_i}^{T_f} b(T)dT \tag{13}$$

The integration is carried numerically using composite Simpson's rule[26]. In this work, R is considered within the range $0 \leqslant R \leqslant 1$, i.e. the heavy retrapping cases are excluded. An alternative analytical expression for intensity can be obtained by using the Lambert-W function[27] as

$$I = \frac{NRse^{-\frac{E}{kT}}}{(1-R)^2\left[W[e^{Z_1}] + W[e^{Z_1}]^2\right]} \tag{14}$$

where

$$Z_1 = \frac{NR}{n_0(1-R)} - \ln\frac{n_0(1-R)}{NR} + \frac{s}{(1-R)\beta}\int_{T_0}^{T} e^{-\frac{E}{kT}}dT \tag{15}$$

where $W[e^{Z_1}]$ is the principal branch of the Lambert-W function. Except for $R = 0$ and 1, we have used Equation (14) to generate the numerical TL data in OTOR model. For $R = 0$ and 1, Equation (7) is used.

Three-Point Area method

In linear heating scheme, $T = T_0 + \beta t$, where β is the linear heating rate, T_0 is the initial temperature ($t = 0$) and T is the temperature at time t. The expressions for TL intensity from Equation (10) becomes

$$I(T) = sn_0 e^{-\frac{E}{kT}} \exp\left[-\frac{s}{\beta}\int_{T_0}^{T} e^{-\frac{E}{kT'}}dT'\right] \tag{16}$$

$$\text{for } b = 1 \text{ and } I(T) = sn_0 e^{-\frac{E}{kT}}\left[\frac{(b-1))s}{\beta}\int_{T_0}^{T} e^{-\frac{E}{kT'}}dT' + 1\right]^{-\frac{b}{b-1}} \tag{17}$$

for $b \neq 1$. We need to carry out the integral $J(T, T_0) = \int_{T_0}^{T} e^{-\frac{E}{kT'}}dT'$, known as the temperature

integral. Setting $T_0 \rightarrow 0$ and using $u = \frac{E}{kT}$, the integral $J(T, T_0)$ can be expressed as[28]

$$J(T, T_0) \simeq \int_0^T e^{-\frac{E}{kT'}} dT' = \frac{E}{k} \int_u^\infty \frac{1}{u'^2} e^{-u'} du' = \frac{E}{k} \frac{E_2(u)}{u} \tag{18}$$

where $E_2(u)$ is the second-order exponential integral with argument u[29]. Writing $u_m = \frac{E}{kT_m}$, (T_m, I_m) being the peak coordinates, Equations (16) and (17) can be recast as

$$\frac{I}{I_m} = \exp[(u_m - u) + F(u, u_m)] \quad \text{for } b = 1 \tag{19}$$

$$\text{and } \frac{I}{I_m} = \exp(u_m - u)\left[1 - \frac{b-1}{b} F(u, u_m)\right]^{-\frac{b}{b-1}} \text{ for } b \neq 1 \tag{20}$$

$$\text{with } F(u, u_m) = u_m^2 \exp(u_m)\left[\frac{E_2(u_m)}{u_m} - \frac{E_2(u)}{u}\right] \tag{21}$$

For an arbitrary point (T_i, I_i) on the curve, we can write from Equation (10)

$$\ln I_i = -\frac{E}{kT_i} + b \ln \frac{n_i}{N} + \ln sN \tag{22}$$

where n_i is the concentration of trapped electrons at temperatures T_i. For a pair of arbitrary points (T_i, I_i) and (T_j, I_j), using Equation (22), we obtain

$$Y_{ij} = b - \frac{E}{k} X_{ij} \tag{23}$$

$$\text{where } Y_{ij} = \frac{\ln I_j - \ln I_i}{\ln \frac{n_j}{n_0} - \ln \frac{n_i}{n_0}}; X_{ij} = \frac{\frac{1}{T_j} - \frac{1}{T_i}}{\ln \frac{n_j}{n_0} - \ln \frac{n_i}{n_0}} \tag{24}$$

Here, we have used $\frac{n_i}{n_j} = \frac{n_i}{n_0} . \frac{n_0}{n_j}$. n_0 is the initial concentration of trapped electrons and is proportional to the area under the entire glow curve. $\frac{n_i}{n_0}$ and $\frac{n_j}{n_0}$ are estimated by measuring the area under the TL curve (Figure 1), starting from temperature T_i and T_j, respectively, to the endpoint temperature (T_e). Similarly, for another pair of points (T_j, I_j) and (T_l, I_l) (one point is common in both the pairs), we obtain

$$Y_{jl} = b - \frac{E}{k} X_{jl} \tag{25}$$

Solving Equations (23) and (25), we get the expressions of E and b as

$$E = -k \frac{Y_{ij} - Y_{jl}}{X_{ij} - X_{jl}}; \qquad b = \frac{X_{jl} Y_{ij} - X_{ij} Y_{jl}}{X_{ij} - X_{jl}} \tag{26}$$

Thus, the TPA method yields the activation energy and order of kinetics simultaneously. From the knowledge of E and b, the frequency factor (s) is determined from the 'maximum condition'[7]

$$s = \beta \left[\frac{bkT_m^2}{E} \exp\left(-\frac{E}{kT_m}\right) - (b-1) J(T_0, T_m)\right]^{-1} \tag{27}$$

Estimation of area

Considering the initial concentration of trapped electrons n_0 to be proportional to the area under the whole TL peak and the instantaneous concentration of trapped electrons n to be proportional to the partial area under the glow peak from temperature T to T_e, we can write[30]

$$\frac{n}{n_0} = \frac{A(T, T_e)}{A_0(T_0, T_e)} \tag{28}$$

where $A(T, T_e)$ is the area of the TL glow curve from T to T_e (where $T_e >> T_m$) and is given by

$$A(T, T_e) = \int_T^{T_e} I(T') dT' \tag{29}$$

where $A_0(T_0, T_e)$ is the area of the TL glow curve from T_0 to T_e, i.e. the area of the whole curve (Figure 1). Now, for non-first order ($b \neq 1$) kinetics (Equation 20), the area under the portion of the peak from temperature T to T_e is given by

$$A(u, u_e) = \frac{E}{k} \int_u^{u_e} \exp(u_m - u') \times \left[1 - \frac{b-1}{b} F(u', u_m)\right]^{-\frac{b}{b-1}} u'^{-2} du' \tag{30}$$

where $u_e = \frac{E}{kT_e}$. The endpoint temperature T_e is taken at which the intensity of the falling side of the curve becomes 1% of the maximum intensity (I_m). The integral occurring in Equation (30) has been evaluated by splitting the total range of integration (T, T_e) into suitable number of subranges and applying composite Simpson's rule[26]. This area is now used to estimate $\frac{n}{n_0}$ (Equation 28), and then E and b are calculated from Equation (26).

RESULTS AND DISCUSSIONS

The 'Three point area' method is applied to extract E and b from the simulated curves and compared with the input values. In OTOR model, the activation energy can be extracted directly from TPA method. The temperature average of b has been estimated as discussed before. In GOK model, input values of E and b can be directly compared with the corresponding values extracted from the TPA method.

Simulated glow curves

The applicability and accuracy of the TPA method for extracting trapping parameters has been tested at first on simulated glow curve. We have generated TL glow curves in OTOR model for different values of R and filling ratio $\left(f = \frac{n_0}{N}\right)$. The linear heating scheme is adopted with heating rate $\beta = 1\text{Ks}^{-1}$. The TPA method is applied on these curves to extract the activation energy (E_T) and order of kinetics (b_T). The results are displayed in Table 1, where the values of input parameters required to generate the curves are also mentioned. Three arbitrary points on the glow curve are chosen, and Equation (26) is applied to determine E_T and b_T as output values. From 'm' number of points on the curve, we can calculate ${}^mC_3$ sets of values of E_T and b_T. We consider a large number of dataset ($m = 19$), and after averaging, we obtain the final values of E_T and b_T. However, we note here that for all the simulated curves, the lower half of the falling side of the TL curve is excluded while taking the required three points for extraction of trapping parameters. For experimental curves, points are chosen from the rising side of the curve. The reason behind this is explained later in Section 3.3. Table 1 shows that E_T is quite in agreement with the input value of activation energy (E_{in}).

As mentioned before, OTOR model does not involve b explicitly, and a unique value of b should not be assigned to a TL peak due to its temperature dependence. We have studied the temperature variations of n as well as b in detail, and the variations are displayed in Figure 2 for $R = 0.5$, corresponding to an unsaturated ($f = 0.5$) and a saturated ($f = 1$) TL peak. b_{av} is estimated (Equation 13) for these curves and compared with b_T obtained from TPA method. Results displayed in Table 1 show reasonable agreement between the extracted value (b_T) and the average value (b_{av}). To have a further check on the reliability of the parameter b_{av} as an equivalent to R, we reproduce the value of R from b_{av} by rearranging Equation (12) as

$$R = \frac{\left(\frac{N}{n}\right)^{b_{\text{av}}-1} - 1}{\frac{N}{n} - 1} \tag{31}$$

We obtain a set of values of R at different temperatures as n varies with T. Numerical average of R (R_{av}) is then obtained as

$$R_{\text{av}} = \frac{1}{T_f - T_i}\int_{T_i}^{T_f} R(T)dT \tag{32}$$

We now employ the b_{av} values listed in Table 1 along with other parameters to reproduce R_{av} according to Equation (2), and the results are listed in Table 2. It is evident that R_{av} values are in close agreement with the input values of R, and hence b_{av} can be treated as a reliable parameter equivalent to R.

We have also employed the GOK model (Equation 10) to generate the TL curve using different set of input values of activation energy (E_{in}), order of kinetics (b_{in}) and frequency factor (s_{in}). In the input values, we have considered E in the range 0.5–1.5 eV, b in the range 1.0–2.0 and s in the range 10^8–10^{12}s^{-1}. All the input parameters are increased systematically in a step-by-step manner, and TPA method is applied to all the numerical glow curves. In Table 3, we have given a representative set of the results of TPA method corresponding to some selective input parameters ($E_{\text{in}}, b_{\text{in}}, s_{\text{in}}$). The agreement between input values ($E_{\text{in}}, b_{\text{in}}$) and output values ($E_T$ and b_T) is evident from Table 3, which shows that the TPA method performs simultaneous extraction of activation energy and order of kinetics. The frequency factor has been calculated using the peak position (T_m) and values of E_T and b_T from the 'maximum condition' (Equation 27), and the results are given in Table 3. We observe that the output s values are slightly lower than the input values, and this is consistent throughout the dataset. This marginal difference in s values may be due to the approximations inherent in the derivation of Equation (27). For a comparison of the present results, we have evaluated E and b from the same curve using Kirsh method[30] also. The results derived from Kirsh method[30] are listed in Table 3 as E_k and b_k, respectively. It is evident that

Table 1. Kinetic parameters derived by TPA method from numerically simulated TL peaks generated in OTOR model in linear heating scheme. The input parameters are $E_{in} = 1.0$eV, $s = 1.0 \times 10^{12}$sec^{-1}, $N = 1.0 \times 10^{10}$m^{-3} and $\beta = 1.0$Ksec^{-1}. b_{av} is estimated using Equation (13).

Input parameters			Output from TPA method	
f	R_{in}	b_{av}	b_T	E_T (eV)
0.1	0.0	1.0056	1.0004	0.9999
	0.001	1.0328	1.0092	1.0000
	0.25	1.6419	1.7932	1.0001
	0.50	1.8030	1.8631	1.0001
	0.75	1.9208	1.9609	1.0001
	1.0	2.0070	2.0517	1.0000
0.5	0.0	1.0056	1.0004	0.9999
	0.001	1.0238	1.0022	1.0000
	0.25	1.5506	1.4182	1.0002
	0.50	1.7257	1.6632	1.0003
	0.75	1.8819	1.8710	1.0001
	1.0	2.0067	2.0118	1.0001
1.0	0.0	1.0057	1.0004	0.9999
	0.001	1.0213	1.0018	1.0000
	0.25	1.5179	1.2662	1.0002
	0.50	1.6881	1.5074	1.0006
	0.75	1.8588	1.7647	1.0003
	1.0	2.0067	2.0062	1.0002

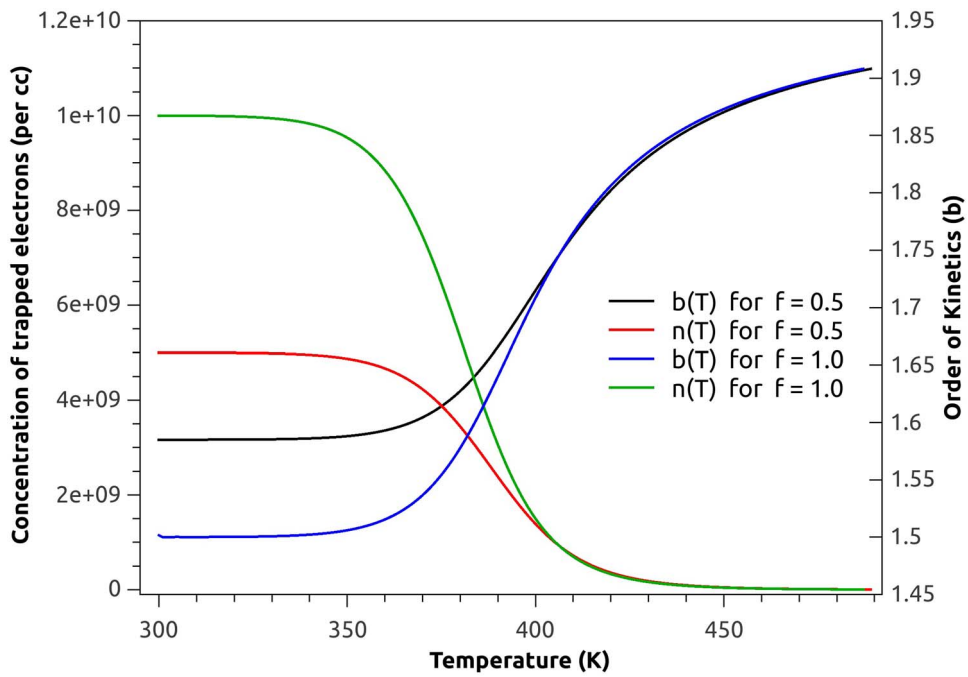

Figure 2: Variation of n and b with respect to T for $R = 0.5$. The input parameters are $E_{in} = 1.0$eV, $s = 1.0 \times 10^{12}$sec^{-1}, $N = 1.0 \times 10^{10}$m^{-3} and $\beta = 1.0$Ksec^{-1}.

Table 2. Average value of R (i.e. R_{av}) estimated from b_{av} using Equations (31and 32) from simulated TL peaks generated in OTOR model in linear heating scheme. The input parameters are same as Table 1.

f	R_{in}	b_{av}	R_{av}
0.1	0.0	1.0056	0.0010
	0.001	1.0328	0.0061
	0.25	1.6419	0.2519
	0.50	1.8030	0.4898
	0.75	1.9208	0.7453
	1.0	2.0070	1.0287
0.5	0.0	1.0056	0.0027
	0.001	1.0238	0.0119
	0.25	1.5506	0.2653
	0.50	1.7257	0.4648
	0.75	1.8819	0.7030
	1.0	2.0067	1.0243
1	0.0	1.0057	0.0041
	0.001	1.0213	0.0153
	0.25	1.5179	0.2795
	0.50	1.6881	0.4568
	0.75	1.8588	0.6784
	1.0	2.0067	1.0232

the present results E_T, b_T are quite consistent with the values E_k, b_k.

Because of the inherent approximations, any phenomenological analysis involves systematic errors. In case of interpretation of experimental data using theoretical methods, experimental errors merge with theoretical errors. So the analysis of systematic errors in theoretical studies gives the lower limit of errors in that method. We have calculated the percentage errors δE and δb in the determination of E and b using TPA method from the simulated glow curves for different values of E, s, b by using the relations $\delta E = \dfrac{E_T - E_{in}}{E_{in}} \times 100\%$ and $\delta b = \dfrac{b_T - b_{in}}{b_{in}} \times 100\%$. It is noted that in TPA method the calculated values of E_T and b_T are always less than the input values in GOK model. The fact that E_T is less than E_{in} is somewhat similar to the case of Initial Rise (IR) method[8], which underestimates activation energy. Figure 3 shows the variation of δE with respect to b and $\log s$ for $E = 1$ eV. Though the percentage error ($\delta E\%$) for the simulated curve is very nominal, Figure 3 displays that δE has dependence on both b and s. δE increases with the increase of b and decreases with increase of $\log s$. However, δE is more sensitive on variations of b than s. For all other values of E_{in}, our observation is that δE does not have much dependence on E_{in}. In Figure 4a, δb is presented as a function of $\log s_{in}$ for different values of E_{in}, and Figure 4b shows the variation of δb with respect to E_{in} for different values of s_{in}. A decrease in δb is observed

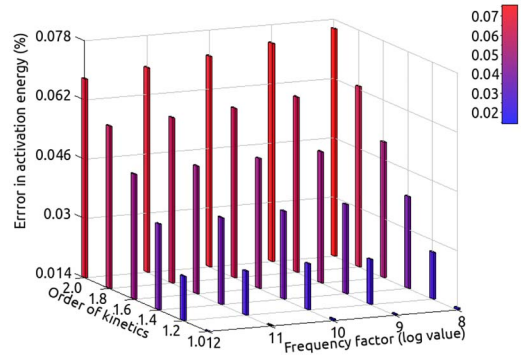

Figure 3: δE (%) plotted against different values of b_{in} and s_{in}. Here, $E_{in} = 1$ eV.

as $\log s$ increases, whereas δb is almost independent of E_{in}.

Application to experimental TL peaks

In the next phase, we apply the TPA method to experimental TL curves reported in literature. At first, we have taken the glow peaks reported by Yazici *et al.*[21], where they analyzed the TL signal of $Sr_2P_2O_7$: Cu, Pr exposed to betaradiation of dose $\sim$ 12 Gy. The glow curve was recorded at a heating rate of 1 $Ksec^{-1}$. The sample exhibited two distinct TL peaks with very small overlapping, and the peak maxima were reported near 363 and 453 K. From the glow curve[21], we have picked up the $I - T$ data points using the browser-based software platform WebPlotDigitizer[31], and the raw data points are shown in Figure 5.

It is worthwhile to mention that to run a numerical code in a systematic manner for calculating the area under the curve, the data points are preferred to be equispaced, which is not possible for experimental data. To avoid this difficulty, we have interpolated the intermediate data to generate the intensities for temperatures in equal interval by using the divided difference algorithm[26], which is a standard technique in case of irregularly spaced data[32, 33]. The composite Simpson's rule[26] is now employed to estimate the area under the glow curve and TPA method is employed to extract the values of activation energy (E_T) and order of kinetics (b_T) for both the peaks. The results are shown in Table 4. We see that the present method estimates a slightly shifted position of the peak maxima (T_m) as compared with[21]. Yazici *et al.*[21] reported the values of activation energy and order of kinetics derived by glow curve deconvolution technique, which are quoted in Table 4, and good agreement with the present values (E_T, b_T) is observed. The values of T_m, E_T and b_T are used to estimate the frequency

Table 3. Kinetic parameters derived by TPA method from numerically simulated TL peaks generated in GOK model in linear heating scheme. The heating rate is $\beta = 1\text{Ksec}^{-1}$.

Input values			Output values					
E_{in}(eV)	$s_{\text{in}}(\text{sec}^{-1})$	b_{in}	$T_m(K)$	E_T(eV)	b_T	$s_T(\text{sec}^{-1})$	E_k(eV)	b_k
0.5	1.0×10^{10}	1.0	229.93	0.4999	0.9995	9.95×10^{9}	0.5000	0.9995
		1.6	229.58	0.4999	1.5977	9.85×10^{9}	0.4999	1.5972
		2.0	229.35	0.4998	1.9957	9.73×10^{9}	0.4998	1.9950
	1.0×10^{12}	1.0	196.52	0.4999	0.9996	9.94×10^{11}	0.5000	0.9995
		1.6	196.29	0.4999	1.5977	9.85×10^{11}	0.4999	1.5973
		2.0	196.15	0.4998	1.9959	9.76×10^{11}	0.4998	1.9953
1	1.0×10^{10}	1.0	448.44	0.9999	0.9995	9.97×10^{9}	0.9999	0.9995
		1.6	447.79	0.9997	1.5977	9.82×10^{9}	0.9998	1.5972
		2.0	447.37	0.9995	1.9958	9.74×10^{9}	0.9997	1.9951
	1.0×10^{12}	1.0	384.57	0.9999	0.9996	9.97×10^{11}	0.9999	0.9995
		1.6	384.15	0.9997	1.5976	9.81×10^{11}	0.9998	1.5973
		2.0	383.87	0.9996	1.9957	9.74×10^{11}	0.9997	1.9954
1.5	1.0×10^{10}	1.0	663.02	1.4998	0.9995	9.96×10^{9}	1.4999	0.9995
		1.6	662.07	1.4995	1.5977	9.83×10^{9}	1.4997	1.5972
		2.0	661.47	1.4993	1.9957	9.73×10^{9}	1.4995	1.9951
	1.0×10^{12}	1.0	569.68	1.4998	0.9995	9.96×10^{11}	1.4999	0.9995
		1.6	569.06	1.4995	1.5978	9.82×10^{11}	1.4997	1.5973
		2.0	568.67	1.4994	1.9960	9.74×10^{11}	1.4995	1.9954

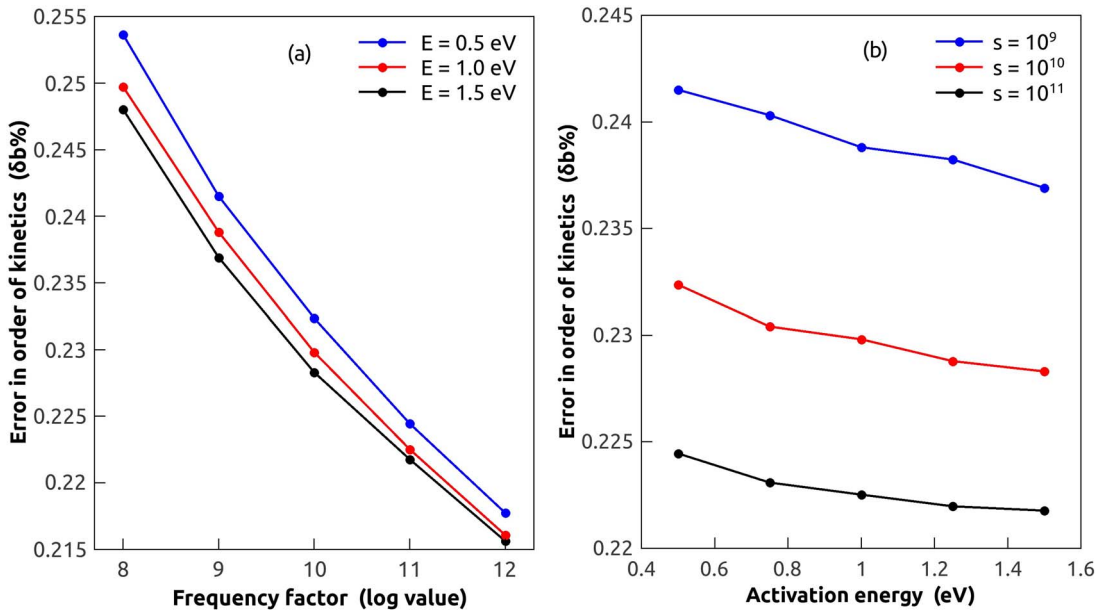

Figure 4: (**a**) Variation of δb (%) against $\log s_{\text{in}}$ for different values of E_{in}, (**b**) Variation of δb (%) against E_{in} for different values of s_{in}.

factors (s_T), and the values are given in Table 4. We have taken all the data points from the rising side of the curve and the errors from TPA method in estimating E and b are about 0.4 and 0.2%, respectively. If the data points from the upper half of the falling side are included, the respective errors

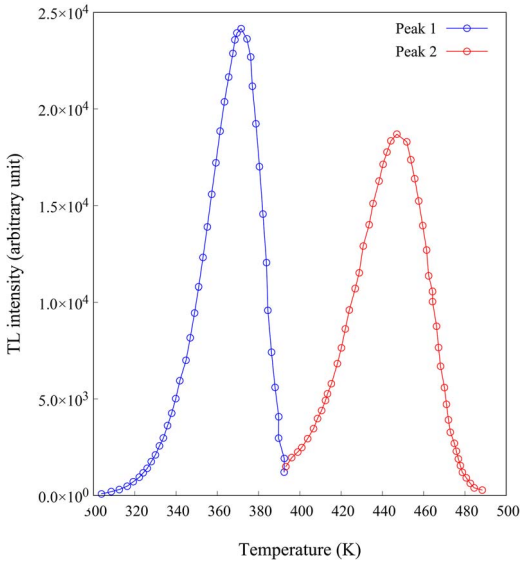

Figure 5: Data points picked up using WebPlotDigitizer from the TL curves of $Sr_2P_2O_7 : Cu, Pr$ reported by Yazici *et al.*[21].

are about 3 and 2%. The error values are due to the inherent theoretical approximations and hence exclude experimental uncertainties.

In a similar manner, we have analyzed the TL curve of gamma-irradiated $LiF : Sm^{3+}, Dy^{3+}$ reported by Kumar *et al.*[22], where the dose was 30 kGy and heating rate was 5 $Ksec^{-1}$. Five deconvoluted peaks were reported by Kumar *et al.*[22], from which we have considered the fist two peaks. The results are quite in agreement and are displayed in Table 4. The present values of T_m, E_T and b_T are used to estimate the frequency factors (s_T), which are in conformity with those reported by Kumar *et al.*[22]. Similar errors as mentioned in the previous paragraph are also obtained here.

Dependence of the results on the location of data points

We have verified the consistency of the results obtained from the TPA method choosing three points from different locations of the curve. For this purpose, we have divided the TL curve in four 'zones': (i) Zone-I: lower half of the rising side (T_0 to $T_{\frac{1}{2}}^-$), (ii) Zone-II: upper half of the rising side ($T_{\frac{1}{2}}^-$ to T_m), (iii) Zone-III: upper half of the falling side (T_m to $T_{\frac{1}{2}}^+$) and (iv) Zone-IV: lower half of the falling side ($T_{\frac{1}{2}}^+$ to T_e). Here, $T_{\frac{1}{2}}^-$ and $T_{\frac{1}{2}}^+$ are half maxima temperatures in rising and falling sides, respectively. We have tested the simulated and experimental TL curves mentioned so far, and a representative dataset showing how the final results are influenced by the location of the chosen points are given in Table 5. It is observed for all the cases that the results are quite consistent if the points are chosen from Zone-I and Zone-II. The activation energy is marginally lowered if the points are chosen from Zone-III. However, in Zone-IV, the results are quite inconsistent. These deviations are not much significant for first-order simulated curves, but becomes noticeable for second order, as is evident from Table 5. In case of experimental peaks, the deviations of the results are prominent for Zone-III and quite large for Zone-IV. In Table 5, the TL data of peak no. 1 of $Sr_2P_2O_7 : Cu, Pr$[21] taking points from different zones are reported showing such behavior. We have also considered the cases where the points are chosen from different zones and found that if the points from Zone-IV are excluded, then the results are quite satisfactory. On the basis of such findings, we have excluded Zone-IV for simulated curves and considered only the rising part of experimental curves for TL analysis in TPA method.

TL analysis of $K_2SrP_2O_7 : Pr$ (0.1 mole%) phosphor in TPA method

In practical aspects, TL study finds its application in studying the properties of a phosphor by analyzing the glow curves. To examine the validity of the present theory, we have made an attempt to prepare a phosphor and apply the TPA method to find out the trapping parameters from the experimental TL curve. A new phosphor potassium strontium pyrophosphate doped with praseodymium, $K_2SrP_2O_7 : Pr$ (0.1 mole%) has been synthesized by combustion method and then exposed to gamma irradiation. Strontium pyrophosphate doped with some rare earth element exhibits considerable TL intensity, which is useful for radiation dosimetry[34], and hence has attracted interest from researchers. However, we emphasize that the preparation of an efficient phosphor is not the primary aim of this work, rather our interest is on the applicability of the present method. Hence, we focus on the analysis of the TL data of the new phosphor rather than the technical details of the material synthesis and its characterization.

As the TPA method should be applied on a single or isolated peak, we have resolved the component peaks from the experimental glow curve of gamma-irradiated $K_2SrP_2O_7 : Pr$ using the deconvolution R-package 'tgcd'[35]. Figure 6 shows the experimental TL curve of $K_2SrP_2O_7 : Pr$ corresponding to heating rate 10 $Ksec^{-1}$ along with the component peaks. The

Table 4. Trapping parameters of TL peaks of different phosphors taken from literature.

Material	Peak	Present work: TPA method				Literature		
		T_m (K)	E_T(eV)	b_T	s_T(sec^{-1})	E_{gcd}(eV)	b_{gcd}	s(sec^{-1})
$Sr_2P_2O_7$: Cu, Pr[21]	1	368.52	0.9332	1.0891	4.55×10^{11}	0.933	1.1	
	2	446.21	1.2283	1.3910	5.25×10^{12}	1.228	1.4	
LiF : Sm^{3+}, Dy^{3+}[22]	1	373.16	0.8291	0.9951	5.39×10^{10}	0.82	1	5.40×10^{10}
	2	408.21	1.0323	1.7860	1.88×10^{12}	1.03	2	1.89×10^{12}

Table 5. Activation energy and order of kinetics derived from three data points chosen from various locations of the TL curve. For simulated curves, $E_{in} = 1.0$ eV, $s_{in} = 1.0 \times 10^{12}$sec^{-1}, $\beta = 1.0$Ksec^{-1}.

Peak	T_m	$T^-_{\frac{1}{2}}$	$T^+_{\frac{1}{2}}$	Location of	Coordinates of the points			E_T	b_T
	(K)	(K)	(K)	three points	(T_1, I_1)	(T_2, I_2)	(T_3, I_3)	(eV)	
Simulated peak with $b_{in} = 1.0$	384.57	367.22	397.06	Zone-I	(347.59, 0.1)	(355.35, 0.2)	(360.27, 0.3)	0.9999	0.9999
				Zone-II	(372.76, 0.7)	(375.48, 0.8)	(378.52, 0.9)	0.9999	0.9999
				Zone-III	(392.11, 0.8)	(393.90, 0.7)	(395.51, 0.6)	0.9987	0.9990
				Zone-IV	(397.06, 0.5)	(398.63, 0.4)	(400.33, 0.3)	0.9927	0.9968
				Mixed zone	(360.27, 0.3)	(375.48, 0.8)	(397.06, 0.5)	0.9999	0.9997
Simulated peak with $b_{in} = 2.0$	383.87	363.59	405.69	Zone-I	(351.45, 0.2)	(356.42, 0.3)	(360.28, 0.4)	0.9999	1.9990
				Zone-II	(366.62, 0.6)	(369.56, 0.7)	(372.61, 0.8)	0.9999	1.9986
				Zone-III	(391.79, 0.9)	(395.59, 0.8)	(398.93, 0.7)	0.9954	1.9910
				Zone-IV	(405.69, 0.5)	(409.58, 0.4)	(414.27, 0.3)	0.9588	1.9491
				Mixed zone	(360.27, 0.4)	(372.61, 0.8)	(395.59, 0.8)	0.9997	1.9977
Peak no. 1 in experimental curve[21] of $Sr_2P_2O_7$:Cu,Pr	362.53	351.34	382.11	Zone-I	(336, 0.1477)	(342, 0.2495)	(346, 0.3448)	0.9330	1.0993
				Zone-II	(354, 0.6035)	(358, 0.7526)	(361, 0.8580)	0.9329	1.0987
				Zone-III	(375, 0.8636)	(378, 0.7184)	(380, 0.6056)	0.9194	1.0876
				Zone-IV	(383, 0.4326)	(385, 0.3264)	(388, 0.1950)	0.7879	1.0306
				Mixed zone	(344, 0.2942)	(358, 0.7526)	(376, 0.8196)	0.9327	1.0978

second derivative of intensity with respect to temperature $\left(\frac{d^2I}{dT^2}\right)$[36] shows a prominent central peak at around 470 K and two very weak satellite peaks. In our analysis, we concentrate on the central peak (peak 2 of Figure 6) as the satellite peaks are extremely weak.

The TPA method is now applied on the experimental glow curve for the determination of E_T and b_T by taking the points from the rising side of the curve, and the results are given in Table 6. The values of E_T and b_T are used to determine the frequency factor (s_T) following Equation (27), which is also given in Table 6. To check the reliability of these results, the 'Area method' of Kirsh[30] is also applied, and the values are given in Table 6 for ready comparison. It is obvious that the results are quite in agreement. It is noted that the errors in extracting E and b in this case are 0.3 and 0.2%, respectively.

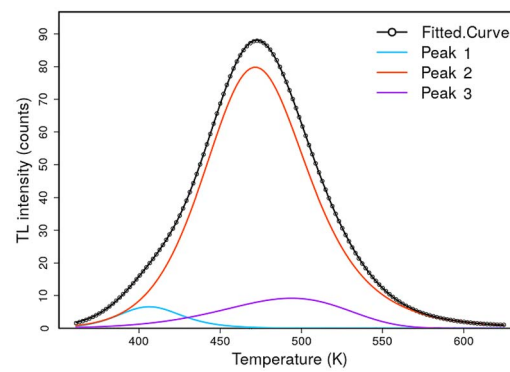

Figure 6: TL glow curve of gamma-irradiated $K_2SrP_2O_7$: Pr and the component peaks deconvoluted using the R-package 'tgcd'[35].

Table 6. Kinetic parameters of $K_2SrP_2O_7$: Pr.

Method	$T_m(K)$	Activation energy (eV)	Order of kinetics	Frequency factor (sec^{-1})
TPA method	472.7	0.7501	1.9853	3.37×10^7
Kirsh method[30]	472.7	0.7504	1.9928	3.47×10^7

CONCLUDING REMARKS

Three-Point Area method, developed as a tool to analyze single or isolated TL glow curves for simultaneous determination of activation energy and order of kinetics, has been discussed. OTOR and GOK models have been adopted for simulating TL glow curves in linear heating scheme. For OTOR model, from the ratio of retrapping and recombination probabilities, the temperature average of order of kinetics is calculated for a ready comparison with the present results. It is found that this temperature average of order of kinetics can be treated as a parameter equivalent to the ratio of retrapping and recombination probabilities. The agreement between output values and input values, in combination with the systematic error analysis, establishes the applicability of the present method. The applications of this method on experimental peaks already available in literature and also on the TL data of a newly synthesized phosphor show reasonable agreement with other results. It is observed that any set of three points excluding those on the lower half portion of the falling side of the curve can yield activation energy and order of kinetics, given the entire area and the relevant partial areas under the curve are known. However, the results are more accurate if the data points are chosen from the rising side of the curve. The present results are quite consistent and encouraging enough to employ the TPA method further on TL curves based on other models like NMTS, IMTS, etc. However, future works are to be carried out in this direction with emphasis on comparative analysis of experimental data by various state-of-the-art methods. The cases of heavy retrapping along with those beyond QE approximations in different models are also in the pipeline.

ACKNOWLEDGMENTS

The authors are grateful to Dr. S. J. Dhoble, Department of Physics, R.T.M. Nagpur University, India, for extending his support to avail the laboratory facilities. S.B. is also thankful to Dr. Arabinda Das of Department of Statistics and Dr. Saurish Chakraborty, Department of Physics, APC College for computational support. The authors are also thankful to anonymous referees for providing useful suggestions.

REFERENCES

1. Xu, X., Zhang, X., Wang, T., Qiu, J. and Yu, X. *Color variation of photo-stimulated luminescence in strontium ortho-silicate with the assistance of trap centers*. Materials Letters. **127**, 40–43. Available from: (2014). http://www.sciencedirect.com/science/article/pii/S0167577X14006697.
2. Pardha Saradhi M, Lakshminarasimhan N, Boudin S, Vijay Kumar Gupta K, Varadaraju UV, Raveau B. Enhanced luminescence of Sr_2SiO_4:Dy^3+ by sensitization (Ce^3+/Eu^2+) and fabrication of white light-emitting-diodes. Materials Letters. 2014; **117**:302–304. Available from:http://www.sciencedirect.com/science/article/pii/S0167577X13016777.
3. Khiem, D. D., Matsuura, H. and Akiyoshi, M. *Measurement of dose distribution from a crookes tube using thermoluminescent dosimeter*. Radiation Measurements. **134**, 106312. Available from: (2020). http://www.sciencedirect.com/science/article/pii/S1350448720300767.
4. Dewangan, P., Bisen, D. P., Brahme, N., Tamrakar, R. K., Upadhyay, K., Sharma, S.et al. *Studies on thermoluminescence properties of alkaline earth silicate phosphors*. Journal of Alloys and Compounds. **735**, 1383–1388. Available from: (2018). http://www.sciencedirect.com/science/article/pii/S0925838817340756.
5. Atlhan, M. A. *Thermoluminescence properties of two natural colorful fluorite samples of Anatolian origin for dosimetric applications*. Nuclear Instruments and Methods in Physics Research Section B: Beam Interactions with Materials and Atoms. **467**, 33–39. Available from: (2020). http://www.sciencedirect.com/science/article/pii/S0168583X20300471.
6. Martini, M. and Meinardi, F. *Thermally stimulated luminescence: New perspectives in the study of defects in solids*. Rivista del Nuovo Cimento. **20**(8), 1. Available from: (1997). https://doi.org/10.1007/BF02897907.
7. Chen, R. and Kirsh, Y. Analysis of thermally stimulated processes. (Oxford: Pergamon Press) (1981).
8. Chen, R. and SWS, M. Theory Of Thermoluminescence And Related Phenomena. (World Scientific Publishing Company) (1997).
9. Pagonis, V., Kitis, G. and Furetta, C. Numerical and Practical Exercises in Thermoluminescence. (Springer New York) (2006).
10. Horowitz, Y. S. Thermoluminescence & Thermoluminescent Dosimetry. Vol. **2**. (CRC Press) (2020).

11. Liritzis, I., Laskaris, N., Vafiadou, A., Karapanagiotis, I., Volonakis, P., Papageorgopoulou, C.et al. *Archaeometry: an overview*. Scientific Culture. **6**, 49 (2020 Jan).
12. Biswas, R. H., Herman, F., King, G. E., Lehmann, B. and Singhvi, A. K. *Surface paleothermometry using low temperature thermoluminescence of feldspar*. Climate of the Past Discussions. **2020**, 126. Available from: (2020). https://cp.copernicus.org/preprints/cp-2019-173/.
13. Chen, R. *On the Calculation of Activation Energies and Frequency Factors from Glow Curves*. Journal of Applied Physics. **40**(2), 570–585. Available from: (1969). https://doi.org/10.1063/1.1657437.
14. Chen, R. *Glow Curves with General Order Kinetics*. Journal of The Electrochemical Society. **116**(9), 1254. Available from: (1969). https://doi.org/10.1149.
15. Bhattacharyya S, Majumdar PS. *An Overview on Peak Shape Method for Thermoluminescence Glow Curve Analysis: Application on Tremolite and Actinolite Glow Peaks*. In: Emerging Synthesis Techniques for Luminescent Materials. IGI Global; 2018. p. 26–52. Available from:http://doi:10.4018/978-1-5225-5170-6.ch002.
16. Kitis, G., Polymeris, G. S. and Pagonis, V. *Stimulated luminescence emission: From phenomenological models to master analytical equations*. Applied Radiation and Isotopes. **153**, 108797. Available from: (2019). http://www.sciencedirect.com/science/article/pii/S0969804319304142.
17. Sunta, C. M. Unraveling thermoluminescence; Springer Series in Materials Science. Vol. **202**. (New Delhi: Springer India) (2014).
18. May, C. and Partridge, J. *Thermoluminescent kinetics of alpha-irradiated alkali halides*. The Journal of Chemical Physics. **40**(5), 1401–1409. Available from: (1964). https://doi.org/10.1063/1.1725324.
19. Natarajan, V., Bhide, M. K., Dhobale, A. R., Godbole, S. V., Seshagiri, T. K., Page, A. G.et al. *Photoluminescence, thermally stimulated luminescence and electron paramagnetic resonance of europium-ion doped strontium pyrophosphate*. Materials Research Bulletin. **39**(13), 2065–2075. Available from: (2004). http://www.sciencedirect.com/science/article/pii/S0025540804002326.
20. Aruna, S. T. and Mukasyan, A. S. *Combustion synthesis and nanomaterials*. Current Opinion in Solid State and Materials Science. **12**(3), 44–50. Available from: (2008). http://www.sciencedirect.com/science/article/pii/S1359028608000533.
21. Yazici, A. N., Seyyidoğlu, S., Toktamiş, H. and Yilmaz, A. *Thermoluminescent properties of Sr2P2O7 doped with copper and some rare earth elements*. Journal of Luminescence. **130**, 1744–1749. Available from: (2010). http://www.sciencedirect.com/science/article/pii/S002223131000164X.
22. Kumar, A., Kumar, A., Dogra, R., Manhas, M., Sharma, S. and Kumar, R. *Effect of gamma irradiation on thermoluminescence studies of LiF:Sm3+,Dy3+ nanophosphor. Emerging*. Materials Research. **9**(1), 122–131. Available from: (2020). https://doi.org/10.1680/jemmr.18.00101.
23. Randall, J. T. and Wilkins, M. H. F. *Phosphorescence and electron traps-I. The study of trap distributions. Proceedings of the Royal Society of London Series A Mathematical and Physical*. Sciences. **184**(999), 365–389. Available from: (1945). https://royalsocietypublishing.org/doi/abs/10.1098/rspa.1945.0024.
24. Randall, J. T. and Wilkins, M. H. F. *Phosphorescence and electron traps-II. The interpretation of long-period phosphorescence. Proceedings of the Royal Society of London Series A Mathematical and Physical*. Sciences. **184**(999), 390–407. Available from: (1945). https://royalsocietypublishing.org/doi/abs/10.1098/rspa.1945.0025.
25. Garlick, G. F. J. and Gibson, A. F. *The Electron Trap Mechanism of Luminescence in Sulphide and Silicate Phosphors*. Proceedings of the Physical Society. **60**(6), 574–590. Available from: (1948 jun). https://doi.org/10.1088.
26. Burden, R. L., Faires, J. D. and Reynolds, A. C. Numerical Analysis: 9th Ed. (Boston, USA: Brooks/Cole Cengage Learning) (2001).
27. Corless, R. M., Gonnet, G. H., Hare, D. E., Jeffrey, D. J. and Knuth, D. E. *On the Lambert W function*. Advances in Computational mathematics. **5**(1), 329–359. Available from: (1996). https://doi.org/10.1007/BF02124750.
28. Christodoulides, C. *Determination of activation energies by using the widths of peaks of thermoluminescence and thermally stimulated depolarisation currents*. Journal of Physics D: Applied Physics. **18**(8), 1501–1510. Available from: (1985). http://stacks.iop.org/0022-3727/18/i=8/a=015.
29. Abramowitz, M. and Stegun, I. A. Handbook of Mathematical Functions. (New York: Dover) (1972).
30. Kirsh, Y. *Kinetic Analysis of Thermoluminescence*. physica status solidi (a) **129**, 15–48. Available from (1992). https://onlinelibrary.wiley.com/doi/abs/10.1002/pssa.2211290102.
31. WebPlotDigitizer webpage. https://apps.automeris.io/wpd.
32. Salzer, H. E. *Divided differences for functions of two variables for irregularly spaced arguments*. Numerische Mathematik. **6**(1), 68–77. Available from: (1964 Dec). https://doi.org/10.1007/BF01386056.
33. Gill, P. E. and Miller, G. *An algorithm for the integration of unequally spaced data*. The Computer Journal. **15**, 80–83. Available from: (1972). https://doi.org/10.1093/comjnl/15.1.80.
34. Seyyidoğlu, S. Synthesis and Characterization of Novel Rare Earth Phosphates and Rietveld Structural Analysis of Rare Earth Orthoborates [Ph.D. thesis]. (Ankara, Turkey: Middle East Technical University) (2009).
35. Peng, J., Dong, Z. and Han, F. *tgcd: An R package for analyzing thermoluminescence glow curves*. SoftwareX. **5**, 112–120. Available from: (2016). http://www.sciencedirect.com/science/article/pii/S2352711016300140.
36. Karmakar, M., Bhattacharyya, S., Sarkar, A., Mazumdar, P. S. and Singh, S. D. *Analysis of Thermoluminescence Glow Curves using Derivatives of different Orders*. Radiation Protection Dosimetry. **175**(4), 493–502. Available from: (2017). http://dx.doi.org/10.1093/rpd/ncw378.

physica status solidi b
www.pss-b.com

Reappraisal of Peak Shape Method Based on Average Geometrical Symmetry Factor and Its Application to Thermoluminescence Glow Curves

Mohan Kundu, Saurish Chakrabarty, Sukhamoy Bhattacharyya, and Partha Sarathi Majumdar*

A new set of peak shape formulas at different fractional intensities is proposed to extract the activation energy from a thermoluminescence (TL) glow curve. The peak shape coefficients are formulated on the basis of the average geometrical symmetry factor which is estimated considering its dependence on the relevant TL parameters. An empirical dependence of the geometrical symmetry factor on order of kinetics and other parameters is also reported. The present method is used on TL peaks generated in general order kinetics (GOK) approximation and in one trap one recombination center (OTOR) model using a wide range of TL parameters. During the course of TL peak simulation, an alternative analytical approach to evaluate the "temperature integral" is developed. The present method seems to be useful to evaluate the activation energy for all peaks except for the heavy retrapping cases when the initial trap saturation is considerably high. A probable reason behind this limitation is also explored by examining the correspondence between the temperature average of order of kinetics and the retrapping-to-recombination probability. Finally, the new peak shape formulas are tried on isolated single peaks deconvoluted from composite experimental TL curves reported in the literature and the results are quite satisfactory.

1. Introduction

Thermoluminescence (TL) has long been a phenomenon that draws the attention of researchers in the fields of radiation dosimetry, dating, and defect studies.[1–3] In solid-state physics, estimation of trap depth is crucial for basic understanding of a material and its application to various electronic and luminescence devices and TL study has been a very useful tool for this purpose. When a TL material is exposed to high-energy radiation (like X-ray, γ-ray, etc.), charge carriers from the valence band are either excited to the conduction band or trapped in trap states. Those trapped carriers get detrapped on heating and move to the conduction band and subsequently either get retrapped at trap states or recombine at recombination centers. On recombination, electromagnetic wave radiates as TL signal. The plot of this TL signal intensity against temperature gives the TL glow curve or TL peak. There are various phenomenological models to theoretically realize the TL process.[4] Among these, the most widely used models are general order kinetics (GOK), one trap one recombination center (OTOR), interactive multitrap system (IMTS), etc. TL curves simulated in such models are studied in various methods to extract important TL parameters like activation energy, that is, trap depth (E), frequency factor (s), order of kinetics (b), etc. Some of the methods commonly adopted by researchers are area method, initial rise (IR), prompt isothermal decay (PID), variable heating rates (VHRs), peak shape method, etc.[3,5]

The peak shape method is perhaps the most widely used one in TL research to extract the activation energy from an experimental TL curve. Since the early days of TL research, several attempts have been made to calculate the activation energy (E) from certain parameters that depend on the shape of a TL peak.[6–10] However, the most popular version of peak shape method is by Chen,[11,12] where a set of peak shape relations was established empirically on the basis of the GOK model. As prescribed by Chen, the peak shape formulae[12] to extract E from a TL curve were given by $E_\alpha = C_\alpha \frac{kT_m^2}{\alpha} - D_\alpha(2kT_m)$, where α stands for the peak shape parameters $\tau = T_m - T_1$, $\delta = T_2 - T_m$, and $\omega = T_2 - T_1$. Here, T_m is the temperature at the maximum intensity (I_m), and T_1, T_2 are temperatures ($T_2 > T_1$) at half-intensity points. The peak shape coefficients (C_α, D_α) were expressed as a function of the geometrical symmetry factor $\mu_g' = \frac{\delta}{\omega}$, which was approximated as a function of only b though a weak dependence of μ_g' on E and s was mentioned.[12] In **Figure 1**, a schematic diagram is shown, where the peak shape parameters are shown at an arbitrary fractional intensity $x = \frac{I}{I_m}$.

M. Kundu, S. Chakrabarty, S. Bhattacharyya, P. S. Majumdar
Department of Physics
Acharya Prafulla Chandra College
New Barrackpore, Kolkata 700131, India
E-mail: sukhamoy@apccollege.ac.in, sukhamoy.b@gmail.com

M. Kundu
Sadhanpur Uludanga Tulsiram High School (H.S)
24 PGS (N), Amdanga 743221, India

The ORCID identification number(s) for the author(s) of this article can be found under https://doi.org/10.1002/pssb.202100277.

DOI: 10.1002/pssb.202100277

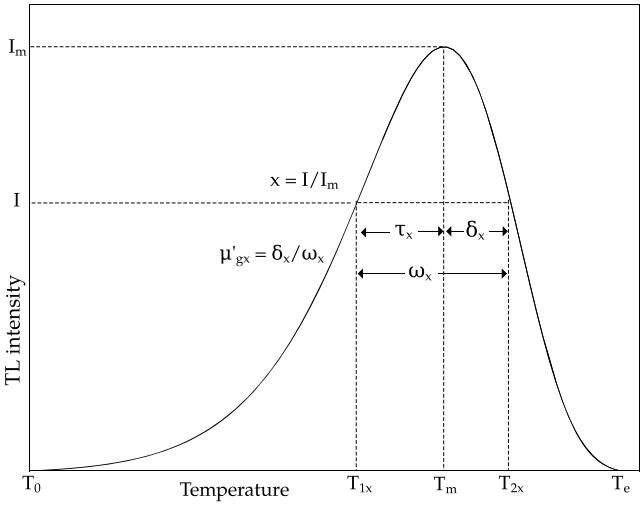

Figure 1. A schematic diagram of a TL peak showing the peak shape parameters for arbitrary fractional intensity $x = \frac{I}{I_m}$. Chen[12] used $x = 0.5$.

In later decades, several attempts were made to develop different variants of peak shape formulae. Christodoulides[13] proposed an alternative set of peak shape relations of the form $E(T_i, T_j) = \frac{T_i T_j}{C(T_i - T_j)} - \frac{T_j}{D}$ for first-order peaks using the peak shape parameters $(\tau_x, \delta_x, \omega_x)$ at fractional intensities $x = 0.25, 0.5, 0.75$. Here T_i and T_j are any two of T_{1x}, T_m, and T_{2x} (see Figure 1) and the coefficients C, D were evaluated numerically.[13] In a subsequent work, Christodoulides[14] reported another set of peak shape relations using GOK theory in the hyperbolic heating scheme. Mazumder et al.[15] further developed the expressions analogous to those of Christodoulides[13] to extract E from nonfirst-order TL peaks at fractional intensities $x = 0.5, 0.667, 0.8$. Gartia et al.[16] reported another version of peak shape relations similar to those reported by Chen,[12] where the peak shape coefficients were expressed as a quadratic function of b at various fractional intensities. Using this methodology,[16] an empirical technique to estimate b in a modified peak shape method was suggested by Singh et al.[17] Kitis and Pagonis[18] reforged the peak shape method for GOK, where the peak shape coefficients were expressed analytically as a function of b multiplied by some pseudoconstants. In this work, Kitis and Pagonis[18] made a comprehensive effort to improve the peak shape coefficients and provide physical insights into them. This work,[18] due to the accuracy it yields in estimating activation energy, has drawn considerable attention among researchers.[19–21] In a subsequent work, Kitis et al.[22] also attempted an alternative approach to derive a set of peak shape formulae in terms of integral symmetry factor in the mixed-order kinetics (MOK) model.

In the present report, we have revisited the peak shape formula from a different perspective, retaining the original form proposed by Chen.[12] We have considered the dependence of geometrical symmetry factor μ'_{gx} at some fractional intensity x (see Figure 1) on E, b, and s (through T_m).[16] An empirical dependence of μ'_g on E, b, and T_m is given here. In the present method, the peak shape coefficients are formulated with respect to an average geometrical symmetry factor $\langle \mu'_{gx} \rangle$ instead of μ'_g or μ'_{gx}. A systematic account is given here to apply the methodology for any arbitrary value of x and in particular, results are given for $x = 0.8, 0.667, 0.5, 0.25$, and 0.11. The present peak shape relations have been applied to extract E from TL peaks simulated in GOK and OTOR models. It is important to note that, instead of b, the charge carrier trafficking mechanism involving the retrapping–recombination processes is reflected in the OTOR model through R which is the ratio of retrapping probability to recombination probability. During the course, we have developed a new analytical method to evaluate the well-known temperature integral which is of the form $\int_{T_i}^{T_f} e^{-\frac{E}{kT}} dT$. The output of the temperature integral as per the new method is compared with those obtained by some of the existing approximated methods.[13,23] The extracted activation energies from GOK and OTOR model TL curves are quite consistent and satisfactory except for the saturated or highly saturated TL peaks generated in the OTOR model when retrapping dominates over recombination. This limitation of the conventional peak shape method is in agreement with other results reported in literature.[20,24,25] We have made a quantitative effort to explore the reason behind the failure of peak shape method for saturated TL peaks with heavy retrapping by retrieving the equivalent value of b from R and comparing it with the temperature average of b.[26] This comparison gives a notion of the validity limit of the peak shape coefficients. We note here that the present peak shape method is applicable for isolated single peaks. For this reason, in experimental cases, deconvolution techniques are to be adopted for extracting the component peaks from a composite TL signal. Various techniques for such deconvolutions are reported in literature and open-source software packages are also available.[27–29] In this light, the present peak shape method is applied to extract E from the experimental TL peaks of $ZnB_2O_4:0.02La$ phosphor[30] and sillimanite (Al_2SiO_5) mineral,[31] where isolated single peaks are deconvoluted from composite experimental peaks. In both the cases, we have considered the component peaks 1 and 2 of the reported glow curves of the materials. The applicability of the present method has been verified by comparing the results with those obtained from the peak shape methods of Chen[12] and Kitis and Pagonis[18] for both simulated and experimental glow curves.

2. Methodology

The basic set of equations describing the charge trafficking in OTOR model is

$$\frac{dn_c}{dt} = nse^{-\frac{E}{kT}} - A_n(N-n)n_c - A_h n_c n_h \quad (1)$$

$$\frac{dn}{dt} = -nse^{-\frac{E}{kT}} + A_n(N-n)n_c \quad (2)$$

$$I = -\frac{dn_h}{dt} = A_h n_c n_h \quad (3)$$

where n_c = concentration of conduction band electrons, n = concentration of trapped electrons, N = total trap concentration, n_h = concentration of holes or recombination center, k = Boltzmann constant, A_n = retrapping probability,

A_h = recombination probability, and T = absolute temperature at heating time t. The charge neutrality condition is given by $n_h = n + n_c$. Under quasiequilibrium (QE) approximations which are given by $|\frac{dn_c}{dn_i}| \ll |\frac{dn}{dt}|$ and $n_c \ll n$, the TL intensity can be expressed as

$$I \simeq -\frac{dn}{dt} = \frac{n^2 s e^{-\frac{E}{kT}}}{n(1-R)+NR} \tag{4}$$

where $R = \frac{A_n}{A_h}$ is a microscopic parameter. We consider linear heating, that is, $T = T_0 + \beta t$, where T_0 is the initial temperature and β is the heating rate. To produce the simulated TL data, Equation (4) can be solved numerically or can be expressed in terms of the Lambert-W function as[32]

$$I = \frac{sNR\exp(-\frac{E}{kT})}{(1-R)^2 W[e^{z_1}] + W[e^{z_1}]^2} \quad \text{for} \quad R < 1 \tag{5}$$

$$= \frac{sNR\exp(-\frac{E}{kT})}{(1-R)^2 W[-1, -e^{-z_2}]^2 + W[-1, -e^{z_2}]} \quad \text{for} \quad R > 1 \tag{6}$$

where

$$z_1 = \frac{1}{c} - \ln c + \frac{s}{(1-R)\beta}\int_{T_0}^{T} \exp\left(-\frac{E}{kT'}\right)dT'$$

$$z_2 = \frac{1}{|c|} - \ln(|c|) + \frac{s}{(1-R)\beta}\int_{T_0}^{T} \exp\left(-\frac{E}{kT'}\right)dT'$$

and $\quad c = \frac{n_0(1-R)}{NR}$

Here, n_0 is the initial concentration of trapped electrons. It is well known[33] that Equation (4) reduces to the first-order and the second-order kinetic equations for $R = 0$ and 1, respectively. In the GOK model, the TL intensity is expressed as

$$I(T) = sn_0 e^{-\frac{E}{kT}} \exp\left[-\frac{s}{\beta}\int_{T_0}^{T} e^{-\frac{E}{kT'}}dT'\right] \quad \text{for} \quad b = 1 \tag{7}$$

$$= sn_0 e^{-\frac{E}{kT}}\left[\frac{(b-1)s}{\beta}\int_{T_0}^{T} e^{-\frac{E}{kT'}}dT' + 1\right]^{-\frac{b}{b-1}} \quad \text{for} \quad b \neq 1 \tag{8}$$

2.1. Evaluation of the Temperature Integral

To estimate the TL intensity, we have to evaluate the temperature integral of the form $J(T_i, T_f) = \int_{T_i}^{T_f} e^{-\frac{E}{kT}}dT$. However this integral cannot be expressed analytically in a closed form; rather, a few approximated methods have been reported in literature. According to Chen,[23] the integral can be approximated as

$$J(T_i, T_f) = \int_{T_i}^{T_f} e^{-\frac{E}{kT}}dT \simeq \int_{0}^{T_f} e^{-\frac{E}{kT}}dT = T_f e^{-\frac{E}{kT_f}} \sum_{r=0}^{\infty}\left(\frac{kT_f}{E}\right)^r (-1)^{r-1} r! \tag{9}$$

Christodoulides[13] proposed another approximation using exponential integrals to evaluate $J(T_i, T_f)$ as

$$J(T_i, T_f) = \int_{T_i}^{T_f} e^{-\frac{E}{kT}}dT \simeq \int_{0}^{T_f} e^{-\frac{E}{kT}}dT = \frac{E}{k}\int_{u_f}^{\infty}\frac{1}{u^2}e^{-u}du = \frac{E}{k}\frac{E_2(u_f)}{u_f} \tag{10}$$

where $\frac{E}{kT} = u$ and $\frac{E}{kT_f} = u_f$. In this communication, we propose an alternative analytical approach to evaluate the integral which is detailed below.

$$J(T_i, T_f) = \int_{T_i}^{T_f} e^{-\frac{E}{kT}}dT = J_f - J_i$$
$$\text{where } J_f = \int_0^{T_f} e^{-\frac{E}{kT}}dT \quad \text{and} \quad J_i = \int_0^{T_i} e^{-\frac{E}{kT}}dT \tag{11}$$

Now, using u and u_f, we can write

$$J_f = \frac{E}{k}\int_{u_f}^{\infty} e^{-u}\frac{1}{u^2}du = \frac{E}{k}\left[\frac{e^{-u_f}}{u_f} - J_1\right] \quad \text{where} \quad J_1 = \int_{u_f}^{\infty}\frac{e^{-u}}{u}du \tag{12}$$

By substituting $u - u_f = \gamma$, we write

$$J_1 = \int_0^{\infty}\frac{e^{-\gamma-u_f}}{\gamma+u_f}d\gamma = J_{11} + J_{12}$$
$$\text{where } J_{11} = e^{-u_f}\int_0^{u_f}\frac{e^{-\gamma}}{\gamma+u_f}d\gamma \quad \text{and} \quad J_{12} = \int_{u_f}^{\infty}\frac{e^{-\gamma-u_f}}{\gamma+u_f}d\gamma \tag{13}$$

Now, using $e^{-\gamma} = \sum_{n_1=0}^{\infty}(-1)^{n_1}\frac{\gamma^{n_1}}{n_1!}$ and $\frac{1}{\gamma+u_f} = \sum_{k_1=0}^{\infty}(-1)^{k_1}\gamma^{k_1}u_f^{-k_1-1}$, we find

$$J_{11} = e^{-u_f}\int_0^{u_f}\sum_{n_1=0}^{\infty}(-1)^{n_1}\frac{\gamma^{n_1}}{n_1!}\sum_{k_1=0}^{\infty}(-1)^{k_1}\gamma^{k_1}u_f^{-k_1-1}\,d\gamma = e^{-u_f}\sum_{n_1=0}^{\infty}\sum_{k_1=0}^{\infty}(-1)^{n_1+k_1}\frac{u_f^{n_1}}{n_1!(n_1+k_1+1)} \tag{14}$$

The J_{12} integral takes a remarkable form if we retrieve the variable $u = \gamma + u_f$. Thus

$$J_{12} = \int_{2u_f}^{\infty}\frac{e^{-u}}{u}du \tag{15}$$

Equation (12) and (15) show that the integrals are similar but the lower limit in J_{12} is twice that of J_1. Hence, J_{12} in Equation (15) can be expanded in a series similar to that given in Equation (14), where u_f is replaced by $2u_f$ plus another integral of the form $\int_{4u_f}^{\infty}\frac{e^{-u}}{u}du$. In this way, a converging infinite series is obtained to express J_f as

$$J_f = \frac{E}{k}\frac{e^{-u_f}}{u_f} - \frac{E}{k}\left[e^{-u_f}\sum_{n_1=0}^{\infty}\sum_{k_1=0}^{\infty}(-1)^{n_1+k_1}\frac{u_f^{n_1}}{n_1!(n_1+k_1+1)} + e^{-2u_f}\sum_{n_2=0}^{\infty}\sum_{k_2=0}^{\infty}(-1)^{n_2+k_2}\frac{(2u_f)^{n_2}}{n_2!(n_2+k_2+1)} + e^{-4u_f}\sum_{n_3=0}^{\infty}\sum_{k_3=0}^{\infty}(-1)^{n_3+k_3}\frac{(4u_f)^{n_3}}{n_3!(n_3+k_3+1)} + \text{higher terms}\right] \tag{16}$$

Equation (16) can be expressed in a more compact form as

$$J_f = \frac{E}{k}\frac{e^{-u_f}}{u_f} - \frac{E}{k}\sum_{p=0}^{\infty}\sum_{k_1=0}^{\infty}\sum_{n_1=0}^{\infty}(-1)^{n_1+k_1}e^{(-2^p u_f)}\frac{(2^p u)^{n_1}}{n_1!(n_1+k_1+1)} \tag{17}$$

For evaluation of the integral (17), we consider that only the $p = 0$ term in the series is enough to have an acceptable value. The contribution of the next term with $p = 1$ is 10^{-12} order smaller than the previous sum and hence can be safely ignored. The present method seems to be working over a wide range of values of E and T_f, whereas in other methods,[13,23] several limitations were mentioned regarding the accuracy depending on the value of $u_f = \frac{E}{kT_f}$. The series (17) involving only $p = 0$ is found to be working successfully for $u_f < 173$ which covers almost entire range in practical applications. For higher values of u_f, more terms in the sum over p are to be included. To achieve a desired accuracy, the number of terms required in the sums over k_1 and n_1 in Equation (17) depend on the value of u_f. However, the integral (17) converges almost instantly in a computer with modest hardware for any value of u_f. To ensure numerical accuracy, we have done the calculations in quadruple precision.

J_i is also evaluated in a similar manner to yield the final expression for $J(T_i, T_f)$ in Equation (11). To check the accuracy of the present method, we compare the present values of the integral with those obtained from Equation (9) and (10). The results are shown in **Table 1**, which shows excellent agreement.

2.2. Modification of Peak Shape Coefficients

The seminal work of Chen[12] on peak shape method suggests the relation

$$E_\alpha = C_\alpha\frac{kT_m^2}{\alpha} - D_\alpha(2kT_m) \tag{18}$$

where α denotes the peak shape parameters τ, δ, and ω measured at $x = 0.5$. The coefficients C_α, D_α were developed in terms of μ'_g assuming a one-to-one correspondence with b.[12] However, μ'_g depends on both b and $u_m = \frac{E}{kT_m}$.[16,34] In this work, we express the geometrical symmetry factor at any arbitrary fractional intensity (x) as

Table 1. Values of the temperature integral evaluated from the present analytical method (Equation (16)), Chen's approximation (Equation (9)), and Christodoulide's method (Equation (10)).

E [eV]	T_0 [K]	T [K]	Present method	Chen[23]	Christodoulides[13]
1.0	250	400	3.24673×10^{-12}	3.24673×10^{-12}	3.24673×10^{-12}
1.0	250	500	1.65474×10^{-9}	1.65474×10^{-9}	1.65474×10^{-9}
1.0	250	600	1.12392×10^{-7}	1.12392×10^{-7}	1.12392×10^{-7}
1.5	250	400	1.10758×10^{-18}	1.10758×10^{-18}	1.10758×10^{-18}
1.5	250	500	1.03190×10^{-14}	1.03190×10^{-14}	1.03190×10^{-14}
1.5	250	600	4.87009×10^{-12}	4.87008×10^{-12}	4.87009×10^{-12}

$$\mu'_{gx} = \frac{T_{2x} - T_m}{T_{2x} - T_{1x}} = \frac{(u_m - u_{2x})u_{1x}}{(u_{1x} - u_{2x})u_m} \tag{19}$$

u_{1x}, u_{2x} are similar to u_m calculated at the temperatures T_{1x}, T_{2x} (see Figure 1). To establish a one-to-one correspondence between b and μ'_{gx}, we proceed as follows. For a fixed value of b, μ'_{gx} is calculated for TL curves corresponding to various u_m within a range $u_{m_i} < u_m < u_{m_f}$. Then average μ'_{gx}, that is, $\langle\mu'_{gx}\rangle$ has been estimated as

$$\langle\mu'_{gx}\rangle = \frac{1}{u_{m_f} - u_{m_i}}\int_{u_{m_i}}^{u_{m_f}}\mu'_{gx}du_m \tag{20}$$

The integration is carried out numerically using the 16-point Gauss–Legendre quadrature.[35] This value of $\langle\mu'_{gx}\rangle$ corresponds to the input value of b that is used to generate the TL peak.

We now proceed to developing the peak shape coefficients with respect to $\langle\mu'_{gx}\rangle$ for various values of fractional intensities. Retaining the forms of the original peak shape relations of Chen,[12] we recast the new peak shape relations as

$$E_{\alpha_x} = C_{\alpha_x}\frac{kT_m^2}{\alpha_x} - D_{\alpha_x}(2kT_m) \tag{21}$$

where x is the fractional intensity and α_x stands for $\tau_x, \delta_x, \omega_x$ (Figure 1). Varying u_m over a wide range, a linear relation between u_m and $\frac{u_p u_q}{u_m|u_p - u_q|}$ can be fit, which yields the peak shape coefficients $C_{\alpha_x}, D_{\alpha_x}$. Here u_p and u_q are any two of u_m, u_{1x}, and u_{2x}. The selection of peak shape parameter α_x from τ_x, δ_x, and ω_x in Equation (21) depends on the choice of u_p and u_q. C_{α_x} and D_{α_x} are fit in a linear relation with $\langle\mu'_{gx}\rangle$ and are expressed as

$$C_{\alpha_x} = C_{1\alpha_x}\langle\mu'_{gx}\rangle + C_{2\alpha_x} \tag{22}$$

$$D_{\alpha_x} = D_{1\alpha_x}\langle\mu'_{gx}\rangle + D_{2\alpha_x} \tag{23}$$

We summarize the entire procedure below to estimate peak shape coefficients for fractional intensity x. 1) Initialize b. 2) Initialize u_m. 3) Estimate μ'_{gx}, u_{1x}, and u_{2x} from the generated TL peak. 4) Increase u_m. Go to step (3) and form new set of μ'_{gx}, u_{1x}, and u_{2x}; repeat the process up to the highest value of u_m. 5) Calculate $\langle\mu'_{gx}\rangle$. 6) Plot $\frac{u_p u_q}{u_m|u_p - u_q|}$ against u_m and fit the plot by a linear relation to find C_{α_x} and D_{α_x}. 7) Increase b. Go to step (2) and form new set of $\langle\mu'_{gx}\rangle$, C_{α_x}, and D_{α_x}; repeat the process up to the highest value of b. 8) Obtain a linear fit of C_{α_x} and D_{α_x} with respect to $\langle\mu'_{gx}\rangle$ to find out ($C_{1\alpha_x}$, $C_{2\alpha_x}$) and ($D_{1\alpha_x}$, $D_{2\alpha_x}$) for the particular value of x.

In the next section, we tabulated the peak shape coefficients for fractional intensities $x = 0.11, 0.25, 0.5, 0.667$, and 0.8, which can be used directly for the estimation of activation energy from the geometrical symmetry factor of a single TL peak.

3. Results and Discussions

The activation energies determined from peak shape parameters $\tau_x, \delta_x, \omega_x$ at different fractional intensity points of the same TL

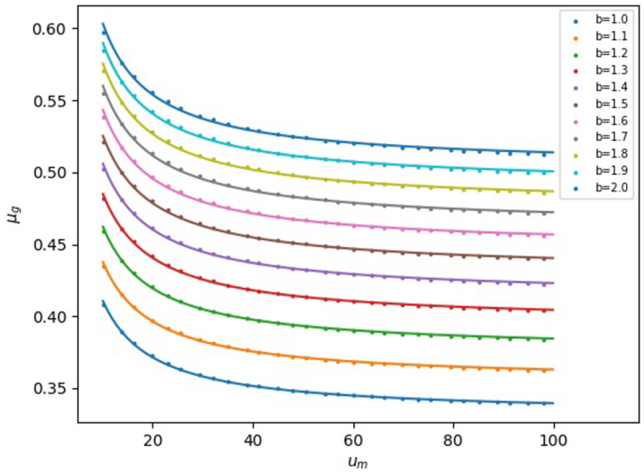

Figure 2. Variation of symmetry factor (μ'_{gx}) with u_m for different b at $x = 0.5$. Here, glow curves are generated for $E_{in} = 1$ eV and $s_{in} = 10^{12}$ s^{-1}.

curve should be consistent among themselves. The peak shape coefficients of activation energies in terms of $\langle \mu'_{gx} \rangle$ are determined for various x. For generating TL curves, values of E and s are taken in wide ranges to yield u_m within the limits $10 \leq u_m \leq 100$. For a fixed value of b, μ'_{gx} is calculated from simulated TL curves corresponding to each u_m value. This process is repeated by varying b in step 1 within the range $0.7 \leq b \leq 2.5$. The variation of μ'_g (i.e., μ'_{gx} at $x = 0.5$) with respect to u_m for $1 \leq b \leq 2$ is shown in **Figure 2**, which shows a clear dependence of μ'_g on b and u_m. The present procedure enables us to establish an empirical dependence of μ'_g on b and u_m by multiparameter fitting. For $x = 0.5$, this relation may be written as

$$\mu'_g = -1.52 + 1.85b^{0.127} + \frac{1}{u_m}(0.094 + 0.919b - 0.227b^2) \quad (24)$$

Similar relations can be formulated for other fractional intensities. After computation of μ'_{gx}, we estimated $\langle \mu'_{gx} \rangle$ according to Equation (20).

3.1. Peak Shape Coefficients at Different Fractional Intensities

The peak shape coefficients (C_{α_x}, D_{α_x}) are needed to evaluate E according to Equation (21). From Equation (22) and (23), the dependence of (C_{α_x}, D_{α_x}) on $\langle \mu'_{gx} \rangle$ is expressed through the fitting constants $C_{1_{\alpha_x}}, C_{2_{\alpha_x}}, D_{1_{\alpha_x}}, D_{2_{\alpha_x}}$, which are obtained in the linear regression method. In **Table 2**, we have listed the values of $C_{1_{\alpha_x}}, C_{2_{\alpha_x}}, D_{1_{\alpha_x}}, D_{2_{\alpha_x}}$ corresponding to different values of fractional intensities (x), where α stands for τ, δ, and ω. We have applied the final peak shape coefficients (C_{α_x}, D_{α_x}) to evaluate E from the TL curve generated in the GOK model and OTOR model.

3.2. Application to GOK Model TL Peaks

For the sake of initial standardization of the present method, we have applied the peak shape formula (Equation 21) to extract

Table 2. Fitting constants in Equation (22) and (23) to evaluate peak shape coefficients in Equation (21) calculated at various fractional intensities.

$x = \frac{I}{I_m}$	α	$C_{1\alpha x}$	$C_{2\alpha x}$	$D_{1\alpha x}$	$D_{2\alpha x}$
0.8	τ	3.6701	−0.9010	8.0509	−2.8304
	δ	6.3094	−2.2376	6.9813	−2.8956
	ω	9.9768	−3.1377	6.9644	−2.5935
0.667	τ	3.3405	−0.3900	5.8890	−1.6311
	δ	6.9339	−2.2181	4.7095	−1.8662
	ω	10.2689	−2.6063	4.5399	−1.3810
0.5	τ	2.9865	0.2260	4.3810	−0.7228
	δ	7.7658	−2.2194	3.0187	−1.1556
	ω	10.7414	−1.9904	2.6723	−0.4477
0.25	τ	2.4611	1.3484	2.8957	0.3388
	δ	9.4782	−2.2821	1.0579	−0.4413
	ω	11.9081	−0.9264	0.3977	0.6851
0.11	τ	2.0872	2.4286	2.1323	1.0754
	δ	11.3057	−2.3975	−0.3198	−0.0337
	ω	13.3205	0.0464	−1.2923	1.5175

activation energy from simulated TL peaks generated in the GOK mode. TL glow curves from the GOK model are generated using Equation (7) and (8) in linear heating scheme with temperature-independent frequency factor. The heating rate (β) is taken as 1 K s^{-1}. The output values $E_{\tau x}$, $E_{\delta x}$, and $E_{\omega x}$ are shown in **Table 3** where first-order, second-order, and GOK are considered. Table 3 shows that the extracted values of activation energy are quite consistent with the input value $E_{in} = 1$ eV. From a theoretical

Table 3. Activation energies $E_{\tau x}$, $E_{\delta x}$, and $E_{\omega x}$ (eV) derived using the present peak shape method from TL peaks simulated in the GOK model for different order of kinetics (b). Here $E_{in} = 1$ eV, $s_{in} = 10^{12}$ s^{-1}, and $\beta = 1$ K s^{-1}.

$x = \frac{I}{I_m}$	b	T_m [K]	τ_x	δ_x	ω_x	μ'_{gx}	$E_{\tau x}$	$E_{\delta x}$	$E_{\omega x}$
0.8	1	384.57	9.09	7.54	16.63	0.4533	1.01	1.03	1.02
	1.5	384.22	10.32	9.79	20.11	0.4869	1.02	1.05	1.03
	2	383.88	11.26	11.71	22.97	0.5098	1.01	1.02	1.01
0.667	1	384.57	12.70	9.87	22.56	0.4373	1.01	1.04	1.02
	1.5	384.22	14.17	13.21	27.38	0.4824	1.02	1.06	1.04
	2	383.88	15.29	16.13	31.42	0.5134	1.01	1.02	1.01
0.5	1	384.57	17.36	12.48	29.84	0.4183	1.01	1.04	1.02
	1.5	384.22	19.03	17.38	36.41	0.4773	1.01	1.07	1.04
	2	383.88	20.29	21.82	42.10	0.5181	1.01	1.02	1.02
0.25	1	384.57	26.56	16.7	43.26	0.3860	1.01	1.05	1.03
	1.5	384.22	28.38	25.09	53.48	0.4692	1.01	1.09	1.05
	2	383.88	29.75	33.24	62.99	0.5278	1.01	1.03	1.02
0.11	1	384.57	35.96	20.11	56.07	0.3587	1.00	1.06	1.03
	1.5	384.22	37.77	32.64	70.41	0.4635	1.01	1.12	1.06
	2	383.88	39.12	45.62	84.74	0.5383	1.01	1.04	1.03

perspective, the present method should work for any value of x, whereas it is observed that admissible values of activation energies are not obtained for $x < 0.11$. It is also evident that the $E_{\tau x}$ values are in greater agreement with E_{in} as compared with $E_{\delta x}$ and $E_{\omega x}$. In fact, $E_{\delta x}$ shows highest deviation from E_{in}.

3.3. Application to OTOR Model TL Peaks

In a similar manner, we have studied the OTOR glow curves for a fairly large number of TL peaks corresponding to a wide range of parameters. For curve generation, the input values of activation energy are taken in the range $0.8 \leq E_{\text{in}} \leq 1.5$ eV and the frequency factor lies in the range $10^8 \leq s_{\text{in}} \leq 10^{12}\ \text{s}^{-1}$. The filling ratio $f = \frac{n_0}{N}$ is taken from 0.01 to 1 to cover the order of trap saturation in a wide range corresponding to different irradiation stages. Retrapping to recombination ratio (R) is considered from 10^{-2} to 10^2 to cover low-to-high retrapping situations during the heating stage. The extracted values of $E_{\tau x}$, $E_{\delta x}$, and $E_{\omega x}$ are shown in **Table 4** for some selected set of input parameters. From Table 4, it is observed that $E_{\tau x}$ values are more consistent with E_{in}, whereas $E_{\delta x}$ values show maximum deviation, as is observed in case of GOK glow curves. The results are consistent for $0 \leq R \leq 1$. However, for $R > 1$, that is, in case of heavy retrapping, $E_{\tau x}$, $E_{\delta x}$, and $E_{\omega x}$ yield acceptable values when f is quite small, which corresponds to low dose rates. In case of saturated or almost saturated cases ($f \simeq 1$) with heavy retrapping ($R > 1$), the output values of activation energy are quite away from the input value. Table 4 shows that even for $f = 0.5$, $E_{\tau x}$, $E_{\delta x}$, and $E_{\omega x}$ show deviation from E_{in} and are underestimated by as much as 9%. We have shown the variation of the average value of activation energy $[E = \frac{1}{3}(E_\tau + E_\delta + E_\omega)]$ plotted against R for different filling ratios at fractional intensities $x = 0.8$ and 0.11 in **Figure 3**. A similar pattern is observed for other x values also. It is evident that for very low values of f (say, $f = 0.01$), the output

Table 4. Activation energies $E_{\tau x}$, $E_{\delta x}$, and $E_{\omega x}$ (eV) derived using the present peak shape method from TL peaks simulated in OTOR model. Here $E_{\text{in}} = 1$ eV, $s_{\text{in}} = 10^{12}\ \text{s}^{-1}$, and $\beta = 1\ \text{K s}^{-1}$.

x	f	R	T_m [K]	τ_x	δ_x	ω_x	μ'_{gx}	$E_{\tau x}$	$E_{\delta x}$	$E_{\omega x}$
0.8	0.01	0	384.57	9.09	7.54	16.63	0.4536	1.02	1.05	1.03
		0.5	436.68	14.39	15.04	29.43	0.5109	1.02	1.07	1.02
		1	447.37	15.11	15.80	30.91	0.5112	1.01	1.08	1.02
		10	487.17	17.81	18.70	36.51	0.5122	1.02	1.08	1.02
	0.5	0	384.57	9.09	7.54	16.63	0.4536	1.02	1.04	1.02
		0.5	388.30	10.78	10.79	21.57	0.5002	1.05	1.07	1.06
		1	392.29	11.74	12.22	23.96	0.5100	1.01	1.02	1.01
		10	416.38	14.92	16.25	31.17	0.5214	0.92	0.91	0.91
	1	0	384.57	9.09	7.54	16.63	0.4536	1.02	1.04	1.05
		0.5	383.31	10.13	9.85	19.98	0.4929	1.06	1.09	1.09
		1	383.87	11.26	11.72	22.97	0.5099	1.01	1.02	1.03
		10	400.08	20.04	20.02	40.06	0.4997	0.56	0.59	0.60
0.667	0.01	0	384.57	12.7	9.88	22.58	0.4374	1.01	1.04	1.02
		0.5	436.68	19.54	20.74	40.28	0.5149	1.01	1.05	1.02
		1	447.37	20.5	21.8	42.31	0.5154	1.01	1.05	1.02
		10	487.17	24.15	25.83	49.98	0.5168	1.01	1.06	1.02
	0.5	0	384.57	12.7	9.88	22.58	0.4374	1.01	1.04	1.02
		0.5	388.30	14.75	14.81	29.55	0.5010	1.04	1.07	1.06
		1	392.29	15.95	16.85	32.8	0.5138	1.01	1.02	1.01
		10	416.38	20.02	22.43	42.46	0.5284	0.92	0.92	0.92
	1	0	384.57	12.7	9.88	22.58	0.4374	1.01	1.04	1.06
		0.5	383.31	13.93	13.45	27.38	0.4913	1.05	1.09	1.11
		1	383.87	15.3	16.15	31.44	0.5136	1.01	1.02	1.05
		10	400.08	26.95	27.12	54.07	0.5016	0.57	0.61	0.63
0.5	0.01	0	384.57	17.35	12.49	29.84	0.4185	1.01	1.04	1.03
		0.5	436.68	25.89	28.06	53.95	0.5201	1.01	1.05	1.02
		1	447.37	27.15	29.51	56.66	0.5208	1.01	1.05	1.02
		10	487.17	31.94	34.99	66.93	0.5228	1.01	1.06	1.03
	0.5	0	384.57	17.35	12.49	29.84	0.4185	1.01	1.04	1.02
		0.5	388.30	19.72	19.93	39.65	0.5027	1.04	1.07	1.06
		1	392.29	21.14	22.77	43.92	0.5185	1.01	1.02	1.02
		10	416.38	26.17	30.28	56.45	0.5364	0.93	0.93	0.93
	1	0	384.57	17.35	12.49	29.84	0.4185	1.01	1.04	1.07
		0.5	383.31	18.71	18.02	36.73	0.4907	1.05	1.10	1.12
		1	383.87	20.28	21.82	42.10	0.5182	1.01	1.02	1.06
		10	400.08	34.94	35.83	70.77	0.5063	0.58	0.63	0.66
0.25	0.01	0	384.57	26.56	16.7	43.26	0.3861	1.01	1.05	1.03
		0.5	436.68	37.88	42.86	80.75	0.5308	1.01	1.04	1.03
		1	447.37	39.69	45.1	84.79	0.5319	1.01	1.05	1.03
		10	487.17	46.6	53.57	100.17	0.5348	1.01	1.05	1.04
	0.5	0	384.57	26.56	16.7	43.26	0.3861	1.01	1.05	1.03
		0.5	388.30	29.26	30.34	59.61	0.5090	1.03	1.08	1.06
		1	392.29	30.99	34.71	65.7	0.5284	1.01	1.03	1.02
		10	416.38	37.46	45.77	83.23	0.5499	0.94	0.95	0.94
	1	0	384.57	26.56	16.7	43.26	0.3861	1.01	1.05	1.03
		0.5	383.31	27.97	27.3	55.28	0.4939	1.04	1.11	1.08
		1	383.87	29.74	33.25	62.99	0.5278	1.01	1.03	1.02
		10	400.08	48.04	52.26	100.3	0.5210	0.63	0.69	0.66
0.11	0.01	0	384.57	35.95	20.11	56.07	0.3588	1.00	1.06	1.03
		0.5	436.68	49.71	58.99	108.7	0.5427	1.01	1.03	1.04
		1	447.37	52.04	62.09	114.13	0.5440	1.01	1.03	1.04
		10	487.17	60.98	73.9	134.88	0.5479	1.01	1.04	1.05
	0.5	0	384.57	35.95	20.11	56.07	0.3588	1.00	1.06	1.03
		0.5	388.30	38.83	41.86	80.68	0.5188	1.03	1.09	1.06
		1	392.29	40.74	47.66	88.39	0.5391	1.01	1.04	1.03
		10	416.38	48.35	62.06	110.4	0.5621	0.95	0.97	0.96
	1	0	384.57	35.95	20.11	56.07	0.3588	1.00	1.06	1.10
		0.5	383.31	37.31	37.67	74.98	0.5024	1.04	1.12	1.15
		1	383.87	39.12	45.62	84.74	0.5384	1.01	1.04	1.10
		10	400.08	58.93	68.84	127.78	0.5388	0.68	0.75	0.80

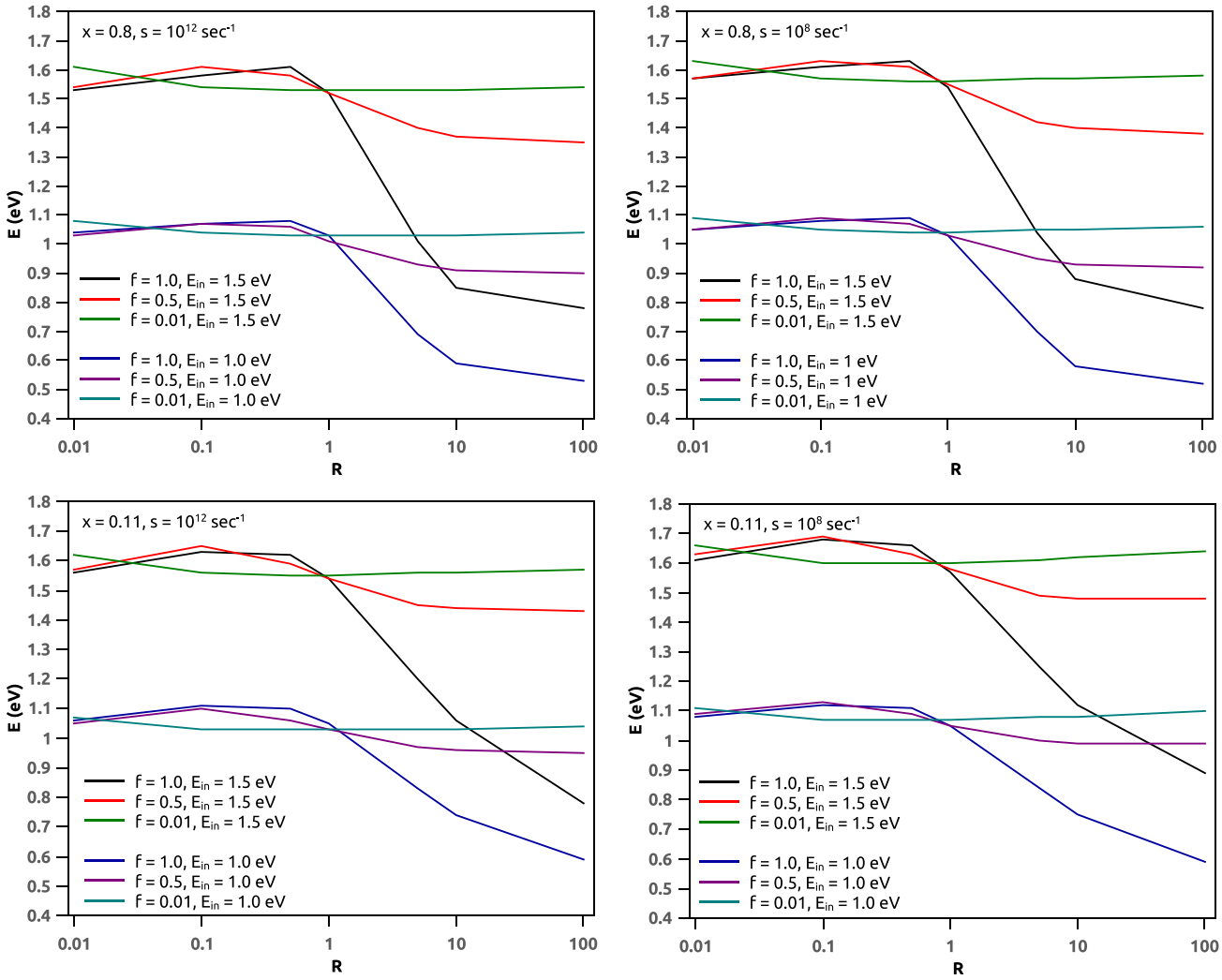

Figure 3. Average activation energy (E) plotted against R for fractional intensities $x = 0.8, 0.11$. Here, $E_{in} = 1$ eV and 1.5 eV, $s_{in} = 10^{12}$ and 10^{8} s^{-1}, and $\beta = 1$ K s^{-1}.

energy is slightly overestimated near $R = 0$. The error decreases with increase in R and even in the heavy retrapping domain ($R > 1$), the activation energy is quite consistent with E_{in}. For higher filling ratio, the error is less near $R = 0$ and 1, but within this range, the extracted activation energy is overestimated. The method starts to fail for heavy retrapping cases ($R > 1$) and the departure becomes more prominent with the gradual filling of trap states. This behavior is uniform for all values of fractional intensities and input parameters for glow curve generation. To gain a deeper insight into the limitation of these peak shape relations for heavy retrapping cases with a higher filling ratio, we have plotted the average activation energy measured at different values of x along with the corresponding error for $R = 10$ in **Figure 4**. We observe a gradual decrease in the output value of E as f increases and the departure is minimum for the parameters corresponding to the lower portion of the curve.

To investigate the primary reason of the failure of the present peak shape method for saturated curves with heavy retrapping, we conducted a detailed study on the symmetry factor (μ'_{gx}) of TL peaks generated with various R and f. The dependence of μ'_{gx} on R and f is shown in **Figure 5** for $x = 0.8$ and 0.11. Similar patterns are observed for other values of x also. It is found that for $0 \leq R \leq 1$, μ'_{gx} increases gradually. Beyond $R > 1$, it increases very slowly in an almost well-behaved way for low values of f. For higher values of f (say, $f = 0.5$), the growth rate of μ'_{gx} with respect to R is quite high, as shown in Figure 5, and above $R = 1$, μ'_{gx} increases and the extracted values of activation energy start deviating. Even the $E_{\tau x}$ values, which are otherwise consistent for $0 \leq R \leq 1$, show a considerable departure from E_{in} for $R > 1$. The behavior of μ'_{gx} for $f = 1$ is quite remarkable. The rate of increase in μ'_{gx} is maximum in this case and above $R = 1$ it shows an anomalous behavior, showing initial growth and then an abrupt fall, which finally reflects through the spurious values of activation energies.

It is to note that in the OTOR model b does not occur explicitly, whereas R does not appear in the GOK model. However, a functional relation between these two can be written as[3,26]

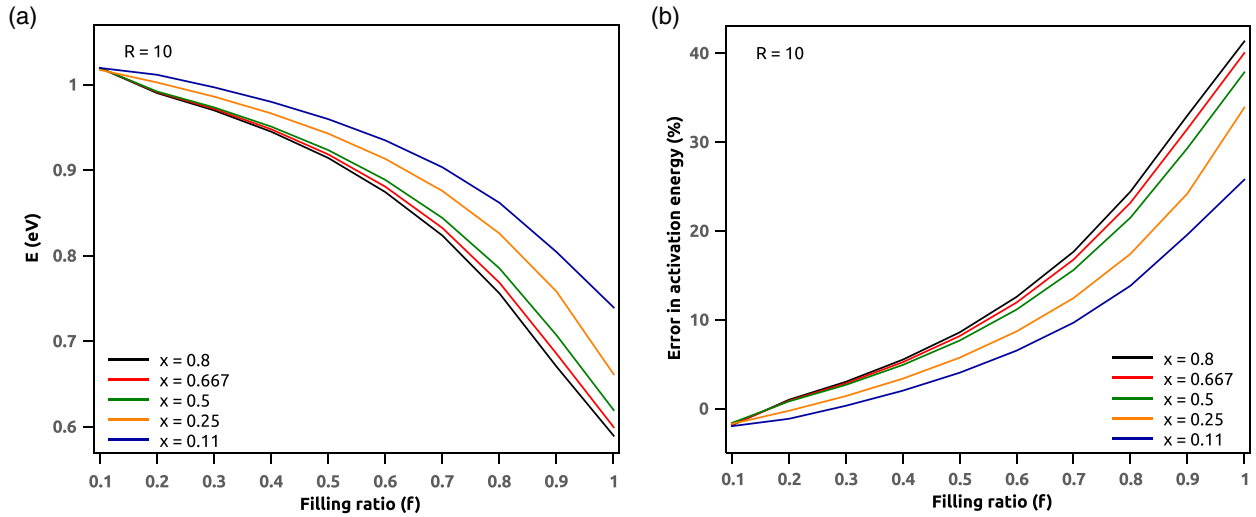

Figure 4. Estimated values of a) activation energy (E) and b) the error inherent in it as derived from TL peaks simulated in OTOR model for different x plotted against f for heavy retrapping ($R = 10$). Here $E_{in} = 1$ eV and $s_{in} = 10^{12}$ s^{-1} and $\beta = 1$ K s^{-1}.

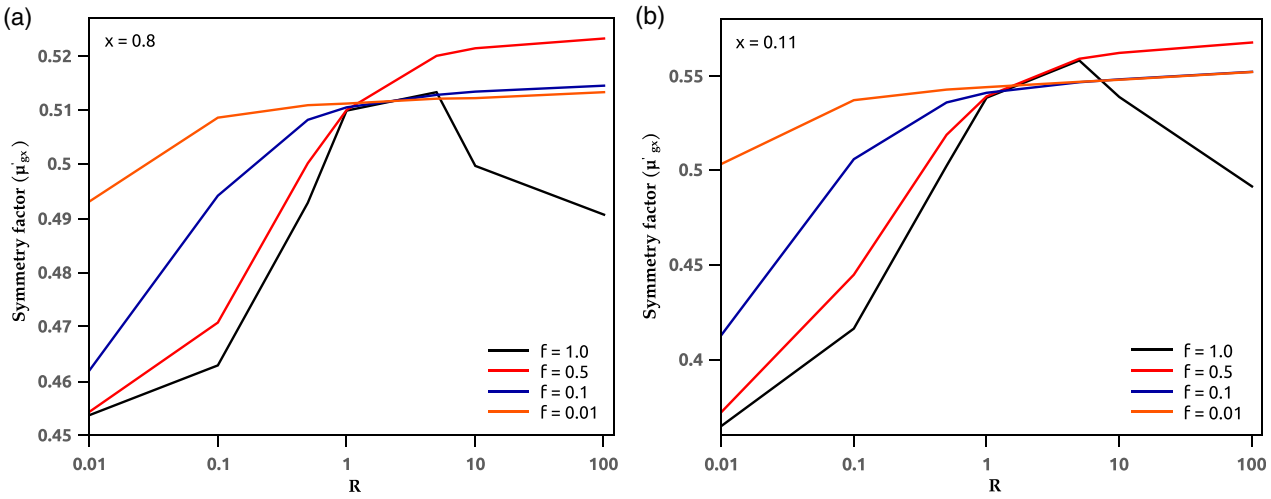

Figure 5. Variation of symmetry factor (μ'_{gx}) plotted against R for TL peaks simulated in OTOR model for various filling ratios with fractional intensities $x = 0.8$ and 0.11. Here $E_{in} = 1$ eV, $s_{in} = 10^{12}$ s^{-1}, and $\beta = 1$ K s^{-1}.

$$b(T) = 1 + \frac{\ln\left[1 + R\left(\frac{N}{n(T)} - 1\right)\right]}{\ln\frac{N}{n(T)}} \tag{25}$$

Equation (25) shows that b has no temperature dependence only for $R = 0$ and 1, which yield $b = 1$ and 2, respectively. For all other values of R, b has a dependence on T due to the temperature dependence of $n(T)$ and hence an entire TL curve should not be described using a fixed value of b. Instead, the temperature average of $b(T)$ (i.e., b_{av}) given by

$$b_{av} = \frac{1}{T_f - T_i}\int_{T_i}^{T_f} b(T)dT \tag{26}$$

is supposed to provide a more reliable correspondence to R.[26] To estimate $b(T)$, we need to integrate Equation (4), so that the required values of $n(T)$ are obtained. The integration in Equation (26) is done here using composite Simpson's rule.[35] We have estimated b_{av} for a large number of TL peaks generated with different values of R and initial filling ratio $f = \frac{n_0}{N}$ and in **Table 5** we have given a representative set of these values. Table 5 shows that for $R \leq 1$, the b_{av} values lie below 2.5 irrespective of the values of f. Even for $R = 10$, we find $b_{av} < 2.5$ for low filling ratio ($f = 0.01$). For all such cases, the activation energies derived from peak shape relations are quite acceptable, as shown in Table 4. This is because the present peak shape coefficients are determined for b lying between 0.7 and 2.5. When trap saturation (i.e., f) increases for $R > 1$, the b_{av} values exceed 2.5, and the peak shape results fail. For $R >> 1$, the peak shape results fail entirely, irrespective of the value of f. The same argument also holds for the failure[24,26] of conventional peak

Table 5. Average value of order of kinetics (b_{av}) for OTOR peaks. The input parameters are $E_{in} = 1.0$ eV, $s = 1.0 \times 10^{12}$ s^{-1}, $N = 1.0 \times 10^{10}$ m^{-3}, and $\beta = 1$ K s^{-1}.

R	f	b_{av}
0.5	0.01	1.9
	0.1	1.8
	0.5	1.7
	1	1.7
1	0.01	2.0
	0.1	2.0
	0.5	2.0
	1	2.0
10	0.01	2.4
	0.1	2.6
	0.5	3.3
	1	5.2
100	0.01	2.8
	0.1	3.3
	0.5	5.1
	1	28.6

shape relations for saturated or highly saturated TL peaks with heavy retrapping.

In **Table 6**, we have given a comparison of the present activation energies for some selected input parameters with those derived using the methods by Chen[12] and Kitis and Pagonis.[18] We note that both the existing methods[12,18] are applicable for $x = 0.5$. The present results for $x = 0.5$ are shown in Table 6 for a ready comparison though this method can yield activation energies at various fractional intensity points. It is evident from Table 6 that the output values' activation energies are quite consistent and in reasonable agreement with other methods. Moreover, the activation energies derived from a particular TL curve at different fractional intensities should be consistent and the present method provides a scope to verify this.

3.4. Application to Experimental TL Peaks

In the final step, we apply the present peak shape relations (Equation (21)) to extract the activation energy from some experimental TL peaks reported in literature. This method works for an isolated component peak deconvoluted from a composite experimental peak. Kucuk et al.[30] reported the TL curves along with the component peaks of γ-irradiated phosphor ZnB_2O_4:0.02La recorded at a heating rate of 5 K s^{-1}. The recorded TL data show a multipeak system of this phosphor and we have considered the first two component peaks with maxima at 456 and 472 K. We have picked the datapoints from the deconvoluted $I - T$ curves[30] for which we have used the browser-based software tool WebPlotDigitizer.[36] It is to note that datapoints picked up in this manner are not equispaced, whereas it is preferred to have equispaced data to conduct some

Table 6. A comparison of present results at $x = 0.5$ with other peak shape methods.[12,18] Here, $E_{in} = 1$ eV, $s_{in} = 10^{12}$ s^{-1}, $\beta = 1$ K s^{-1}, and, for OTOR model, $f = 0.5$.

Model	Input parameters	T_m [K]	μ_g	Activation energy [eV]		
				E_τ	E_δ	E_ω
GOK	$b = 1.0$	384.57	0.4183	1.01	1.04	1.02
				1.00[a)]	0.98[a)]	1.00 [a)]
				0.99[b)]	1.00[b)]	0.99[b)]
	$b = 1.5$	384.22	0.4773	1.01	1.07	1.04
				1.00[a)]	1.02[a)]	1.02[a)]
				0.99[b)]	1.00[b)]	0.99[b)]
	$b = 2.0$	383.88	0.5181	1.01	1.02	1.01
				1.00[a)]	0.98[a)]	1.00[a)]
				0.99[b)]	1.01[b)]	0.99[b)]
OTOR	$R = 0.0$	384.57	0.4185	1.01	1.04	1.02
				1.00[a)]	0.98[a)]	1.00[a)]
				0.99[b)]	1.00[b)]	0.99[b)]
	$R = 0.5$	388.30	0.5027	1.04	1.07	1.05
				1.03[a)]	1.03[a)]	1.04[a)]
				1.01[b)]	0.98[b)]	0.99[b)]
	$R = 1.0$	392.29	0.5186	1.01	1.02	1.01
				1.00[a)]	0.99[a)]	1.00[a)]
				0.99[b)]	1.01[b)]	0.99[b)]

[a)]Chen[12]; [b)]Kitis and Pagonis.[18]

systematic numerical analyses. Moreover, accurate $I - T$ data are essential to estimate the peak shape parameters τ, δ, and ω for a given fractional intensity (x). We have, therefore, adopted the method of interpolation to generate the intermediate data at equal-temperature intervals using the divided difference algorithm[35] which is a standard process for nonequispaced data.[37] The $I - T$ data thus obtained are now exploited to extract the activation energy as per the present version of peak shape formulas. In **Table 7**, we have given the present results ($E_{\tau x}$, $E_{\delta x}$, and $E_{\omega x}$) of activation energies corresponding to the experimental curves. The reported experimental values (E_{expt}) are also shown in Table 7 for a ready comparison of the present results. Moreover, in Table 7, we have also given the activation energies (E_τ, E_δ, and E_ω) estimated according to the formulae of Chen[12] and Kitis and Pagonis,[18] which are valid for $x = 0.5$ only. It is evident from Table 7 that the $E_{\tau x}$, $E_{\delta x}$, and $E_{\omega x}$ values of ZnB_2O_4:0.02La are quite consistent among themselves and are also in agreement with those obtained by other methods.[12,18] The average values of the present activation energy of ZnB_2O_4:0.02La are 1.45 and 1.59 eV for peak 1 and 2, respectively, which are marginally overestimated as compared with E_{expt} values.[30] The relative standard deviation is measured using the formula $\sigma = \frac{1}{E_{avg}}\sqrt{\frac{1}{n}\sum_n (E_{\alpha x} - E_{avg})^2} \times 100\%$. Here, from the values shown in Table 7, $E_{\alpha x}$ are the activation energies ($\alpha = \tau, \delta, \omega$) for all values of x, and n is the number of $E_{\alpha x}$ values (15 for each peak) and E_{avg} is the average of these $E_{\alpha x}$ values.

Table 7. Activation energies derived using the present peak shape method from experimental TL peaks.

Material	Peak	E_{expt} [eV]	$x = \frac{I}{I_m}$	Activation energy [eV]		
				$E_{\tau x}$	$E_{\delta x}$	$E_{\omega x}$
ZnB_2O_4:0.02La phosphor[30]	1	1.36 ± 0.07[30]	0.8	1.49	1.53	1.51
			0.667	1.42	1.49	1.46
			0.5	1.43	1.46	1.44
				1.43[a)]	1.40[a)]	1.43[a)]
				1.39[b)]	1.31[b)]	1.35[b)]
			0.25	1.39	1.44	1.41
			0.11	1.39	1.46	1.42
	2	1.48 ± 0.07[30]	0.8	1.63	1.67	1.65
			0.667	1.58	1.63	1.59
			0.5	1.57	1.62	1.60
				1.56[a)]	1.54[a)]	1.57[a)]
				1.51[b)]	1.40[b)]	1.46[b)]
			0.25	1.52	1.58	1.54
			0.11	1.52	1.59	1.55
Sillimanite (Al_2SiO_5) mineral[31]	1	0.88[31]	0.8	0.75	0.76	0.76
			0.667	0.79	0.82	0.80
			0.5	0.86	0.91	0.88
				0.85[a)]	0.86[a)]	0.86[a)]
				0.85[b)]	0.89[b)]	0.87[b)]
			0.25	0.87	0.95	0.90
			0.11	0.87	0.98	0.92
	2	1.08[31]	0.8	1.14	1.18	1.16
			0.667	1.12	1.17	1.15
			0.5	1.11	1.17	1.14
				1.10[a)]	1.11[a)]	1.11[a)]
				1.08[b)]	1.05[b)]	1.06[b)]
			0.25	1.09	1.18	1.13
			0.11	1.07	1.19	1.13

[a)]Chen[12]; [b)]Kitis and Pagonis.[18]

For ZnB_2O_4:0.02La, the $E_{\tau x}$, $E_{\delta x}$, and $E_{\omega x}$ values yield $\sigma = 2.80$ and 2.75% for peak 1 and 2, respectively.

In a similar manner, we have also determined the activation energies from the component peaks 1 and 2 of the experimental TL curve of X-ray-irradiated sillimanite (Al_2SiO_5) mineral reported by Kalita and Wary.[31] The sample was annealed at 773 K and heated at a rate of 2 K s^{-1}. The reported peak maxima were at 359.6 and 387.3 K.[31] The present results as shown in Table 7 yield $E_{avg} = 0.85$ eV for peak 1 with $\sigma = 8.14\%$. It is evident that for peak 1 that $E_{\tau x}$, $E_{\delta x}$, and $E_{\omega x}$ values of Al_2SiO_5 are consistent except for $x = 0.8$ and 0.667 and also in agreement with the values derived from other methods.[12,18] Given that $E_{expt} = 0.88$ eV for peak 1, the results corresponding to $x = 0.8$ are quite underestimated. Compared with peak 1, the results of peak 2 of (Al_2SiO_5) show more consistency and yield $E_{avg} = 1.14$ eV with $\sigma = 2.93\%$. The probable reason behind such an inflated value of σ corresponding to peak 1 of Al_2SiO_5 might be inherent in the quality of the $I - T$ data picked up from the experimental plot. However, for all the cases, the $E_{\tau x}$ results are always consistent and in better agreement with experimental values.

4. Concluding Remarks

A new set of peak shape formulae for different fractional intensities has been developed to extract activation energy from isolated single TL peaks for which the coefficients are determined using the average symmetry factor of TL curve with b lying between 0.7 and 2.5. During the process, a new analytical method to evaluate the temperature integral using converging infinite series is developed. A numerical relationship to express of μ'_g in terms of b and $\frac{E}{kT_m}$ has been reported. Application of this peak shape method to TL peak simulated in the GOK model gives consistent results of activation energies. When applied to OTOR model TL peaks, the present peak shape relations are found to be working successfully for $R \leq 1$. When R is slightly greater than 1, the newly developed formulae are useful if the trap saturation is low but the method starts to fail if the initial trap saturation increases. For $R >> 1$, the present method fails except for very low initial trap saturation cases. A close look on the values of the symmetry factor reveals that the pattern of its gradual variation breaks down for highly saturated TL peaks with heavy retrapping. The temperature average of b for a TL curve shows that for heavy retrapping cases with sufficiently high trap saturation, the equivalent value of b exceeds 2.5 for $R > 1$, which justifies the failure of peak shape relations as they are estimated by assuming that b lies below 2.5. The development of peak shape formulae for $b > 2.5$ corresponding to $R > 1$ for saturated or highly saturated peaks is in the pipeline, which is supposed to address the limitation of the present method. However, experimental observations of such peaks are not yet reported. The application of the present peak shape method to experimental peaks produces encouraging results with a caution on the accuracy of picking the datapoints from experimental curves. The activation energies derived from the τ parameter appear to be more accurate and the lower portion of the curve seems to produce better results. The present study shows that this modified version of the peak shape method is likely to be useful in case of experimental curves.

Conflict of Interest

The authors declare no conflict of interest.

Data Availability Statement

Research data are not shared. The data are given in the tables and plots and are also available from the authors on request.

Keywords

one trap one recombination model, peak shape methods, symmetry factors, temperature integrals, thermoluminescence

Received: June 14, 2021
Revised: July 21, 2021
Published online:

[1] D. D. Khiem, H. Matsuura, M. Akiyoshi, *Radiat. Meas.* **2020**, *134*, 106312.
[2] R. Chen, Y. Kirsh, *The Analysis of Thermally Stimulated Processes*, Pergamon Press, Oxford **1981**.
[3] C. M. Sunta, *Unraveling thermoluminescence*, Springer Series in Materials Science, Vol. *202*, Springer India, New Delhi **2014**.
[4] G. Kitis, G. S. Polymeris, V. Pagonis, *Appl. Radiat. Isot.* **2019**, *153*, 108797.
[5] G. S. Polymeris, V. Pagonis, G. Kitis, *J. Lumin.* **2020**, *222*, 117142.
[6] F. Urbach, *Zur Lumineszenz der Alkalihalogenide.* Sitzungsber. Akad. Wiss. Wien, Naturwiss.-Mathem. Kl., Vol. *139*, **1930**, pp. 353–372.
[7] L. I. Grossweiner, *J. Appl. Phys.* **1953**, *24*, 1306.
[8] C. B. Lushchik, *Sov. Phys. JETP* **1956**, *3*, 390.
[9] A. Halperin, A. A. Braner, *Phys. Rev.* **1960**, *117*, 408.
[10] P. N. Keating, *Proc. Phys. Soc.* **1961**, *78*, 1408.
[11] R. Chen, *J. Appl. Phys.* **1969**, *40*, 570.
[12] R. Chen, *J. Electrochem. Soc.* **1969**, *116*, 1254.
[13] C. Christodoulides, *J. Phys. D: Appl. Phys.* **1985**, *18*, 1501.
[14] C. Christodoulides, *J. Phys. D: Appl. Phys.* **1986**, *19*, 1555.
[15] P. S. Mazumdar, S. J. Singh, R. K. Gartia, *J. Phys. D: Appl. Phys.* **1988**, *21*, 815.
[16] R. K. Gartia, S. J. Singh, P. S. Mazumdar, *Phys. Status Solidi A* **1988**, *106*, 291.
[17] S. J. Singh, M. Karmakar, S. D. Singh, *Radiat. Eff. Defects Solids* **2013**, *168*, 352.
[18] G. Kitis, V. Pagonis, *Nucl. Instrum. Methods Phys. Res. Sect. B* **2007**, *262*, 313.
[19] S. J. Singh, M. Karmakar, M. Bhattacharya, S. D. Singh, W. S. Singh, S. Azharuddin, *Indian J. Phys.* **2012**, *86*, 113.
[20] M. Karmakar, S. Bhattacharyya, A. Sarkar, P. S. Mazumdar, S. D. Singh, *Radiat. Prot. Dosim.* **2017**, *175*, 493.
[21] M. Talebi, M. Zahedifar, E. Sadeghi, *Nucl. Instrum. Methods Phys. Res. Sect. B* **2019**, *458*, 97–104.
[22] G. Kitis, R. Chen, V. Pagonis, *Phys. Status Solidi A* **2008**, *205*, 1181.
[23] R. Chen, *J. Comput. Phys.* **1969**, *4*, 415.
[24] C. Sunta, A. W. Feria, T. Piters, S. Watanabe, *Radiat. Meas.* **1999**, *30*, 197.
[25] A. Sadek, H. Eissa, A. Basha, G. Kitis, *J. Lumin.* **2014**, *146*, 418.
[26] M. Kundu, S. Bhattacharyya, M. Karmakar, P. S. Majumdar, *Radiat. Prot. Dosim.* **2021**, *193*, 247.
[27] A. Sadek, H. Eissa, A. Basha, E. Carinou, P. Askounis, G. Kitis, *Appl. Radiat. Isot.* **2015**, *95*, 214.
[28] J. Peng, Z. Dong, F. Han, *SoftwareX* **2016**, *5*, 112.
[29] J. Peng, G. Kitis, A. M. Sadek, E. C. Karsu Asal, Z. Li, *Appl. Radiat. Isot.* **2021**, *168*, 109440.
[30] N. Kucuk, A. H. Gozel, M. Yüksel, T. Dogan, M. Topaksu, *Appl. Radiat. Isot.* **2015**, *104*, 186.
[31] J. Kalita, G. Wary, *Spectrochim. Acta, Part A* **2017**, *175*, 61.
[32] G. Kitis, N. Vlachos, *Radiat. Meas.* **2013**, *48*, 47.
[33] R. Chen, S. W. S. McKeever, *Theory of Thermoluminescence and Related Phenomena*, World Scientific Publishing Company, Singapore **1997**.
[34] S. Bhattacharyya, P. S. Majumdar, in *Emerging Synthesis Techniques for Luminescent Materials*, IGI Global, Hershey, PA, USA **2018**, pp. 26–52. https://doi.org/10.4018/978-1-5225-5170-6.ch002.
[35] R. L. Burden, J. D. Faires, A. C. Reynolds, *Numerical Analysis*, 9th ed., Brooks/Cole Cengage Learning, Boston **2001**.
[36] WebPlotDigitizer webpage, https://apps.automeris.io/wpd (accessed: April 2021).
[37] P. E. Gill, G. Miller, *Comput. J.* **1972**, *15*, 80.

Radiation Measurements 156 (2022) 106820

Contents lists available at ScienceDirect

Radiation Measurements

journal homepage: www.elsevier.com/locate/radmeas

Thermoluminescence glow curve analysis using temperature dependent frequency factor in OTOR model

M. Kundu [a,b], S. Chakrabarty [c], S. Bhattacharyya [a,*], P.S. Majumdar [c]

[a] Department of Physics, Jadavpur University, Kolkata 700032, India
[b] Sadhanpur Uludanga Tulsiram High School (H.S), Amdanga, 24 PGS (N) 743221, India
[c] Department of Physics, Acharya Prafulla Chandra College, New Barrackpore, Kolkata 700131, India

ARTICLE INFO

Keywords:
Thermoluminescence
OTOR model
Temperature dependent frequency factor
Temperature integral
Lambert-W function

ABSTRACT

The frequency factor in a thermoluminescent material depends on temperature which can be expressed as $s(T) = s_0 T^a$ $(-2 \leq a \leq 2)$. In practice, analysis of thermoluminescence (TL) glow curves are performed assuming the frequency factor to be temperature independent due to the difficulties involved in estimating a. Such assumption may introduce some limitations in estimating TL parameters of a material and hence, a thorough investigation on the effect of temperature dependent frequency factor (TDFF) on TL analysis has its own importance. In this communication, a comprehensive study using 'One Trap One Recombination centre' (OTOR) model considering TDFF is reported. The prerequisite for such a study is to reproduce the same curve for different values of 'a' as it is not possible to have *a priori* knowledge of 'a' in experimental scenario. This issue is addressed in this work and we have described a methodology for such peak simulation. The OTOR equations are solved and pioneering calculations to derive the peak maxima condition is developed using Lambert-W function considering TDFF. An analytical approach to evaluate the extended temperature integral of the form $\int_{T_i}^{T_f} T^a e^{-\frac{E}{kT}} dT$ is also presented. We have extracted the activation energy for different values of 'a' from a particular TL peak using peakshape method and estimated the subsequent error that may incur out of the assumption of temperature independent frequency factor. The present study has been extended to analyse experimental TL peak reported in literature. TL Peak simulation with TDFF based on Interactive Multi Trap System (IMTS) model has also been explored for a sample case.

1. Introduction

Insulating materials can possess localized energy levels within their forbidden energy gap which are created either naturally or artificially. When such a material is exposed to radiation *e.g.* γ-ray, X-ray *etc.*, electrons and holes are generated in conduction and valence band respectively. Subsequently the electrons from the conduction band are trapped in electron traps and the holes in hole traps (luminescence centres). Various stimulation methods are commonly used to liberate these trapped electrons to conduction band which may further recombine at the luminescent centres and stimulated luminescence signals are produced. Depending on the type of stimulation the process may be termed as thermally stimulated luminescence or thermoluminescence (TL), optically stimulated luminescence (OSL) *etc.* Different stimulation processes are analysed in terms of various stimulating functions. For thermoluminescence the stimulating function is written as

$$p(t) = se^{-\frac{E}{kT(t)}} \tag{1}$$

where E is the activation energy or trap depth, k is Boltzmann constant and s is the pre-exponential factor (in $\sec^{-1}$) known as frequency factor which varies slowly with temperature. To impart a physical significance to s, the trap may be regarded as a potential box (Chen, 1969a) and s is defined as the product of the reflection coefficient and the frequency with which the trapped electron strikes the wall of the box (Mott and Gurney, 1940). The pre-exponential factor was reported more explicitly from comprehensive theoretical background (Bube, 1960; Simmons and Taylor, 1971; Bosacchi et al., 1974) and can be expressed as

$$s(T) = N_c(T) v_t(T) \sigma_n(T) \tag{2}$$

Here N_c is the effective density of states in the conduction band and v_t is the thermal velocity of electrons which are approximated as

$$N_c = 2\left(\frac{km^*T}{2\pi\hbar^2}\right)^{3/2} \quad \text{and} \quad v_t = \sqrt{\frac{3kT}{m^*}} \tag{3}$$

* Corresponding author.
E-mail addresses: sukhamoyb.physics@jadavpuruniversity.in, sukhamoy.b@gmail.com (S. Bhattacharyya).

https://doi.org/10.1016/j.radmeas.2022.106820
Received 8 April 2022; Received in revised form 23 May 2022; Accepted 7 June 2022
Available online 13 June 2022

m^* is the effective mass of electron. σ_n is the transition cross section for trapped electrons to transit into conduction band which is same as the retrapping cross section according to the principle of detailed balance (Salzmann, 1998). Though there is no explicit expression available in literature for σ_n, it has been reported to vary with temperature differently for different materials (Lax, 1960; Bemski, 1958; Lewandowski and McKeever, 1991). The temperature dependence of capture cross section may be summarized in the form $\sigma_n \sim T^{-l}$, where l is a positive number that has been observed to have values $0 \leq l \leq 4$ (Lax, 1960). Thus using Eq. (3) the temperature dependence of frequency factor (Keating, 1961; Chen, 1969a; Fleming, 1990; Bhattacharya et al., 2000; Shambhunath Singh et al., 2000; Karmakar et al., 2010) can be expressed from Eq. (2) as

$$s(T) = s_0 T^a \tag{4}$$

where a is a number with values $-2 \leq a \leq 2$ and s_0 is the temperature independent part of the frequency factor.

A theoretical account explaining the impact of temperature dependent frequency factor (TDFF) on TL peaks and subsequently a method that estimates the activation energy and temperature exponent a from such peaks was reported by Keating (1961) using General Order Kinetic (GOK) model. In a later work, Fleming (1990) showed that it is not possible to determine the value of a from TL measurements alone. Thus determination of the index a from separate experiment not only enhances experimental intricacy, it also introduces additional experimental error. For this reason all the widely used methods (Chen and Kirsh, 1981) assume the frequency factor to be temperature independent (*i.e.* $a = 0$) for TL analysis. However, the quantitative idea about the error originating from this approximation is important for having a deeper physical insight of the underlying processes and also for practical measurements.

Theoretical studies of TL processes considering TDFF is quite limited in literature and almost all of them are carried out using the GOK model. However, GOK model has its inherent limitations for which it is imperative to go beyond GOK model. More physically realistic models based on the band theory *e.g.* One Trap One Recombination centre (OTOR), Interactive Multi Trap System (IMTS) models *etc.* may be adopted for this purpose. In a recent work, Singh (Lovedy Singh, 2020) studied the TL process in OTOR model considering TDFF, where only T^2 dependence of s (*i.e.* $a = 2$ in Eq. (4)) was considered and a significant mismatch was visible between the TL curves generated for $a = 2$ and $a = 0$. Thus an elaborate study of the TL process in OTOR model for the entire range of a should be carried out which is also applicable for study of other thermally stimulated processes like thermally stimulated conductivity (TSC) *etc.* The primary difficulty in the theoretical analysis using TDFF is to reproduce the same curve for different values of a (which is not known beforehand in experimental scenario) by tuning other TL parameters, which has been also mentioned by Singh (Lovedy Singh, 2020).

In this work, a comprehensive study using OTOR model for investigating the effect of TDFF on TL peaks is reported. Analytical expression for TL intensity is derived by solving relevant differential equations. A brief account of the procedure to simulate the same TL peak for different values of a ($-2 \leq a \leq 2$) is given. For this purpose, the value of s_0 for various a (Eq. (4)) is to be evaluated which can be obtained from peak maximum condition. The peak maximum condition with TDFF in OTOR model is developed analytically using Lambert-W function (Corless et al., 1997) as well as Wright ω function (Corless and Jeffrey, 2002). In order to simulate TL peaks we need to evaluate the extended temperature integral of the form $J(a, E, T_i, T_f) = \int_{T_i}^{T_f} T^a e^{-\frac{E}{kT}} dT$ which cannot be expressed in a closed form and various approximated methods were suggested in earlier works (Keating, 1961; Chen, 1970; Gorbachev, 1976; Petty et al., 1977; Gartia et al., 1992; Bhattacharya et al., 2001). In this work we report an analytical approach to estimate the integral $J(a, E, T_i, T_f)$ for both fractional and integral values of a. The applicability of the present method of peak simulation is tested in IMTS model also for a sample dataset using different values of a. However, it is to mention that the present work is in the purview of OTOR model and hence, for further analysis, only the OTOR model is considered. The activation energies are extracted from a particular peak simulated with different 'a' values by using two versions of peakshape method (Kundu et al., 2021b; Chen, 1969a). A thorough investigation to quantify the error incurred due to not considering the temperature dependence of frequency factor while estimating activation energy is carried out. We have also extended the present study using the parameters of the glow peak of $Sr_2P_2O_7 : Cu, Pr$ reported by Yazici et al. (2010) and estimated the activation energy for different values of a.

2. TL equations in OTOR model using temperature dependent frequency factor

The basic charge trafficking equations in OTOR model (Sunta, 2014) can be recast considering TDFF as

$$\frac{dn_c}{dt} = ns_0 T^a e^{-\frac{E}{kT}} - A_n(N-n)n_c - A_h n_c n_h \tag{5}$$

$$\frac{dn}{dt} = -ns_0 T^a e^{-\frac{E}{kT}} + A_n(N-n)n_c \tag{6}$$

$$I = -\frac{dn_h}{dt} = A_h n_c n_h \tag{7}$$

The parameters used in the Eqs. (5)–(7) are: n_c = concentration of conduction band electrons, n = concentration of trapped electrons, N = total trap concentration, n_h = concentration of holes or recombination centre, k = Boltzmann constant, A_n = retrapping probability, A_h = recombination probability and T = absolute temperature at heating time t. The charge neutrality condition is given by: $n_h = n + n_c$. The quasi-equilibrium (QE) approximations *i.e.* $\left|\frac{dn_c}{dt}\right| \ll \left|\frac{dn}{dt}\right|$ and $n_c \ll n$ can also be applied here as, during the TL process, the heating is generally done rather slowly (Dussel and Bube, 1967; Sunta, 2014). Hence, the TL intensity may be expressed as

$$I(t) \simeq -\frac{dn}{dt} = \frac{n^2 s_0 T^a e^{-\frac{E}{kT}}}{n(1-R) + NR} \tag{8}$$

where $R = \frac{A_n}{A_h}$. It may be noted that, in an earlier work, Halperin and Braner (1960) mentioned the dependence of σ_n on A_n and v_t as $\sigma_n = \frac{A_n}{v_t}$ where A_n was considered independent of temperature. In the present work, A_n and A_h are incorporated in the process of peak generation through the parameter R. As R is the ratio of retrapping to recombination probabilities, it may be approximated as independent of temperature.

In linear heating scheme *i.e.* $T = T_0 + \beta t$ where T_0 is the initial temperature and β is the heating rate, Eq. (8) reduces to

$$I(T) \simeq -\frac{dn}{dT} = -\frac{1}{\beta}\frac{dn}{dt} = \frac{n^2 s_0 T^a e^{-\frac{E}{kT}}}{\beta\left[n(1-R) + NR\right]} \tag{9}$$

The initial condition $n = n_0$ at $T = T_0$ is employed to solve Eq. (9). Here n_0 is the initial concentration of trapped electrons. The initial trap filling ratio is defined as $f = \frac{n_0}{N}$. Eq. (9) can be solved numerically or in terms of Lambert-W function to yield TL intensity in OTOR model considering TDFF. The analytical solution of Eq. (9) can be expressed as (Kitis and Vlachos, 2013)

For $R < 1$

$$I(T) = \frac{s_0 T^a NR \exp\left(-\frac{E}{kT}\right)}{\beta(1-R)^2 W[e^{z_1(T)}]\left(1 + W[e^{z_1(T)}]\right)} \tag{10}$$

where $z_1(T) = \frac{1}{c} - \ln c + \frac{s_0}{\beta(1-R)} \int_{T_0}^{T} T'^a \exp\left(-\frac{E}{kT'}\right) dT'$

and $c = \frac{n_0}{N}\frac{(1-R)}{R} = f\frac{(1-R)}{R}$

For $R > 1$

$$I(T) = \frac{s_0 T^a N R \exp\left(-\frac{E}{kT}\right)}{\beta(1-R)^2 W[-1,-e^{-z_2(T)}]\left(1+W[-1,-e^{z_2(T)}]\right)} \quad (11)$$

where $z_2(T) = \frac{1}{|c|} + \ln(|c|) + \frac{s_0}{(1-R)\beta}\int_{T_0}^{T} T'^a \exp\left(-\frac{E}{kT'}\right) dT'$

In the present study we have considered the cases where R lies between 0 and 1.

The peak position can be located from the maximum condition that can be obtained from Eq. (10) by setting $\frac{dI(T)}{dT} = 0$. However for mathematical convenience we set $\frac{d\ln I(T)}{dT} = 0$ and obtain

$$\frac{d\ln I(T)}{dT} = \frac{a}{T} + \frac{E}{kT^2} - \frac{d\ln[W[e^{z_1(T)}] + W[e^{z_1(T)}]^2]}{dW[e^{z_1(T)}]}\frac{dW[e^{z_1(T)}]}{dz_1(T)}\frac{dz_1(T)}{dT} \quad (12)$$

The derivative of $W[e^{z_1(T)}]$ is given by Corless et al. (1997)

$$\frac{dW[e^{z_1(T)}]}{dz_1(T)} = \frac{W[e^{z_1(T)}]}{1+W[e^{z_1(T)}]} \quad (13)$$

Setting $\frac{d\ln I(T)}{dT} = 0$ in Eq. (12) and using Eq. (13), the maximum condition can be expressed after simplification as

$$\frac{a}{T_m} + \frac{E}{kT_m^2} = \frac{s_0}{(1-R)\beta}\left[\frac{1+2W[e^{z_1(T_m)}]}{(1+W[e^{z_1(T_m)}])^2}\right] T_m^a \exp\left(-\frac{E}{kT_m}\right) \quad (14)$$

The TL intensity in OTOR model can also be expressed in terms of Wright ω (denoted by $\omega(z)$) function when $R < 1$ (Singh and Gartia, 2013). The Wright ω function is related to the Lambert-W function as $\omega(z) = W_{k(z)}[e^z]$, where $k(z) = \frac{Im(z)-\pi}{2\pi}$ and hence the TL intensity for TDFF in (Eq. (10)) can be expressed as

$$I(T) = \frac{s_0 T^a N R \exp\left(-\frac{E}{kT}\right)}{\beta(1-R)^2 \omega(z_1(T))(1+\omega(z_1(T)))} \quad (15)$$

The peak maximum condition takes the form

$$\frac{a}{T_m} + \frac{E}{kT_m^2} = \frac{s_0}{(1-R)\beta}\left[\frac{1+2\omega(z_1(T_m))}{(1+\omega(z_1(T_m)))^2}\right] T_m^a \exp\left(-\frac{E}{kT_m}\right) \quad (16)$$

where the derivative of $\omega(z_1(T))$ is given by Corless and Jeffrey (2002)

$$\frac{d\omega(z_1(T))}{dz_1(T)} = \frac{\omega(z_1(T))}{1+\omega(z_1(T))}. \quad (17)$$

3. Evaluation of the extended temperature integral

From Eqs. (10) and (11) it is seen that to simulate TL peak in OTOR model for TDFF, the extended temperature integral of the form $J(a,E,T_i,T_f) = \int_{T_i}^{T_f} T^a e^{-\frac{E}{kT}} dT$ is to be evaluated. A few approximated approaches have been reported in literature for the evaluation of $J(a,E,T_i,T_f)$. Keating (1961) gave an approximated formula by an asymptotic series which involved ~3% error in estimating the integral and the expression is given by

$$J(a,E,T_i,T_f) \simeq \frac{kT^{a+2}}{E}\left[1-(a+2)\frac{kT}{E}\right]\exp\left(-\frac{E}{kT}\right) \quad (18)$$

Later, Chen (1970) proposed an improved version of the formula which is valid unless a is an integer less than −2 and can be expressed as

$$J(a,E,T_i,T_f) = \frac{kT^{a+2}}{E}\left[1-\frac{1}{\Gamma(a+2)}\sum_{n=2}(-1)^{n-1}\Gamma(a+n+1)\right]\exp\left(-\frac{E}{kT}\right) \quad (19)$$

Petty et al. made further improvement of Eq. (19) for $a < -2$ (Petty et al., 1977; Chen and Kirsh, 1981) which is given by

$$J(a,E,T_i,T_f) = \left(\frac{k}{E}\right)^{(|a|-1)}(a-2)!\left[\sum_{n=0}^{|a|-2}\frac{(-\frac{E}{kT})^n}{n!}\right]\exp\left(-\frac{E}{kT}\right) \quad (20)$$

Gorbachev (1976) and Chen and Kirsh (1981) presented another approximation for the integral which can be written as

$$J(a,E,T_i,T_f) \simeq \left[\frac{kT^{a+2}}{E+(a+2)kT}\right]\exp\left(-\frac{E}{kT}\right) \quad (21)$$

Though the expression in Eq. (21) is easier to use but yields limited accuracy (Chen and Kirsh, 1981). In this work, we describe an expression for the evaluation of $J(a,E,T_i,T_f)$ in an analytical approach which does not assume any approximation but involves converging infinite series.

$$J(a,E,T_i,T_f) = \int_{T_i}^{T_f} T^a e^{-\frac{E}{kT}} dT = J_f(a,E,T_f) - J_i(a,E,T_i) \quad (22)$$

where $J_f = \int_0^{T_f} T^a e^{-\frac{E}{kT}} dT$ and $J_i = \int_0^{T_i} T^a e^{-\frac{E}{kT}} dT$

Now, using $\frac{E}{kT} = u$ and $\frac{E}{kT_f} = u_f$, we can write

$$J_f(a,E,T_f) = \left(\frac{E}{k}\right)^{a+1}\int_{u_f}^{\infty}\frac{e^{-u}}{u^{a+2}}du = \left(\frac{E}{k}\right)^{a+1} J_1$$

where $J_1 = \int_{u_f}^{\infty}\frac{e^{-u}}{u^{a+2}}du$ (23)

By substituting $u - u_f = u_1$, we write

$$J_1 = \int_0^{\infty}\frac{e^{-u_f-u_1}}{(u_f+u_1)^{a+2}}du_1 = J_{11} + J_{12} \quad (24)$$

where $J_{11} = e^{-u_f}\int_0^{\frac{u_f}{2}}\frac{e^{-u_1}}{(u_f+u_1)^{a+2}}du_1$ and

$$J_{12} = \int_{\frac{u_f}{2}}^{\infty}\frac{e^{-u_f-u_1}}{(u_f+u_1)^{a+2}}du_1 \quad (25)$$

From Eq. (24) we see J_1 has been decomposed into a finite integral J_{11} and an infinite integral J_{12}.

To evaluate J_{11} we use the binomial expansion as

$$\frac{1}{(u_f+u_1)^{a+2}} = (u_f+u_1)^{-(a+2)} = \sum_{k_1=0}^{\infty}\frac{(-a-2)_{k_1}}{k_1!}u_f^{-(a+2)-k_1}u_1^{k_1} \quad (26)$$

In Eq. (26) the Pochhammer symbol (Graham et al., 1994) is used which is schematically expressed as $(\alpha)_m = \alpha(\alpha-1)(\alpha-2)...(\alpha-m+1)$. Using $e^{-u_1} = \sum_{n_1=0}^{\infty}(-1)^{n_1}\frac{(u_1)^{n_1}}{n_1!}$ the integral J_{11} is recast as

$$J_{11} = e^{-u_f}\int_0^{\frac{u_f}{2}}\sum_{n_1=0}^{\infty}(-1)^{n_1}\frac{u_1^{n_1}}{n_1!}\sum_{k_1=0}^{\infty}\frac{(-a-2)_{k_1}}{k_1!}u_f^{-(a+2)-k_1}u_1^{k_1}\,du_1$$
$$= e^{-u_f}\sum_{n_1=0}^{\infty}\sum_{k_1=0}^{\infty}(-1)^{n_1}\frac{(-a-2)_{k_1}}{n_1!k_1!}\frac{2^{-a-2-k_1}}{(n_1+k_1+1)}\left(\frac{u_f}{2}\right)^{n_1-a-1} \quad (27)$$

We note that the upper limit of J_{11} is set to $\frac{u_f}{2}$ in order to facilitate the convergence of the binomial series (26) which requires $u_1 < u_f$ as a necessary condition.

The evaluation of the integral J_{12} is carried out in a different manner. It is seen that on retrieval of the variable $u = u_f + u_1$, J_{12} takes a form similar to J_1 as given in Eq. (23) except the lower limit and is expressed as

$$J_{12} = \int_{\frac{3u_f}{2}}^{\infty}\frac{e^{-u}}{u^{a+2}}du \quad (28)$$

The lower limit of the J_1 integral (Eq. (23)) is u_f whereas for J_{12} integral (Eq. (28)) it becomes $\frac{3u_f}{2}$. Hence, J_{12} in Eq. (28) can be expanded in a similar manner as described for Eq. (27) in addition to another integral of the form $\int_{\frac{5u_f}{2}}^{\infty}\frac{e^{-u}}{u^{a+2}}du$. Finally, the integral J_f (23) is expressed in a converging infinite series as

$$J_f = \left(\frac{E}{k}\right)^{a+1}\left[e^{-u_f}\sum_{n_1=0}^{\infty}\sum_{k_1=0}^{\infty}(-1)^{n_1}\frac{(-a-2)_{k_1}}{n_1!k_1!}\frac{(2)^{-a-2-k_1}}{(n_1+k_1+1)}\left(\frac{u_f}{2}\right)^{n_1-a-1}\right.$$

Table 1
Comparison of the values of the extended temperature integral evaluated in different methods. Here results are presented for $E = 1$ eV.

T_i (K)	T_f (K)	a	Value of the integral			
			Present method	Chen (1970), Petty et al. (1977)	Keating (1961)	Gorbachev (1976)
0	200	−2.0	5.45108×10^{-30}	5.45107×10^{-30}	5.45107×10^{-30}	5.45107×10^{-30}
		−1.5	7.64421×10^{-29}	7.64420×10^{-29}	7.64255×10^{-29}	7.64312×10^{-29}
		0.0	2.10891×10^{-25}	2.10891×10^{-25}	2.10527×10^{-25}	2.10778×10^{-25}
			2.10891×10^{-25}[a]			
		1.5	5.82157×10^{-22}	5.8216×10^{-22}	5.79517×10^{-22}	5.81634×10^{-22}
		2.0	8.16749×10^{-21}	8.16755×10^{-21}	8.12045×10^{-21}	8.15923×10^{-21}
0	600	−2.0	3.43354×10^{-13}	3.43354×10^{-13}	3.43354×10^{-13}	3.43354×10^{-13}
		−1.5	8.20801×10^{-12}	8.20808×10^{-12}	8.193×10^{-12}	8.19848×10^{-12}
		0.0	1.12480×10^{-7}	1.12504×10^{-7}	1.10826×10^{-7}	1.12023×10^{-7}
			1.12480×10^{-7}[a]			
		1.5	1.54796×10^{-3}	1.54995×10^{-3}	1.4879×10^{-3}	1.53828×10^{-3}
		2.0	3.71277×10^{-2}	3.72039×10^{-2}	3.52957×10^{-2}	3.68728×10^{-2}

[a]Kundu et al. (2021b).

$$+e^{-\frac{3u_f}{2}}\sum_{n_2=0}^{\infty}\sum_{k_2=0}^{\infty}(-1)^{n_2}\frac{(-a-2)_{k_2}}{n_2!k_2!}\frac{(\frac{3}{2})^{-a-2-k_2}}{(n_2+k_2+1)}\left(\frac{2u_f}{2}\right)^{n_2-a-1}$$
$$+e^{-\frac{5u_f}{2}}\sum_{n_3=0}^{\infty}\sum_{k_3=0}^{\infty}(-1)^{n_3}\frac{(-a-2)_{k_3}}{n_3!k_3!}\frac{(\frac{5}{2})^{-a-2-k_3}}{(n_3+k_3+1)}\left(\frac{4u_f}{2}\right)^{n_3-a-1}$$
$$+\text{ higher order terms}\Bigg] \tag{29}$$

A concise form of the J_f integral of Eq. (29) can be written as

$$J_f(a,E,T_f) = \left(\frac{E}{k}\right)^{a+1}\sum_{p=0}^{\infty}\sum_{n=0}^{\infty}\sum_{k=0}^{\infty}e^{-(2^p+1)\frac{u_f}{2}} \times (-1)^n\frac{(-a-2)_k}{n!k!}\frac{(1+\frac{1}{2^p})^{-a-2-k}}{(n+k+1)}\left(2^p\frac{u_f}{2}\right)^{n-a-1} \tag{30}$$

In practical scenario, for given values of E and a, $J(a,E,T_i,T_f)$ is insensitive to T_i if T_f and T_i are not too close to each other since the integral is a very strongly increasing function of T. Thus $J_i(a,E,T_i)$ can be ignored comfortably and the final expression for $J(a,E,T_i,T_f)$ equals $J_f(a,E,T_f)$ of Eq. (30). However, the $J_i(a,E,T_i)$ integral can be evaluated in a similar manner as $J_f(a,E,T_f)$, if needed. A computer with standard hardware specification can evaluate the integral (30) almost in no time. It has been investigated that only the $p = 0$ term in the series (30) is sufficient to have a value of the extended temperature integral appropriate for TL studies. In that case the integral becomes

$$J_f = \int_0^{T_f} T^a e^{-\frac{E}{kT}}dT \simeq \left(\frac{E}{k}\right)^{a+1}e^{-u_f}\sum_{n_1=0}^{\infty}\sum_{k_1=0}^{\infty}(-1)^{n_1}\frac{(-a-2)_{k_1}}{n_1!k_1!}\frac{(2)^{-a-2-k_1}}{(n_1+k_1+1)}\left(\frac{u_f}{2}\right)^{n_1-a-1} \tag{31}$$

We have estimated the extended temperature integral for different sets of parameters and the results are compared with those obtained from some of the other methods available in literature (Chen, 1970; Petty et al., 1977; Keating, 1961; Gorbachev, 1976). The calculations are carried out in quadruple precision. The results are displayed in Table 1 which shows excellent agreement. In Table 1, we have given the values of the integral for both integer and fractional values of a within the range $-2 \leqslant a \leqslant 2$. However, we have verified that the integral works satisfactorily for other values of a beyond this range In a previous work (Kundu et al., 2021b), we have reported the temperature integral for $a = 0$. The present results for $a = 0$ are also in excellent agreement with those reported in Kundu et al. (2021b).

4. Glow curve simulation

The prerequisite in investigating the effect of temperature dependence of frequency factor on TL peaks is to simulate the same peak for different values of a (Eq. (4)) which poses a challenge before theoretical analysis. If a particular TL curve cannot be reproduced for different values of a, it will not be possible to apply any method to extract trapping parameters by glow curve analysis. In this study we have addressed this issue and have been able to simulate the same TL curve for different values of a lying in the range $-2 \leq a \leq 2$. For obvious reasons the determined values of s_0 and E corresponding to a peak will vary if a is varied. It is reported in literature that when TDFF is taken into account, a correction term akT_m is to be incorporated in E (Aramu et al., 1966; Ingraham and Marier, 1964; Chen, 1969b,a; Chen and Kirsh, 1981). Since T_m is known for an experimental TL peak, s_0 can be determined for a particular value of a from the peak maximum condition (Eqs. (14) or (16)) with $E = E_0 - akT_m$ where E_0 is the input value of E for $a = 0$. We have observed that the exclusion of the correction factor akT_m results in a mismatch in peak height and a deviation in peak position (T_m) occurs if s_0 is not estimated properly. We have simulated glow curves for various values of a and the matching among the glow curves are quite remarkable as depicted in Fig. 1.

In Fig. 1(a) TL glow peaks for $R = 0$ and $f = 0.5$ simulated in OTOR model are shown where s is temperature dependent. The $R = 0$ peak is equivalent to the first order case in GOK model. Fig. 1(a) exhibits that the same TL peak with $T_m = 386.8$ K is generated with various values of a. Similar glow curves for $R = 0.5$ (general order case in GOK model) and $R = 1$ (second order in GOK model) are given in Fig. 1(b) and (c) respectively. The input parameters used for simulating the peaks in Fig. 1(a)–(c) are given in Table 2. The peak maximum (T_m) is seen to shift as R changes and the values of T_m are also tabulated. In addition to that, we have also given the values of frequency factor at peak temperature $s_m = s(T_m) = s_0 T_m^a$ in Table 2 for convenience. We have studied numerous TL curves for different values of input parameters (E, s_0, f, R) covering a wide range of T_m and observed that the present methodology can reproduce the same TL curve for different values of a. We have extended the present method of peak simulation in IMTS model also and found it to be equally applicable which is evident from Fig. 1(d). The differential equations governing the TL process in IMTS model are taken from Sunta (2014) and modified them accordingly for TDFF.

In order to have a quantitative measure of the accuracy of simulation of a particular peak in OTOR model for different values of a, we have estimated the area under the curves as well as the geometric symmetry factor $\mu_g' = \frac{T_2 - T_m}{T_2 - T_1}$ for the curves. Here T_1, T_2 are the temperatures at rising side and falling side respectively of the glow curve at half intensity points. In Fig. 2 we have shown the variation in area under the curve for different a related to peaks given in Fig. 1(a–c). From Fig. 2 it is seen that, in case of $R = 0$, area under the curves is almost insensitive to a and a gradually increasing trend with respect to a is there as R goes from 0 to 1, though not much variation is seen. In Fig. 3 we have shown the variation of μ_g' with respect to $\frac{E}{kT_m}$ for the

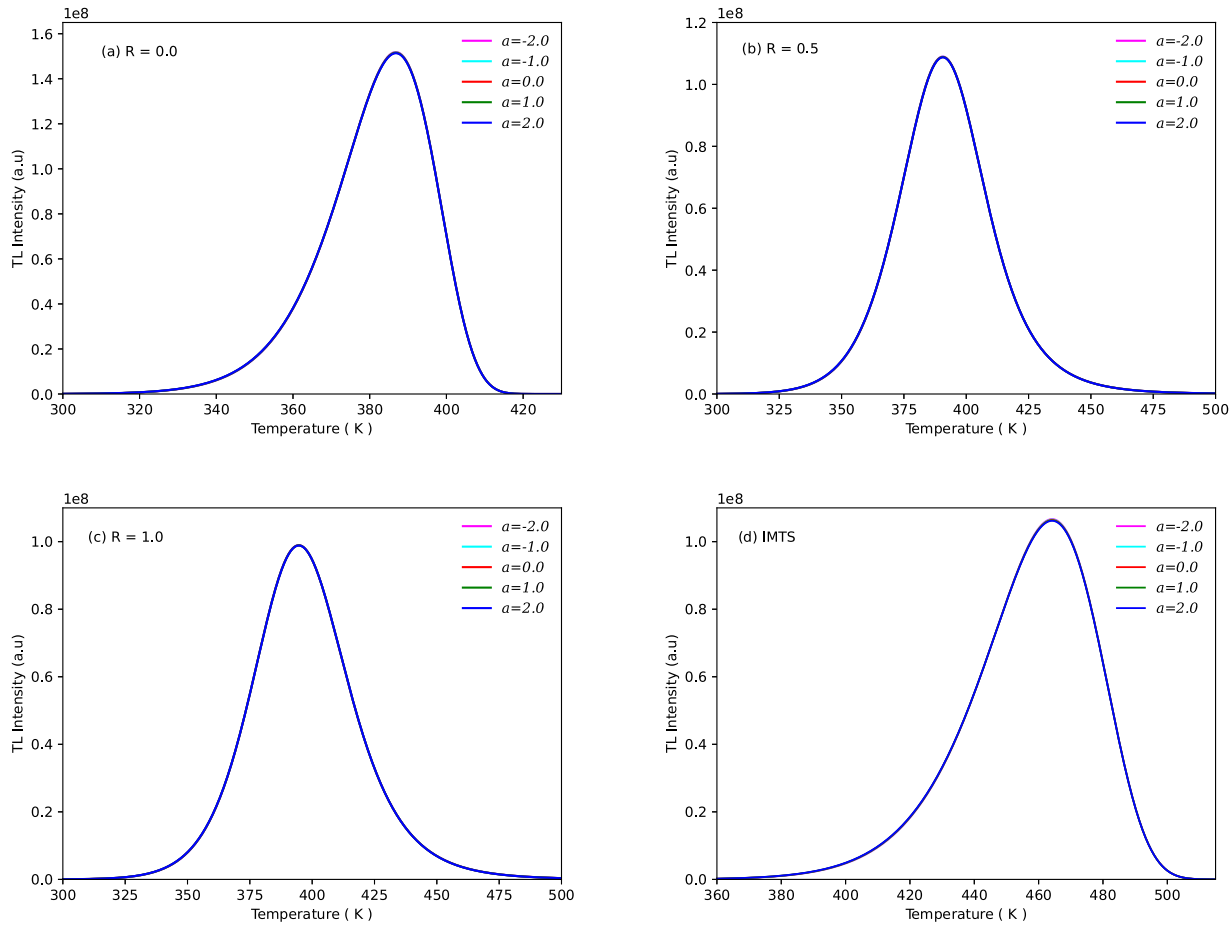

Fig. 1. Simulation of TL glow peaks for TDFF. (a)–(c) Particular TL peak simulated in OTOR model with different values of a where $s = s_0 T^a$. Here a has been considered in the range $-2 \leq a \leq 2$. Corresponding input parameters are given in Table 2. (d) IMTS glow peak, equivalent to first order peak in GOK model, simulated for temperature dependent s by varying a. For peak generation, we have taken $E_0 = 1$ eV and $\beta = 1$ Ksec^{-1}.

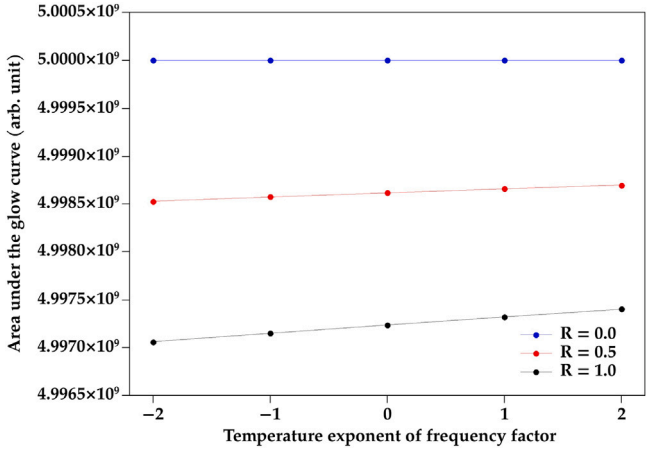

Fig. 2. Comparison of area under the curve plotted against a. Here TL peaks in Fig. 1(a)–(c) for different R have been used.

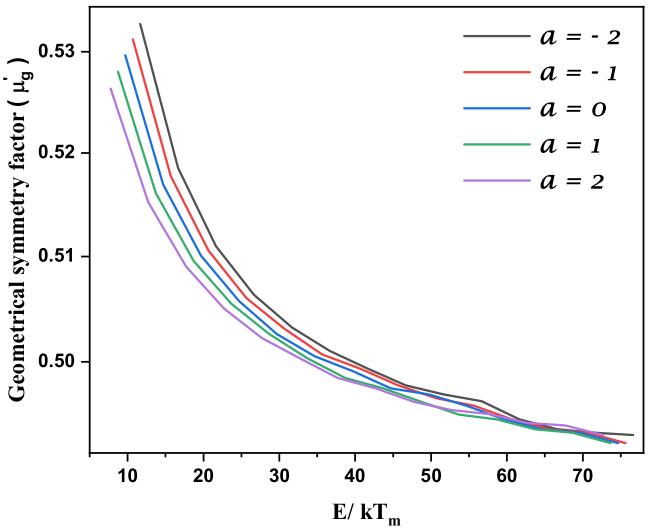

Fig. 3. Comparative variation of geometric symmetry factor of TL peaks with TDFF with respect to $\frac{E}{kT_m}$ for different values of a. Here $R = 0.5$ and $f = 0.5$ are taken.

glow curves generated with $R = 0.5$ and $f = 0.5$. It is seen that μ'_g does not exhibit much difference with respect to a when $\frac{E}{kT_m} > 30$.

We have further investigated the variation of frequency factor with respect to temperature for different values of a related to a particular peak and repeated the study for a large number of TL curves. Here we present the analysis in Fig. 4(a) in respect of the TL curves having $\frac{E}{kT_m} = 30$. Corresponding values of s_0 (unit s^{-1}/K^a) are also given in log scale in Fig. 4(a). It is observed that $s(T)$ decreases with temperature for $a < 0$ while an opposite behaviour is seen for $a > 0$. The impact of

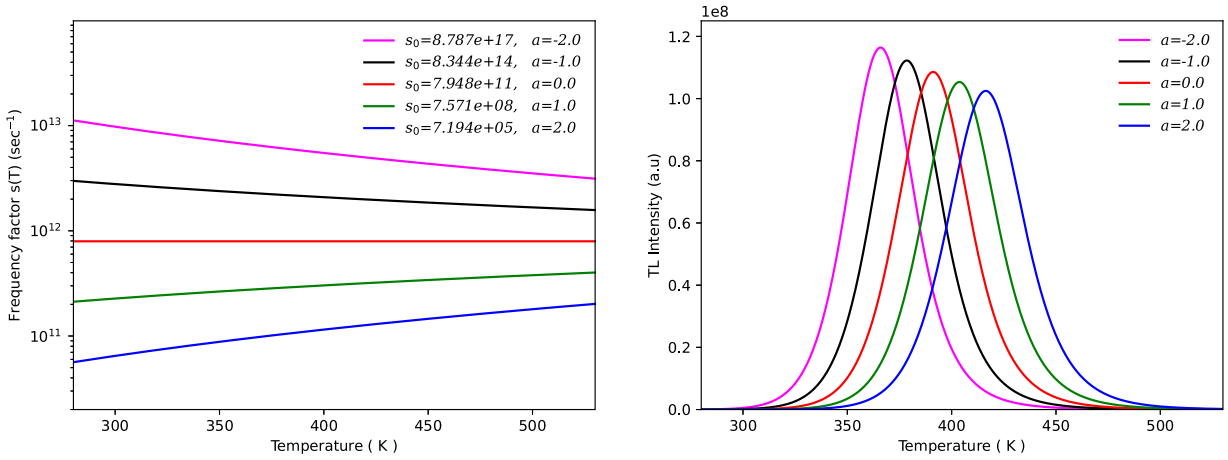

Fig. 4. (a) Variation of frequency factors with temperature for different values of a. Here s_0 values are given in unit s^{-1}/K^a. The vertical axis is presented in log scale. (b) The TL peaks corresponding to each $s(T)$ in figure (a) are shown. Here $E = 1$, $R = 0.5$ and $f = 0.5$ is used for curve simulation.

Table 2
The input parameters used for different values of a to yield the same glow peak simulated in OTOR model when s depends on temperature. The peaks are given in Fig. 1(a)–(c). Here $E = E_0 - akT_m$. $E_0 = 1$ eV and $f = 0.5$ are considered for all the cases.

a	E (eV)	s_0 ($s^{-1}K^{-a}$)	$R = 0.0$		$R = 0.5$		$R = 1.0$	
			T_m (K)	s_m (s^{-1})	T_m (K)	s_m (s^{-1})	T_m (K)	s_m (s^{-1})
−2	1.067	9.182×10^{17}	386.8	6.14×10^{12}	390.6	6.02×10^{12}	394.6	5.90×10^{12}
−1	1.033	8.714×10^{14}		2.25×10^{12}		2.23×10^{12}		2.21×10^{12}
0	1.0	8.296×10^{11}		8.30×10^{11}		8.30×10^{11}		8.30×10^{11}
1	0.967	7.898×10^{08}		3.05×10^{11}		3.08×10^{11}		3.12×10^{11}
2	0.933	7.495×10^{05}		1.12×10^{11}		1.14×10^{11}		1.17×10^{11}

TDFF on TL peaks are visible when we simulate TL peaks using these values of $s(T)$ corresponding to different a keeping E, f, R fixed and it is displayed in Fig. 4(b). As the values of a vary from −2 to 2, the peak maxima show a rightward shift with decrease in peak height.

5. Systematic error analysis

In the next phase we attempt to extract activation energy from the TL curves simulated in OTOR model with TDFF and we employ the peakshape method for this purpose. We have considered different values of input parameters to generate TL peaks in such a way that the value of $u_m = \frac{E}{kT_m}$ remains in the range of experimental interest. At first, the peak for $R = 0$ is simulated with $a = 0$ and $u_m = 30$ where $E = 1.0$ eV that yields $T_m = 386.8$ K. The value of s_0 comes out to be $s_0 = 8.296\times10^{11}$ s^{-1} from maximum condition. Setting this glow peak as reference, we simulate the same peak (similar to $a = 0$) for other values of a ($-2 \le a \le 2$) keeping T_m unaltered. Following the peakshape method proposed in a previous work (Kundu et al., 2021b) we have estimated the activation energy (E_τ) using the peakshape parameter $\tau_x = \frac{T_m - T_{1x}}{T_{2x} - T_{1x}}$ where $x = \frac{I}{I_m}$ is the fractional intensity. T_{1x}, T_{2x} are the temperatures at rising side and falling side of the glow curve respectively at fractional intensity x. We have taken $x = \frac{1}{4}, \frac{1}{2}, \frac{2}{3}$ in this work. Moreover, for $x = \frac{1}{2}$, we have also used the peakshape method proposed by Chen (1969a) to estimate the activation energy. The results are listed in Table 3. E_{in} is the input values of activation energy used in peak simulation and E_{out} is the output activation energy derived by peakshape method. It is to note that in both the versions of peakshape method, the geometrical symmetry factor (μ_g') plays a central role and the difference in μ_g' values for different a, as is shown in Fig. 3, is reflected through the output values of E. The results extracted by using two versions of peakshape method as given in Table 3 are quite in agreement. The same procedure is followed to investigate other peaks corresponding to $R = 0.5$ and 1.0 and the results are also displayed in Table 3.

In experimental scenario, T_m is measured from a TL peak where a is unknown and hence E is usually estimated from the recorded TL data considering $a = 0$. Hence there is a scope to investigate theoretically the effect of non-zero values of a on the extracted values of activation energy using peakshape method. We have carried out a systematic error analysis in extracting activation energy from TL data. In Table 3 we have also given the error ($\delta E = \frac{E_{out} - E_{in}}{E_{in}} \times 100\%$) explicitly for each TL peak corresponding to different values of a. It can be seen from Table 3 that for $R = 0$ and 1, the inherent error in activation energy arising due to the temperature variation of frequency factor lie within 8% whereas for $R = 0.5$, the error may go beyond 11%. In Fig. 5 we have given the variation of error $\delta E(\%)$ as a function of $\frac{E}{kT_m}$. For this purpose we have generated a sufficiently large number of TL peaks where $u_m = \frac{E}{kT_m}$ is varied from 10 to 75. Each peak is reproduced for five values of a *i.e.* $\pm2, \pm1, 0$. The plot in Fig. 5 for $R = 0$, 0.5, 1 are presented in the same scale to facilitate a comparative study. In all the cases it is seen that the magnitude of error increases as $\frac{E}{kT_m}$ decreases and the amount of error becomes quite significant when $\frac{E}{kT_m}$ goes below 30. Moreover, for $R = 0$ and 1, δE is minimum with $a = 0$ when $\frac{E}{kT_m} > 20$ whereas, for $R = 0.5$, δE is minimum for $a = -1$.

In order to verify the applicability of the present study in case of experimental TL peaks, we have considered the glow curve of $Sr_2P_2O_7$: Cu, Pr reported by Yazici et al. (2010) where the sample was exposed to β-radiation with dose ∼12 Gy and the heating rate was 1 Ks^{-1}. The composite TL signal was deconvoluted into two component peaks. In this work we have considered only the peak-1 and carried out the analysis based on OTOR model for different values of a to estimate E using peakshape methods (Kundu et al., 2021b; Chen, 1969a). In the original work of Yazici et al. (2010) the glow curve analysis was carried out in GOK model and the order of kinetics was reported as $b = 1.1$ for peak-1 of $Sr_2P_2O_7$: Cu, Pr. As the present study is done in terms of OTOR model where b does not arise explicitly, we have estimated the

Table 3
Activation energies (E) and corresponding error ($\delta E\%$) for fractional intensities $x = \frac{1}{4}$, $\frac{1}{2}$ and $\frac{2}{3}$ estimated using the peakshape method proposed in Kundu et al. (2021b). For $x = \frac{1}{2}$, Chen's (1969a) peakshape results are also given that are marked by asterisks. Here $f = 0.5$ has been considered for all the peaks.

T_m (K)	$\frac{E}{kT_m}$	Input parameters				Output values of activation energy (E_{out} in eV)					
		R	a	s_0 ($s^{-1}K^{-1}$)	E_{in} (eV)	$x = \frac{1}{4}$		$x = \frac{1}{2}$		$x = \frac{2}{3}$	
						E_τ	δE (%)	E_τ	δE (%)	E_τ	δE (%)
386.8	32.00	0.0	−2	9.182×10^{17}	1.067	1.010	−5.34	1.013	−5.06	1.014	−4.97
								1.004[a]	−5.90		
	31.00		−1	8.714×10^{14}	1.033	1.008	−2.42	1.011	−2.13	1.013	−1.94
								1.002[a]	−3.00		
	30.00		0	8.296×10^{11}	1.000	1.006	0.60	1.010	1.00	1.012	1.20
								1.001[a]	0.10		
	29.00		1	7.898×10^{8}	0.967	1.005	3.93	1.008	4.24	1.010	4.45
								0.999[a]	3.31		
	28.00		2	7.495×10^{5}	0.933	1.003	7.50	1.007	7.93	1.008	8.04
								0.998[a]	6.97		
391.1	31.65	0.5	−2	8.787×10^{17}	1.067	1.037	−2.81	1.042	−2.34	1.045	−2.06
								1.033[a]	−3.19		
	30.66		−1	8.344×10^{14}	1.033	1.035	0.19	1.041	0.77	1.044	1.06
								1.031[a]	−0.19		
	29.67		0	7.948×10^{11}	1.000	1.033	3.30	1.039	3.90	1.042	4.20
								1.029[a]	2.90		
	28.68		1	7.571×10^{8}	0.967	1.032	6.72	1.038	7.34	1.041	7.65
								1.028[a]	6.31		
	27.69		2	7.194×10^{5}	0.933	1.03	10.40	1.036	11.04	1.039	11.36
								1.026[a]	9.97		
395.3	31.31	1.0	−2	8.642×10^{17}	1.067	1.010	−5.34	1.011	−5.25	1.011	−5.25
								1.001[a]	−6.19		
	30.33		−1	8.208×10^{14}	1.033	1.009	−2.32	1.009	−2.32	1.010	−2.23
								0.998[a]	−3.39		
	29.35		0	7.821×10^{11}	1.000	1.007	0.70	1.009	0.90	1.008	0.80
								0.998[a]	−0.20		
	28.37		1	7.451×10^{8}	0.967	1.005	3.93	1.007	4.14	1.007	4.14
								0.996[a]	3.00		
	27.39		2	7.083×10^{5}	0.933	1.004	7.61	1.005	7.72	1.005	7.72
								0.995[a]	6.65		

[a]Chen (1969a).

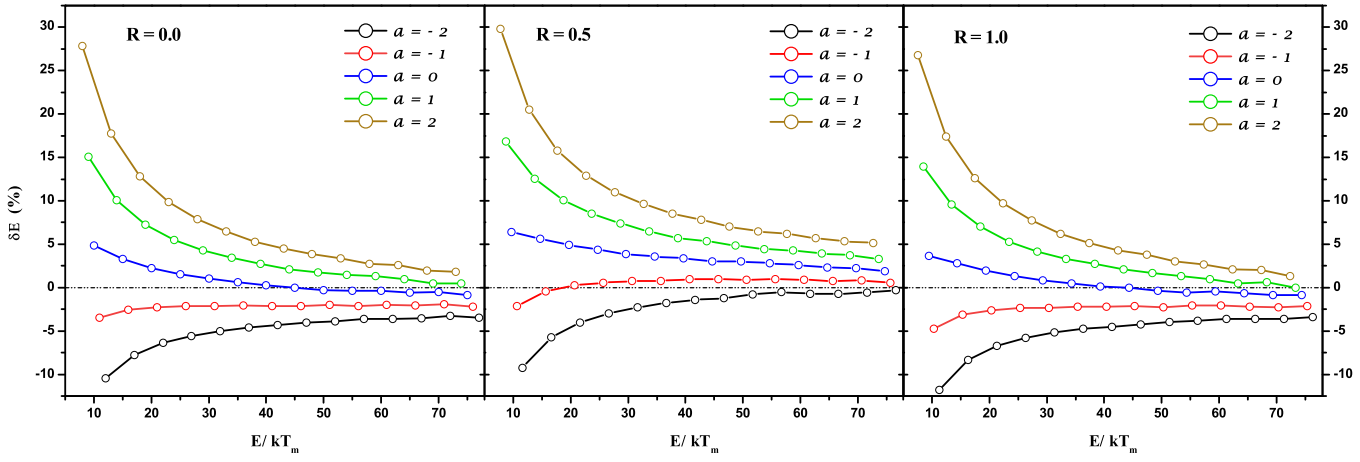

Fig. 5. Variation in error $\delta E\%$ due to temperature dependence of frequency factor plotted against $\frac{E}{kT_m}$. Here $f = 0.5$ has been used for peak generation.

value of R corresponding to $b = 1.1$ using the empirical relation (Sunta, 2014; Kundu et al., 2021a).

$$b = 1 + \frac{\ln\left[1 + R(\frac{N}{n} - 1)\right]}{\ln \frac{N}{n}} \tag{32}$$

The reported value of E for peak-1 was 0.933 eV (Yazici et al., 2010). In the present work, the activation energy derived in peakshape method (Kundu et al., 2021b) lies within the range from 0.948 to 0.936 eV when a is varied from −2 to 2.

6. Concluding remarks

In this work we have solved the TL equations in OTOR model considering TDFF. Analytical expressions for peak maxima condition using Lambert-W function and Wright ω function in OTOR model are presented. A new approach for an analytical evaluation of the extended temperature integral of the form $\int_{T_i}^{T_f} T^a e^{-\frac{E}{kT}} dT$ is described and it can be computationally realized in a simple manner. It has become possible to generate a particular TL peak for different values of temperature exponent a lying within the range $-2 \leqslant a \leqslant 2$ by tuning other relevant parameters. The activation energies are derived from the TL

curves using two different versions of peakshape method. The error incurred in activation energy due to the approximation of temperature independent frequency factor is also reported quantitatively. The error in activation energy becomes significant if the value of $\frac{E}{kT_m}$ goes below 20. We have also been able to simulate a sample IMTS peak for different values of a to check the validity of the present method and a detailed analysis in this line is in progress. The overall outcome of the present study is quite encouraging and expected to be useful in future research in the backdrop of recent advancements in experimental as well as computational techniques.

Declaration of competing interest

The authors declare that they have no known competing financial interests or personal relationships that could have appeared to influence the work reported in this paper.

References

Aramu, F., Brovetto, P., Rucci, A., 1966. Activation energy in the NaCl thermoluminescence. Phys. Lett. 23 (5), 308–309.

Bemski, G., 1958. Recombination properties of gold in silicon. Phys. Rev. 111 (6), 1515–1518.

Bhattacharya, M., Deb, N., Msezane, A., Mazumdar, P., 2001. On the thermoluminescence glow curve deconvolution functions for different orders of kinetics. Phys. Status Solidi (A) 185 (2), 291–299.

Bhattacharya, M., Singh, W.S., Mazumdar, P., 2000. Determination of the temperature exponent for the case of the temperature-dependent frequency factor in thermoluminescence. Can. J. Phys. 78 (4), 253–260.

Bosacchi, A., Franchi, S., Bosacchi, B., 1974. Thermoluminescence and continuous distributions of traps. Phys. Rev. B 10 (12), 5235–5238.

Bube, R.H., 1960. Photoconductivity of Solids. Wiley, New York.

Chen, R., 1969a. Glow curves with general order kinetics. J. Electrochem. Soc. 116, 1254–1257.

Chen, R., 1969b. On the calculation of activation energies and frequency factors from glow curves. J. Appl. Phys. 40, 570–585.

Chen, R., 1970. On the computation of the generalized integral in glow curve theory. J. Comput. Phys. 6 (2), 314–316.

Chen, R., Kirsh, Y., 1981. Analysis of Thermally Stimulated Processes. Pergamon Press, Oxford.

Corless, R.M., Jeffrey, D.J., 2002. The Wright ω function. In: Artificial Intelligence, Automated Reasoning, and Symbolic Computation. Springer, pp. 76–89.

Corless, R.M., Jeffrey, D.J., Knuth, D.E., 1997. A sequence of series for the Lambert W function. In: Proceedings of the 1997 International Symposium on Symbolic and Algebraic Computation. pp. 197–204.

Dussel, G.A., Bube, R.H., 1967. Theory of thermally stimulated conductivity in a previously photoexcited crystal. Phys. Rev. 155 (3), 764–779.

Fleming, R., 1990. Activation energies and temperature-dependent frequency factors in thermally stimulated luminescence. J. Phys. D: Appl. Phys. 23 (7), 950–954.

Gartia, R., Singh, S.D., Subodh, T., Singh, T., Mazumdar, P., 1992. Determination of the activation energy of a thermally stimulated luminescence peak for the case of a temperature-dependent frequency factor. J. Phys. D: Appl. Phys. 25 (3), 530–534.

Gorbachev, V., 1976. Algorism for the solution of the exponential integral in non-isothermal kinetics at linear heating. J. Thermal Anal. Calorim. 10 (3), 447–449.

Graham, R.L., Knuth, D.E., Patashnik, O., Liu, S., 1994. Concrete mathematics: a foundation for computer science, 2nd ed. Addison-Wesley Publishing Company, Reading, USA.

Halperin, A., Braner, A.A., 1960. Evaluation of thermal activation energies from glow curves. Phys. Rev. 117, 408–415.

Ingraham, T.R., Marier, P., 1964. Activation energy calculation from a linearly-increasing-temperature experiment. Can. J. Chem. Eng. 42 (4), 161–163.

Karmakar, M., Sarkar, B., Azharuddin, S., Mazumdar, P., Singh, S.D., Singh, W.S., Bhattacharya, M., 2010. On the temperature dependent frequency factor in thermoluminescence. Indian J. Phys. 84 (5), 529–537.

Keating, P.N., 1961. Thermally stimulated emission and conductivity peaks in the case of temperature dependent trapping cross sections. Proc. Phys. Soc. 78, 1408–1415.

Kitis, G., Vlachos, N., 2013. General semi-analytical expressions for TL, OSL and other luminescence stimulation modes derived from the OTOR model using the Lambert W-function. Radiat. Meas. 48, 47–54.

Kundu, M., Bhattacharyya, S., Karmakar, M., Majumdar, P.S., 2021a. Three-point area method for thermoluminescence glow curve analysis and its application to the glow peak of $K_2SrP_2O_7 : Pr$. Radiat. Prot. Dosim. 193, 247–258.

Kundu, M., Chakrabarty, S., Bhattacharyya, S., Majumdar, P.S., 2021b. Reappraisal of peak shape method based on average geometrical symmetry factor and its application to thermoluminescence glow curves. Phys. Status Solidi (B) 258 (11), 2100277.

Lax, M., 1960. Cascade capture of electrons in solids. Phys. Rev. 119 (5), 1502–1523.

Lewandowski, A., McKeever, S., 1991. Generalized description of thermally stimulated processes without the quasiequilibrium approximation. Phys. Rev. B 43 (10), 8163–8178.

Lovedy Singh, L., 2020. Formulation of OTOR differential equation for thermoluminescence using temperature dependent frequency factor. Nucl. Instrum. Methods Phys. Res. B 474, 63–67.

Mott, N.F., Gurney, R.W., 1940. Electronic processes in ionic crystals. University press, oxford.

Petty, H.R., Arakawa, E.T., Baird, J.K., 1977. Methods to determine the temperature dependence of the pre-exponential factor of the Arrhenius equation from thermogravimetric data. J. Therm. Anal. 11 (3), 417–422.

Salzmann, D., 1998. Atomic Physics in Hot Plasmas. Oxford University Press.

Shambhunath Singh, W., Bhattacharya, M., Dorendrajit Singh, S., Mazumdar, P., 2000. Activation energies and temperature dependent frequency factors in thermoluminescence recorded with hyperbolic heating scheme. Phys. Status Solidi (A) 179 (1), 265–273.

Simmons, J., Taylor, G., 1971. Nonequilibrium steady-state statistics and associated effects for insulators and semiconductors containing an arbitrary distribution of traps. Phys. Rev. B 4 (2), 502–511.

Singh, L.L., Gartia, R., 2013. Theoretical derivation of a simplified form of the OTOR/GOT differential equation. Radiat. Meas. 59, 160–164.

Sunta, C.M., 2014. Unraveling Thermoluminescence; Springer Series in Materials Science, Vol. 202. Springer India, New Delhi.

Yazici, A.N., Seyyidoğlu, S., Toktamiş, H., Yilmaz, A., 2010. Thermoluminescent properties of $Sr_2P_2O_7$ doped with copper and some rare earth elements. J. Lumin. 130, 1744–1749.

Nuclear Instruments and Methods in Physics Research B 542 (2023) 214–222

Contents lists available at ScienceDirect

Nuclear Inst. and Methods in Physics Research, B

journal homepage: www.elsevier.com/locate/nimb

Estimation of activation energy using skewness of TL data as symmetry parameter in peak shape method

M. Kundu [a,b], S. Chakrabarty [c], S. Bhattacharyya [a,*], P.S. Majumdar [c]

[a] Department of Physics, Jadavpur University, Kolkata 700032, India
[b] Sadhanpur Uludanga Tulsiram High School (H.S), Amdanga, 24 PGS (N) 743221, India
[c] Department of Physics, Acharya Prafulla Chandra College, New Barrackpore, Kolkata 700131, India

ARTICLE INFO

Keywords:
Thermoluminescence
Activation energy
Peak shape method
Skewness
OTOR model

ABSTRACT

The retrapping and recombination mechanism of charge carriers in a thermoluminescence (TL) process governs the shape of a glow curve. In peak shape method the shape of a glow curve is exploited through various symmetry parameters to estimate activation energy. In statistical sense, skewness is a measure of distribution asymmetry of a dataset and hence may be useful to reflect the shape of a TL curve through its asymmetry. In this work, we investigate the applicability of skewness as a symmetry parameter and propose a new set of peak shape relations in terms of skewness of the data to extract activation energy from an isolated TL peak. The applicability of present method is verified by employing it to the TL peaks simulated in General Order Kinetics (GOK) and One Trap One Recombination centre (OTOR) equations. The present method yields consistent results for all the glow curves except for highly saturated cases with heavy retrapping. This limitation is investigated by studying the dependence of skewness on the ratio of retrapping to recombination probabilities. Finally, the present peak shape formulae are tried on experimental TL curves reported in literature and the results are quite satisfactory. The present peak shape coefficients are listed explicitly so that they can be used to estimate activation energy using skewness of isolated peaks deconvoluted from experimental TL data.

1. Introduction

A thermoluminescence (TL) glow curve is obtained by plotting the TL signal intensity as a function of temperature during the heating stage of a previously irradiated thermoluminescent material. An analytical expression of TL intensity as a function of temperature can be formulated using General Order Kinetics (GOK) equation [1] where the trapping parameters *viz.* activation energy (E), frequency factor (s) and order of kinetics (b) are used explicitly. A TL curve with $b = 1$ is known as first order [2,3] glow curve and $b = 2$ corresponds to the second order kinetics [4]. For other values of b, TL glow curves of general order are obtained. Other band theory based models like One Trap One Recombination center (OTOR), Interactive Multi Trap System (IMTS) *etc.* are also adopted to describe TL process. Glow curve analysis has been one of the widely used tools to estimate the trapping parameters in TL materials. Various methods [5–7] like Initial Rise [4,8,9], Fractional Glow Technique [10], Various Heating Rates [11], Area method [12,13], Curve Fitting [14,15] and Computerized Glow Curve Deconvolution (CGCD) [16–18], Peak shape method *etc.* have been developed for analyzing glow curves to estimate trapping parameters. All of these methods can be used to estimate activation energy but only a few of them can extract the order of kinetics 'b' (in GOK model). Different variants of area methods [12,13], Curve fitting methods [14,15] and Computerized Glow Curve Deconvolution (CGCD) [16–18] can be applied to estimate $\}b'$ from a TL peak. An empirical technique was reported by Singh et al. [19] using a modified peak shape method to estimate $\}b'$ in an indirect manner. Apart from these, Kitis and Pagonis [20] and later Kundu et al. [21] reported other empirical techniques to estimate $\}b'$ using the symmetry factor of TL curves.

The peak shape method is one of the most extensively used methods to estimate activation energy from a well isolated single TL peak where different shape parameters of glow curve are used. The first ever peak shape formula was proposed by Grossweiner [22] to calculate E from a first order TL peak. After incorporating the modification proposed by Dussel and Bube [23] the formula is expressed as

$$E = 1.41\left(\frac{kT_mT_1}{\tau}\right) \tag{1}$$

Here k is Boltzmann constant, T_m is the peak temperature, T_1 is the half intensity temperature on rising side of the curve and $\tau = T_m - T_1$ is a

* Corresponding author.
E-mail addresses: sukhamoy.b@gmail.com, sukhamoyb.physics@jadavpuruniversity.in (S. Bhattacharyya).

https://doi.org/10.1016/j.nimb.2023.07.006
Received 31 May 2023; Received in revised form 5 July 2023; Accepted 11 July 2023
Available online 24 July 2023

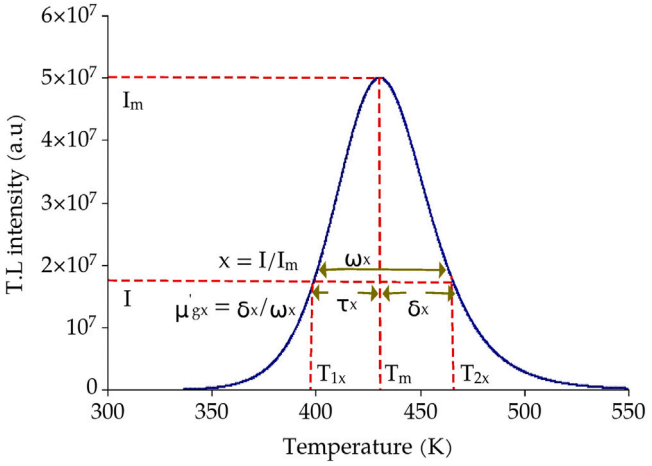

Fig. 1. A sample TL peak showing the peak shape parameters (τ_x, δ_x, ω_x) at arbitrary fractional intensity $x = \frac{I}{I_m}$. For $x = \frac{1}{2}$, τ_x, δ_x, ω_x are denoted by τ, δ, ω respectively.

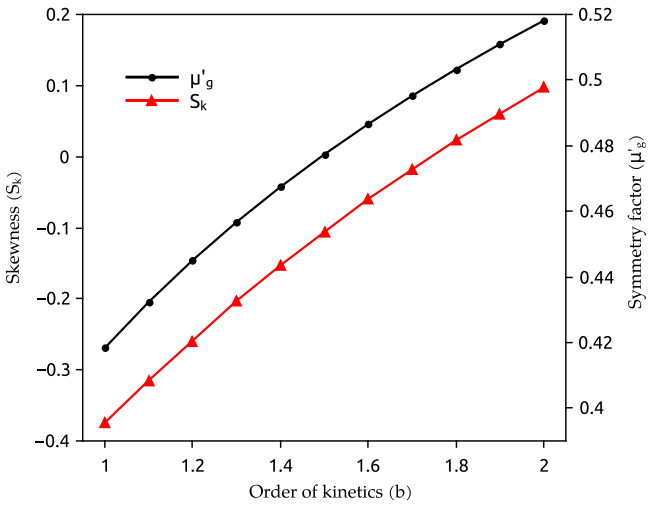

Fig. 2. Variation of skewness (S_k) and geometric symmetry factor (μ'_g) with order of kinetics (b).

peak shape parameter (see Fig. 1). Later, Lushchik [24] gave peak shape formulae for both first and second order peaks using another peak shape parameter $\delta = T_2 - T_m$ where T_2 is the half intensity temperature on the falling side of the curve (see Fig. 1). The peak shape relations of Luschik [24] were modified by Chen [25] and can be expressed as

$$\begin{aligned} E &= 0.976\left(\frac{kT_m^2}{\delta}\right) && \text{for first order} \\ &= 1.71\left(\frac{kT_m^2}{\delta}\right) && \text{for second order} \end{aligned} \tag{2}$$

Halperin and Braner [26] proposed another variant of peak shape relation for first order curves which can be written, after considering the numerical correction suggested by Chen [25], as

$$E = 1.52\left(\frac{kT_m^2}{\tau}\right) - 1.58\,(2kT_m) \tag{3}$$

In formulating Eq. (3), the geometric symmetry factor (μ'_g) was used where $\mu'_g = \frac{\delta}{\omega}$ and $\omega = T_2 - T_1$ (see Fig. 1). After revisiting the previous peak shape formulae [24,26], Chen [25,27] proposed the peak shape relations using τ, δ and ω which can be summarized as

$$E_\alpha = C_\alpha \frac{kT_m^2}{\alpha} - D_\alpha(2kT_m) \tag{4}$$

Here α stands for the peak shape parameters τ, δ or ω. The peak shape coefficients (C_α, D_α) were estimated numerically and expressed in terms of μ'_g.

In later decades, several attempts were made to develop different variants of peak shape method. Christodoulides [28] proposed an alternative set of peak shape relations for first order ($b = 1$) peaks at different fractional intensities. Mazumder et al. [29] developed the peak shape formula analogous to those of Christodoulides [28] for non-first order ($b \neq 1$) TL peaks. The peak shape method of Chen [27] was revisited by Gartia et al. [30] by expressing the peak shape coefficients as a quadratic function of b. Kitis and Pagonis [20] used some pseudo-constants to express the peak shape coefficients in terms of b. The peak shape method was also addressed in mixed order kinetics (MOK) model by Kitis et al. [31] where the integral symmetry factor was used. In a recent work, Kundu et al. [21] proposed a set of peak shape relations to estimate E at arbitrary fractional intensity ($x = \frac{I}{I_m}$, see Fig. 1) where average symmetry factor ($\langle\mu'_g\rangle$) was used to develop peak shape coefficients considering the dependence of μ'_g on E and s along with b.

The peak shape relations based on μ'_g are quite popular in use. In experimental scenario, μ'_g can be estimated easily from a TL peak as it involves only three points on a glow curve *viz.* (T_{1x}, I_{1x}), (T_m, I_m), (T_{2x}, I_{2x}) (see Fig. 1). For obvious reasons, μ'_g varies at different fractional intensities (Fig. 1) and all the choices of x may not yield results with same accuracy [13,21]. The primary motivation of the work is to develop a peak shape method using a symmetry parameter which is unique to a set of TL data and can involve the whole data set instead of choosing few particular points. The nature of symmetry of TL curve has direct dependence on the retrapping–recombination mechanism in a TL material at the heating stage of TL process. This retrapping–recombination mechanism is reflected through b in GOK model and through R ($= \frac{A_n}{A_h}$) in OTOR model. Here A_n and A_h are the probabilities of retrapping and recombination respectively. The dependence of the shape of a glow curve on b (or R) can be reflected through the skewness which is unique for a particular dataset. In fact, the variations of skewness and μ'_g as a function b exhibit almost similar nature as is shown in Fig. 2. Hence, as a measure of asymmetry, skewness can be a useful parameter to represent the shape of a TL curve. The calculation of skewness involves the entire TL dataset and thus avoids the limitation of choosing particular points or portion of the curve.

In the present study we have carried out a thorough investigation on the shape and nature of asymmetry of glow curves by studying their skewness (S_k). Within the perview of GOK framework glow curves are simulated by varying E, s and b and the variation of S_k with respect to these parameters are studied in detail. We note that variation of S_k with E and s is studied through the parameter $u_m = \frac{E}{kT_m}$. In OTOR model, S_k is estimated from glow curves simulated for different values of R and trap filling ratio (f). The heavy retrapping cases ($R > 1$) are also considered exhaustively. A new set of peak shape relations similar to Eq. (4) are developed for τ_x, δ_x and ω_x where the peak shape coefficients are formulated in terms of skewness of the TL data. The present peak shape relations are applied to extract E from TL peaks simulated in GOK and OTOR models. Finally, the present method is successfully employed to estimate E from reported experimental TL glow curves of 110°C peak of quartz [32,33] and peaks of MgO [34].

2. Methodology

Before we proceed, we summarize the basic mathematical expressions used here for TL glow curve generation. In OTOR model [7,26] the relevant differential equations are

$$\frac{dn_c}{dt} = nse^{-\frac{E}{kT}} - A_n(N-n)n_c - A_h n_c n_h \tag{5}$$

$$\frac{dn}{dt} = -nse^{-\frac{E}{kT}} + A_n(N-n)n_c \tag{6}$$

$$I = -\frac{dn_h}{dt} = A_h n_c n_h \tag{7}$$

Here n_c = the concentration of electrons at conduction band, n = concentration of trapped electrons, n_h = concentration of holes at recombination centre, N = concentration of available trap in the forbidden energy gap. s = frequency factor related to trap, A_n = probability of retrapping, A_h = probability of recombination and T = absolute temperature at time t. The charge neutrality condition is $n_h = n + n_c$. Considering quasi-equilibrium (QE) approximations which are given by $\left|\frac{dn_c}{dt}\right| \ll \left|\frac{dn}{dt}\right|$ and $n_c \ll n$, the TL intensity in OTOR model is obtained by solving Eqs. (5)–(7) and expressed as

$$I(t) \simeq -\frac{dn}{dt} = \frac{n^2 s e^{-\frac{E}{kT}}}{n(1-R)+NR} \tag{8}$$

where $R = \frac{A_n}{A_h}$. To simulate $I-T$ data in linear heating scheme (*i.e.* $T = T_0 + \beta t$; T_0 being the temperature at $t = 0$ and β is the heating rate) Eq. (8) can be solved either numerically or analytically in terms of Lambert-W function [35] as

$$I = \frac{sNR\exp\left(-\frac{E}{kT}\right)}{(1-R)^2\left[W[e^{z_1}] + W[e^{z_1}]^2\right]} \quad \text{for} \quad R<1 \tag{9}$$

$$= \frac{sNR\exp\left(-\frac{E}{kT}\right)}{(1-R)^2\left[W[-1,-e^{-z_2}]^2 + W[-1,-e^{z_2}]\right]} \quad \text{for} \quad R>1 \tag{10}$$

where $z_1 = \frac{1}{c} - \ln c + \frac{s}{(1-R)\beta}\int_{T_0}^{T}\exp\left(-\frac{E}{kT'}\right)dT'$

$$z_2 = \frac{1}{|c|} - \ln(|c|) + \frac{s}{(1-R)\beta}\int_{T_0}^{T}\exp\left(-\frac{E}{kT'}\right)dT'$$

and $c = \frac{n_0(1-R)}{NR}$

Here n_0 is the initial concentration of trapped electrons. Eq. (8) reduces to the first order and the second order kinetic equations for $R = 0$ and 1 respectively. The general order kinetics (GOK) equation for TL intensity is given by

$$I(T) = sn_0 e^{-\frac{E}{kT}}\exp\left[-\frac{s}{\beta}\int_{T_0}^{T} e^{-\frac{E}{kT'}}dT'\right] \quad \text{for } b=1 \tag{11}$$

$$= sn_0 e^{-\frac{E}{kT}}\left[\frac{(b-1)s}{\beta}\int_{T_0}^{T} e^{-\frac{E}{kT'}}dT' + 1\right]^{-\frac{b}{b-1}} \quad \text{for } b\neq 1 \tag{12}$$

The fractional intensity (x) can be expressed [36] using Eqs. (11) and (12) as

$$x = \frac{I(T)}{I_m}$$

$$= \exp\left[1 - \frac{2}{u_m} + u_m\left(1-\frac{T_m}{T}\right) - \left(\frac{T}{T_m}\right)^2\left(1-\frac{2kT}{E}\right)\right.$$

$$\left.\times \exp\left[u_m\left(1-\frac{T_m}{T}\right)\right]\right] \quad \text{for } b=1$$

$$= b^{\frac{b}{b-1}}\left[1+(b-1)\left[\frac{2}{u_m} + \left(\frac{T}{T_m}\right)^2\left(1-\frac{2kT}{E}\right)\right.\right.$$

$$\left.\left.\times \exp\left(u_m\left(1-\frac{T_m}{T}\right)\right)\right]\right]^{\frac{-b}{b-1}} \exp\left[u_m\left(1-\frac{T_m}{T}\right)\right] \quad \text{for } b\neq 1 \tag{13}$$

2.1. Skewness as peak shape parameter for TL study

Skewness is a statistical parameter that represents the extent of asymmetry in a set of recorded data. When the frequency distribution of the data set is symmetric, skewness is zero. A longer tail toward left in frequency distribution represents negative skewness while the opposite condition yields positive skewness. Skewness of a set of TL data estimated from Pearson's first measure [37] can be given by

$$S_k = \frac{\text{mean} - \text{mode}}{\text{standard deviation}} = \frac{\overline{T} - T_m}{\sigma} \tag{14}$$

$$\text{where,} \quad \text{mean} = \overline{T} = \frac{\sum_j T_j I_j}{\sum_j I_j}$$

$$\text{mode} = T_m = \text{Peak temperature}$$

$$\text{standard deviation} = \sigma = \sqrt{\frac{\sum_j \left(T_j - \overline{T}\right)^2 I_j}{\sum_j I_j}}$$

Here I_j can be considered as the equivalent frequency of occurrence of the variable T_j.

It is to mention that skewness is measured by considering the departure of data from the central tendency, *i.e.*, from mean temperature in the present case. However the mean temperature which is a weighted average, has a dependence on the intensity values (Eq. (14)). Though the temperature is increased systematically to simulate a TL curve, the mean temperature depends on the data distribution in 'I – T' plot and not on the initial and the final temperatures only. The 'I – T' data distribution depends on system properties. For example if we generate the 'I – T' data with input parameters E = 1 eV, s = 10^{12} s^{-1}, β = 1 K/s between the temperatures T_i = 300 K and T_f = 500 K, then the mean temperature is 379 K for first order TL peaks and 386 K for second order peak respectively. Clearly the mean values differ as the charge dynamics in the system changes and they are in general not equal to the arithmetic mean which is 400 K in the example given above, irrespective of order of kinetics.

The skewness of a TL dataset can be calculated instantly using Eq. (14) by writing a simple computer code where the $I-T$ data are fed as input values. In Fig. 3, a schematic diagram related to the calculation of skewness from a TL data set is given. A TL peak with negative skewness is shown in Fig. 3(a) where the peak is simulated in OTOR model with $R = 0$. The blue vertical dotted line indicates the position of mean whereas the vertical solid black line indicates the mode (*i.e.* T_m) of TL data. The two vertical red lines indicate the range of temperature representing standard deviation. It is seen from Fig. 3(a) that the mean is on the left to the mode which corresponds to negative skewness. In Fig. 3(b), another TL peak simulated in OTOR model with $R = 1$ is shown. It is evident from Fig. 3(b) that the mean is on the right to the mode which is the signature of positive skewness. It is to mention that skewness is associated to a particular data set, therefore S_k of a TL dataset depends on the initial and final data points and also on stepsize (ΔT). To have an accurate estimation of skewness of a glow curve, it is imperative to include as many datapoints as possible. In an experimental scenario it is sometimes difficult to get clean data at low intensity regions due to presence of various noise signals. Throughout the work we have calculated S_k considering all the data points for which $I(T) \geq \frac{I_m}{10}$. The stepsize for simulation of TL peaks is $\Delta T = 0.1$K. We note that $\overline{T}$ does not significantly depend on the size of ΔT.

The shape of a TL curve depends on the retrapping and recombination kinetics represented through the empirical parameter b (or R). However, small dependence on E and s is also observed [21,27]. Since in case of a TL curve, S_k relates to the shape and symmetry, it is expected to have some dependence on b as well as on E and s. To have a close insight in this context we have carried out an exhaustive study with a large number of TL peaks. Glow curves are simulated in systematic manner using Eq. (13) by varying b in step 0.1 within the range $1.0 \leq b \leq 2.0$. For each b, E is varied from 0.2 to 2.0 eV in step 0.1, whereas for each set of b and E, s is chosen in such a way that

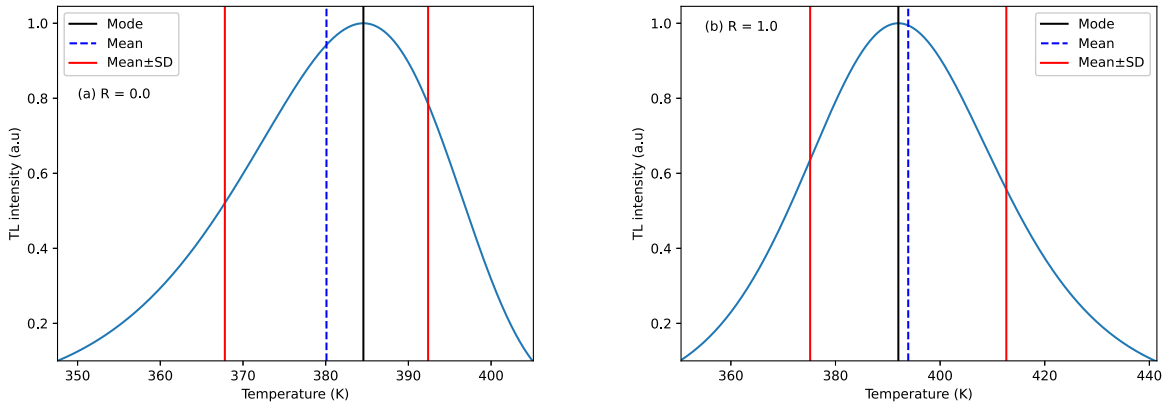

Fig. 3. Schematic diagram to calculate S_k of a TL peak generated in OTOR model (a) for $R = 0$ (b) for $R = 1$. The input parameters are: $E = 1$ eV, $s = 10^{12}$ s^{-1}, $f = 0.5$.

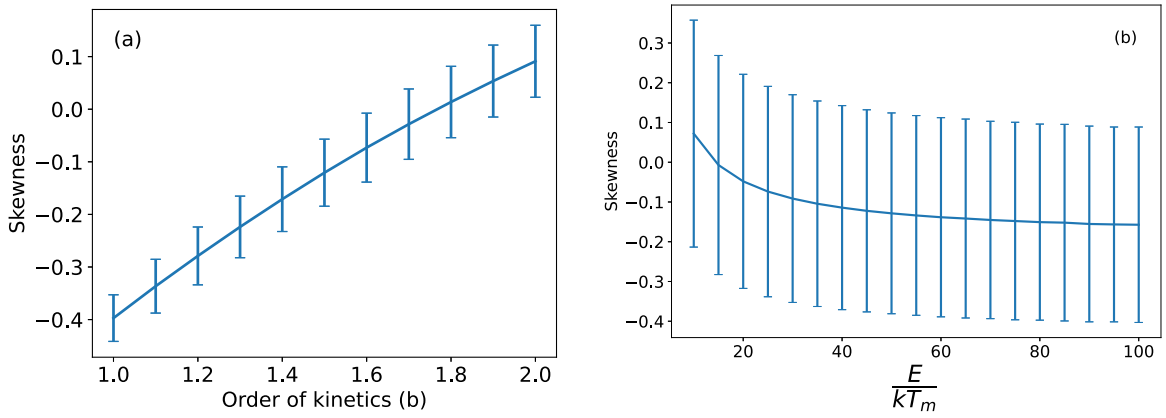

Fig. 4. Variation of S_k of TL peak with: (a) b and (b) $u_m = \frac{E}{kT_m}$.

u_m varies from 10 to 100 in step 5. We estimate S_k of the synthetic glow peaks using Eq. (14) and the results are presented in Fig. 4. From Fig. 4(a) it is seen that S_k varies with b in a systematic manner. As b increases S_k also increases gradually from –ve to +ve values. For a fixed value of b, the possible variation in S_k due to change in u_m is also studied and the results are depicted in Fig. 4(a) through vertical error bars. Dependence of S_k on u_m is presented in Fig. 4(b) from which it appears that S_k decreases by small amount from +ve to –ve value as u_m increases. However, for $u_m > 50$ the change in S_k is almost negligible. For a fixed u_m, significant variation in S_k is observed due to variation in b and presented through vertical error bars in Fig. 4(b).

2.2. Determination of Peak Shape coefficients using skewness

The above study reveals that S_k of a TL peak for a particular b cannot be defined specifically because of the simultaneous dependence of S_k on u_m. However, the shape of a TL curve has direct dependence on b and hence, to use S_k as a symmetry parameter for glow curve analysis in peak shape method, it is required to establish a one-to-one correspondence between b and S_k. For this purpose, we propose to use the average value of skewness *i.e.* $\langle S_k \rangle$ to determine peak shape coefficients where the averaging is done over a range of u_m ($u_{m_i} \le u_m \le u_{m_f}$) for a fixed value of b. Therefore,

$$\langle S_k \rangle = \frac{1}{u_{m_f} - u_{m_i}} \int_{u_{m_i}}^{u_{m_f}} S_k \, du_m \tag{15}$$

Retaining the forms of the original peak shape relations (Eq. (4)) as suggested by Chen [27], the new peak-shape relations are given by

$$E_{\alpha_x} = C_{\alpha_x} \frac{kT_m^2}{\alpha_x} - D_{\alpha_x}(2kT_m) \tag{16}$$

where C_{α_x} and D_{α_x} are peak shape coefficients estimated at the fractional intensity x and α_x stands for $\tau_x, \delta_x, \omega_x$ (see Fig. 1). We express C_{α_x} and D_{α_x} in a linear relation with S_k as

$$C_{\alpha_x} = C_{1\alpha_x} S_k + C_{2\alpha_x} \tag{17}$$

$$D_{\alpha_x} = D_{1\alpha_x} S_k + D_{2\alpha_x} \tag{18}$$

Now we proceed to determine $C_{1\alpha_x}$, $C_{2\alpha_x}$, $D_{1\alpha_x}$, $D_{2\alpha_x}$ in Eqs. (17) and (18) using $\langle S_k \rangle$. For a particular value of b we generate TL peaks by varying u_m. For calculation of S_k, we consider all the datapoints for which $I(T) \ge \frac{I_m}{10}$ where the stepsize is $\Delta T = 0.1$ K. From each of these curves S_k, u_m and $\frac{u_p u_q}{u_m |u_p - u_q|}$ are estimated. Here u_p and u_q are any two of u_{1x}, u_m and u_{2x} where u_{1x}, u_{2x} are similar to u_m calculated at the temperatures T_{1x}, T_{2x} respectively (see Fig. 1). For the three peak shape parameters $\tau_x, \delta_x, \omega_x$, we mention that

(i) If $u_p = u_{1x}$ and $u_q = u_m$, in Eq. (16) $\alpha_x = \tau_x$ is to be considered.
(ii) $u_p = u_m$ and $u_q = u_{2x}$ are to be considered to obtain the peak shape relation using δ_x.
(iii) Peak shape coefficients for ω_x are obtained when $u_p = u_{1x}$ and $u_q = u_{2x}$.

For a particular value of b, Eq. (15) is used to calculate $\langle S_k \rangle$ from the set of S_k values obtained from each curve corresponding to different values of u_m. From $\left(u_m, \frac{u_p u_q}{u_m |u_p - u_q|}\right)$ data of all the curves generated for a particular b, a linear relation between u_m and $\frac{u_p u_q}{u_m |u_p - u_q|}$ can be fitted to obtain $C_{\alpha_x}, D_{\alpha_x}$ in Eq. (16) for that particular b. In this way we obtain C_{α_x}, D_{α_x}, $\langle S_k \rangle$ corresponding to a particular b. Now, by varying

Table 1
Linear constants in Eqs. (17), (18) for the determination of peak shape coefficients in Eq. (16) estimated at different values of x.

x	α	$C_{1\alpha_x}$	$C_{2\alpha_x}$	$D_{1\alpha_x}$	$D_{2\alpha_x}$
1/4	τ	0.7627	2.5570	0.8984	1.7609
	δ	2.9453	2.3730	0.3309	0.0784
	ω	3.6983	4.9219	0.1250	0.8806
1/2	τ	0.6591	1.6971	0.9685	1.4354
	δ	1.7186	1.6064	0.6711	0.3318
	ω	2.3753	3.3012	0.5931	0.8689
2/3	τ	0.5652	1.2603	0.9985	1.2783
	δ	1.1760	1.2075	0.8022	0.4608
	ω	1.7402	2.4669	0.7719	0.8620

b in suitable stepsize and following the procedure discussed above, we obtain the sets of $\left[C_{\alpha_x}, D_{\alpha_x}, \langle S_k \rangle\right]$ corresponding to different values of b. The coefficients $C_{1\alpha_x}, C_{2\alpha_x}, D_{1\alpha_x}, D_{2\alpha_x}$ (Eqs. (17) and (18)) are obtained from a linear fit of C_{α_x} and D_{α_x} with $\langle S_k \rangle$.

It is important to note that the role of average skewness in the present work is only to estimate the coefficients C_{α_x} and D_{α_x}. For practical purposes the skewness of a TL dataset can be used directly in Eqs. (17) and (18). The required coefficients are given later in Table 1, 'Results and discussions' section.

3. Results and discussions

The present peak shape formulae provide an opportunity to estimate E at different fractional intensities of the same TL curve using τ_x, δ_x, ω_x and by estimating skewness of the TL data. Thus the peak shape coefficients are to be determined for various x. For generating TL curves, we considered b within the range $0.7 \leqslant b \leqslant 2.5$ in step $\Delta b = 0.1$. For each value of b, we have taken E (eV) in step 0.1 within the range $0.2 \leqslant E \leqslant 2.0$ and varied s (in s^{-1}) in a wide range so that u_m lies within the limits $10 \leqslant u_m \leqslant 100$. In the present work we have increased u_m systematically in step of 5 for simulating glow curves. For a fixed value of b, S_k is calculated for simulated TL data corresponding to each u_m value.

3.1. Peak shape coefficients at different fractional intensities

In Table 1 we have listed the values of $C_{1\alpha_x}$, $C_{2\alpha_x}$, $D_{1\alpha_x}$, $D_{2\alpha_x}$ (Eqs. (17), (18)) to determine C_{α_x}, D_{α_x} (Eq. (16)) corresponding to different fractional intensities using the shape parameters τ_x, δ_x and ω_x. To check the applicability of the present method we have applied the peak shape coefficients (C_{α_x}, D_{α_x}) to evaluate E from TL curves generated in GOK and OTOR models and finally applied them on some experimental TL peaks. We note that by adopting the present methodology it is possible to determine peak shape coefficients for any reasonable value of x. Moreover, in Table 1, the coefficients at $x = \frac{1}{4}, \frac{1}{2}, \frac{2}{3}$ are listed that can be used directly on simulated as well as experimental glow curves to extract E using skewness of the TL data.

3.2. Application to TL peaks simulated in GOK model

TL glow curves in GOK model are generated by using equations ((11), (12)) in linear heating scheme where the heating rate (β) is 1 K s^{-1} and the input values of activation energy (E_{in}) and frequency factor (s_{in}) are 1 eV and 10^{12} s^{-1} respectively. The coefficients given in Table 1 are used to estimate the output values $E_{\tau x}$, $E_{\delta x}$ and $E_{\omega x}$. The results are given in Table 2 where first order, second order and general order kinetics are taken into account. It is evident from Table 2 that the extracted values of activation energy are quite consistent with the input value $E_{in} = 1$ eV. Table 2 also reveals that $E_{\tau x}$ values show comparatively better agreement with E_{in} whereas $E_{\delta x}$ shows maximum deviation.

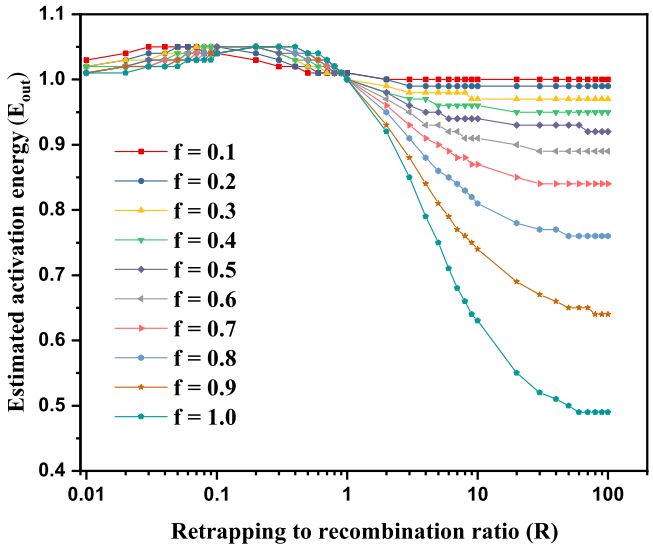

Fig. 5. Estimated values of activation energy plotted against R measured at fractional intensity $x = 0.5$. Here $E_{in} = 1$ eV, $s_{in} = 10^{12}$ s^{-1} and $\beta = 1$ K s^{-1}.

3.3. Application to TL peaks simulated in OTOR model

In the next phase, we investigate the applicability of the present peak shape formulae in case of OTOR glow curves. For curve simulation, the input values of activation energy and frequency factor are taken in the range $0.5 \leqslant E_{in} \leqslant 1.5$ eV and $10^7 \leqslant s_{in} \leqslant 10^{13}$ s^{-1} respectively. The filling ratio $f = \frac{n_0}{N}$ is taken from 0.1 to 1 to cover almost the entire range of trap saturation. The ratio of retrapping to recombination probabilities (R) is considered by varying in step $\Delta R = 0.01$ when $0 \leq R \leq 1$ and in step $\Delta R = 1$ when $1 < R \leq 100$ to cover low to heavy retrapping situations during heating stage.

In Table 3, $E_{\tau x}$, $E_{\delta x}$ and $E_{\omega x}$ extracted from TL peaks generated for some selected values of f and R with input values $E_{in} = 1$ eV and $s_{in} = 10^{12}$ s^{-1} are given. It is observed that $E_{\tau x}$ values are more in agreement with E_{in} whereas $E_{\delta x}$ values show maximum departure, similar to GOK curves. The results are consistent for the TL peaks having $0 \leqslant R \leqslant 1$. As trap saturation increases, the error in activation energy for $R = 0.5$ goes up to 6% and 11% when $E_{\tau x}$ and $E_{\delta x}$ are considered respectively. For $R > 1$, *i.e.* in case of heavy retrapping, $E_{\tau x}$, $E_{\delta x}$ and $E_{\omega x}$ yield acceptable values when f is quite small which corresponds to low-dose irradiation. In case of saturated or nearly saturated TL peaks (*i.e.* $f \simeq 1$) with heavy retrapping ($R > 1$), the output values of activation energy are quite away from the input value. Table 3 shows that even for $f = 0.5$ and $R = 10$, $E_{\tau x}$, $E_{\delta x}$ and $E_{\omega x}$ show deviation from E_{in} and are underestimated by as much as 10%. The results show that for $f = 1$ and $R = 10$, the version of peak shape method using skewness as a symmetry parameter does not work at all. This observation is consistent with earlier reports [21,38–40] on the limitation of peak shape methods in case of saturated TL peaks with heavy retrapping.

In Table 4 we have given a representative set of present results corresponding to some other values of input parameters. However, as output values of activation energy (E_{out}) we have presented $E_{\tau x}$ only. In Fig. 5 we have plotted $E_{\tau x}$ measured at $x = \frac{1}{2}$ against R for different filling ratios (f). Fig. 5 represents the data corresponding to $E_{in} = 1$eV and $s_{in} = 10^{12}$ used as input parameters, though similar variation of $E_{\tau x}$ is observed for other values of E_{in} and s_{in} with different x. Moreover, in all the cases, $E_{\delta x}$ and $E_{\omega x}$ also exhibit similar pattern. It is seen from Fig. 5 that the present method yields quite consistent values of activation energy (E_{out}) near $R = 0$ and 1 whereas, within the range $0 < R < 1$, the estimated activation energy is marginally overestimated. In heavy retrapping region ($R > 1$), the activation

Table 2
Values of $E_{\tau x}$, $E_{\delta x}$, $E_{\omega x}$ (eV) estimated using the present peak shape method from TL curves simulated in GOK model. Here $E_{in} = 1$ eV, $s_{in} = 10^{12}$ s^{-1} and $\beta = 1$ K s^{-1}.

b	T_m (K)	S_k	x	τ	δ	ω	$E_{\tau x}$	$E_{\delta x}$	$E_{\omega x}$
1	384.57	−0.3745	1/4	26.56	16.70	43.26	1.00	1.04	1.02
			1/2	17.36	12.48	29.84	1.01	1.03	1.02
			2/3	12.70	9.87	22.56	1.01	1.02	1.02
1.5	384.22	−0.1062	1/4	28.38	25.09	53.48	1.00	1.07	1.04
			1/2	19.03	17.38	36.41	1.01	1.05	1.03
			2/3	14.17	13.21	27.38	1.01	1.04	1.02
2	383.88	0.0973	1/4	29.75	33.24	62.99	1.00	1.02	1.01
			1/2	20.29	21.82	42.10	1.00	1.02	1.01
			2/3	15.29	16.13	31.42	1.01	1.01	1.01

Table 3
Activation energies $E_{\tau x}$, $E_{\delta x}$, $E_{\omega x}$ (eV) estimated using the present peak shape method from TL curves simulated in OTOR model. Here $E_{in} = 1$ eV, $s_{in} = 10^{12}$ s^{-1} and $\beta = 1$ K s^{-1}.

f	R	T_m (K)	S_k	x	τ	δ	ω	$E_{\tau x}$	$E_{\delta x}$	$E_{\omega x}$
0.1	0	384.57	−0.3633	1/4	26.56	16.70	43.26	1.01	1.06	1.03
				1/2	17.35	12.49	29.84	1.01	1.05	1.03
				2/3	12.70	9.88	22.58	1.01	1.04	1.02
	0.5	405.08	0.0900	1/4	32.60	36.03	68.63	1.01	1.04	1.03
				1/2	22.18	23.62	45.80	1.02	1.04	1.03
				2/3	16.70	17.48	34.18	1.02	1.04	1.03
	1	413.28	0.1052	1/4	34.19	38.51	72.70	1.01	1.03	1.02
				1/2	23.35	25.24	48.59	1.01	1.02	1.02
				2/3	17.62	18.67	36.29	1.01	1.02	1.01
	10	446.07	0.1250	1/4	39.87	46.04	85.91	1.00	1.02	1.01
				1/2	27.36	30.15	57.51	1.00	1.01	1.01
				2/3	20.70	22.27	42.97	1.00	1.01	1.00
0.5	0	384.57	−0.3633	1/4	26.56	16.70	43.26	1.01	1.06	1.03
				1/2	17.35	12.49	29.84	1.01	1.05	1.03
				2/3	12.70	9.88	22.58	1.01	1.04	1.02
	0.5	388.31	0.0395	1/4	29.27	30.33	59.60	1.03	1.08	1.06
				1/2	19.73	19.92	39.65	1.04	1.08	1.06
				2/3	14.76	14.80	29.56	1.05	1.08	1.06
	1	392.29	0.1006	1/4	30.99	34.71	65.70	1.00	1.02	1.02
				1/2	21.14	22.77	43.91	1.01	1.02	1.01
				2/3	15.95	16.85	32.80	1.01	1.02	1.01
	10	416.38	0.1676	1/4	37.46	45.77	83.23	0.94	0.93	0.93
				1/2	26.17	30.28	56.45	0.92	0.91	0.91
				2/3	20.02	22.43	42.45	0.91	0.90	0.90
1	0	384.57	−0.3633	1/4	26.56	16.7	43.26	1.01	1.06	1.03
				1/2	17.35	12.49	29.84	1.01	1.05	1.03
				2/3	12.70	9.88	22.58	1.01	1.04	1.02
	0.5	383.31	−0.0081	1/4	27.97	27.3	55.27	1.04	1.10	1.07
				1/2	18.71	18.03	36.74	1.06	1.11	1.09
				2/3	13.93	13.45	27.38	1.06	1.11	1.09
	1	383.88	0.0985	1/4	29.75	33.24	62.99	1.00	1.02	1.01
				1/2	20.29	21.81	42.10	1.00	1.02	1.01
				2/3	15.30	16.14	31.44	1.01	1.02	1.01
	10	400.09	0.0673	1/4	48.04	52.25	100.29	0.63	0.68	0.66
				1/2	34.94	35.82	70.76	0.59	0.64	0.62
				2/3	26.96	27.11	54.07	0.57	0.63	0.60

energy is quite consistent with E_{in} for low values of f (*i.e.* $f \leq 0.4$). It is also evident from Fig. 5 that for heavy retrapping cases ($R > 1$) the deviation of output values (E_{out}) from E_{in} grows higher as trap filling increases. Hence it may be said that skewness (S_k) can be used as a symmetry parameter in peak shape method to estimate activation energy (E) with the only limitation in cases of nearly saturated peaks with heavy retrapping, as is evident from Tables 3, 4 and Fig. 5.

To have a deeper insight on the limitation of peak shape relations for heavy retrapping cases, we have plotted in Fig. 6 the percentage error in activation energy $\delta E_{\tau_x}(\%)$ measured at $x = \frac{1}{2}$ with respect to f for different values of R. We observe that the error in E becomes significant for $R > 1$. To be precise, for $R > 1$, activation energy is underestimated and the magnitude of error gradually increases as f increases. For low filling ratios, (*i.e.* when $f \leq 0.4$) the present method works well even for $R > 1$ as $|\delta E_{\tau_x}|$ lie within 5%. The magnitude of error increases with increase in R also, however, Fig. 6 reveals that this error does not change much for $R > 50$.

We have performed a detailed study on S_k of TL peaks generated with various R and the results are shown in Fig. 7 for different values of filling ratio (f). It is found that for $0 \leqslant R \leqslant 1$, S_k increases gradually with R in a systematic manner for a fixed value of f. When R is fixed within this range, S_k decreases as f increases. The estimated values of S_k for all f are equal at $R = 1$. Fig. 7 shows that the pattern of variation of S_k changes remarkably beyond $R > 1$ where crossing of the plots takes place. For low values of f, S_k slowly increases with R in an almost well-behaved manner. For high values of f, this pattern becomes quite anomalous for $R > 1$ and the present peak shape method fails in such cases.

To validate the applicability of skewness as symmetry parameter in peak shape method we have compared the present results with some other variants of peak shape method [20,21,27]. The activation

Table 4
Activation energies estimated by present peak shape method from OTOR glow peaks simulated with different input parameters.

Input parameters				T_m	S_k	E_{out}		
E	s	f	R			$x=\frac{1}{4}$	$x=\frac{1}{2}$	$x=\frac{2}{3}$
0.5	10^7	0.1	0.1	314.76	0.0458	0.52	0.53	0.54
			10	387.87	0.1935	0.51	0.51	0.51
		0.9	0.1	306.08	−0.1933	0.52	0.53	0.53
			10	327.10	0.2356	0.38	0.36	0.34
	10^{13}	0.1	0.1	186.08	−0.0018	0.52	0.52	0.53
			10	210.92	0.1197	0.50	0.50	0.50
		0.9	0.1	182.81	−0.2351	0.51	0.52	0.52
			10	191.20	0.1319	0.37	0.35	0.34
1.5	10^7	0.1	0.1	896.07	0.0399	1.57	1.59	1.61
			10	1092.93	0.1843	1.51	1.52	1.52
		0.9	0.1	872.41	−0.1985	1.56	1.58	1.59
			10	930.14	0.2235	1.13	1.06	1.03
	10^{13}	0.1	0.1	540.36	−0.0043	1.55	1.57	1.58
			10	610.07	0.1159	1.49	1.49	1.49
		0.9	0.1	531.13	−0.2361	1.54	1.56	1.57
			10	554.83	0.1271	1.10	1.03	1.01

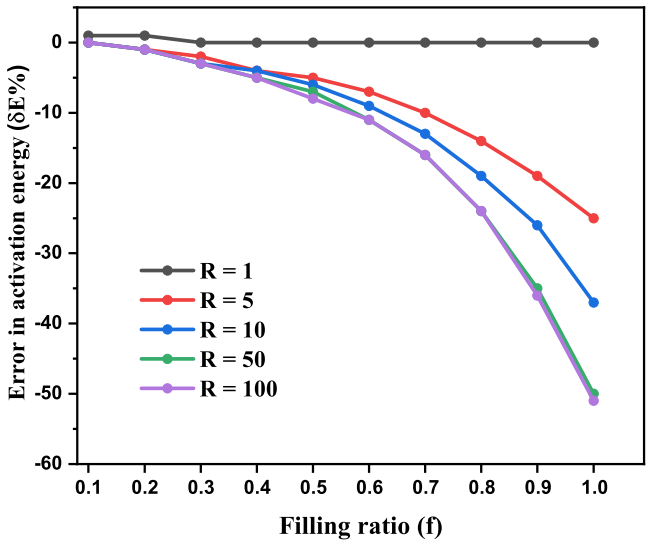

Fig. 6. Inherent error (δE%) plotted against f for different values of R. Here $E_{in} = 1$ eV, $s_{in} = 10^{12}$, $x = 0.5$ and $\beta = 1$ K s^{-1} is considered.

energies derived from TL curves simulated in GOK and OTOR models using different methods are given in Table 5 and it is evident that the present results are quite in agreement with those obtained by other established methods. It is to note that both the methods of Refs. [20,27] are applicable for $x = 0.5$ whereas that of Ref. [21] provides a scope to compare the present results for various values of x. Table 5 exhibits that present peak shape method using skewness as the symmetry parameter more often than not yields better results than Ref. [21] where the symmetry factor was used as symmetry parameter.

3.4. Application to experimental TL peaks

We have applied the present peakshape method in case of some widely studied TL peaks. We note that the present peakshape method is applicable for single or well isolated glow peaks and hence we have selected few such peaks reported in literature. In all the cases we have picked up the data from the experimental curves by using the browser-based software tool WebPlotDigitizer [41] and the skewness (S_k) is calculated using Eq. (14). For 110°C peak of quartz, we have used the glow curves reported by Petrov and Bailiff [32] and Lovedy [33] where the activation energy was reported as 0.99 and 0.973 eV respectively. The present method yields the activation energies as for the dataset of

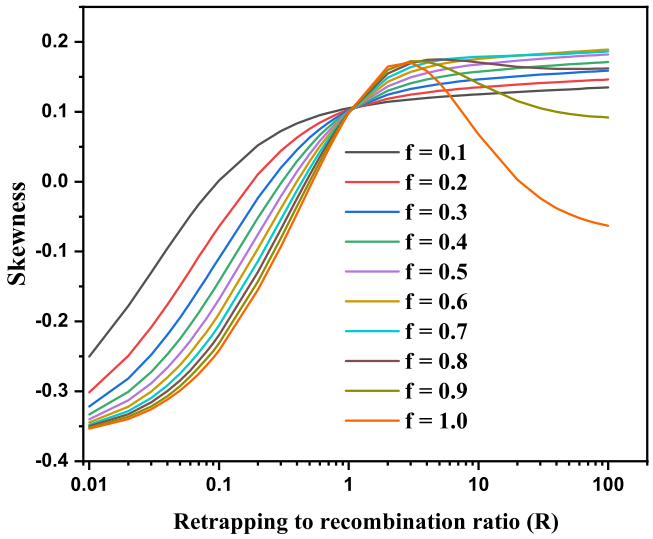

Fig. 7. Variation of skewness (S_k) plotted against R for TL peaks simulated in OTOR model. Here $E_{in} = 1$ eV, $s_{in} = 10^{12}$ s^{-1}, $\beta = 1$ K s^{-1}.

Ref. [32] 1.03 eV and 1.05 eV for Ref. [33]. We have also considered the TL peaks of MgO which are well separated and applied the present method on the 1st peak of the glow curve reported by Thomas and Houston [34]. The reported value [34] of activation energy was 0.66 eV and the present calculation comes out to be 0.71 eV. It is quite evident from the results that the present peak shape method works satisfactorily for experimental TL curves.

4. Concluding remarks

A new set of peak shape relations are developed where activation energy from a well isolated single TL peak can be estimated from the skewness of the TL data. The present peak shape method is quite effective to determine activation energy from TL peaks simulated using GOK equations. When applied to TL peaks simulated in OTOR model, the present method is found to work satisfactorily for $0 \le R \le 1$. Beyond $R > 1$ *i.e.* for heavy retrapping cases, the present peak shape method shows limitation for the TL glow peaks when the traps are highly saturated. This limitation is consistent with other versions of peak shape method reported in literature. The application of present peak shape method to experimental peaks produces encouraging results. The activation energies derived from the τ parameter appears to be more accurate. The procedure of TL glow curve analysis of an experimental sample using the present peak shape method is summarized below.

(i) After recording the TL signal, the complex glow curve is to be resolved into component peaks so that well isolated single peaks are obtained.
(ii) The 'intensity – temperature' data are to be obtained from isolated single glow peaks.
(iii) Skewness (S_k) of the data can be calculated from Eq. (14) by writing an elementary computer programme. For this purpose, all the datapoints for which $I(T) \ge \frac{I_m}{10}$ are to be considered.
(iv) The $I-T$ data are preferred to be taken in an uniform temperature interval (say, $\Delta T = 0.1$ K) so that the peak shape parameters τ_x, δ_x and ω_x are accurately measured at fractional intensities $x = \frac{1}{4}, \frac{1}{2}, \frac{2}{3}$.
(v) With these values of S_k, τ_x, δ_x and ω_x, activation energies ($E_{\tau x}$, $E_{\delta x}$ and $E_{\omega x}$) can be determined in a straightforward manner following Eqs. (16)–(18) where the coefficients are given in Table 1.

Table 5
Comparison of activation enrgies (eV) obtained using present peak shape method and other established peak shape methods [20,21,27]. Here E_{in} = 1 eV, $s_{in} = 10^{12}$ s^{-1} are used.

Model	Input parameters		T_m (K)	$x = \frac{I}{I_m}$	Present method			Other methods		
					E_τ	E_δ	E_ω	E_τ	E_δ	E_ω
GOK	b = 1		384.57	1/4	1.00	1.04	1.02	1.01[a]	1.05[a]	1.03[a]
				1/2	1.01	1.03	1.02	1.01[a]	1.04[a]	1.02[a]
								1.00[b]	0.98[b]	1.00[b]
								0.99[c]	1.00[c]	0.99[c]
				2/3	1.01	1.02	1.02	1.01[a]	1.04[a]	1.02[a]
	b = 1.5		384.22	1/4	1.00	1.07	1.04	1.01[a]	1.09[a]	1.05[a]
				1/2	1.01	1.05	1.03	1.01[a]	1.07[a]	1.04[a]
								1.00[b]	1.02[b]	1.02[b]
								0.99[c]	1.00[c]	0.99[c]
				2/3	1.01	1.04	1.02	1.02[a]	1.06[a]	1.04[a]
	b = 2		383.88	1/4	1.00	1.02	1.01	1.01[a]	1.03[a]	1.02[a]
				1/2	1.00	1.02	1.01	1.01[a]	1.02[a]	1.02[a]
								1.00[b]	0.99[b]	1.00[b]
								0.99[c]	1.01[c]	0.99[c]
				2/3	1.01	1.01	1.01	1.01[a]	1.02[a]	1.01[a]
OTOR	f = 0.5	R = 0	384.57	1/4	1.01	1.06	1.03	1.01[a]	1.05[a]	1.03[a]
				1/2	1.01	1.05	1.03	1.01[a]	1.04[a]	1.02[a]
								1.00[b]	0.99[b]	1.00[b]
								0.99[c]	1.00[c]	0.99[c]
				2/3	1.01	1.04	1.02	1.01[a]	1.04[a]	1.02[a]
		R = 0.5	388.30	1/4	1.03	1.08	1.06	1.03[a]	1.08[a]	1.06[a]
				1/2	1.04	1.08	1.06	1.04[a]	1.07[a]	1.05[a]
								1.03[b]	1.03[b]	1.04[b]
								1.01[c]	0.99[c]	0.99[c]
				2/3	1.05	1.08	1.06	1.04[a]	1.07[a]	1.06[a]
		R = 1	392.29	1/4	1	1.02	1.02	1.01[a]	1.03[a]	1.02[a]
				1/2	1.01	1.02	1.01	1.01[a]	1.02[a]	1.01[a]
								1.00[b]	0.99[b]	1.00[b]
								0.99[c]	1.01[c]	0.99[c]
				2/3	1.01	1.02	1.01	1.01[a]	1.02[a]	1.01[a]

[a]Kundu et al. [21].
[b]Chen [27].
[c]Kitis et al. [20].

CRediT authorship contribution statement

M. Kundu: Conceptualization, Methodology, Software, Data curation, Writing – original draft, Visualization, Investigation. **S. Chakrabarty:** Software, Validation. **S. Bhattacharyya:** Supervision, Conceptualization, Methodology, Writing – review & editing. **P.S. Majumdar:** Conceptualization, Methodology.

Declaration of competing interest

The authors declare that they have no known competing financial interests or personal relationships that could have appeared to influence the work reported in this paper.

Data availability

Data will be made available on request.

References

[1] C.E. May, J.A. Partridge, Thermoluminescent kinetics of alpha-irradiated alkali halides, J. Chem. Phys. 40 (5) (1964) 1401–1409.
[2] J.T Randall, M.H.F Wilkins, Phosphorescence and electron traps-I. The study of trap distributions, Proc. R. Soc. Lond. Ser. A. Math. Phys. Sci. 184 (999) (1945) 365–389.
[3] J.T Randall, M.H.F Wilkins, Phosphorescence and electron traps-II. The interpretation of long-period phosphorescence, Proc. R. Soc. Lond. Ser. A. Math. Phys. Sci. 184 (999) (1945) 390–407.
[4] G.F.J. Garlick, A.F. Gibson, The electron trap mechanism of luminescence in sulphide and silicate phosphors, Proc. Phys. Soc. 60 (6) (1948) 574–590.
[5] C.S. Shalgaonkar, A.V. Narlikar, Review: a review of the recent methods for determining trap depth from glow curves, J. Mater. Sci. 7 (12) (1972) 1465–1471.
[6] Reuven Chen, On the methods for determining trap depth from glow curves, J. Mater. Sci. 9 (2) (1974) 345–347.
[7] C.M. Sunta, Unraveling thermoluminescence; Springer Series in Materials Science, Vol. 202, Springer India, New Delhi, 2014.
[8] A. Halperin, A.A. Braner, A. Ben-Zvi, N. Kristianpoller, Thermal activation energies in NaCl and KCl crystals, Phys. Rev. 117 (2) (1960) 416–422.
[9] J. Nahum, A. Halperin, Thermoluminescence and the relation between thermal and optical activation energies in diamond, J. Phys. Chem. Solids 24 (7) (1963) 823–834.
[10] H. Gobrecht, D. Hofmann, Spectroscopy of traps by fractional glow technique, J. Phys. Chem. Solids 27 (3) (1966) 509–522.
[11] Antonín Bohun, Thermoemission und photoemission von Natriumchlorid, Cechoslov. Fiziceskij Z. 4 (1) (1954) 91–93.
[12] Yoram Kirsh, Kinetic analysis of thermoluminescence, Phys. Status Solidi a 129 (1992) 15–48.
[13] M. Kundu, S. Bhattacharyya, M. Karmakar, P.S. Majumdar, Three-point area method for thermoluminescence glow curve analysis and its application to the glow peak of $K_2SrP_2O_7$:Pr, Radiat. Prot. Dosim. 193 (2021) 247–258.
[14] D. Shenker, R. Chen, Numerical curve fitting of general order kinetics glow peaks, J. Phys. D: Appl. Phys. 4 (2) (1971) 287–291.
[15] N.S. Mohan, R. Chen, Numerical curve fitting for calculating glow parameters, J. Phys. D: Appl. Phys. 3 (2) (1970) 243–247.
[16] M. Puchalska, P. Bilski, GlowFit—a new tool for thermoluminescence glow-curve deconvolution, Radiat. Meas. 41 (6) (2006) 659–664.
[17] Y.S. Horowitz, M. Moscovitch, Highlights and pitfalls of 20 years of application of computerised glow curve analysis to thermoluminescence research and dosimetry, Radiat. Prot. Dosim. 153 (2012) 1–22.
[18] Th Basanta Singh, L. Rey, R.K. Gartia, Applications of PeakFit software in thermoluminescence studies, 2011, NISCAIR-CSIR, India.
[19] S. Joychandra Singh, Mahua Karmakar, S. Dorendrajit Singh, On the determination of the order of kinetics in thermoluminescence by peak-shape method, Radiat. Eff. Defects Solids 168 (2013) 352–357.
[20] G. Kitis, V. Pagonis, Peak shape methods for general order thermoluminescence glow-peaks: A reappraisal, Nucl. Instrum. Methods Phys. Res. B 262 (2007) 313–322.

[21] Mohan Kundu, Saurish Chakrabarty, Sukhamoy Bhattacharyya, Partha Sarathi Majumdar, Reappraisal of peak shape method based on average geometrical symmetry factor and its application to thermoluminescence glow curves, Phys. Status Solidi b 258 (11) (2021) 2100277.
[22] Leonard I. Grossweiner, A note on the analysis of first-order glow curves, J. Appl. Phys. 24 (1953) 1306–1307.
[23] Gustavo A. Dussel, Richard H. Bube, Theory of thermally stimulated conductivity in a previously photoexcited crystal, Phys. Rev. 155 (3) (1967) 764–779.
[24] Ch. B. Lushchik, The investigation of trapping centers in crystals by the method of thermal bleaching, Sov. Phys.—JETP 3 (1956) 390–399.
[25] Reuven Chen, On the calculation of activation energies and frequency factors from glow curves, J. Appl. Phys. 40 (1969) 570–585.
[26] A. Halperin, A.A. Braner, Evaluation of thermal activation energies from glow curves, Phys. Rev. 117 (1960) 408–415.
[27] Reuven Chen, Glow curves with general order kinetics, J. Electrochem. Soc. 116 (1969) 1254–1257.
[28] C. Christodoulides, Determination of activation energies by using the widths of peaks of thermoluminescence and thermally stimulated depolarisation currents, J. Phys. D: Appl. Phys. 18 (1985) 1501–1510.
[29] P.S. Mazumdar, S.J. Singh, R.K. Gartia, The determination of activation energy from the shape of a thermoluminescence peak, J. Phys. D: Appl. Phys. 21 (1988) 815–819.
[30] R.K. Gartia, S.J. Singh, P.S. Mazumdar, Symmetry factor and order of kinetics in thermally stimulated luminescence, Phys. Status Solidi a 106 (1988) 291–296.
[31] George Kitis, Reuven Chen, Vasilis Pagonis, Thermoluminescence glow-peak shape methods based on mixed order kinetics, Phys. Status Solidi a 205 (2008) 1181–1189.
[32] S.A. Petrov, I.K. Bailiff, The '110 °C' TL peak in synthetic quartz, Radiat. Meas. 24 (4) (1995) 519–523.
[33] L. Lovedy, Glow curve analysis of the 110 °C glow peak of quartz in the simplified got equation, Int. J. Lumin. Appl. (2017).
[34] B. Thomas, E. Houston, Correlation of optical absorption and thermoluminescence curves for single crystals of magnesium oxide, Br. J. Appl. Phys. 15 (8) (1964) 953.
[35] G. Kitis, N.D. Vlachos, General semi-analytical expressions for TL, OSL and other luminescence stimulation modes derived from the OTOR model using the Lambert W-function, Radiat. Meas. 48 (2013) 47–54.
[36] Georgios Kitis, J.M. Gomez-Ros, Jan W.N. Tuyn, Thermoluminescence glow-curve deconvolution functions for first, second and general orders of kinetics, J. Phys. D: Appl. Phys. 31 (19) (1998) 2636–2641.
[37] Y. Dodge, The Concise Encyclopedia of Statistics, Springer, New York, 2008.
[38] C.M. Sunta, Ayta W.E. Feria, T.M. Piters, S. Watanabe, Limitation of peak fitting and peak shape methods for determination of activation energy of thermoluminescence glow peaks, Radiat. Meas. 30 (1999) 197–201.
[39] A.M. Sadek, H.M. Eissa, A.M. Basha, G. Kitis, Resolving the limitation of the peak fitting and peak shape methods in the determination of the activation energy of thermoluminescence glow peaks, J. Lumin. 146 (2014) 418–423.
[40] M. Karmakar, S. Bhattacharyya, A. Sarkar, P.S. Mazumdar, S.D. Singh, Analysis of thermoluminescence glow curves using derivatives of different orders, Radiat. Prot. Dosim. 175 (2017) 493–502.
[41] WebPlotDigitizer webpage, https://apps.automeris.io/wpd.

Skew normal distribution function for deconvolution of thermoluminescence glow curves

M. Kundu[1,2], S. Sarkar[1], A.Das[3], and S. Bhattacharyya[*1]

[1]Department of Physics, Jadavpur University, Kolkata 700032, India
[2]Sadhanpur Uludanga Tulsiram High School (H.S), Amdanga, 24 PGS (N) 743221, India
[3]Department of Physics, Acharya Prafulla Chandra College, New Barrackpore, Kolkata 700131, India

Abstract

Thermoluminescence (TL) glow curve analysis is a widely used technique to characterize a material by estimating trapping parameters. The difficulty in this analysis is that a complex experimental glow curve generally comprises of several superposed peaks whereas the theoretical methods of analysis are mostly developed on single peaks. Thus, it is important to isolate the component peaks for further analysis and glow curve deconvolution (GCD) is a widely used method for this purpose. A few GCD functions based on different statistical distribution (*e.g.* Gaussian distribution, Weibull distribution, logistic asymmetric distribution *etc.*) were reported in literature, but the success is quite limited. In this work, we report pilot calculations using the skew normal distribution for analyzing TL data to explore its applicability as a GCD function. In particular, we propose a five-parameter skew-normal distribution function which has been used to fit a large number of TL glow curves equivalent to both first and second order peaks, simulated using One-Trap-One-Recombination center (OTOR) model with a wide range of input parameters. The quality of fitting TL curves using proposed skew normal function is also studied. Results obtained here are quite encouraging to explore the applicability of skew-normal distribution function as a potential GCD function in TL analysis.

Keywords: Thermoluminescence, OTOR model, Glow curve deconvolution, skew normal distribution, Curve fitting.

1 Introduction

A thermoluminescence (TL) glow curve is the plot of TL signal intensity as a function of temperature obtained during heating a previously irradiated thermoluminescent material. The glow curve analysis has been a major subject in various field of research. Extensive theoretical and experimental researches have been carried out to develop different methods of glow curve analysis, *e.g.* peak shape methods [1, 2], Initial rise method [3–5], Variable heating rate method [6], Curve Fitting [7, 8] and Computerized Glow Curve Deconvolution (CGCD) [9–11] *etc.* Each technique has its own merits and limitations as well. Glow curve deconvolution (GCD) is a technique which is used to deconvolute an experimentally obtained complex TL glow curve into its individual component peaks. Computerized Glow Curve Deconvolution (CGCD) [9–11] is one of the most widely used methods for TL analysis to extract

*Corresponding author. Email: sukhamoy.b@gmail.com, sukhamoyb.physics@jadavpuruniversity.in

relevant parameters like activation energy (E), frequency factor (s) and order of kinetics (b). In CGCD, a complex experimental glow curve is analyzed by constituting and then analyzing its component peaks. Several CGCD software packages have been developed to analyze complex TL data [9, 11–17]. In CGCD, the experimental TL curve is reconstituted by iterative process using proper GCD function to build up the constituent single TL glow peaks. Therefore, choosing appropriate GCD function plays a key role to have an efficient CGCD program. Many functions have been proposed [12–14] to describe the constituent peaks used in various CGCD programs. Kitis *et. al.* [18] proposed GCD functions on the basis of general order kinetics (GOK) model for first, second and general order of kinetics.

Glow curve analysis has also been carried out from the point of view of statistical distribution of TL data. A few probability distribution functions have been tried by various researchers to develop suitable GCD functions. Pagonis *et. al.* [19] have proposed a GCD function using 3 parameter Weibull probability function which can only be used to describe first order TL peaks. In a later work, Pagonis and kitis [20] proposed another GCD function where logistic asymmetric statistical probability function was used which could describe second order TL curves only. Moreover, in TL literature, [21, 22] the application of Gaussian function to deconvolute complex TL data is also available. However, Chandrashekhar and Gartia [22] have shown that Gaussian function is not suitable for this purpose. Conceptually it is also understandable as the Gaussian function is composed of two parameters (the mean (λ) and variance (σ^2)), whereas a single TL peak is characterized by at least three kinetic parameters (E, s, b) in GOK model or four parameters in band theory based OTOR model (E, s, f, R). Here f is the initial trap filling ratio and $R = \dfrac{A_n}{A_h}$ (A_n = retrapping probability and A_h = recombination probability). It is further remarkable that the Gaussian (normal) distribution is symmetric in nature whereas the shape of a single TL peak is usually asymmetric. The nature of asymmetry in TL curve depends on the retrapping-recombination mechanism during the heating stage. This dependence can be systematically reflected through the skewness of a TL dataset. In a recent work [23], it is shown that, as a measure of asymmetry, skewness of TL data may be exploited to reflect the shape of a single TL curve. Hence a probability distribution function involving skewness of the data may be a potential candidate for developing an appropriate GCD function. It is to mention that all the proposed GCD functions mentioned above were derived on the basis of GOK model.

The primary motivation of this work is to develop a GCD function from a statistical view point to analyze band theory based OTOR model TL data. Since in OTOR model a TL intensity is characterized by four parameters (E, s, f, R), the probability distribution function is likely to be composed of at least four parameters. Keeping all this in mind we consider a version of skew normal distribution function. At first we critically investigate the normal distribution function to describe some experimental TL peaks mentioned in Ref. [22], simulated using GOK model and highlight the limitations. In next step we consider the OTOR model and apply the skew normal distribution to examine its suitability as GCD function. It is to note that the present work is carried out in OTOR model using $R = 0$ and 1 which corresponds to first and second order kinetics respectively.

2 Methodology

In this section we describe TL data simulation in GOK and OTOR model under linear heating scheme and the method of analysis using normal and skew normal distribution functions.

2.1 TL glow curves simulation in GOK model

The general order kinetics (GOK) equation for TL intensity at temperature T is given by [24–26]

$$\begin{aligned} I(T) &= sn_0 e^{-\frac{E}{kT}} \exp\left[-\frac{s}{\beta}\int_{T_0}^{T} e^{-\frac{E}{kT'}}dT'\right] && \text{for b} = 1 \\ &= sn_0 e^{-\frac{E}{kT}}\left[\frac{(b-1))s}{\beta}\int_{T_0}^{T} e^{-\frac{E}{kT'}}dT' + 1\right]^{-\frac{b}{b-1}} && \text{for b} \neq 1 \end{aligned} \tag{1}$$

Here, n_0 = initial concentration of trapped electrons, T_0 = initial temperature, β = linear heating rate, k = Boltzmann constant. The input parameters for curve simulation in GOK model are TL kinetic parameters E, s, b.

2.2 Fitting with normal distribution functions

We use the two-parameter Gaussian function for fitting TL data are given by

$$I_g(T) = I_0 + \frac{A}{\sigma}\sqrt{\frac{2}{\pi}}\, exp\left[-2\left(\frac{T - T_{mg}}{\sigma}\right)^2\right] \tag{2}$$

where $I_g(T)$ = TL intensity at temperature T, I_0 = offset, A = area. The peak maxima occurs at the mean position (T_{mg}) and σ is the width at inflection points (T_i^- in the rising side and T_i^+ in the falling side of the curve). Hence,

$$\frac{d^2 I_g}{dT^2} = 0 \qquad \text{at} \quad T = T_i^{\pm} = T_{mg} \pm \frac{\sigma}{2} \tag{3}$$

The Gaussian fitting is carried out using 'QtiPlot' software where the inbuilt Levenberg-Marquardt algorithm is adopted. We have also estimated the figure of merit (FOM) for all the curves by using the relation

$$\text{FOM} = \frac{\sum_n |I(T) - I_g(T)|}{\sum_n I_g(T)} \times 100\% \tag{4}$$

Here n is the number of data points and $I(T)$ is calculated according to equation (1). We have also estimated the χ^2-values for all the peaks according to the method suggested by Vejnović *et al.* [27].

2.3 TL glow curve simulation in OTOR model

The basic charge trafficking equations in OTOR model [28] are

$$\frac{dn_c}{dt} = nse^{-\frac{E}{kT}} - A_n(N-n)n_c - A_h n_c n_h \tag{5}$$

$$\frac{dn}{dt} = -nse^{-\frac{E}{kT}} + A_n(N-n)n_c \tag{6}$$

$$I = -\frac{dn_h}{dt} = A_h n_c n_h \tag{7}$$

The parameters used in the equations (5−7) are: n_c = concentration of conduction band electrons, n = concentration of trapped electrons, n_h = concentration of holes or recombination centre, N = total trap concentration. The charge neutrality condition is: $n_h = n + n_c$. Under the quasi-equilibrium (QE) approximations *i.e.* $\left|\frac{dn_c}{dt}\right| << \left|\frac{dn}{dt}\right|$ and $n_c << n$ and in linear heating scheme *i.e.* $T = T_0 + \beta t$, the TL intensity is expressed as

$$I(T) \simeq \frac{n^2 s e^{-\frac{E}{kT}}}{\beta\left[n(1-R)+NR\right]} \tag{8}$$

The initial condition $n = n_0$ at $T = T_0$ is employed to solve equation (8). The initial trap filling ratio is defined as $f = \frac{n_0}{N}$. Equation (8) can be solved numerically or in terms of Lambert-W function [29] to yield TL intensity in OTOR model. Here we have adopted numerical method for curve simulation using Eq. (8) where the input parameters are E, s, f, R.

2.4 Fitting the OTOR glow curves using skew normal distribution function

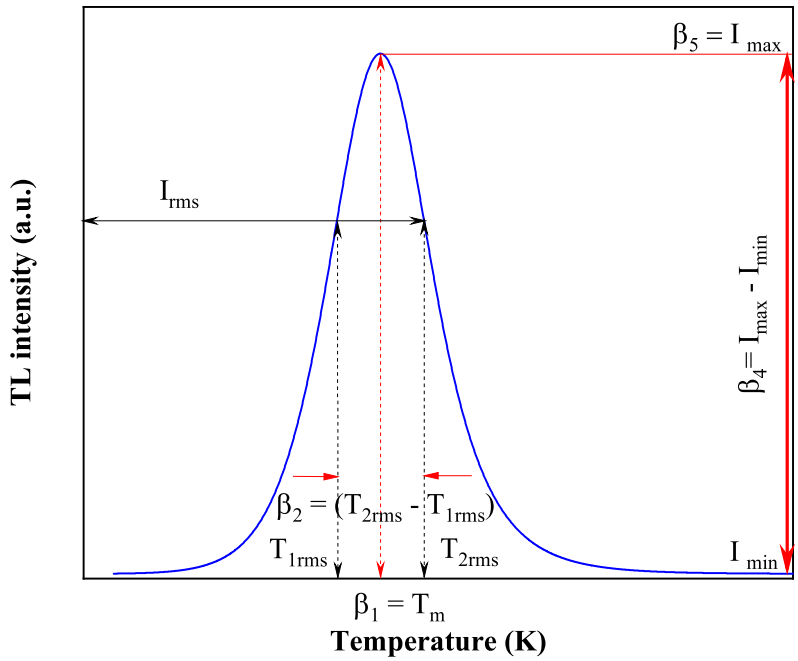

Figure 1: Schematic diagram showing relations between the characteristic parameters of proposed skew normal distribution and the various features of TL glow curve

The basic version of a skew normal distribution function is characterized by mainly three parameters, *viz.* the mean (λ), variance (σ^2) and skewness (S_k). However, depending on the nature of the system and quality of data, number of parameters may be more. Our study reveals that to fit TL data simulated in OTOR model, the skew normal distribution function characterized by five parameters is

more suitable.

The required computation is done by writing a computer code written in programming language 'R' which is widely used for statistical computation and data visualization. According to the present proposition the TL intensity in skew normal distribution is written as

$$I(T) = \frac{2}{\sqrt{\pi}} exp\left[\frac{1}{2}\left(\frac{T-\beta_1}{\beta_2}\right)^2\right] pnorm\left(\beta_3 T, \beta_3\beta_1, \beta_2\right)\beta_4 + \beta_5 \tag{9}$$

Here *'pnorm'* is an inbuilt function in 'R' for calculation of the cumulative distribution function. The characteristic parameters in the probability function are related to the glow data which is to be fitted (Fig. 1). The relations are as follows: β_1 = Peak temperature (T_m), β_2 = peak width at inflection points, β_3 = skewness of TL data, β_4 = Peak height *i.e.* $(I_{max} - I_{min})$ and $\beta_5 = I_{max}$.

The simulated TL data in OTOR model is fed to the 'R' code and a set of initial (guess) values for β_1, β_2 and β_3 are given as input. Based on these initial values, iteration is performed to yield the best values of the fitting parameters. Our experience on this process is that the initial guess values need to be closer to the actual values, otherwise the process of iteration fails.To do away with this difficulty we first fit the input TL data by using a normal distribution function to have better initial guess of β_1 and β_2. The initial guess of β_3 is given intuitively by seeing the skewed nature of input TL data. The code does not require initial values of β_4 and β_5 as they are calculated within the process and final iterated values of all the fitting parameters are obtained as output.

3 Results and discussions

The TL glow curve analysis is carried out first on GOK model curves using Gaussian distribution function and then on OTOR model curves using skew normal function.

3.1 Fitting of glow curve using Gaussian function.

The GOK curves are simulated using the kinetic parameters mentioned in Ref. [22] in respect of experimental TL peaks corresponding to different phosphors. Each glow curve is fitted with the Gaussian function (2). Table 1 shows the input parameters (E, s, b) for all the peaks [22] along with the fitted parameters (I_0, A, σ, T_{mg}) of Gaussian functions (equation 2). Table 1 also lists the FOM and χ^2 values. These FOM values are far higher than those reported in Ref. [22] where a different expression of FOM was used. The FOM values of Table 1 indicate that fitting of TL curves using Gaussian functions should not be treated as a good choice. We see that only when 'b' lies around $1.6-1.7$, FOM lies below 5% which is still very high [30] and beyond the range of good fitting. In Fig. 2, the TL curves with Gaussian fitting of Peak 3 of $Ca_{0.79}Sr_{0.21}S : Eu$ and Peak 1 of $Sr_2MgSi_2O_7 : Eu^{2+}Dy^{3+}$ are shown along with the respective residues. The residue corresponding to the peak with $b = 1.68$ in Fig. 2(a) varies within a smaller range as compared to that in Fig. 2(b) corresponding to the peak with $b = 1.10$.

Table 1: The input values [22] for TL curve generation (equation 1) along with the Gaussian function parameters (equation 2). The linear heating rate is $\beta = 1.0\ K.s^{-1}$

		Input parameters [22]			Present Gaussian curve parameters					
Sample	Peak	$E\ (eV)$	$s\ (s^{-1})$	b	I_0	A	σ	T_{mg}	FOM (%)	χ^2
$ZnS : Eu^{+}, Co^{2+}$	P1	0.79	3.82×10^{10}	2.00	0.0108	44.5337	36.8755	340.94	7.43	3.36×10^{-04}
	P2	0.80	7.52×10^{09}	2.00	0.0155	49.8293	41.3912	365.63	6.95	3.98×10^{-04}
	P3	1.00	1.02×10^{10}	2.00	0.0169	59.8393	49.7542	448.38	6.70	4.08×10^{-04}
	P4	1.10	3.28×10^{11}	2.00	0.0151	52.3507	43.4713	437.06	6.50	3.58×10^{-04}
$Ca_{0.79}Sr_{0.21}S : Eu$	P1	0.70	1.88×10^{09}	1.23	0.0052	38.4437	31.1458	336.43	9.59	5.68×10^{-04}
	P2	0.70	3.04×10^{08}	1.10	0.0063	41.5859	33.7484	361.15	12.19	1.08×10^{-03}
	P3	0.89	1.46×10^{10}	1.68	0.0115	48.3173	39.7807	394.61	4.41	1.38×10^{-04}
	P4	0.95	8.02×10^{09}	1.20	0.0071	45.1346	36.7273	427.63	10.32	8.06×10^{-04}
	P5	1.00	2.98×10^{09}	1.60	0.0150	58.2297	47.9792	467.50	3.62	1.35×10^{-04}
$Sr_2MgSi_2O_7 :$	P1	0.55	1.22×10^{08}	1.10	0.0040	36.0792	29.2260	297.79	12.26	8.10×10^{-04}
$Eu^{2+}Dy^{3+}$	P2	0.60	6.15×10^{07}	1.10	0.0054	41.2657	33.4532	333.38	11.91	9.68×10^{-04}
	P3	0.79	3.22×10^{09}	1.57	0.0091	46.6794	38.2830	371.42	4.48	1.39×10^{-04}
	P4	0.95	3.99×10^{10}	1.60	0.0098	46.9125	38.5215	405.51	4.50	1.44×10^{-04}
$BaZrSi_3O_9 :$	P1	0.75	7.93×10^{10}	1.10	0.0041	29.7550	24.1389	314.01	13.52	8.63×10^{-04}
Eu^{2+}, Pr^{3+}	P2	0.75	9.86×10^{08}	1.80	0.0145	51.5815	42.6531	370.47	4.85	2.09×10^{-04}
	P3	1.00	1.16×10^{11}	1.10	0.0060	37.8192	30.7238	409.47	13.32	1.11×10^{-03}
	P4	1.10	7.16×10^{10}	1.20	0.0073	44.5835	36.2954	456.60	10.66	8.45×10^{-04}

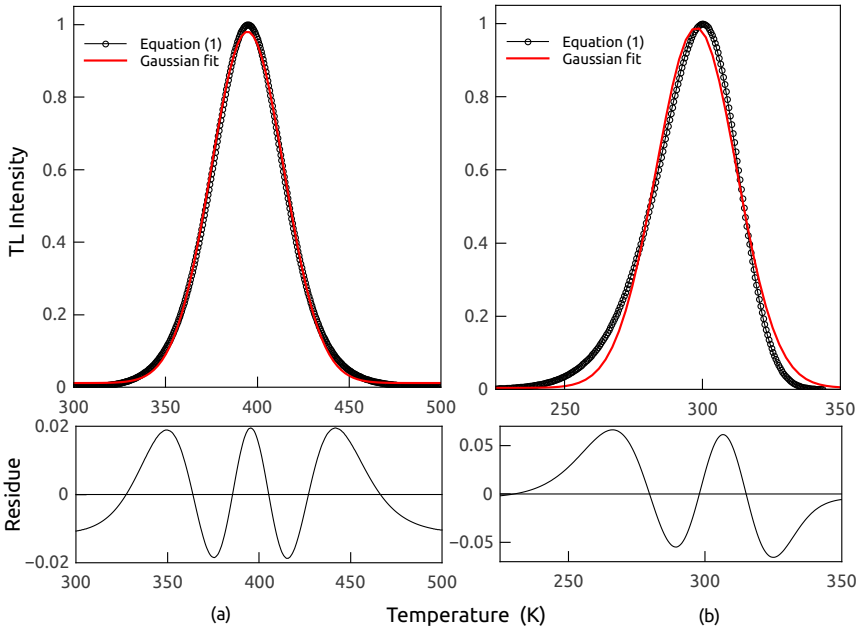

Figure 2: Fitting of TL glow curve using Gaussian functions and the residues. (a) Peak 3 of $Ca_{0.79}Sr_{0.21}S : Eu$; input parameters: $E = 0.89$ eV, $s = 1.46 \times 10^{10}\ s^{-1}$ and $b = 1.684$, (b) Peak 1 of $Sr_2MgSi_2O_7 : Eu^{2+}, Pr^{3+}$; input parameters: $E = 0.55$, $s = 1.22 \times 10^{8}\ s^{-1}$ and $b = 1.10$.

3.2 Fitting the OTOR glow curve using skew-normal distribution function.

For numerical generation of TL curves in OTOR model for $R = 0$ and 1, we have considered E (eV) in the range $0.1 \leq E \leq 2.0$ in step 0.1. For each value of E we have taken seven values of s (s^{-1}) gradually *i.e.* $10^7, 10^8, 10^9, 10^{10}, 10^{11}, 10^{12}, 10^{13}$ and f is varied within $0.1 \leq f \leq 1.0$ in step 0.1. The TL curves simulated in OTOR model have been fitted with the proposed skew normal distribution function (equation(9)). In Fig.(3) we have given a couple of representative cases for $R = 0$. The residues are also plotted in the figure to show the quality of fitting from which it is clear that the fitting is quite satisfactory. In table 2 we have given the output values of the characteristic parameters of the skew normal distribution for some randomly chosen set of input TL parameters corresponding to $R = 0$ *i.e.* for equivalent first order peaks. The correlation between the TL data and fitted data are also given in table 2 and the results are quite satisfactory.

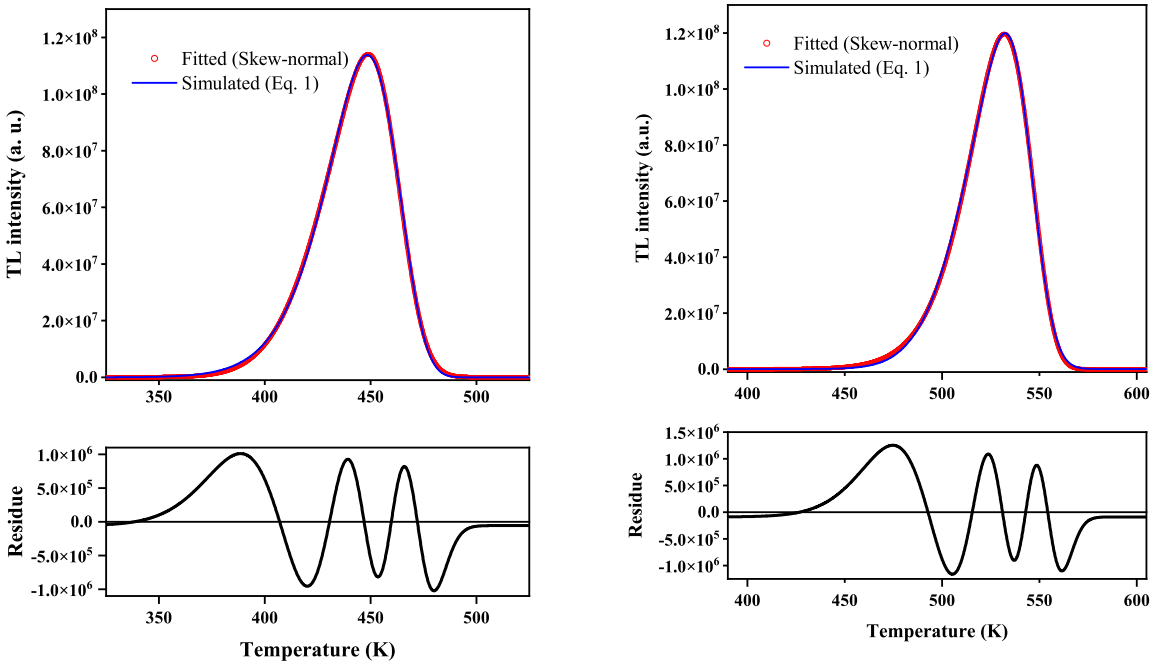

Figure 3: Fitting of TL glow curve using skew normal distribution function. Glow curves are simulated in OTOR model where R = 0 and f = 0.5 were taken. The left glow curve is simulated with $E = 1$ eV and $s = 10^{10}$ s^{-1} whereas the right glow curve is for $E = 1.5$ eV and $s = 10^{13}$ s^{-1}

.

In a similar manner OTOR model TL curves are simulated for $R = 1$ and fitted with the skew normal function. In Fig.(4) a few representative cases are depicted to show the quality of fitting along with the residue plot. The input values for simulation of some TL curves and the fitting parameters obtained from skew normal distribution are shown in the table 3 for $R = 1$. The values of correlation given in table 3 confirms the suitability of the proposed probability distribution to derive a GCD function for OTOR glow curve equivalent to second order kinetics.

Table 2: The input values used for TL curve simulation (equation 8) along with the fitted parameters of skew normal distribution function (equation (9)). Here $R = 0$ and linear heating rate $\beta = 1.0\ K.s^{-1}$ is adopted.

Input parameters			**Parameters obtained after fitting**					
E (eV)	s (s^{-1})	f	β_1 (K)	β_2 (K)	β_3	β_4	β_5	Correlation
0.1	10^{07}	0.1	69.51	5.84	-2.43	1.71×10^{8}	1.86×10^{4}	0.99995
0.2	10^{10}	0.5	98.36	6.25	-2.64	7.96×10^{8}	2.27×10^{5}	0.99991
0.3	10^{13}	1.0	114.52	5.87	-2.76	1.69×10^{9}	5.17×10^{5}	0.99989
0.4	10^{07}	0.5	258.81	20.54	-2.48	2.43×10^{8}	4.58×10^{4}	0.99994
0.5	10^{10}	1.0	237.39	14.64	-2.66	6.79×10^{8}	2.54×10^{5}	0.99991
0.6	10^{13}	0.1	224.24	11.28	-2.77	8.81×10^{7}	3.28×10^{4}	0.99988
0.7	10^{07}	1.0	440.54	34.20	-2.50	2.91×10^{8}	7.96×10^{4}	0.99993
0.8	10^{10}	0.1	373.19	22.68	-2.67	4.39×10^{7}	1.44×10^{4}	0.99991
0.9	10^{13}	0.5	332.28	16.53	-2.77	3.00×10^{8}	1.60×10^{5}	0.99988
1.0	10^{07}	0.1	618.55	47.37	-2.51	2.10×10^{8}	5.09×10^{4}	0.99993
1.1	10^{10}	0.5	507.13	30.52	-2.67	1.63×10^{8}	4.75×10^{4}	0.99991
1.2	10^{13}	1.0	439.26	21.69	-2.78	4.58×10^{8}	1.97×10^{5}	0.99988
1.3	10^{07}	0.5	794.09	60.22	-2.52	8.28×10^{7}	1.74×10^{4}	0.99993
1.4	10^{10}	1.0	639.76	38.22	-2.68	2.60×10^{8}	7.81×10^{4}	0.99991
1.5	10^{13}	0.1	545.46	26.78	-2.78	3.71×10^{7}	1.77×10^{4}	0.99988
1.6	10^{07}	1.0	967.78	72.81	-2.52	1.37×10^{8}	2.84×10^{4}	0.99993
1.7	10^{10}	0.1	771.38	45.80	-2.68	2.17×10^{7}	6.91×10^{3}	0.99991
1.8	10^{13}	0.5	651.06	31.81	-2.78	1.56×10^{8}	7.03×10^{4}	0.99988
1.9	10^{07}	0.1	1139.99	85.22	-2.53	1.17×10^{7}	2.41×10^{3}	0.99993
2.0	10^{13}	0.5	721.16	35.14	-2.78	1.41×10^{8}	7.26×10^{4}	0.99988

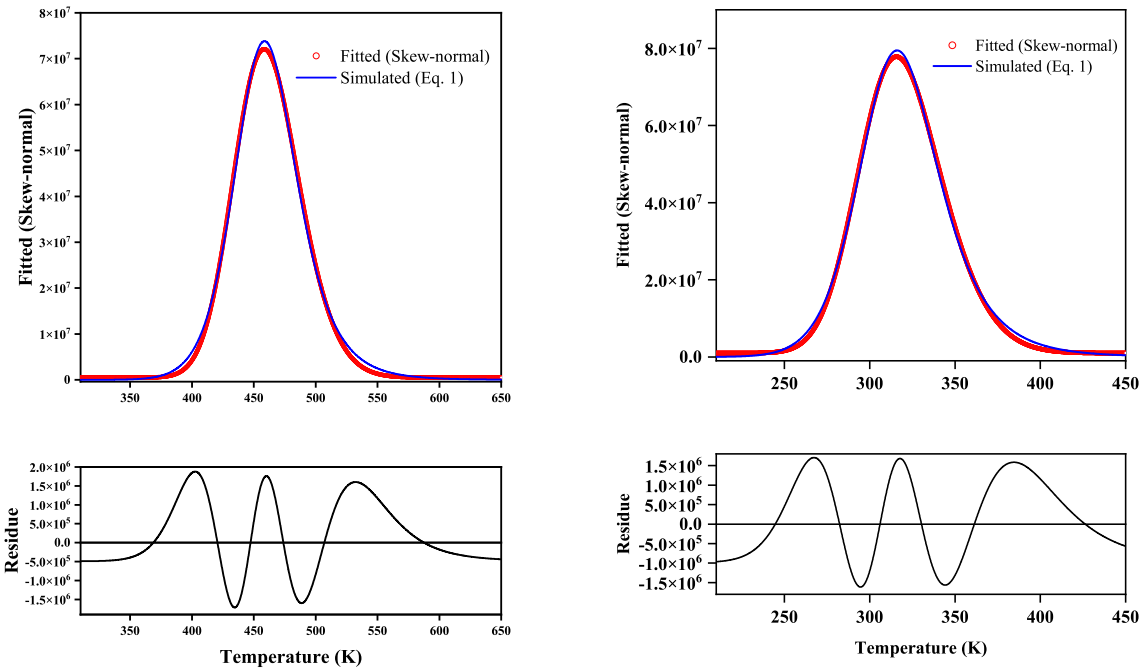

Figure 4: Fitting of TL glow curve using skew normal distribution function. Glow curves are simulated in OTOR model where $R = 1$ and $f = 0.5$ were taken. The left glow curve is simulated with $E = 1$ eV and $s = 10^{10}\ s^{-1}$ whereas the right glow curve is for $E = 1.5$ eV and $s = 10^{13}\ s^{-1}$

Table 3: The input values used for TL curve simulation (equation 8) along with the fitted parameters of skew normal distribution function (equation (9)). Here $R = 1$ and linear heating rate $\beta = 1.0\ K.s^{-1}$ is adopted.

Input parameters			**Parameters obtained after fitting**					
E (eV)	s (s^{-1})	f	β_1 (K)	β_2 (K)	β_3	β_4	β_5	Correlation
0.1	10^{07}	0.1	69.60	9.58	1.68	9.85×10^{7}	6.56×10^{5}	0.99914
0.2	10^{10}	0.5	93.03	8.04	1.41	5.94×10^{8}	2.24×10^{6}	0.99914
0.3	10^{13}	1.0	107.60	6.94	1.28	1.38×10^{9}	3.25×10^{6}	0.99912
0.4	10^{07}	0.5	240.26	27.72	1.57	1.70×10^{8}	1.09×10^{6}	0.99919
0.5	10^{10}	1.0	219.60	17.71	1.38	5.38×10^{8}	2.36×10^{6}	0.99914
0.6	10^{13}	0.1	225.67	15.29	1.30	6.25×10^{7}	2.18×10^{5}	0.99912
0.7	10^{07}	1.0	397.50	42.72	1.52	2.20×10^{8}	1.64×10^{6}	0.99919
0.8	10^{10}	0.1	375.25	32.62	1.41	2.92×10^{7}	1.36×10^{5}	0.99914
0.9	10^{13}	0.5	319.10	20.13	1.26	2.37×10^{8}	1.06×10^{6}	0.99912
1.0	10^{07}	0.1	620.67	74.03	1.58	1.27×10^{7}	9.87×10^{4}	0.99915
1.1	10^{10}	0.5	481.40	38.85	1.38	1.23×10^{8}	4.09×10^{5}	0.99913
1.2	10^{13}	1.0	413.81	25.44	1.26	3.76×10^{8}	1.22×10^{6}	0.99911
1.3	10^{07}	0.5	740.30	80.54	1.53	5.89×10^{7}	3.16×10^{5}	0.99916
1.4	10^{10}	1.0	593.46	46.20	1.36	2.07×10^{8}	6.49×10^{5}	0.99913
1.5	10^{13}	0.1	549.10	35.91	1.28	2.65×10^{7}	1.18×10^{5}	0.99912
1.6	10^{07}	1.0	876.17	91.32	1.51	1.04×10^{8}	4.81×10^{5}	0.99915
1.7	10^{10}	0.1	775.70	65.42	1.40	1.46×10^{7}	6.23×10^{4}	0.99914
1.8	10^{13}	0.5	625.76	38.76	1.26	1.23×10^{8}	4.40×10^{5}	0.99911
1.9	10^{07}	0.1	1144.00	132.50	1.57	7.14×10^{6}	4.40×10^{4}	0.99917
2.0	10^{13}	0.5	693.32	42.68	1.25	1.12×10^{8}	4.64×10^{5}	0.99911

4 Concluding remarks

In this work, at first we have critically examined the suitability of Gaussian distribution as a GCD function for TL glow curve analysis and the results are not at all satisfactory. Looking into the skewed nature of TL glow curve, for the first time we propose a version of skew normal distribution characterized by five parameters. We investigate the suitability of this new probability function and apply it to large number of TL glow curves simulated in OTOR model. As a pilot investigation we have considered the TL curves which are equivalent to first and second order kinetics. The quality of fitting is judged through residue plots as well as through the correlation between the TL data and fitted data. The outcome is quite encouraging which will definitely pave the way to formulate an efficient GCD function that may lead to the development of a CGCD technique based on OTOR model.

5 Acknowledgement

This work was partially carried out using the facilities of UGC-DAE CSR. The authors acknowledge the financial support from UGC-DAE CSR through a collaborative Research Scheme (CRS) project number CRS/2022-23/02/833.

References

1. R. Chen. On the calculation of activation energies and frequency factors from glow curves. *Journal of Applied Physics*, 40:570–585, 1969.

2. R. Chen. Glow curves with general order kinetics. *Journal of The Electrochemical Society*, 116: 1254–1257, 1969.

3. G. F. J. Garlick and A. F. Gibson. The electron trap mechanism of luminescence in sulphide and silicate phosphors. *Proceedings of the Physical Society*, 60(6):574–590, 1948.

4. A. Halperin, A. Braner, A. Ben-Zvi, and N. Kristianpoller. Thermal activation energies in NaCl and KCl crystals. *Physical Review*, 117(2):416–422, 1960.

5. J. Nahum and A. Halperin. Thermoluminescence and the relation between thermal and optical activation energies in diamond. *Journal of Physics and Chemistry of Solids*, 24(7):823–834, 1963.

6. A. Bohun. Thermoemission und photoemission von natriumchlorid. *Cechoslovackij fiziceskij zurnal*, 4(1):91–93, 1954.

7. D. Shenker and R. Chen. Numerical curve fitting of general order kinetics glow peaks. *Journal of Physics D: Applied Physics*, 4(2):287–291, 1971.

8. N. S. Mohan and R. Chen. Numerical curve fitting for calculating glow parameters. *Journal of Physics D: Applied Physics*, 3(2):243–247, 1970.

9. M. Puchalska and P. Bilski. GlowFit—a new tool for thermoluminescence glow-curve deconvolution. *Radiation Measurements*, 41(6):659–664, 2006.

10. Y. S. Horowitz and M. Moscovitch. Highlights and pitfalls of 20 years of application of computerised glow curve analysis to thermoluminescence research and dosimetry. *Radiation Protection Dosimetry*, 153:1–22, 2012.

11. T. B. Singh, L. Rey, and R. Gartia. Applications of peakfit software in thermoluminescence studies. *NISCAIR-CSIR, India*, 2011.

12. A. Bos, T. Piters, J. Go'mez-Ros, and A. Delgado. An intercomparison of glow curve analysis computer programs: I. synthetic glow curves. *Radiation Protection Dosimetry*, 47(1-4):473–477, 1993.

13. A. Bos, T. Piters, J. Gómez Ros, and A. Delgado. An Intercomparison of Glow Curve Analysis Computer Programs: II. Measured Glow Curves. *Radiation Protection Dosimetry*, 51(4):257–264, 1994.

14. D. Yossian and Y. Horowitz. Computerized glow curve deconvolution applied to the analysis of the kinetics of peak 5 in lif: Mg, ti (tld-100). *Journal of Physics D: Applied Physics*, (7):1495, 1995.

15. A. Delgado and J. M. G. mez Ros. Computerised glow curve analysis: A tool for routine thermoluminescence dosimetry. *Radiation Protection Dosimetry*, 96(1):127–132, 2001.

16. J. Peng, Z. Dong, and F. Han. tgcd: An R package for analyzing thermoluminescence glow curves. *SoftwareX*, 5:112 – 120, 2016.

17. J. Peng, G. Kitis, A. M. Sadek, E. C. K. Asal, and Z. Li. Thermoluminescence glow-curve deconvolution using analytical expressions: A unified presentation. *Applied Radiation and Isotopes*, 168: 109440, 2021.

18. G. Kitis, J. Gomez-Ros, and J. W. Tuyn. Thermoluminescence glow-curve deconvolution functions for first, second and general orders of kinetics. *Journal of Physics D: Applied Physics*, 31(19): 2636–2641, 1998.

19. V. Pagonis, S. Mian, and G. Kitis. Fit of first order thermoluminescence glow peaks using the weibull distribution function. *Radiation Protection Dosimetry*, 93(1):11–17, 2001.

20. V. Pagonis and G. Kitis. Fit of second order thermoluminescence glow peaks using the logistic distribution function. *Radiation Protection Dosimetry*, 95(3):225–229, 2001.

21. A. Perepelitsa, M. Smirnov, O. Ovchinnikov, A. Latyshev, and A. Kotko. Thermostimulated luminescence of colloidal ag2s quantum dots. *Journal of Luminescence*, 198:357–363, 2018.

22. N. Chandrasekhar and R. K. Gartia. Gaussian approximation of thermoluminescence (TL) peaks: A common misconception for analysis of TL of persistent luminescent materials. *Journal of Alloys and Compounds*, 745:773–778, 2018.

23. M. Kundu, S. Chakrabarty, S. Bhattacharyya, and P. Majumdar. Estimation of activation energy using skewness of tl data as symmetry parameter in peak shape method. *Nuclear Instruments and Methods in Physics Research Section B: Beam Interactions with Materials and Atoms*, 542:214–222, 2023.

24. J. Randall and M. Wilkins. Phosphorescence and electron traps-I. the study of trap distributions. *Proceedings of the Royal Society of London. Series A. Mathematical and Physical Sciences*, 184 (999):365–389, 1945.

25. J. Randall and M. Wilkins. Phosphorescence and electron traps-II. the interpretation of long-period phosphorescence. *Proceedings of the Royal Society of London. Series A. Mathematical and Physical Sciences*, 184(999):390–407, 1945.

26. C. May and J. Partridge. Thermoluminescent kinetics of alpha-irradiated alkali halides. *The Journal of Chemical Physics*, 40(5):1401–1409, 1964.

27. Z. Vejnović, M. B. Pavlović, and M. Davidović. Fitting the glow curve and calculating TL parameters. *Journal of Physics D: Applied Physics*, 32:72, 1999.

28. C. M. Sunta. *Unraveling thermoluminescence; Springer Series in Materials Science*, volume 202. Springer India, New Delhi, 2014.

29. G. Kitis and N. Vlachos. General semi-analytical expressions for TL, OSL and other luminescence stimulation modes derived from the OTOR model using the Lambert W-function. *Radiation Measurements*, 48:47–54, 2013.

30. H. Balian and N. W. Eddy. Figure-of-merit (FOM), an improved criterion over the normalized chi-squared test for assessing goodness-of-fit of gamma-ray spectral peaks. *Nuclear Instruments and Methods*, 145(2):389–395, 1977.

National Conference on Atomic, Molecular and Nano Sciences
(NCAMNS- 2019)
April 3-4, 2019

DEPARTMENT OF PHYSICS
ALIAH UNIVERSITY
New Town, Kolkata- 700160, India

Certified that Prof./Dr./Mr./Ms. MOHAN KUNDU

of SADHANPUR UTR HIGH SCHOOL, ANDANGA, NADIA *participated (Invited talk/ Oral presentation/ Poster presentation) in the National Conference on Atomic, Molecular and Nano Sciences (NCAMNS-2019)*

Secretary & HoD	Convener	Co-convener
Dr. Sk. Faruque Ahmed	**Dr. Md. Mabud Hossain**	**Dr. Jayanta K. Saha**

3rd INTERNATIONAL CONFERENCE

ON

RECENT TRENDS IN RENEWABLE ENERGYANDSUSTAINABLE DEVELOPMENT

29th–30th April 2022

Organized by

BHILAI INSTITUTE OF TECHNOLOGY, RAIPUR

Certificate of Participation

Paper ID : ICRTRESD2022_ET&T_018

This is to certify that Prof./Dr./Mr./Mrs./Ms ***M. Kundu*** *of* ***Acharya Prafulla Chandra College, Kolkata*** *has Presented/Participated his/her oral presentation through hybrid mode on* ***A critical appraisal on the validity of the thermoluminescence glow curve analysis of luminescent materials using gaussian function.*** *during "3rd International Conference on Recent Trends in Renewable Energy and Sustainable Development" organized by Bhilai Institute of Technology Raipur on 29th and 30th of April 2022.*

Dr. T. Rama Rao
Director, BITR

Dr. Anup Mishra
Principal, BITR

Dr. Vikas Dubey
Convener, BITR

Dr. Md. Khaja Mohiddin
Convener, BITR

ICAMNOP - 2023

International Conference on
Atomic, Molecular, Material, Nano, and Optical Physics with Applications

20th - 22nd December, 2023

Organized by:
Department of Applied Physics, Delhi Technological University, Delhi, India

Certificate

This is to certify that

Prof./Dr./Mr./Ms. Mohan Kundu

has presented Poster / Oral Presentation in the **"International Conference on Atomic, Molecular, Material, Nano and Optical Physics with Applications (ICAMNOP-2023)"** held at Delhi Technological University, Delhi, India during 20th-22nd December, 2023.

Prof. Rinku Sharma
President, ICAMNOP-2023

Prof. A. S. Rao
Chairperson, ICAMNOP-2023

Prof. Vinod Singh
Convener, ICAMNOP-2023

Metrohm